UNIVERSIDAD AUTÓNOMA DE MADRID

FACULTAD DE CIENCIAS

Departamento de Biología Molecular

MITOPHAGY DYSFUNCTION IN PERIPHERAL AND NEURAL MODELS OF ALZHEIMER DISEASE

TESIS DOCTORAL

Patricia Martín-Maestro Rojas

Madrid, 2016

CSIC
CONSEJO SUPERIOR DE INVESTIGACIONES CIENTÍFICAS
UAM
UNIVERSIDAD AUTONOMA DE MADRID
CENTRO DE BIOLOGÍA MOLECULAR "SEVERO OCHOA"

Madrid, 30 de Mayo de 2016

Jesús Ávila de Grado, Profesor de Investigación del Consejo Superior de Investigaciones Científicas, y Vega García-Escudero Barreras, Profesora Ayudante Doctor de la Universidad Autónoma de Madrid

INFORMAN

Que la presente tesis doctoral titulada "Mitophagy dysfunction in peripheral and neural models of Alzheimer disease" ha sido realizada bajo nuestra dirección por Dña. Patricia Martín-Maestro Rojas. Consideramos que el trabajo reviste las características de originalidad y calidad científica requeridas para ser defendida como Tesis Doctoral para optar al Grado de Doctor.

Los directores de la tesis,

Dr. Jesús Ávila de Grado **Dr. Vega García-Escudero Barreras**

INDEX

Abbreviations

ABAD: Aβ-binding alcohol dehydrogenase

AD: Alzheimer disease

ADDLs: Aβ-derived diffusible ligands

Aβ: Amyloid beta

AP: Autophagosome

APP: Amyloid beta (A4) precursor protein

ATG: autophagy related proteins

ATP: Adenosine triphosphate

AVs: Autophagic vacuoles

CCCP: Carbonyl cyanide m-chlorophenylhydrazone

CMA: Chaperone-mediated autophagy

COX4: Complex IV

DLP1: Dynamin-like protein 1

DMEM: Dulbecco´s modified Eagle´s medium

DAPI: 4',6-Diamidino-2-Phenylindole, Dihydrochloride

EB: Embryoid body

ER: Endoplasmic reticulum

FAD: Familial Alzheimer disease

FBS: Fetal Bovine Serum

FL: Full-length

GAPDH: Glyceraldehyde-3-phosphate dehydrogenase

GTP: Guanosine triphosphate

IMM: Inner mitochondrial membrane

iNs: Induced neurons

iPSC: induced pluripotent stem cell

IP3R: Inositol triphosphate receptor

KLF4: Kruppel-like factor 4

KO: Knock-out

LAMP1: Lysosomal-associated membrane protein 1

MAM: Mitochondria-associated ER membranes

MAP1LC3/LC3: Microtubule-associated protein 1 light chain 3

MAPT/Tau: Microtubule-associated protein tau

Mfn: Mitofusin

MPP: Mitochondrial processing protease

mtDNA: mitochondrial DNA

NBR1: Neighbor of BRCA1 gene 1 protein

NDP52: Nuclear dot protein 52 kDa

Abbreviations

NTF: Neurofibrillary tangles

OCT4: Octamer-binding transcription factor 4

OMM: Outer mitochondrial membrane

OPA1: Optic atrophy 1

PHF: Paired helical filaments

PSEN: Presenilin

PARK2: Parkin RBR E3 ubiquitin protein ligase

PARL: Presenilin-associated rhomboid-like

PINK1: PTEN-induced putative kinase 1

ROS: Reactive oxygen species

SCaMC-1: Short calcium-binding mitochondrial carrier 1

SAD: Sporadic Alzheimer disease

SOX2: Sex determining Region Y-box 2

SQSTM1: Sequestosome 1

TOMM20: Translocase of outer mitochondrial membrane 20 homolog

VDAC1: Voltage-dependent anion channel 1

WB: Western blot

WT: Wild type

$\Delta\Psi m$: Mitochondrial membrane potential

Abstract

Alzheimer disease (AD) is a neurodegenerative disorder characterized by the accumulation of Aβ peptide and hyperphosphorylated Tau protein. Mitochondrial dysfunction and oxidative damage have been previously reported not only in the vulnerable regions of affected brain but also in peripheral cells in the disease. Autophagy has been demonstrated to play a fundamental role in AD related proteinopathy. Moreover, anomalies at different levels of autophagy pathway have been described suggesting that autophagy failure might be considered an early event of the disease. Therefore, the aim of this work was the study of autophagy pathway besides mitochondrial recycling process in human cellular models of both familial and sporadic types of AD.

The overexpression of *APP* in human fibroblasts demonstrated an activation of autophagy flux due to an enhanced degradation phase correlating with higher lysosomal activity. Increased mitochondrial content revealed a defect in mitophagy due to defective labeling of damaged mitochondria by PARK2. The addition of *Tau* to *APP* overexpression model aggravated the mitophagy dysfunction leading to unachievable recovery of mitochondrial membrane potential after an insult that resulted in the further accumulation of dysfunctional mitochondria labeled by PINK1.

The study of fibroblasts derived from familial AD patients associated to presenilin mutation revealed a deregulation of autophagy degradation phase correlating with lysosome acidification deficiency leading to accumulation of autophagic vesicles. This resulted in a mitochondrial recycling failure that caused the accumulation of mitochondria and PARK2. Worsened mitophagy dysfunction was observed in neurons derived from induced pluripotent stem cells harboring the same presenilin mutation triggering increased accumulation of mitochondria, PARK2 and PINK1.

Fibroblasts derived from sporadic AD patients demonstrated compromised mitochondrial dynamics and function as well as deficient autophagy induction and lysosomal anomalies resulting in the accumulation of oxidized and ubiquitinated proteins. Mitophagy impairment has been proven in these cells due to diminished PARK2 recruitment that caused the accumulation of depolarized mitochondria and PINK1. Patients' hippocampal samples at early stages of the disease exhibited similar mitophagy alterations showing abnormally increased mitochondrial content together with accumulation of PINK1.

Overexpression of PARK2 in sporadic AD fibroblasts diminished ubiquitinated proteins accumulation, improved its targeting to mitochondria and potentiated autophagic vesicle synthesis allowing the reversion of mitophagy failure. This suggests that autophagy enhancement is a powerful therapeutic strategy.

Our findings indicate that, although there are differences in the deregulation pattern of the mitochondrial recycling process in sporadic and familial AD models, both converge in the same mitophagy failure that causes the accumulation of dysfunctional mitochondria.

La enfermedad de Alzheimer (EA) es un trastorno neurodegenerativo caracterizado por la acumulación del péptido Aβ y la proteína Tau hiperfosforilada. Se ha demostrado un fallo en la función mitocondrial así como un daño oxidativo no solo en las regiones afectadas en el cerebro si no en células periféricas en la enfermedad. Se han descrito anomalías en las diferentes etapas de la autofagia sugiriendo que la insuficiencia autofágica podría ser considerada un evento temprano de la patología. Teniendo en cuenta estos antecedentes, el objetivo de este trabajo fue el estudio del proceso de autofagia así como el mecanismo de reciclaje mitocondrial en modelos celulares humanos tanto de la forma familiar como esporádica de la EA.

La sobreexpresión de *APP* en fibroblastos humanos demostró una activación de la fase degradativa de la autofagia en correlación con una mayor actividad lisosomal. El incremento del contenido mitocondrial reveló un defecto en mitofagia debido a un incorrecto marcaje de mitocondrias dañadas por PARK2. La adición de *Tau* al modelo de sobreexpresión de *APP* agravó la disfunción en mitofagia que se reflejó en la falta de recuperación del potencial de membrana, lo que provocó una mayor acumulación de mitocondrias no funcionales marcadas con PINK1.

El estudio de fibroblastos de pacientes de EA familiar asociados a una mutación en presenilina mostró una desregulación de la fase degradativa de la autofagia en correlación con una incorrecta acidificación de los lisosomas, lo que resultó en la acumulación de vesículas autofágicas. Esto provocó un fallo en el reciclaje mitocondrial que causó la acumulación de mitocondrias y PARK2. Las neuronas derivadas de células madre pluripotentes inducidas (iPSC) con la misma mutación en presenilina presentaron un empeoramiento del proceso de mitofagia que conllevó a un aumento de la acumulación mitocondrial, PARK2 y PINK1.

Los fibroblastos derivados de pacientes de EA esporádica manifestaron una dinámica y función mitocondrial menoscabada, así como una inducción de autofagia deficiente unida a anomalías lisosomales, dando como resultado la acumulación de proteínas oxidadas y ubiquitinadas. En estas células se demostró un deterioro en mitofagia debido a un menor reclutamiento de PARK2 que causó la acumulación de mitocondrias despolarizadas y PINK1. Muestras de hipocampo de pacientes en etapas tempranas de la enfermedad presentaron alteraciones similares en mitofagia con acumulación anormal de mitocondrias y PINK1.

La sobreexpresión de PARK2 en fibroblastos de EA esporádica generó una disminución de los niveles de proteínas ubiquitinadas, mejoró su reclutamiento a la mitocondria, además de potenciar la síntesis de vesículas autofágicas permitiendo la reversión del defecto en mitofagia. Esto sugiere que la mejora del proceso de autofagia es una poderosa estrategia terapéutica.

Nuestros resultados indican que, aunque existen diferencias en el patrón de desregulación del proceso de reciclaje mitocondrial en los modelos esporádicos y familiares de la EA, ambos convergen en el mismo fallo en mitofagia que causa la acumulación de mitocondrias no funcionales.

Introduction

1. Alzheimer Disease

Alzheimer disease (AD) is a progressive and fatal neurodegenerative disorder and the leading cause of dementia accounting for 50–70% of cases. Due to the fact that the primary risk factor for AD is old age, the prevalence of the disease is increasing dramatically with progressive ageing of population in developed countries. The *World Alzheimer Report* revealed that over 46 million people worldwide live with dementia in 2015 and this number will almost double every 20 years.

AD was first described by Alois Alzheimer in 1907 (Alzheimer et al, 1995), and it is manifested by cognitive and memory deterioration, progressive impairment of activities of daily living, as well as a variety of neuropsychiatric symptoms and behavioral disturbances (Cummings, 2004).

AD is classified in two different types: familial Alzheimer disease (FAD) and sporadic Alzheimer disease (SAD). FAD is early-onset AD (<65 years) and genetically heterogeneous with autosomal dominant inheritance (Tanzi et al, 1996). Only less than 5% of AD cases can be related to mutations in *Amyloid beta (*Aβ*) precursor protein* (*APP*) located in chromosome 21, *Presenilin 1* (PSEN1) in chromosome 14 and *Presenilin 2* (PSEN2) in chromosome 1 (Rademakers et al, 2003). SAD or late-onset AD (>65 years) which accounts for more than 95% of cases, is a multifactorial disease where several genes are implicated in increasing the risk as well as environmental factors. Undoubtedly, the main risk factor is aging since the incidence of AD increases exponentially from 65 years (Jicha et al, 1999; Kawas & Corrada, 2006; Kukull et al, 2002). Moreover, it has been described different types of lifestyle risk factors such as smoking, hypertension, obesity, atherosclerosis, hypercholesterolemia, previous brain injury or diabetes mellitus type II (Carlsson, 2010; de Toledo Ferraz Alves et al, 2010; Fotuhi et al, 2009; Schmidt et al, 2001). On the other hand, the polymorphic *apolipoprotein E* (apoE) gene confers susceptibility to develop the disease. The apoE4 allele is the largest known genetic risk factor for late-onset SAD in a variety of ethnic groups in contrast to apoE2 and apoE3 alleles (Coon et al, 2007; Corder et al, 1993; Raber et al, 2004; Strittmatter et al, 1993).

The confirmed diagnosis of AD requires the presence of two major neuropathological lesions: accumulation of extracellular amyloid beta (Aβ) senile plaques and intracellular microtubule-associated protein Tau (MAPT/Tau) neurofibrillary tangles. These structures are normally visible at the patient autopsy although increasing efforts has been made to develop techniques that allow their identification *in vivo* (Fodero-Tavoletti et al, 2011; Klunk et al, 2004). However, it is widely accepted that Alzheimer is a silent neurodegeneration where neuronal damage occurs before the diagnosis, and plaques, tangles and cellular degeneration appear previous to the onset of disease symptoms.

1.1 APP & amyloid plaques

Amyloid precursor protein (APP) is an integral membrane protein expressed in various organs and tissues which belongs to a larger evolutionarily conserved APP superfamily found in diverse organisms from nematode to mammals. Although still not fully understood, the role of APP in normal functioning of the brain and other organs had been intensively studied. The protein sequence analysis of the APP superfamily members strongly suggests that the normal function of APP relates to cell–cell interaction and cell–substrate adhesion (Coulson et al, 2000; Soba et al, 2005). Moreover, it has been implicated as a regulator of synapse formation (Priller et al, 2006), neural plasticity (Turner et al, 2003), iron export (Duce et al, 2010) and hormonal regulation (Gallego et al, 2010; Porayette et al, 2009). However, there are some data suggesting that membrane localization and processing of APP in neurons differ from those in peripheral cells (e.g. lymphoid cells, hepatocytes or kidney) which suggests that functioning of this transmembrane holoprotein and production of Aβ in the brain is a critical determinant of its receptor-transducer properties unique to this organ (Jung et al, 1996).

The Aβ senile plaques are extracellular deposits mainly composed by Aβ peptide crucially involved in Alzheimer disease but also shown in brains of advance age (Dickson et al, 1992; Morris et al, 1996; Wolf et al, 1999), without evidence of a cognitive deficit associated with their presence (Aizenstein et al, 2008; Katzman et al, 1988; Rowe et al, 2007). The peptides result from the sequential proteolytic cleavage of APP (Masters et al, 1985), which is proteolyzed by α-, β- y γ-secretase to yield Aβ. The sequential cleavage of α- and γ-secretase generates a small non-amyloidogenic peptide of 3 kDa, (Haass et al, 1993; Haass et al, 1992). Consecutive cleavages of β- and γ-secretase generates a peptide of 40 or 42 amino acids (Aβ40 or Aβ42), which is released into the extracellular space (Selkoe, 2001). Aβ42 is more hydrophobic than Aβ40, and tends to aggregate and fold in β-sheet structure, recruiting other extracellular proteins, which could result in the formation of senile plaques (Citron et al, 1996; Neve et al, 2000). Mutations associated with FAD, both APP and presenilin genes (involved in the activity of γ-secretase), carry out an increased Aβ42/ Aβ40 ratio (Selkoe, 2002). Aβ molecules can aggregate to form flexible soluble oligomers which may exist in several forms. On the other hand, calcium dysregulation has been observed in cells exposed to amyloid oligomers. These small aggregates can form ion channels in planar lipid bilayer membranes. Channel formation has been hypothesized to account for calcium dysregulation and mitochondrial dysfunction by allowing indiscriminate leakage of ions across cell membranes (Kagan et al, 2004). Moreover, studies have shown that amyloid deposition is associated with mitochondrial dysfunction and it results in the generation of reactive oxygen species (ROS), which can initiate a signaling pathway leading to apoptosis (Kadowaki et al, 2005).

1.2 Tau & Neurofibrillary tangles

Tau protein is a microtubule-associated protein (MAP) that under physiological conditions regulates microtubules assembly, dynamic behavior, and spatial organization (Drechsel et al, 1992; LoPresti et al, 1995). Tau is abundant in neurons of the central nervous system but is also expressed at very low levels in astrocytes and oligodendrocytes (Shin et al, 1991). Therefore, modification of Tau by phosphorylation or a change in the amount of Tau can result in destabilization of neuronal microtubules. This can affect the placement and function of mitochondria, lysosomes, and other cellular structures (Avila et al, 2004; Ebneth et al, 1998). Moreover, it is known that autophagosome clearance by lysosomes is a microtubule-dependent process (Jahreiss et al, 2008; Matteoni & Kreis, 1987). Therefore, abnormal function of Tau may disrupt neuronal function including axonal transport, which also involves trafficking of autophagic cargos (Yue, 2007) and lead to the buildup of autophagosomes in AD dystrophic neurites or axons (Nixon et al, 2005).

Neurofibrillary tangles (NFT) are filamentary aggregates of hyperphosphorylated Tau protein (Grundke-Iqbal et al, 1986b). It appears within neurons, taking up the perinuclear cytoplasm and, after neuronal death, remain in the extracellular space where they are called extracellular neurofibrillary or ghost tangles (Braak & Braak, 1991). The NFT are mainly composed by paired helical filaments (PHF) and in lower proportion by straight filaments (Hirano et al, 1968). In the 80s, the biochemical composition of the PHF was described, composed mainly by the Tau protein (Goedert et al, 1988; Grundke-Iqbal et al, 1986a; Kosik et al, 1986; Wischik et al, 1988; Wood et al, 1986). Further studies revealed that Tau is hyperphosphorylated in the PHF (Grundke-Iqbal et al, 1986b; Lee et al, 1991; Wolozin et al, 1986).

2. Mitochondria

Mitochondria are a double membrane organelle found in most eukaryotic cells. The organelle is comprised of two separate and functionally distinct outer and inner membranes that encapsulate the intermembrane space and matrix compartments. They also contain a circular genome, mitochondrial DNA (mtDNA), that has been reduced during evolution through gene transfer to the nucleus. mtDNA is organized into discrete nucleoids in the matrix.

Mitochondria are cellular energy powerhouses that play important roles in maintaining cell survival, cell death and cellular metabolic homeostasis. They perform diverse interconnected functions producing ATP and many biosynthetic intermediates while also coordinating cellular stress responses such as autophagy and apoptosis (Galluzzi et al, 2012). Mitochondria form a dynamic, interconnected network that are intimately integrated with other cellular compartments. In addition, mitochondrial functions extend beyond the boundaries of the cell and influence an organism's physiology by regulating communication between cells and tissues. It is therefore not surprising that

mitochondrial dysfunction has emerged as a key factor in multiple diseases, including neurodegenerative and metabolic disorders.

2.1 Organization and distribution

Mitochondria are dynamic organelles that continuously undergo fission and fusion events (Fig.1), which are necessary for cell survival as well as adaptation to changing conditions needed for cell growth, division, and distribution of mitochondria during differentiation (van der Bliek et al, 2013). Mitochondrial fusion in mammals is mediated by the fusion proteins mitofusin 1 (Mfn1) and mitofusin 2 (Mfn2) and optic atrophy 1 (OPA1) (Ni et al, 2015). Mfn1 and Mfn2 are dynamin-related GTPases that are responsible for fusion of outer mitochondrial membranes (OMM). OPA1 is also a dynamin-related GTPase, which is responsible for fusion of inner mitochondrial membranes. Presenilin-associated rhomboid-like (PARL) and paraplegin (an AAA protease family present in the mitochondrial matrix) induce alternative splicing and alternative processing of OPA1 to generate eight OPA1 isoforms (Cipolat et al, 2006; Ishihara et al, 2006). Mitochondrial fission in mammals is mediated by dynamin-like protein 1 (DLP1), which is also a large GTPase (Ni et al, 2015). DLP1 is a cytosolic protein that can be recruited to the outer mitochondrial membrane to constrict mitochondria resulting in eventual division of a mitochondrion into two separate organelles. DLP1 interacts with four mitochondrial receptor proteins: fission 1 (Fis1), mitochondria fission factor (Mff), mitochondrial dynamics protein of 49 kDa (MID49) and 51kDa (MID51) (Loson et al, 2013; Palmer et al, 2011). In mammalian cells, it seems that the interaction between Fis1 and DLP1 has a minor role in regulating mitochondrial fission whereas the interactions of DLP1 with the other three receptor proteins play prominent roles for fission. Moreover, during cell division, mitochondrial fission is essential for separating mitochondria into two daughter cells.

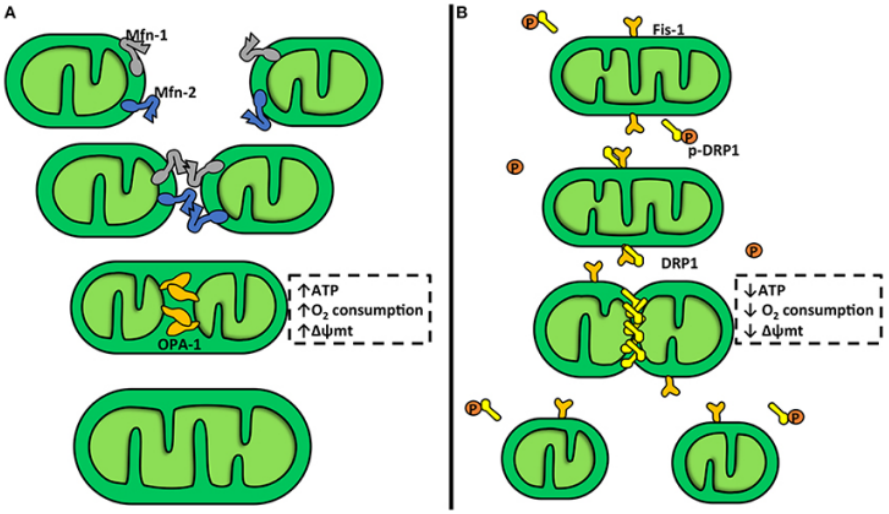

Figure 1. Scheme of the mitochondrial dynamics. A. Mitochondrial fusion. **B.** Mitochondrial fission (Chiong et al, 2014).

In addition to fission and fusion, the movement of mitochondria through the cytoskeleton is also important for the cellular distribution and turnover of mitochondria (Mishra & Chan, 2014). Mitochondria in mammalian cells are mostly transported on microtubules using a kinesin motor towards the plus end and a dynein motor towards the minus end of microtubules (Saxton &

Hollenbeck, 2012). The attachment of mitochondria to the kinesin motor is regulated by several molecular adapters. The adapter protein Milton directly interacts with the outer mitochondrial membrane protein Mitochondrial Rho GTPase (Miro) and in turn links mitochondria to kinesin (Saxton & Hollenbeck, 2012).

It has been suggested that mitochondria fission and fusion may serve as important quality control mechanisms for preserving mitochondria and are fundamental for the correct distribution of the mitochondria in the cell (Detmer & Chan, 2007). This is particularly important for neurons that may have very long axons and also for the function of synapses, which are subcellular regions with high metabolic requirement (Frazier et al, 2006). Dysfunctional mitochondria may lose their fusion capacity by inactivating fusion or activating fission machineries to prevent the damaged mitochondria from incorporating back into the healthy mitochondrial network. Daughter mitochondria with higher membrane potential (presumably good quality mitochondria) proceed to fusion while depolarized daughter mitochondria (presumably bad quality mitochondria) are degraded by mitophagy (Twig et al, 2008). On the other hand, although fission plays a pivotal role in apoptosis, it has described that inhibition of the mitochondrial fission blocks cell death, resulting in a significantly reduced cellular susceptibility toward apoptosis (Frank et al, 2001).

2.2 Removal of defective mitochondria

2.2.1 Autophagy

Autophagy is a stress-induced catabolic process in which components of the cell are degraded by the lysosomes (or, in yeast, the analogous vacuole) and recycled (Esclatine et al, 2009; Klionsky, 2005). Based on how substrates are delivered to the lysosomal compartment, autophagy is classified into three main subtypes:

Chaperone-mediated autophagy (CMA): In CMA, a chaperone protein binds first to its cytosolic target substrate and then to a receptor on the lysosomal membrane where the unfolding of the protein occurs. The unfolded cytosolic target protein is subsequently translocated directly into the lysosome for its degradation (Cuervo, 2010; Massey et al, 2004).

Microautophagy: Microautophagy is a non-selective lysosomal degradative process that translocates direct engulfment of cytoplasmic cargo to the lysosome for degradation by either direct invagination, protrusion, or septation of the lysosomal membrane (Li et al, 2012).

Macroautophagy: Macroautophagy is characterized by the formation of a cytosolic double-membrane vesicle, the autophagosome (AP). During macroautophagy, cytoplasmic proteins, organelles or other materials are surrounded by phagophores, which expand and close to form APs (Fig.2). The AP generation is characterized by the participation of autophagy related proteins (ATG) family. The AP maturation requires the cleavage of autophagy related protein 8/Microtubule-associated proteins 1A/1B light chain 3 (ATG8/LC3) by autophagy related protein 4 (ATG4) producing the cytosolic form of the protein known as LC3I. The covalent bond of this protein to a residue of phosphatidylethanolamine (PE), which gives the name of LC3II, allows it to join to the AP membrane facilitating its expansion (Xie et al, 2008). The PE residue gives to LC3II a different electrophoretic mobility compare with LC3I detectable by Western blotting (WB) correlated directly with the number of mature APs and autophagolysosomes. Moreover, the LC3II protein is essential in the recognition of the cargo that should be incorporated into the AP (Wild et al, 2014). Adaptor proteins that recognize post translational modifications, often polyubiquitinations, such as Sequestosome 1 (p62/SQSTM1), have binding domains to AP. p62 bins to lysine 63-linked ubiquitination (Tan et al, 2008) abundant on the surface of protein aggregates. On the other hand, p62 can bind to LC3II promoting cargo recruitment by the AP (Pankiv et al, 2007) regulating the protein aggregates and inclusions clearance (Komatsu et al, 2007). p62 may also modulate aggregate formation and regulates stress-response genes as well as damage organelle clearance (Wong & Cuervo, 2010). Excess of p62 as a result of autophagy block inhibits the clearance of ubiquitinated proteins destined for proteasomal degradation suggesting a possible cytotoxic role (Korolchuk et al, 2009). Additionally, it has been described two more adaptor proteins such as Neighbor of BRCA1 gene 1 protein (NBR1) (Kirkin et al, 2009) and nuclear dot protein 52 kDa (NDP52) (Thurston et al, 2009) which also recognize ubiquitin. NBR1 binds to proteins while NDP52 may act in infections caused by pathogenic bacteria. Then, the trafficking of APs along microtubules towards lysosomes is necessary to allow effective fusion. These APs fuse with lysosomes to form autolysosomes, in which the cytoplasmic cargos are degraded by resident

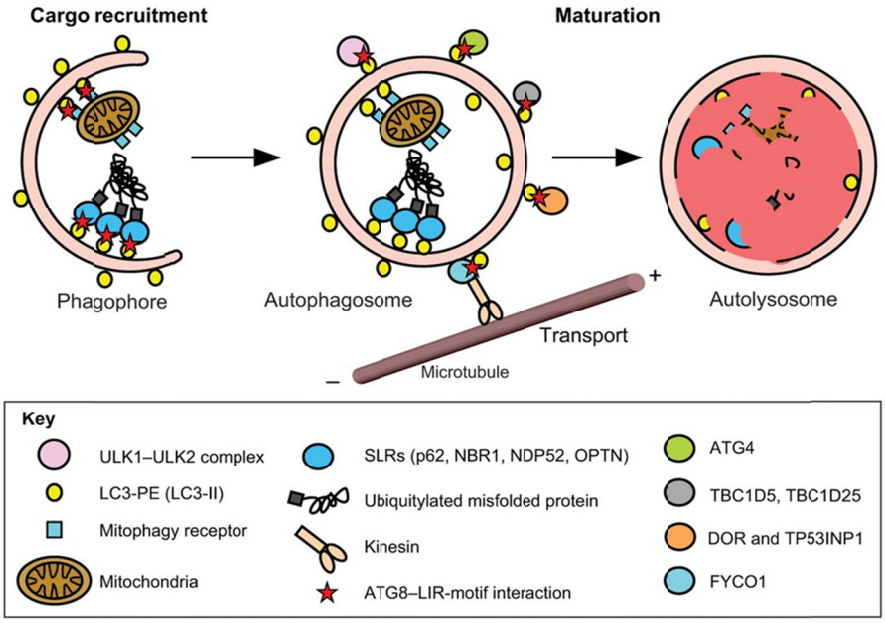

Figure 2. Representative stages of autophagy. (Birgisdottir, 2013).

hydrolases. Fusion is an extremely regulated process. Most of the molecular effectors that controls fusion process are characterized in yeast but there are some articles which revealed some of the proteins involved in fusion in mammal cells such as Rab7, Rab22 y Rab24 (Ganley et al, 2011) as well as proteins of SNARE complex such as Vti1b (Fraldi et al, 2010) and Sintaxin 17 (Itakura et al, 2012). The ATP-dependent proton pump V-ATPase ensures low intralysosomal pH, which is essential for lysosomal hydrolase activity. Based on studies with the V-ATPase inhibitor Bafilomycin A1, lysosomal acidification is also thought to be required for fusion with incoming vesicles from the autophagic and endocytic pathways (Wang et al, 2014a). The resulting degradation products are then transported back into the cytosol through the activity of membrane permeases for reuse (Klionsky, 2007). Although macroautophagy is generally considered to be nonspecific, there are many examples of selective autophagy, including mitophagy (for mitochondria), ribophagy (for ribosomes), pexophagy (for peroxisomes) and reticulophagy (for the endoplasmic reticulum, ER) (He & Klionsky, 2009).

Among the three main forms of autophagy, macroautophagy is the most widely studied and best characterized process. In this thesis, we will focus on macroautophagy process, referred to as autophagy and more specifically in mitophagy.

2.2.2 Mitophagy

As it referred previously, mitophagy is the selective degradation of mitochondria by autophagy. It often occurs to defective mitochondria following damage or stress. It promotes turnover of mitochondria and prevents accumulation of dysfunctional mitochondria which can lead to cellular degeneration (Lemasters, 2005). There are two different ways to carry out the mitochondrial recycling process.

PARK2-dependent mitophagy: One of the best studied mechanisms for mitophagy in mammalian cells is the PINK1–PARK2-mediated mitophagy pathway (Ding & Yin, 2012; Youle & Narendra, 2011). The PARK2-dependent mitophagy pathway has been shown to require both PARK2 and PINK1 proteins. PARK2 RBR E3 ubiquitin protein ligase (PARK2) is a cytosolic E3 ubiquitin l ligase that translocates to depolarized mitochondria and initiates their degradation via mitophagy (Narendra et al, 2008).

Molecular regulation of PINK1: PTEN induced putative kinase 1 (PINK1) is a mitochondrial serine/threonine kinase. Levels of PINK1 are normally undetectable in most cells because PINK1 is cleaved in the mitochondria and then degraded by mitochondrial peptidases. However, PINK1 turned out to be accumulated in depolarized mitochondria rapidly (Narendra et al, 2010b; Vives-Bauza et al, 2010), suggesting that PINK1 is subjected to a posttranslational degradation (**Fig.3**). Several studies report that PARL, which is localized in the inner mitochondrial membrane (IMM), processes PINK1 in

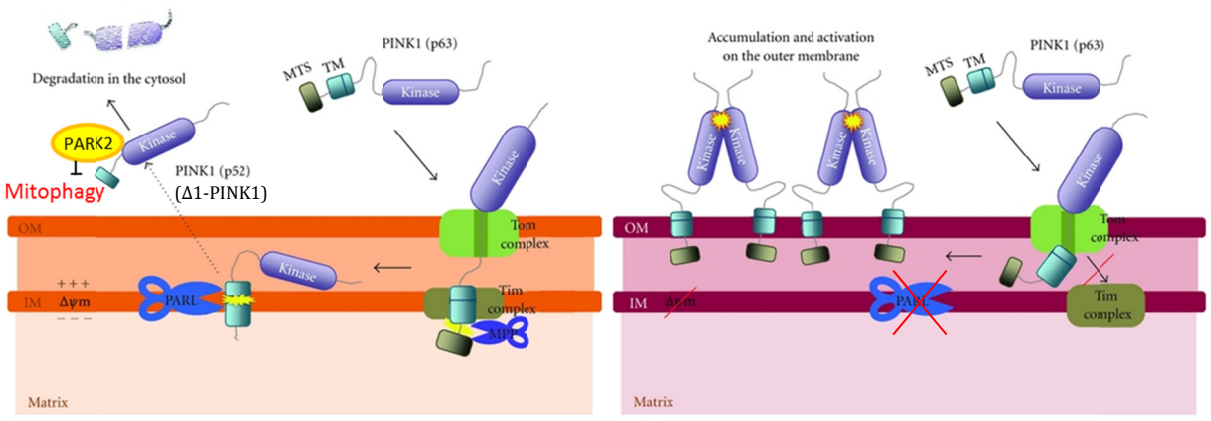

Figure 3. Model of posttranslational processing of PINK1. Modified from Imai, 2012.

a mitochondrial membrane potential (ΔΨm)-dependent manner (Jin et al, 2010). Newly synthesized PINK1 in the cytosol is inserted into the IMM, through the mitochondrial import activity of the TOMM and TIMM complexes (Lazarou et al, 2012). Full-length (FL)-PINK1 is proteolyzed by mitochondrial processing protease (MPP), which cleaves the mitochondrial targeting sequence (Greene et al, 2012). Then, PINK1 is cleaved in its putative transmembrane domain by PARL to generate the Δ1-PINK1 isoform. Δ1-PINK1 is rapidly removed by a proteasome-dependent pathway, most likely after its release from the mitochondrial intermembrane space to the cytosol (Meissner et al, 2011). It has been recently described that cytosolic cleaved Δ1-PINK1 represses PARK2 translocation to mitochondria. Δ1-PINK1 is able to physically bind PARK2 in the cytosol inhibiting its translocation to the mitochondria impairing the elimination of damaged mitochondria (Fedorowicz et al, 2014). Upon the depolarization of the ΔΨm, PINK1 IMM insertion and the subsequent processing of PINK1 by PARL may be inhibited, leading to the accumulation of FL-PINK1 in the OMM (Jin et al, 2010) to begin the mitophagy process.

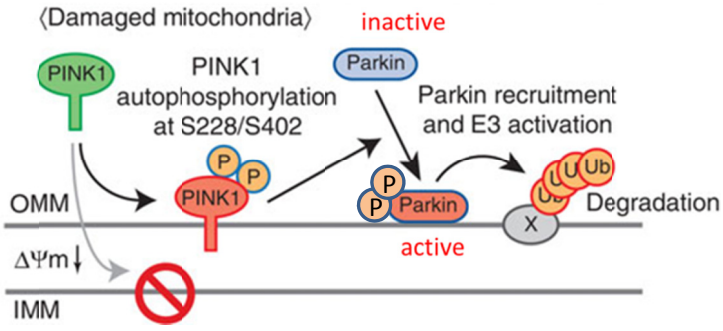

Figure 4. Steps of PARK2/Parkin recruitment and activation. Modified from Okatsu et al, 2012.

Molecular crosstalk between PINK1 and PARK2: After dissipation of ΔΨm, the autophosphorylation of PINK1 is essential for its activation promoting the recruitment of PARK2 to the mitochondria (Fig.4). PINK1 directly phosphorylates PARK2 at Thr175 and Thr217 within PARK2's linker region, which promotes PARK2 mitochondrial translocation (Kim et al, 2008b). In addition, phosphorylation of PARK2 by PINK1 at Ser65 activates PARK2 E3 ubiquitin ligase activity, enabling it to ubiquitinate mitochondrial proteins (Sha et al, 2010). Moreover, it is known that PINK1 also phosphorylates ubiquitin at Ser65, and the

phospho-ubiquitin activates PARK2 E3 ubiquitin ligase activity through a feed-forward mechanism (Kane et al, 2014; Koyano et al, 2014).

PARK2 activation and mitophagy initiation: Once recruited to the mitochondria, PARK2 ubiquitinates several mitochondrial outer membrane proteins including the mitochondrial fusion proteins Mfn1 and Mfn2, Miro, translocase of outer mitochondrial membrane 20 (TOMM20), and voltage-dependent anion channel 1 (VDAC1) to initiate mitophagy. Ubiquitination and proteasomal degradation of Mfn1 and Mfn2 results in mitochondrial fragmentation. Following PARK2-mediated ubiquitination of outer mitochondrial membrane proteins, the selective autophagy adapter protein p62/SQSTM1 (Sequestosome 1) is recruited to mitochondria and play a role in mitophagy due to its capacity to directly interact with LC3 via its LC3 interacting region (Geisler et al, 2010; Huang et al, 2011; Manley et al, 2013). However, it seems that the role of p62 in mitophagy is not essential, likely due to the presence of other compensatory or redundant similar autophagy receptor proteins (Narendra et al, 2010a; Okatsu et al, 2010). Interestingly, it was recently found that optineurin, another autophagy receptor protein, was also recruited to ubiquitinated mitochondria via its ubiquitin binding domain after PARK2 activation on mitochondria. Optineurin induces autophagosome formation around the damaged mitochondria by recruiting double FYVE-containing protein 1 and LC3 to damaged mitochondria (Wong & Holzbaur, 2014). In addition, PARK2 also recruits Ambra1 (a Beclin-1 interacting protein) to depolarized mitochondria to initiate engulfment of damaged mitochondria by autophagosomes (Van Humbeeck et al, 2011).

PARK2-independent mitophagy: Although the goal of this thesis is focused in PARK2-dependent mitophagy is necessary to note that increasing evidence supports that mitophagy can occur independent of PARK2. Several autophagy receptor proteins have been shown to localize on mitochondria and interact with LC3 to recruit autophagosomes to damaged mitochondria including Bcl2/adenovirus E1B 19 kDa protein-interacting protein 3, NIX (also called BNIP3L), Fun14 Domain containing 1 besides other mitochondrial E3 ligases such as SMURF1.

3. Mitochondrial dysfunction & AD

3.1 Oxidative stress production

Oxidative stress is a primary event in the development of AD (Bonda et al, 2010a). This oxidative stress may be due to the presence of dysfunctional mitochondria resulting in generation of reactive oxygen species (ROS) (Santos et al, 2010) that may be toxic for cells with a long life span and a deficiency in antioxidant defenses, such as neurons (Moreira et al, 2010). Additionally, mitochondria are at the same time a target of ROS causing the oxidation of their components such as

mtDNA, lipids, and proteins increasing mitochondrial deterioration. Mitochondrial dysfunction is one of the earliest and most prominent features of AD (Hauptmann et al, 2009; Schmitt et al, 2012). In fact, a decreased expression of either nuclear or mitochondrial genes of the oxidative phosphorylation in the neocortex of AD patients has been shown to correlate with progressive reductions in brain glucose metabolism that can be visualized by positron emission tomography (Chandrasekaran et al, 1996; Chandrasekaran et al, 1997).

Alterations of several enzymes involved in the tricarboxylic acid cycle such as pyruvate dehydrogenase and α-ketoglutarate dehydrogenase have been reported in Alzheimer disease (Fig.5). Postmortem brains showed a reduction of pyruvate dehydrogenase, ATP-citrate lyase, and acetoacetyl-CoA thiolase correlating with decreased production of acetylcoenzyme A and the subsequent cholinergic defects observed in these patients (Perry et al, 1980). Reduced activity of α-ketoglutarate dehydrogenase was also observed in brain tissue as well as in peripheral cells from AD patients (Gibson et al, 1988; Sheu et al, 1994). Additionally in AD brain, there is a loss of α-ketoglutarate-enriched cells, therefore causing the degeneration of α-ketoglutarate-enriched areas (cortical layers II and IV) which are the ones that are selectively degenerated in AD (Ko et al, 2001). On the other hand, products of the toxic action of ROS, like hydroxynonenal (HNE), or the presence of

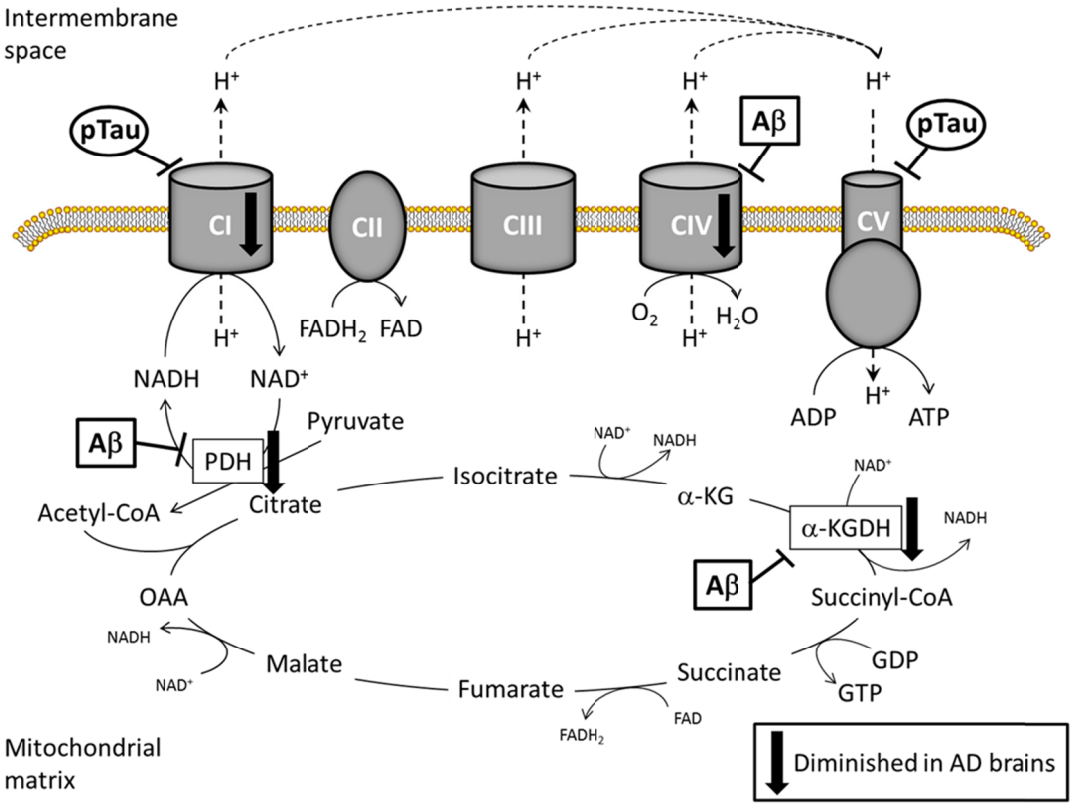

Figure 5. AD-related alterations of mitochondrial respiratory chain and tricarboxylic acid cycle. Oxidative phosphorylation complexes are labeled as CI to CIV. PDH: pyruvate dehydrogenase, α-KG: α-ketoglutarate, α-KGDH: α-ketoglutarate dehydrogenase, OAA: oxaloacetate (Garcia-Escudero et al, 2013).

quinones (like coenzyme Qo) may facilitate the self-assembly of Tau protein into fibrillar polymers similar to those paired helical filaments present in the brain of AD patients (Santa-Maria et al, 2004). These findings suggest another possible link between oxidative stress, neuronal dysfunction, and AD.

It is possible that mitochondrial dysfunction in AD patients not only takes place in the central nervous system but also in cells from peripheral tissues. Increased oxidative stress levels and reduced antioxidant defenses have been observed in AD fibroblasts (Cecchi et al, 2002). Regarding this, it has been described that lipoic acid and N-acetylcysteine may decrease the mitochondrial-related oxidative stress in Alzheimer disease patients (Moreira et al, 2007a).

3.2 Mitochondrial dynamics alteration

Mitochondria failure may arise from a deficient dynamic balance of mitochondrial fission and fusion that, in AD (**Fig.6**), is greatly shifted toward fission and it may result in the presence of dysfunctional mitochondria in damaged neurons as well as fibroblasts from AD patients characterized by their accumulation into perinuclear areas (Bonda et al, 2010b; Zhu et al, 2013). Vulnerable neurons in AD brain exhibit significant reduction in mitochondrial length and increased width with a significant increased overall size consistent with unopposed fission suggesting alterations of mitochondrial dynamics (Wang et al, 2008b). In agreement with these findings, an abnormal distribution of mitochondria was found in pyramidal neurons of AD-affected individuals where mitochondria were redistributed away from axons in the pyramidal neurons (Wang et al, 2009). Accordingly, levels of fusion proteins OPA1, Mfn1, and Mfn2 were significantly reduced whereas levels of Fis1 were significantly increased in AD. In the case of the fission protein DLP1, it has been described a reduction in neurons (Bossy et al, 2010; Wang et al, 2008a) and fibroblasts of sporadic patients (Wang et al, 2008a). Primary hippocampal neurons treated with Aβ-derived diffusible ligands (ADDLs) demonstrated shortened mitochondria in neurons and alteration of fission and fusion proteins (Wang et al, 2009). Moreover, time-lapse recordings in these neurons showed impairment of both, fission and fusion processes, with fusion process being more severely affected (Wang et al, 2009). Additional evidence has shown an abnormal interaction of Aβ monomers and oligomers with DLP1 that increases with the progression of the disease suggesting a possible cause of abnormal mitochondrial dynamics and synaptic damage (Manczak et al, 2011). On the other hand, the expression of AD-causing Swedish APP mutation in M17 cells also induced shorter and fatter mitochondria, with a slight but significant increase in size, but a decrease in the total mitochondrial number while the number of damaged mitochondria was increased (Wang et al, 2008b). Similar observations have been found in transgenic mice (Tg2574) harboring the APP Swedish mutation (Calkins et al, 2011). Abnormal mitochondrial morphology has been found in fibroblasts from sporadic AD patients, where they become significantly elongated and form a highly connected network (Wang et al, 2008a). This discrepancy in mitochondrial morphology may be due to differences in the expression pattern of proteins involved in dynamics, showing decreased DLP1 and

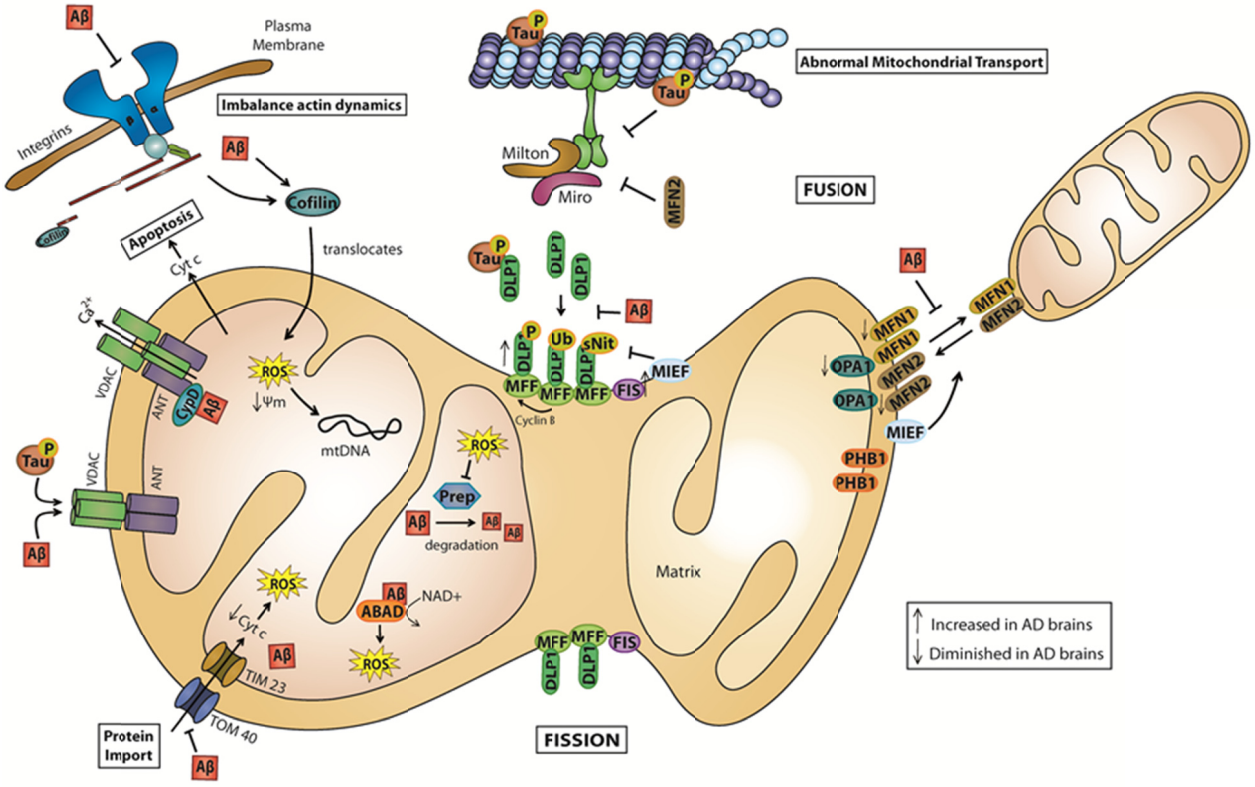

Figure 6. Mitochondrial alterations found in AD. Scheme of the effect of Aβ and phosphorylated-Tau (pTau) over mitochondrial dynamics, transport, protein import, membrane permeabilization, apoptosis as well as actin dynamics (Garcia-Escudero et al, 2013).

unchanged OPA1. Mitochondrial mobility has also been altered in AD causing a mitochondrial reduction in neurites (Zhu et al, 2013) (Fig.6). Aβ induces a reduction in motile mitochondria (Rui et al, 2006) and ADDL impairs anterograde and retrograde axonal transport of mitochondria in hippocampal neurons (Wang et al, 2010). Primary neurons from Tg2576 APP transgenic mice showed a specific impairment of anterograde mitochondrial transport. These results suggest that mitochondrial fission/fusion and mitochondrial transport can be coupled. In fact, it has been demonstrated that Mfn2 interacts with Miro and Milton, two adaptor proteins involved in the regulation of mitochondrial transport (Misko et al, 2010), although further work is necessary to clarify this relationship. Moreover, Neuronal pentraxin 1, a pro-apoptotic protein increased in damaged neurites in Alzheimer disease-affected brains, regulates mitochondrial dynamics and trafficking during apoptotic neurodegeneration (Clayton et al, 2012).

The alteration in mitochondrial dynamics leads to severe consequences in the cell such as structural changes in the cristae formation and assembly of electron transport complex compromising bioenergetics and causing calcium dyshomeostasis, increased oxidative stress, mtDNA damage, and synaptic dysfunction (Zhu et al, 2013).

3.3 Relationship between mitochondrial dysfunction and AD-related pathology

3.3.1 Amyloid beta

In FAD, an increase in the level of Aβ may result in oxidative damage (Belkacemi & Ramassamy, 2012; Butterfield, 2002; Schmitt et al, 2012). APP and Aβ accumulate in mitochondrial membranes causing structural and functional damage (Pagani & Eckert, 2011). Non-glycosylated full-length and C-terminal truncated APP has been found to accumulate in the protein import channels of mitochondria of human AD brains (Devi et al, 2006) (**Fig.6**). APP forms stable complexes with the translocase of the outer mitochondrial membrane 40 (TOMM40) import channel and the translocase of the inner mitochondrial membrane 23 (TIMM23) inhibiting the entry of nuclear-encoded cytochrome *c* oxidase subunits IV and Vb proteins, which was associated with decreased cytochrome *c* oxidase activity and increased ROS production. Additionally, an interaction has been discovered between Aβ and phosphorylated Tau with VDAC1 in the brains of AD patients and from APP, APP/PSEN1, and 3XTg AD mice which may block the mitochondrial pores leading to mitochondrial dysfunction (Manczak & Reddy, 2012).

Aβ interacts with the mitochondrial protein ABAD (Aβ-binding alcohol dehydrogenase) which is upregulated in the temporal lobe of AD patients as well as in APP transgenic mice (Lustbader et al, 2004) (**Fig.6**). This complex prevents the binding of nicotinamide adenine dinucleotide NAD to ABAD, thereby changing mitochondrial membrane permeability and reducing the activities of respiratory enzymes causing elevated ROS.

Moreover, it has been suggested that the oxidative stress induced by Aβ may oxidize and inactivate presequence protease, PreP, one of the proteins involved in Aβ degradation in the mitochondria thus increasing Aβ concentration in mitochondrial matrix and its pathologic effects (Alikhani et al, 2009) (**Fig.6**).

Aβ has been also involved in alterations of mitochondrial dynamics. In fact, the overexpression of human APP Swedish double mutation in neuroblastoma cell lines induces a higher percentage of highly fragmented and slower mitochondria correlating with an alteration of the levels of the proteins involved in mitochondrial dynamics such as increased fission protein Fis1 and reduced levels of fusion proteins like OPA1 and DLP1 (Wang et al, 2008b) (**Fig.6**). In agreement with these *in vitro* findings, an abnormal distribution of mitochondria was also found in pyramidal neurons of AD affected individuals.

Additionally, Aβ enhances nitrosative stress-inducing S-nitrosylation of DLP1, which favors mitochondrial fission followed by mitochondrial depletion from axons and dendrites and subsequently synaptic loss (Bossy et al, 2010) (**Fig.6**).

Mitochondrial Aβ may also interact with cyclophilin D, an integral part of the mitochondrial permeability transition pore (mPTP), which potentiates free radical production, causes synaptic failure, and promotes the opening of the mPTP leading to apoptosis (Du et al, 2008) (**Fig.6**).

On the other hand, Aβ accumulation could result in cytoskeletal aberrations (Kang et al, 2011) (**Fig.6**). Aβ oligomers interact with integrins leading to improper control of focal adhesion assembly and signaling, therefore causing the dysregulation of cofilin, which is involved in the regulation of actin dynamics. The inhibition of actin dynamics is associated with increased ROS production and reduced mitochondrial potential. Moreover, cofilin in response to oxidative stress translocates to the mitochondria where it induces swelling, a drop in ΔΨm, and cytochrome *c* release promoting the opening of mPTP and apoptosis.

3.3.2 Presenilin

Presenilins 1 and 2 are multi-transmembrane proteins associated with nicastrin, APH-1, and PEN-2, that form high-molecular γ-secretase complex, and are involved in Aβ production by intramembrane cleavage of APP. *PSEN1* gene mutations are the most prevalent in FAD, but besides the generation of Aβ, little is known about its implication in mitochondrial dysfunction and oxidative damage. It has been demonstrated that PSEN1 (Ankarcrona & Hultenby, 2002) and PSEN2 are also located in mitochondria as part of the γ-secretase complex (Hansson et al, 2004). Noteworthy, presenilin mutations have been shown to sensitize cells to apoptosis by mechanisms suggested to involve impaired mitochondrial function and PSEN2/γ-secretase activity can modify ΔΨm (Behbahani et al, 2006). Moreover, PSEN2 KO mouse embryonic fibroblasts exhibit lower basal respiratory rate. On the other hand, in at least two transgenic mouse models expressing human Tau with AD mutations at *PSEN1*, $PSEN_{1M146L}$ (Schuessel et al, 2006) and $PSEN1_{A246E}$ (Strazielle et al, 2009), the existence of mitochondrial abnormalities prior to cognitive deficits has been described. Also, in the case of $PSEN1_{M146L}$ mice, it was found that the mutation increases mitochondria ROS formation and oxidative damage. Finally, it has been recently shown that presenilins and γ-secretase activities are concentrated in a specialized subcompartment of the endoplasmic reticulum (ER) that is physically and biochemically connected to mitochondria, called mitochondria-associated ER membranes (MAM) which are involved in mitochondrial function and dynamics, among others (Area-Gomez et al, 2012; Schon & Area-Gomez, 2010) . Either in presenilin KO mice or fibroblasts from FAD and SAD patients, MAM function is increased correlating with a significantly increased area of apposition between ER and mitochondria.

3.3.3 Tau

Tau is involved in the axonal transport of organelles such as mitochondria (Trinczek et al, 1999). It is known that Tau-dependent mitochondrial axonal trafficking is regulated by the activity of Glycogen synthase kinase 3 beta (Llorens-Martin et al, 2011). Hyperphosphorylated Tau may block

the transport of mitochondria leading to energy deprivation and oxidative stress at the synapse as well as to neurodegeneration (Stamer et al, 2002) (**Fig.6**). Analysis of brain proteins from *P301L* mutant human *Tau* transgenic mice revealed deregulation of mitochondrial respiratory chain complex components such as complex V and reduced complex I activity as well as an impaired mitochondrial respiration with the subsequent ROS accumulation with aging (David et al, 2005) (**Fig.5**). Accordingly, the overexpression of *P301L Tau* mutation in human neuroblastoma cells has been shown to induce substantial complex I deficit accompanied by decreased ATP levels and increased susceptibility to oxidative stress (Schulz et al, 2012). This was paralleled by pronounced changes in mitochondrial morphology, decreased fusion and fission rates accompanied by reduced expression of OPA1 and DLP1. Moreover, an abnormal interaction of hyperphosphorylated Tau and mitochondrial fission protein DLP1 has been described suggesting a relationship with mitochondrial dynamics alteration (Manczak et al, 2011) (**Fig.6**). Other researchers have found that the expression of human Tau mutations in both *Drosophila* (*R406W*) and mouse neurons (*P301L*) results in elongation of mitochondria, which is accompanied by mitochondrial dysfunction and cell cycle mediated cell death (DuBoff et al, 2012). We have previously mentioned an interaction of phospho-Tau and VDAC1 that may in turn block the mitochondrial pores leading to mitochondrial dysfunction (Manczak & Reddy, 2012) (**Fig.6**). On the other hand, increased oxidative stress has been shown to cause Tau hyperphosphorylation in a superoxide dismutase 2 knockout mouse model (Melov et al, 2007). Furthermore, the inhibition of complex I with annonacin led to a redistribution of Tau from the axons to the cell body which correlates with a retrograde transport of mitochondria and finally to cell death (Escobar-Khondiker et al, 2007). Lastly, the downregulation of the proteins involved in the axonal transport of mitochondria such as Miro and Milton in *Drosophila* has shown loss of axonal mitochondria that promotes Tau phosphorylation in Ser262 via partitioning defective-1 (*Drosophila* homolog of mammalian microtubule affinity-regulating kinase) causing late-onset neurodegeneration in the fly (Iijima-Ando et al, 2012).

3.4 Autophagy and Mitophagy failure

In AD, Aβ and Tau aggregation has been associated with mitochondrial damage, oxidative stress, and cytoskeletal alteration of neurons. Autophagy plays a fundamental role in neuronal function and is intensively involved in AD-related protein aggregation (Nixon et al, 2005). Indeed, it has been demonstrated that autophagy is the major degradational pathway following unfolded protein response activation in neuronal cells, as early event in AD brain, suggesting a connection between its activation and the observed autophagic pathology (Scheper et al, 2011). Accordingly, an accumulation of autophagic vesicles in the cortex of AD patients compared to non-demented ones has been shown (Nixon et al, 2005). Moreover, an increase of autophagic vesicles containing mitochondria in pyramidal neurons from AD patients has been found, suggesting a mitophagy alteration (Moreira et al, 2007b; Moreira et al, 2007c). According to this, PARK2, as previously

mentioned, one of the proteins involved in the target of mitochondria to be degraded by mitophagy, has been shown to be reduced in the cortex of AD brains (Rosen et al, 2010). Additionally, autophagy alterations have been described in AD brain and animal models. Beclin1, a protein that plays a key role in autophagy, has been shown to be diminished in the affected brain regions in AD patients early in the disease process (Pickford et al, 2008). In the same work, in an APP transgenic mouse model, the downregulation or overexpression of Beclin1 increased or diminished, respectively, the Aβ accumulation, extracellular Aβ deposition, and neurodegeneration, highlighting the relevance of autophagy in AD-related pathology. Moreover, a link between FAD and autophagy has been recently indicated (Lee et al, 2010), showing that autophagy requires functional, PSEN1 for lysosomal maturation and that is impaired by Alzheimer-related PSEN1 mutations. Thus, PSEN1 mutations could indirectly affect mitochondrial function by impairing its recycling by mitophagy.

On the other hand, autophagy has been proposed to play an active role in AD pathogenesis. In this regard, autophagic vesicles have been demonstrated to be an active compartment for Aβ generation and their abnormal accumulation in affected neurons of AD brain contributes to Aβ deposition (Yu et al, 2004). Additionally, PARK2-induced autophagy facilitated clearance of vesicles containing debris and defective mitochondria counteracting oxidative stress and preventing mitochondrial dysfunction (Khandelwal et al, 2011). PARK2 reverses intracellular Aβ accumulation and its negative effects on proteasome function (Rosen et al, 2010).

Other strategies for the induction of autophagy as a therapeutic strategy in AD have been tested in animal models for the disease. With this aim several molecules have been tested such as rapamycin (Caccamo et al, 2010; Spilman et al, 2010), cystatin B (Yang et al, 2011), trehalose (Schaeffer et al, 2012), *scyllo*-Inositol (Lai & McLaurin, 2012), and latrepirdine (Steele & Gandy, 2013), although effects on improving mitochondrial recycling were not studied in these works.

4. Models for the study of AD

Disease models are indispensable tools for understanding the molecular mechanisms that drive pathogenesis and enable the development of novel therapies. As primary patient cells are only available in very small quantities, AD studies typically use transgenic animals or transformed cell lines. The advantage of animal models is that they can be used to examine a disease *in vivo*, and primary animal cells are easily to isolate in large numbers for applications such as high-throughput screening. Transformed cell lines are accessible in large quantities and can be engineered to express a disease-causing gene of interest. However, the physiology of animal models and transformed cell lines is different from that of patient cells, which may partly explain why sometimes it is difficult to recapitulate the features of the disease and why many drug candidates are not effective in patients when tested in clinical trials. Therefore, developing these treatments using human models from the outset would be a distinct advantage.

4.1 Human fibroblasts

The main advantages of using skin fibroblasts as an *in vitro* model of AD are their availability and robustness. Furthermore, skin fibroblasts represent a model of primary human cells, which comprise the chronological and biological aging of the patients according to their polygenic predisposition and environmental etiopathology.

Skin fibroblasts can be easily isolated from 2 mm punch skin biopsies, a procedure which does not need stitches and has practically as few complications as a venous puncture (Auburger et al, 2012). It should be performed by a dermatologist and is not a routine measure in the management of AD patients, thus requiring written consent and ethics commission approval.

The ensuing cell culture is a mixture of primary fibroblasts and keratinocytes at the beginning of the culturing process and a pure culture of fibroblasts is only achieved in the third passage. However, the fibroblast population consists most probably of a mixture of mitotic and postmitotic fibroblast (Auburger et al, 2012), thus contributing to a heterogeneous cell population even at early passages. Furthermore, cells may be contaminated with the frequent skin microorganism Mycoplasma (Nikfarjam & Farzaneh, 2012), possibly causing deprivation of nutrients, reduced growth, inflammatory responses, and oxidative stress, which makes a periodic testing for *Mycoplasma* necessary. Cell propagation, storage of aliquots in liquid nitrogen, and transport are easy and comparable to standard cell lines, thus fibroblasts from patients with sporadic AD or familiar AD can be obtained from numerous labs and several repositories such as the Coriell Institute in New Jersey.

Since clonal selection and drift in culture are inherent features of fibroblasts, the matching of fibroblasts from a sufficient number of patients with their appropriate controls of similar age and sex is sometimes an inevitable difficulty.

In view of the slow growth of primary cells from aged individuals, it needs weeks in culture to generate sufficient material for a number of biochemical tests. After some cultivation time, primary skin fibroblasts may be similar to mouse embryonic fibroblasts (MEFs) which either transform spontaneously or reach replicative senescence, thus altering the previously established phenotypes. Therefore, as with all primary cell models, a careful documentation of culture history, number of population doublings, and senescence markers such as senescence-activated β-galactosidase (SA-β-galactosidase) staining are indispensable quality controls. Furthermore, control cells and patients fibroblast should have a similar amount of population doublings when comparing biochemical or genetic parameters. On the other hand, immortalization of fibroblasts can be regarded as an advantage since immortalized cells proliferate faster than primary cells, thus allowing a much higher cell yield, and characteristics induced by *in vitro* aging can be disregarded. A study by Sprenger et al. (2010) comparing primary and immortalized fibroblasts shows that both cell types are quite similar in the early passages regarding major cell lineage-specific characteristics but

expression changes of genes and proteins involved in transcription, cell cycle, receptor tyrosine kinase signaling cascade, and in the regulation of the cytoskeleton have been reported (Fridman & Tainsky, 2008; Sprenger et al, 2010), indicating that the use of immortalized fibroblast for studies involving these pathways must be carefully controlled. Additionally, depending on the immortalizing genes combinations used, chromosome instability and tumorigenic transformation may take place what may alter genuine properties of the cell (Garcia-Escudero et al, 2010).

Primary skin fibroblasts are a suitable extraneural model for neurodegenerative diseases because it has been described that these cells are able to reflect cumulative cell damage at the age of the patient. The can be obtained from living patients giving the possibility of benefiting the individual with the findings. Additionally, it can be reprogrammed to induced pluripotent stem cells (iPSC) and differentiated to various types of neurons as a human neuronal *in vitro* model of AD. However, it has to be kept in mind that fibroblasts are quite resistant against most stressors as well as their gene expression profile and their signaling could differ from neurons.

Althought work with human fibroblasts exhibits the disadvantages explain before, they are a powerful source for the study of AD and an excellent tool to develop a model of the pathology.

4.2 Induced pluripotent stem cells and iPSC-derived neurons

4.2.1 Induced pluripotent stem cell technology

The discovery that somatic cells could be reprogrammed to a pluripotent state has profoundly altered the landscape in which stem cell research is conducted. A revolutionary work in 2006 by Takahashi and Yamanaka demonstrated for the first time that adult differentiated cells such as fibroblasts are able to be retrodifferentiated to generate stem cells (Takahashi & Yamanaka, 2006). Four transcriptions factors, Oct4, Sox2, c-Myc, and Klf4, were enough to induce pluripotency in primary fibroblast indicating that cell programming could be reversed. Other groups have generated similarly pluripotent cells from other peripheral cells, such as blood cells (Loh et al, 2009) keratinocytes (Aasen et al, 2008), B lymphocytes (Hanna et al, 2008), neural stem cells (Kim et al, 2008a) or hepatocytes (Stadtfeld et al, 2008). It is important to keep in mind that exogenous factors, genetic background, and epigenetic of tissue origin of cells influences native pluripotency (Hanna et al, 2010). Therefore certain differences on the epigenetic landscape are expected to exist between ES and iPS cells (Bock et al, 2011; Lister et al, 2011).

Patient-specific iPSCs are well suited for generating human disease models. In theory, the limitless self-renewal and differentiation properties of iPSCs enable them to produce the large quantities of specific cell types for basic research and drug discovery. iPSC technology offers a unique tool to dissect the principles of cell fate determination during normal development and its dysregulation in disease (Stadtfeld & Hochedlinger, 2010). The abundance of studies clearly shows that iPSCs are a reliable tool for disease modelling. One advantage of using iPSCs derived from

patients with highly penetrant mutations is that these cells are likely to recapitulate disease phenotypes; indeed, the vast majority of disease models generated so far are from genetic mutations that cause disease in a Mendelian manner. However, most diseases are either sporadic or the result of polymorphisms at multiple loci. The alternative approach for modelling diseases using iPSCs from patients with a risk allele or a sporadic disease has been extremely challenging. Unlike conventional models, a great advantage of iPSCs is that they are derived from individual patients with observable phenotypes, even when there are multiple unknown contributing genetic mutations.

The study of human brain disorderes is hampered by obtaining live material relevant for the disease. The ability to generate neural cultures from post-mortem human brains depends greatly on the quality of the post-mortem brain tissue (Verwer et al, 2002) but in most cases is extremely difficult. The generation of human iPS cells is one way to surmount these limitations. Protocols have been developed to differentiate iPS cells *in vitro* into distinct neuronal types allowing researchers to examine disease onset and progression directly in different models of neurological disorders (Liu et al, 2012; Sandoe & Eggan, 2013).

4.2.2 iPSC differentiation into neural subtypes relevant to AD

Several groups have succeeded in creating functional neurons from FAD and SAD iPSC that recapitulates the features of AD pathology (**Table 1**). The base protocols used for these differentiations include dual-SMAD inhibition in a monolayer culture (Chambers et al, 2009), an embryoid body or aggregate method (Eiraku et al, 2008) or more recently, the formation of cerebral organoids (Lancaster et al, 2013).

Both glutamatergic and GABAergic neuronal fates have been implicated in different aspects of AD pathogenesis. Through modulation of patterning pathways, differentiation can be directed to generate cultures of more dorsal, glutamatergic fates (Vazin et al, 2014; Zeng et al, 2010) or else of more ventral, GABAergic fates (Cunningham et al, 2014; Nicholas et al, 2013). It was recently shown that iPSC-derived GABAergic neurons are less susceptible to Aβ induced cell death (Vazin et al, 2014), thus demonstrating the differential phenotypes that can be understood by specifying cell fates.

The loss of basal forebrain cholinergic neurons is associated with deficits in spatial learning and memory in AD pathology. Since cholinergic neurons are among the first to degenerate in AD, there has been much interest in directing differentiation to this fate. Cholinergic neurons can be generated from human ES cells by sequential treatment with growth factors that are found in the forebrain during different developmental stages (Bissonnette et al, 2011). Alternatively, cholinergic neurons can be generated by the overexpression of transcription factors. Expression of Lhx8 and Gbx1 is necessary and sufficient to generate basal forebrain cholinergic neurons (Bissonnette et al, 2011). Production of cholinergic neurons by nucleofection with Lhx8/Gbx1-IRES-GFP allows for additional purification of cell populations by fluorescence-activated cell sorting. iPSC-derived basal

forebrain cholinergic neurons originated from sporadic AD patients of the apoE3/E4 background using this method displayed typical AD biochemical features including an increase in the Aβ42 to Aβ40 ratio and an augmented vulnerability to glutamate-mediated cell death (Duan et al, 2014).

AD lines		Description
Spordic		Oligomerization of Aβ, endoplasmic reticulum and oxidative stress (Kondo et al, 2013)
		Increased secretion of Aβ40, phosphorylation of Tau, activation of GSK3β, large and very early endosomes (Israel et al, 2012)
		Effect of BDNF on Aβ secretion is SORL1 gene-dependent (Young et al, 2015)
APP	Dominant mutation	Increased secretion of Aβ40, phosphorylation of Tau, activation of GSK3β, large and very early endosomes (Israel et al, 2012)
		Abundance of intracellular Aβ oligomers, increased Aβ42/Aβ40 ratio (Kondo et al, 2013)
		Increased Aβ42/Aβ40 ratio (Mertens et al, 2013)
		Increased β-secretase cleavage of APP, altered γ-secretase cleavage, increased Aβ42, increased phospho-Tau (Muratore et al, 2014)
		Elevation of intracellular tau protein levels (Moore et al, 2015)
	Rec. mut	Decreased secretion of Aβ40, increased oligomerization of Aβ, increased stress response (Kondo et al, 2013)
PSEN1/PSEN2	**$PSEN1_{A79V}$**	Increased Aβ42/Aβ40 ratio (Mertens et al, 2013)
	$PSEN1_{L166P}$	Increase Aβ42/40 ratio, selective decrease in Aβ40 production (Koch et al, 2012)
	$PSEN1_{A246E}$ **$PSEN1_{M146L}$**	Increased Aβ42/Aβ40 ratio (Mahairaki et al, 2014; Sproul et al, 2014; Yagi et al, 2011)
		14 genes differentially regulated in FAD lines. Five of these genes were differentially expressed in brains of late and intermediate AD patients (Sproul et al, 2014)
	$PSEN2_{N141}$	Increase in Aβ42 secretion (Yagi et al, 2011)

Table 1. Summary of published works using human iPSC models of AD.

Objectives

Mitochondrial dysfunction and oxidative damage play a critical role in the pathogenesis of Alzheimer disease. Accumulation of oxidatively damaged proteins and organelles due to inefficient degradation could exacerbate the pathophysiology of the cell in this disorder. It is well known the fundamental function of autophagy in AD related proteopathy. Moreover, autophagy alterations have been described in Alzheimer disease mouse models and patients' samples.

By generating different human cellular models of Alzheimer disease we propose the following objectives:

1. Study of APP and Tau contribution to autophagy and mitochondrial recycling process.

2. Study of autophagy and mitophagy system in the early onset familial form of Alzheimer disease through:

    - a cell model of skin fibroblasts derived from FAD patients.

    - validation of the anomalies found in fibroblasts in a neural model derived from iPSC from FAD patients.

3. Study of mitochondrial function, autophagy and mitochondrial recycling process in the late onset sporadic form of Alzheimer disease through:

    - a cell model of skin fibroblasts derived from SAD patients.

    - validation of the anomalies found in fibroblasts in brain samples from AD patients.

4. Study of autophagy enhancement as a therapeutic strategy in SAD patients.

Materials and Methods

1. Materials

1.2 Primary cells

Primary skin fibroblasts from AD patients and their correspondent healthy sex and age-matched samples were obtained from Coriell Institute for Medical Research (New Jersey, USA). iPSC lines were generated by Andrew Sproul from New York Stem Cell Foundation from fibroblast cell lines AG06842 and AG07671. See **Table 2** for details about age, sex and stage of the disease of these cells.

1.3 Brain tissues

Hippocampal brain samples from SAD patients and control subjects were obtained from Banco de Tejidos (Fundación CIEN, Instituto de Salud Carlos III, Madrid, Spain). On the basis of quantitative pathological features, the SAD brain specimens were classified (**Table 3**) as coming from SAD patients at Braak stages II and III (early AD) (n=5), Braak stage V (n=5) and Braak VI (n=6) (severe AD), and control subjects (n=6). Written informed consent was obtained from all the patients.

Cell Line	Age/Gender	Clinical Diagnosis	ApoE4
AG11362	63/F	Non-affected	No
AG05813	67/F	Non-affected	No
AG07803	66/M	Non-affected	No
AG07310	60/F	Non-affected	No
AG11020	79/F	Non-affected	No
AG04148	56/M	Non-affected	No
AG12988	56/F	Non-affected	No
AG05809	63/F	Moderate dementia	No
AG06263	67/F	Moderate dementia	No
AG06262	66/M	Moderate dementia	No
AG06869	60/F	Moderate dementia	No
AG05810	79/F	Severe dementia	Yes
AG06840	56/M	Moderate dementia FAD1 PSEN A246E	No
AG06848	56/F	Severe dementia FAD1 PSEN A246E	No
AG06842	75/M	Non-affected PSEN WT	Yes
AG07671	44/M	Moderate dementia FAD1 PSEN A246E	Yes

Table 2. Brain samples.

Patient	Age/Gender	Clinical Diagnosis
BCM12	56/M	Non-affected
BCM15	49/M	Non-affected
BCPA65	41/M	Non-affected
BCM67	84/M	Non-affected
BCM81	14/M	Non-affected
BCPA177	58/F	Non-affected
BCM137	78/M	Non-affected
BCPA364	43/M	Non-affected
BCPA14	80/M	Braak II
BCPA8	87/M	Braak II
BCPA19	85/F	Braak II
BCPA158	84/M	Braak II
BCPA268	82/F	Braak II
BCPA25	85/M	Braak III
BCPA206	unknown/F	Braak III
BCPA411	85/M	Braak III
BCPA279	98/F	Braak IV
BCPA18	87/F	Braak V
BCPA41	73/F	Braak V
BCPA73	88/F	Braak V
BCPA139	82/F	Braak V
BCPA202	87/M	Braak V
BCPA221	81/M	Braak V
BCPA30	68/M	Braak VI
BCPA37	76/M	Braak VI
BCPS143	88/M	Braak VI
BCPA151	86/F	Braak VI
BCPA184	81/F	Braak VI

Table 3. Brain samples.

Primary antibody	Protein/Epitope	Species	Provider	WB dilution	ICC dilution
Anti-APP	Amyloid precursor protein	Rabbit	Sigma	1/1000	
Anti-BECN1	Beclin N-terminus	Rabbit	Santa Cruz	1/1000	
Anti-Calbindin	Calcium-binding proteins	Rabbit	Swant		1/1000
Anti-COX4	Mitochondrial Complex IV subunit I	Mouse	Invitrogen	1/1000	1/500
Anti-CTSB	Lysosomal cysteine protease Cathepsin B	Rabbit	Chemicon	1/1000	
Anti-DLP1	Dynamin-like protein 1	Mouse	BD Bioscience	1/1000	
Anti-GAPDH	Glyceraldehyde 3-phosphate dehydrogenase	Rabbit	Abcam	1/5000	
Anti-GFP	Green fluorescent protein	Mouse	Santa Cruz	1/5000	
Anti-LAMP1	Lysosomal-associated membrane proteins -1	Mouse	BD Bioscience	1/1000	
Anti-LC3	Microtubule-associated protein 1 light chain 3	Rabbit	Sigma	1/1500	
Anti-LC3	Microtubule-associated protein 1 light chain 3	Mouse	MBL		1/500
Anti-MAP2	Microtubule-associated protein 2	Mouse	Sigma		1/500
Anti-NANOG	Transcription factor NANOG	Rabbit	Cell Signaling Tech		1/100
Anti-NeuN	Neuronal specific nuclear protein	Rabbit	Millipore		1/200
Anti-OCT4	Transcription factor OCT4	Rabbit	Stemgent		1/250
Anti-Parkin	RBR E3 ubiquitin protein ligase protein	Mouse	Santa Cruz	1/500	1/500
Anti-PHF1	Tau phosphorylated in serines S396 and S404	Mouse	Our lab	1/100	
Anti-PINK1	PTEN-induced putative kinase 1	Rabbit	Novus	1/1000	1/200
Anti-p62	p62 lck ligand cytoplasmic protein	Mouse	BD Bioscience	1/2000	
Anti-SCaMC-1	Short calcium-binding mitochondrial carrier 1	Mouse	Dra. Araceli del Arco		1/500
Anti-SSEA4	Stage-specific embryonic antigen 4	Mouse	Abcam		1/250
Anti-SOX2	Transcription factor SOX2	Rabbit	Stemgent		1/250
Anti-Tau1	Tau protein (central region)	Mouse	Millipore		1/1000
Anti-Tau5	Tau protein (central region)	Mouse	Calbiochem	1/1000	
Anti-TRA1-60	TRA antigen 60	Mouse	Millipore		1/250
Anti-TRA1-81	TRA antigen 81		Millipore		1/250
Anti-TOM20	Full-lenght TOM20 protein	Rabbit	Santa Cruz	1/2000	1/500
Anti-Ubiquitin	Free and conjugated ubiquitin	Rabbit	Dako	1/1000	
Anti-vGlut1	Vesicular glutamate transporter 1	Guinea pig	Millipore		1/500
Anti-514	High molecular weight MAP2 isoforms	Rabbit	Our lab		1/400

Table 4. Antibodies used in this work.

1.1 Antibodies

The primary antibodies used in this work for Western Blot and immunostaining are listed in the following **Table 4**.

For Western Blot analysis the following HRP (horseradish peroxidase) conjugated secondary antibodies were used: anti-mouse, anti- rabbit (DAKO) all produced in goat at 1/1000 dilution. For immunostaining assays the following Alexa secondary conjugated antibodies were used: anti-mouse, anti- rabbit and anti-goat Alexa 488/555/647 (Invitrogen) all produced in donkey at 1/1000 dilution. To nucleic acid staining, 4',6-Diamidino-2-Phenylindole, Dihydrochloride (DAPI) was used.

2. Methods

2.1 Cell culture methods

2.1.1 Fibroblasts culture conditions

Human fibroblasts were cultured in Dulbecco´s modified Eagle´s medium (DMEM) supplemented with 10% (v/v) heat-inactivated Fetal Bovine Serum (FBS), 2 mM glutamine, 10 U/ml penicillin, 10 µg/ml streptomycin, in 5% CO_2 in a humid incubator at 37ºC. The use of fibroblasts has been restricted to a maximum of 10 cell passages to avoid replicative senescence and cultures were always kept below confluence.

2.1.2 iPSC culture conditions

Undifferentiated iPSCs were kept onto Cultrex (Trevigen, 3432-005-01)-coated dishes and grown in feeder-free maintenance basal medium for hESCs and hiPSCs mTesR1 (StemCell Technologies, 05851) supplemented with mTeSR1 5X Supplement (StemCell Technologies, 05852) contained penicillin-streptomycin (100U/mL-0.1mg/mL) in 5% CO_2 in a humid incubator at 37ºC.

2.1.3 Retroviral reprogramming

Fibroblasts were plated at $3x10^4$– $5x10^4$ cells in a single well of a 6-well plate or multiple wells of a 12- well-plate, which was infected the 6-18 hours later with four retroviruses prepared for Oct4, KLF4, Sox2, and c-Myc by the Harvard Gene Therapy Core (Sproul et al, 2014). Infected fibroblasts were split 7-14 days post-infection onto MEFs (γ-irradiated mouse embryonic fibroblasts) and concomitantly treated with three chemical compounds to enhance reprogramming: SB431512 (2 µM), Thiazovivan (0.5 µM), and PD0325901 (0.5 µM) (Lin et al, 2009). iPSC colonies were initially selected by morphology, passaged several times to remove untransformed cells, and expanded before characterization.

2.1.4 Monolayer neuronal cortical differentiation

iPSC colonies were dissociated into single cells by washing with PBS and adding 1 ml Accutase (Life Technologies, A1110501) and then plated onto Cultrex-coated dishes in mTesR1 medium containing 10 µM ROCK inhibitor (Y-27632, Stemgent, 04-0012). Cells were plated at a density of $3x10^5$ cells per 6 well-plate and allowed to recover for 3 days to allow near confluency. Cells were neuronally differentiated with dual-smad inhibition from days 0-9 in custom TesR1 (5x supplement W/o 5 factors mTesR1 and penicillin-streptomycin (100 U/mL-0.1 mg/mL)) using 10 µM SB431542 (Stemgent, 04-0010) and 250 nM LDN193189 (Stemgent, 04-0074). Cell were split with Accutase (Life Technologies, A1110501) on day 10 and plated at a density of $2x10^5$ cells per 6 well-plate on 100µg/mL Poly-L-Ornithine (Sigma-Aldrich, P3655)/ 3 µg/mL laminin plates. Monolayer neuronal differentiation was carried out in Neurobasal (Life Technologies, 21103049) + B27 supplement (Life Technologies, 17504044) and cells were fed every 2 to 3 days until analyzed. At day 30, neuronal differentiation media was supplemented with 20 ng/ml BDNF (R&D system, 2837).

2.1.5 Lentivirus production

Pseudotyped lentivectors were produced using reagents and protocols from Didier Trono with the following modifications: 293T cells were transiently co-transfected with 5 µg of the corresponding lentivector plasmid, 5 µg of the packaging plasmid pCMVdR8.74 (Addgene plasmid 22036) and 2 µg of the VSV G envelope protein plasmid pMD2G (Addgene plasmid 12259) using Lipofectamine and Plus reagents following instructions of the supplier (18324 and 11514, respectively, Life Techonologies). The lentivector used encodes wild type PARK2, and was a gift from Dr. Andrew B. West (University of Alabama) (da Costa et al, 2009).

2.2 Biochemistry methods

2.2.1 Western Blot analysis

The cells and tissue samples were homogenized in lysis buffer (50 mM pH 7.5 HCl-Tris, 300 mM NaCl, 0.5% SDS and 1% Triton X-100) and incubated 15 min at 95ºC. Protein concentration of the extracts was measured using the Dc protein assay kit (500-0111, Bio-Rad). Equal amounts of total protein extract from healthy and SAD cells were resolved by SDS-PAGE and then transferred to nitrocellulose membranes (G9917809, Amersham, Germany). Western blot and immunoreactive proteins were developed using an enhanced chemiluminescence detection kit (NEL105001EA, Perkin Elmer) following instructions of the supplier. Quantification was performed by densitometry of the obtained bands in each lane with respect to the correspondent housekeeping protein in each experiment (Quantity One software, Bio-Rad). When several paired samples were compared very

data was normalized with respect to the values obtained from each correspondent age-matched healthy sample.

2.2.2 Protein oxidation detection

OxyBlot Protein Oxidation Detection Kit (S7150, Millipore) was used to detect oxidized proteins in cell extracts using the supplier guidelines. Briefly stated, carbonyl groups of cell extract proteins were treated with 2,4-dinitrophenylhydrazine. Equal amounts of total protein extract (20 µg) were loaded and Western blot detection was performed as previously described. Quantification was done by densitometry of the obtained bands in each lane (Quantity One software, Bio-Rad) with respect to GAPDH signal and every result was normalized with respect to the values obtained from each correspondent age-matched healthy sample.

2.2.3 Ubiquitination levels detection

A conventional Western blot was performed as described above by using the primary antibody against ubiquitin motive (Z0458, Dako). Quantification was performed by densitometry of each lane (Quantity One software, Bio-Rad) with respect to the correspondent GADPH signal and every result was normalized with respect to the correspondent age-matched healthy sample.

2.2.4 Mitochondrial isolation

The Mitochondria Isolation Kit for Mammalian Cells (89874, Pierce Protein Biology Products) was used to isolate intact mitochondria from cultured cells using the manufacturer´s protocol.

2.2.5 Phos-tag assay

Cells were treated with 20 µM CCCP for 1 h and then lysed in Western blot lysis buffer. We use 7.5% polyacrylamide gels containing 50 µM Phos-tag acrylamide AAL-107 (Wako chemicals) and 100 µM $MnCl_2$. After electrophoresis, gels were washed twice with transfer buffer containing 0.01% SDS and 10 mM EDTA for 20 min, and then replaced with transfer buffer containing 0.01% SDS for 10 min. Proteins were transferred to PVDF membranes and analyzed by conventional immunoblotting. For dephosphorylation, extracts treated with CCCP were incubated for 1 h with 800 U of lambda protein phosphatase (λPP, Sigma, St. Louis Missouri) following the guidelines of the supplier.

2.3 Molecular biology methods

2.3.1 Pluripotency and differentiation score analysis

To ensure that non-reprogrammed or partially reprogrammed fibroblast lines were distinguished from successfully reprogrammed iPSC lines, gene expression signatures were used to

measure the pluripotency and differentiation score. Assays were carried out by the NanoString protocol. Samples of 10^5cells were lysed and RNA hybridized to custom specific molecularly-barcoded reporter and capture probes before processing on the nCounter Prep-station (NanoString). Processed samples were then loaded into an nCounter Digital Analyzer (NanoString) and scanned at high resolution (about 800 frames/sample). nCounter Analyzer data were analyzed on NanoString's nSolver software, normalizing counts to three housekeeping genes, ACTB, POLR2A, and ALAS1. Probe sets include a Pluripotency Codeset of 25 genes indicative of pluripotency and a Lineage Codeset including multiple targets indicative of separate germ layers previously described (Kahler et al, 2013).

2.3.2 Quantitative real-time PCR assays

Frozen brain tissue was homogenized using a TissueLyser (Retsch MM300, Qiagen, GmbH, Hilden, Germany) run at 30 Hz for 5 min with 5 mm stainless steel beads (69989, Qiagen) in 700 µl of QIAzol Lysis Reagent (79306, Qiagen). RNA was extracted using miRNeasy Mini Kit (217004, Qiagen) with RNase-Free DNase Set (79254, Qiagen) following provider's guidelines. RNA integrity number (RIN) of each sample was calculated using the Agilent 2100 Bioanalyzer system (Agilent Technologies) and only RNAs with RIN above 5 were used for RT-qPCR. Retrotranscription was performed with Transcriptor First Strand cDNA Synthesis Kit (04379012001, Roche) using 20 ng/µl of RNA with random primers. Quantitative PCR was performed in a thermocycler AB7.900HT (Applied Biosystems) using the following conditions: 50ºC for 2 min, 95ºC for 10 min and 40 cycles of 95ºC for 15 sec. and 60ºC for 1 min. The oligos used for the detection were PARK2-F: CCCTGGGACTAGTGCAGAAT, PARK2-R: TGCGATCAGGTGCAAAGCTA, PINK1-F: CATGCCTACATTGCCCCAGA, PINK1-R: GAACCTGCCGAGATGTTCCA, TOMM20-F: GCTGGGCTTTCCAAGTTACC, TOMM20-R: AGTAACTGCTGTGGCTGTCC, MTRNR2-F: CGATGGTGCAGCCGCTATTA, and MTRNR2-R: ATCATTTACGGGGGAAGGCG. Genes expression were normalized to GAPDH expression using TaqMan primer human GAPDH (Hs99999905_m1, Applied Biosystems).

2.3.3 Microarray analysis

The expression profiling by array (Affymetrix Human Gene 1.0 ST Array) of *PARK2*, *PINK1* and *TOMM20* of human brain samples classified into healthy (n=47) vs AD (n=32) was retrieved from the Hisayama study (Hokama et al, 2014). Differences in *PARK2*, *PINK1* and *TOMM20* expression between healthy and AD were calculated using Student's T test.

2.4 Functional study methods

2.4.1 MTT assay

Cells were grown in 96-well plates and treated as indicated. Metabolic status was determined by 200 µg/ml MTT (3-[4,5-dimethylthiazo-2-yl]-2,5-diphenyltetrazolium bromide) (Sigma, M2128) as previously described (Mosmann, 1983).

2.4.2 Mitochondrial dynamics study

Cells were infected at an approximate MOI: 5-10 with a lentivector encoding DsRed2-Mito construct obtained from Clontech (632421) kindly provided by Dr. Ismael Santa-María. Cells were treated with CCCP (20 µM, Sigma, St. Louis Missouri) for 6 h and, in the reversible condition, CCCP was removed after 1 h and the medium was replaced for DMEM 10% FCS. After the treatments cells were fixed with 4% PFA and mitochondrial pattern was observed with a Radiance 2000 confocal system (Bio-Rad) coupled to an Axiovert S100 TV inverted microscope (Zeiss). 10 randomly chosen fields containing between 10 and 15 cells were used to quantify the pattern of mitochondria distinguishing between completely filamentous (long and spaghetti-like shape), fragmentated (completely punctated) and intermediate pattern (when both filamentous and punctated mitochondria were found).

2.4.3 Mitochondrial potential measurement

Cells were treated with 20 µM carbonyl cyanide m-chlorophenylhydrazone (CCCP; C2759, Sigma) for 7 h and, in the reversible condition, CCCP was removed and the medium was replaced for DMEM 10% FBS during the last 60 min. Then, fibroblasts were incubated with 50 nM DiOC6(3) (D273, Molecular Probes) for 30 min at 37 ºC and analyzed by flow cytometry (FACSCalibur, BD Biosciences, San Jose, CA). Mitochondrial membrane potential for each condition was represented as the percentage of the fluorescence intensity with respect to fluorescence intensity exhibited when these cells remained untreated.

2.4.4 ATP quantification

ATP was quantified using ATP determination kit (Invitrogen). After correspondent treatments, cell extracts were prepared in PBS 0.5% triton X-100 and, following the manufacturer's instructions, ATP content was determined by luminiscence using a FLUOstar OPTIMA Plate Reader (BMG Labtech) at 28ºC, using Costar 96-well black plates (Fisher Scientific). As a control we used Oligomycin 10 µM for 1 h (O4876, Sigma).

2.4.5 Autophagy flux study

Fibroblasts and iPSC-derived neurons were treated with CCCP (20 µM) for 24h followed by an additional treatment of PBS or NH_4Cl (15 mM) for 6h in the presence of CCCP. After the treatment, cells were lysed in Western blot buffer and immunodetection of autophagy involved proteins was performed as described in Methods 2.2.1. Quantification of autophagic synthesis was represented as the ratio between the values of the cells trated with CCCP and NH_4Cl with respect to the condition without CCCP but maintaining NH_4Cl treatmnt. Quantification of autophagic degradation ratio was obtained by the relation between the values of the cells treated with CCCP and NH_4Cl and the ones without NH_4Cl but maintaining CCCP treatment according to autophagy standard guidelines (Klionsky et al, 2016).

2.4.6 Lysosomal function study

Cells were treated with 100 nM bafilomycin A1 (B1793, Sigma) for 2 h or remain untreated. After that, cells were collected and treated with 500 nM LysoTracker Red DND-99 (L-7528, Molecular Probes, Life Technologies) for 20 min. Then, cells were analyzed by flow cytometry (FACSCalibur, BD Biosciences, San Jose, CA). Relative LysoTracker level represents the ratio of the FL-2 fluorescence intensity of the untreated condition and the bafilomycin treated one.

2.4.7 Cathepsin assay (Magic Red)

Fibroblasts were plated to chambered coverglasses and imaged the following day on FRET in vivo Imaging System (Zeiss, Oberkochen, Germany) coupled to an Axiovert200 microscope (Zeiss). At the start of imaging, Magic Red reagent (937, Immunochemistry Technologies) was diluted 1:365 into PBS, and then this solution was added at a 1:10 dilution into the cell culture media. Images were acquired using a 20X Plan-Apochromat objective (420650-9901-000, Zeiss); numerical aperture of 0.6, at 4 min intervals for a total of 32 min. Image analysis was performed using ImageJ software (Bethesda, MD). Images were thresholded to include only the lysosomal compartment, using the same numerical threshold for all images across a single experiment. The total fluorescence above threshold was normalized to the total area of the lysosomal compartment, measured as the area above threshold at t = 32 min. Graph represents means and standard deviation of normalized fluorescence intensities plotted over time obtained from three Alzheimer and healthy couples.

2.5 Immunochemistry methods

2.5.1 Immunocytochemistry

Fibroblasts and differentiated neurons were grown on sterile glass coverslips, treated as described for each experiment, followed by washing with PBS and fixing with 4% paraformaldehyde in PBS for 30 min or 10 min for fibroblasts or neurons respectively at room temperature. After

blocking with PBS containing 1% BSA, permeabilizing with 0.1% Triton X-100 and Glycine 1 M for 30 minutes, cells were washed with PBS and stained by indirect immunofluorescence using the antibodies described before. When indicated, phalloidin (A-12379, Life Techonolgies) was added at 1:200 during the second antibody incubation. Samples were mounted with Prolong Gold Antifade (P-36930, Life Technologies) and randomly chosen field images were obtained in an Invert Confocal LSM510 (Zeiss, Oberkochen, Germany) fluorescence microscope. iPSC colonies were fixed with 4% for 10 minutes and blocked with blocking buffer (PBS with 0.25% TritonX-100, 2% bovine serum albumin, and 1% sodium azide) for 30 minutes. Cells were then stained with primary antibody diluted according to manufacturer recommendation in blocking buffer overnight at 4°C. Cells were washed with 0.1% PBS and stained with secondary antibody (1:400 in blocking buffer) for two hours at room temperature. Cells were washed again with 0.1% PBS and images were taken on an Olympus IX71 inverted microscope.

2.5.2 Mitochondrial content analysis

Mitochondrial content was measured by ImageJ macro designed by Ruben K. Dagda at the University of Pittsburgh (Dagda et al, 2009). The macro allows to threshold immunostained mitochondria in cells labeled with a mitochondrial antibody or transiently expressing mitochondrially targeted GFP. This macro displays measurements of several mitochondrial parameters such as mitochondrial count, total mitochondrial area or mitochondrial perimeter. Briefly, the macro splits the channels and the image with mitochondria is automatically thresholded. The next step of the macro consists in analyzing the different mitochondrial parameters drawing individual outlines for each mitochondrion. Then, the program displays a panel with the parameters measured. In our case, we used the total area of all mitochondria measured.

2.5.3 Autophagolysosomes quantification

Fibroblasts were transfected with mRFP-GFP tandem fluorescent-tagged LC3 plasmid (Kimura et al, 2007) using Polyethylenimine (PEI; 408727, Sigma). After 24 h, cells were fixed and processed for analysis in an Invert Confocal LSM510 (Zeiss, Oberkochen, Germany) fluorescence microscope. Quantification of only RFP-positive dots per cell was performed with ImageJ software (Bethesda, MD).

2.5.4 Colocalization assay

Colocalization analysis was performed with ImageJ software (Bethesda, MD) and every cell was manually delimited according to phalloidin staining. The background of different channels was edited with Subtract Background tool with a rolling ball radius of 30 pixels; and by a threshold intensity, binary images were obtained. The logical operation AND of the Image Calculator tool was used to generate an image harboring only overlapping structures of both channels. Colocalization

measurement was obtained by quantifying the area occupied by the overlapping elements per cell. At least 200 cells were measured for each cell line.

2.6 Statistical analysis

When paired samples were used, values represented in the graphs were obtained by normalizing every AD sample data with its correspondent age-matched healthy sample. Randomly chosen AD-healthy couples were used for each experiment without any specific exclusion criteria. Graphs represent means and standard deviations of the values obtained from experimental triplicates or from at least three SAD-healthy couples. Statistical comparison of the data sets was performed by the Student's t test. Two-way ANOVA test was performed to examine the differences between experimental factors and their interaction. A post hoc Bonferroni test was used when more than two experimental groups were compared. When the distribution of the data was not normal a nonparametric Mann–Whitney U test was used. The differences are given with their corresponding statistical significance or *p* value, which is the probability that the difference occurred merely by chance under the null hypothesis.

Results

1. Mitophagy analysis in a human cellular model of Alzheimer disease by the overexpression of *Tau* and *APP*

Accumulation of Aβ peptide and hyperphosphorylated Tau protein are two major pathological hallmarks of AD. It is well known that the autophagy is the main degradational pathway after activation of the unfolded protein response, as early event in affected brain (Nixon et al, 2005; Scheper et al, 2011). Several studies have demonstrated that altered processing and impaired degradation by the lysosomal system are implicated in the buildup of Tau neurofibrillary tangles and Aβ deposition in AD (Funderburk et al, 2010). However, the precise role of Aβ and Tau in autophagy deregulation still remains unclear (Yoon, 2016). Mitochondrial damage has been related to Aβ or Tau pathology. The contribution of these factors to mitochondrial dysfunction has been well analyzed (Garcia-Escudero et al, 2013).

According to these previous works, the first approach of this thesis consisted in the study of autophagy-mitophagy process under the presence of APP and Tau proteins. To carry out this work, we generated a cellular model of AD by the overexpression of wild-type (WT) human APP by lentiviral transduction in a human primary cell line of skin fibroblasts obtained from Coriell Institute. APP is ubiquitously expressed; therefore, all the cells of an organism may be susceptible to Aβ pathology. As Tau is mainly expressed in neurons, we next studied the effect of the overexpression of Tau in the observed pathology. With this aim we used a lentiviral construct encoding the longest WT isoform of Tau in human brain harbouring four repeats and two N-terminal inserts followed by GFP (green fluorescent protein) linked by an IRES.

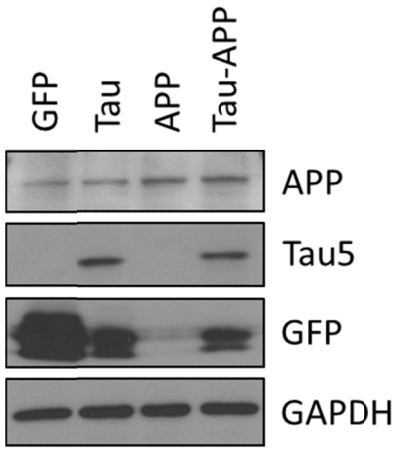

Figure 7. Validation of APP and Tau expression. Representative Western blot of APP, Tau and GFP after the overexpression of WT *APP* and WT *Tau* and *GFP* by lentiviral transduction in a human primary cell line of skin fibroblasts.

First of all, we examined by Western blot the expression of APP and Tau (also by the GFP reporter) (Fig.7). Moreover, the expression analysis of these proteins was carried out in each independent experiment previous to the study of the proteins involved in the recycling machinery. As a control we used a lentivirus encoding GFP to ensure that the observed effect is due to APP and Tau and not the effect of protein overexpression.

1.1 Response of mitochondrial recycling machinery in human fibroblasts after the overexpression of *APP*

APP is the precursor of Aβ whose accumulation is one of the most important features of AD. APP is a protein expressed in different organs and tissues. Although fibroblasts revealed low levels of APP expression we wanted to evaluate the effect of *APP* overexpression over autophagy and, more specifically, over mitophagy.

1.1.1 *APP* overexpression increased autophagy degradation phase

To study the autophagy process, cells were infected with a lentivector encoding *APP* and then treated for 24h with the mitochondrial respiratory chain uncoupler carbonyl cyanide m-chlorophenylhydrazone (CCCP), which triggers loss of mitochondrial membrane potential. This was followed by an additional treatment of NH_4Cl for 6h in the presence of CCCP to block the degradation phase of autophagy. APP-expressing cells showed a decreased amount of autophagic vesicles (AV) revealed by the lower levels of LC3II protein as well as levels of LC3II/LC3I ratio under basal conditions (Fig. 8A-B). These results were accompanied by the reduced synthesis of AV besides the significant increase in their degradation (Fig. 8C-D). This may explain the diminished AV content observed. The proper function of lysosomal system is essential for degrading proteins, organelles and large protein aggregates or inclusions by the autophagic pathway. Therefore, we examined levels of lysosomal-associated membrane protein 1 (LAMP1), which was markedly enhanced in APP-

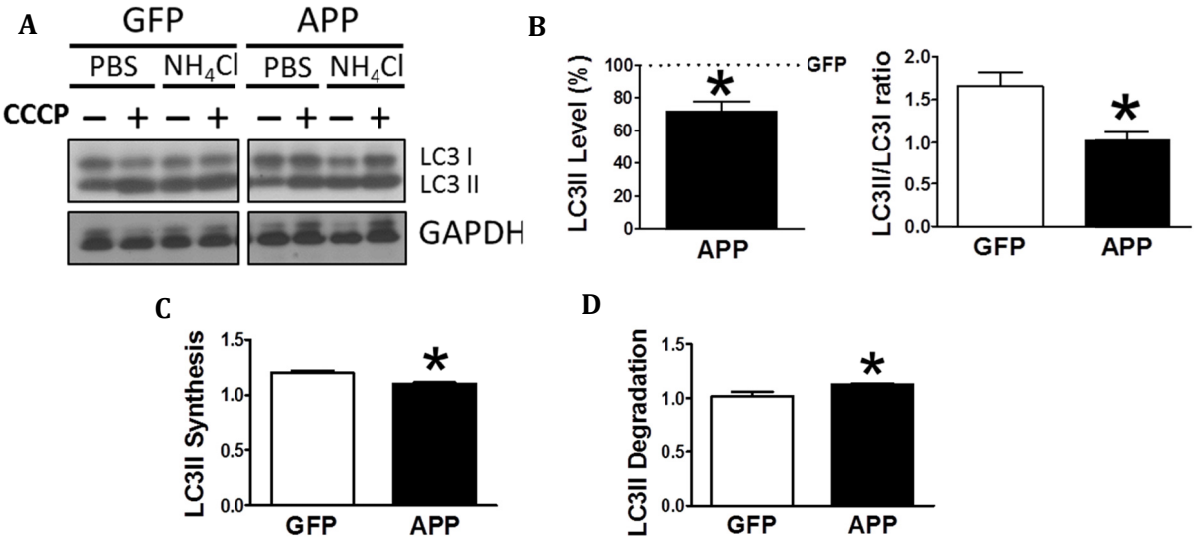

Figure 8. *APP* overexpression induces clearance of autophagic vesicles by increasing their degradation. **A.** Representative Western blot of LC3 expression for the study of autophagy flux as explained in Methods: 2.4.5 in fibroblasts overexpressing *GFP* and *APP*. **B.** Quantification of LC3II levels and LC3II/LC3I ratio in APP-expressing cells with respect to the controls under basal conditions. **C.** Quantification of LC3II synthesis ratio as described in Methods 2.4.5. **D.** Quantification of LC3II degradation ratio as described in Methods 2.4.5. (n=3 independent experiments; *$p<0.05$).

expressing cells (Fig. 9A-B). It is well known that the lysosomal cysteine protease Cathepsin B has been associated with amyloid plaques and increased Aβ production (Cataldo et al, 1997; Cataldo & Nixon, 1990) thus, levels of the active form of this protease were studied and revealed a considerable increase in APP-expressing cells (Fig. 9A-C). These results together suggested an enhanced activity of the autophagy degradation phase correlating with a higher lysosomal content causing reduced AV levels.

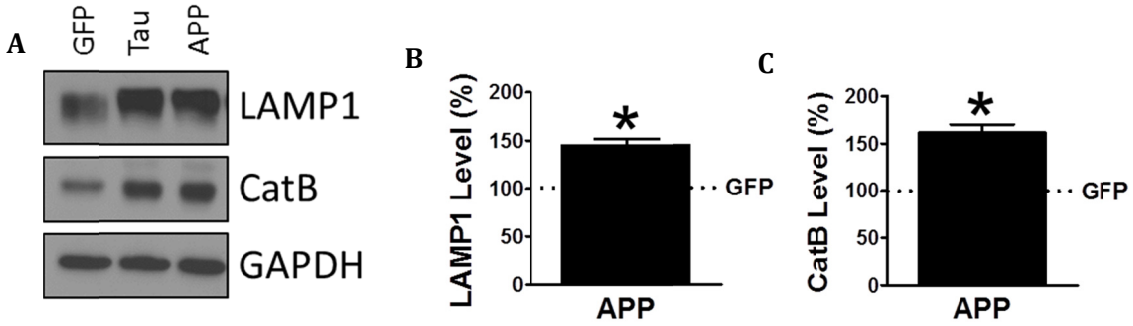

Figure 9. Enhanced lysosomal activity by *APP* overexpression. A. Representative Western blot of LAMP1 and Cathepsin B protein levels in fibroblasts overexpressing *GFP*, *Tau* or *APP* . **B.** Quantification of LAMP1 protein levels under APP overexpression with respect to GFP. **C.** Quantification of Cathepsin B protein levels under similar conditions. (n=3 independent experiments; *$p<0.05$).

1.1.2 Imbalance of mitophagy-related proteins after *APP* overexpression

The removal of damaged mitochondria is critical for maintaining proper cellular functions (Ding & Yin, 2012). PARK2 is an ubiquitin ligase involved in the labeling of defective

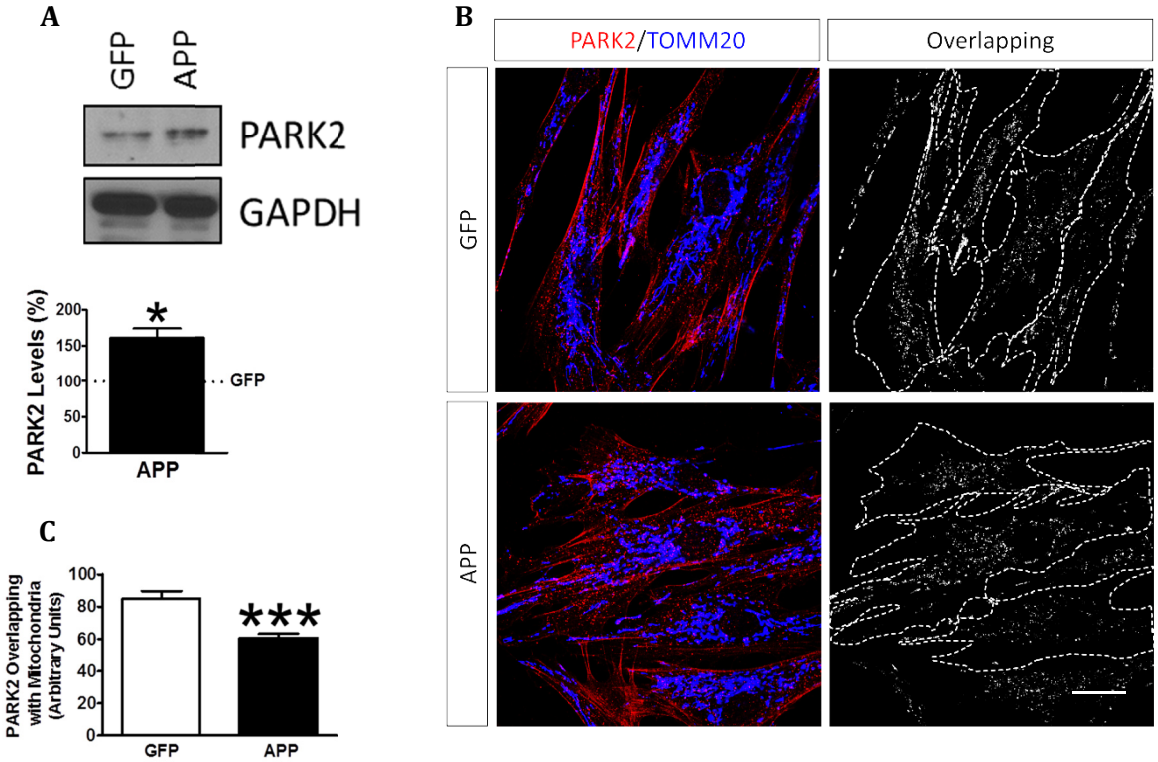

Figure 10. Imbalance pattern of PARK2 in APP-expressing cells. A. Representative Western blot and quantification of PARK2 in fibroblasts overexpressing *GFP* or *APP*. **B.** Representative confocal microscopy immunofluorescence images showing PARK2 in red and TOMM20 as a mitochondrial constitutive marker in blue in the same cells treated with CCCP (20 μM) for 1h. On the right, binary image representing the colocalization of both labels and dotted line delimits cytoplasm of each cell according to phalloidin staining (not shown). **C.** Quantification of the colocalization between PARK2 and TOMM20 expressed as area occupied by the overlapping elements per cell. Scale bar: 40 μm. (n=3 independent experiments; **p<0.05, ***p<0.001*).

mitochondria to be targeted to autophagy recycling. Thus, we examined PARK2 protein, and Western blot analysis revealed substantially increased PARK2 levels in APP-expressing cells (**Fig. 10A**). On the other hand, to test the function of PARK2 in mitophagy, we treated cells with CCCP for 1h and analyzed PARK2 targeting to depolarized mitochondria. It has been demonstrated that within 1h of CCCP addition, endogenous PARK2 was recruited to mitochondria in the majority of cells (Narendra et al, 2008). Immunofluorescence study displayed a decreased mitochondrial localization of PARK2 in APP-expressing cells suggesting a defective labeling of damaged mitochondria to be recycled by mitophagy (**Fig. 10B-C**). It has been described that PARK2 is recruited to the mitochondria by a PTEN-induced putative kinase 1 (PINK1)-dependent mechanism for mitochondrial turnover by the

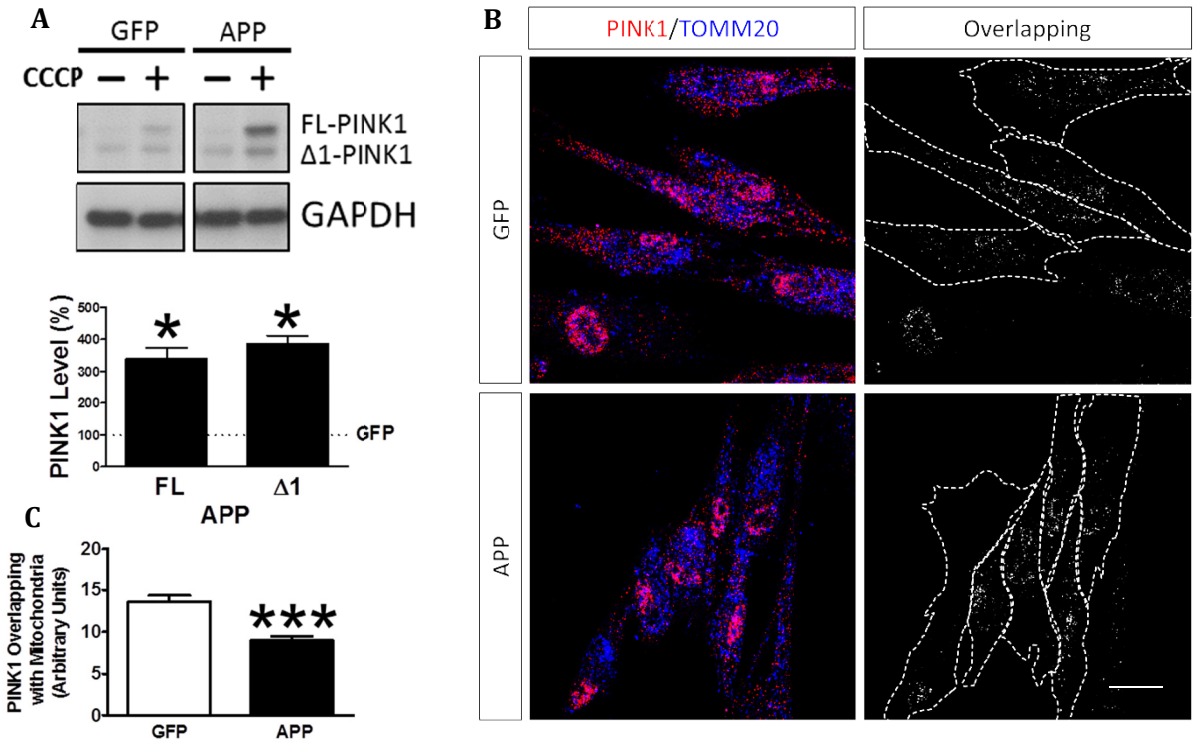

Figure 11. Imbalance pattern of PINK1 in APP-expressing cells. A. Representative Western blot of the expression of PINK1 in fibroblasts overexpressing *GFP* or *APP* treated with CCCP (20 μM) for 24h. Quantification of the levels of FL-PINK1 and Δ1-PINK1 isoform in APP-expressing cells with respect to GFP in the presence of CCCP. **B.** Representative confocal microscopy immunofluorescence images showing PINK1 in red and TOMM20 in blue of APP-expressing fibroblasts treated with CCCP (20 μM) for 1h. On the right, binary image representing the colocalization of both labels and dotted line delimits cytoplasm of each cell according to phalloidin staining (not shown). **C.** Quantification of the colocalization between PINK1 and TOMM20 expressed as area occupied by the overlapping elements per cell. (n=3 independent experiments; **p<0.05, ***p<0.001*). Scale bar: 40 μm.

autophagy system (Vives-Bauza et al, 2010). After mitochondrial damage, PINK1 is stabilized in the mitochondrial membrane as a full length (FL) isoform which recruits PARK2 (Narendra et al, 2010b). On the other hand, it has been recently demonstrated PINK1 may also play a inhibitory role in mitophagy process (Fedorowicz et al, 2014). The main cleaved product of PINK1 (Δ1 fragment), is able to physically bind PARK2 in the cytosol inhibiting its translocation to the mitochondria, therefore, impairing the elimination of damaged mitochondria. Taking this into account, we next checked whether PINK1 protein levels or distribution were altered after CCCP treatment when APP is overexpressed. APP-expressing cells exhibited elevated levels of both FL-PINK1 and Δ1-PINK1 after 24h of CCCP treatment (Fig. 11A). Immunofluorescence analysis of the stabilization of PINK1 in the mitochondria after CCCP challenge for 1h showed a diminished PINK1 protein at this subcellular localization (Fig. 11B-C). Next, we observed that levels of mitochondrial constitutive protein TOMM20 were slightly higher in APP cells respect to controls (Fig. 12A). The increase of mitochondria per cell (Martinez-Vicente et al, 2010) and, even, increased levels of TOMM20 by Western blot have been previously related with the impairment of mitochondrial recycling by autophagy. To test whether there was a mitochondria recycling failure we analyzed the recovery of mitochondrial function represented by the mitochondrial membrane potential (ΔΨm) after a reversible treatment with CCCP. The overexpression of APP did not significantly alter ΔΨm and depolarization took place similarly in both GFP- and APP-expressing cells. After de removal of CCCP, although ΔΨm recovery was not complete in APP-expressing cells the differences were not statistically significant compared to GFP-expressing cells, in which there was practically recovery during the studied period (Fig. 12B). The diminished targeting of PARK2 and PINK1 to mitochondria may correlate with the observed boosted autophagy flux; however, the long term accumulation of these proteins together with increased mitochondrial content suggests a slightly compromised mitophagy. This may be caused by insufficient labelling of depolarized mitochondria by PINK1 and PARK2. Additionally, the enhanced amount of Δ1-PINK1 may point out a further inhibitory

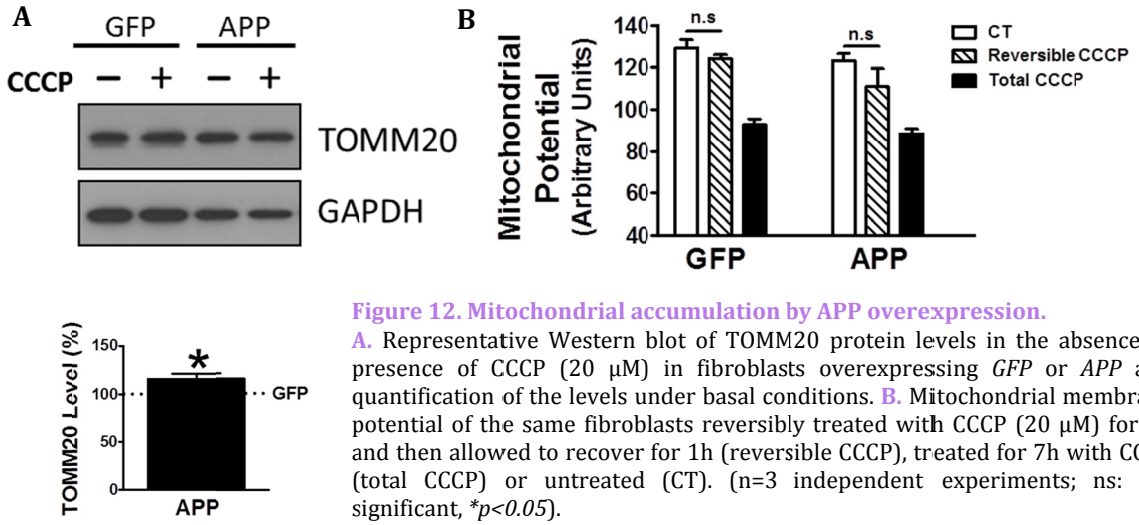

Figure 12. Mitochondrial accumulation by APP overexpression.
A. Representative Western blot of TOMM20 protein levels in the absence or presence of CCCP (20 μM) in fibroblasts overexpressing *GFP* or *APP* and quantification of the levels under basal conditions. B. Mitochondrial membrane potential of the same fibroblasts reversibly treated with CCCP (20 μM) for 6h and then allowed to recover for 1h (reversible CCCP), treated for 7h with CCCP (total CCCP) or untreated (CT). (n=3 independent experiments; ns: not significant, **p<0.05*).

mechanism over PARK2 translocation to mitochondria that may contribute to the deficient labeling of this damage organelle.

1.2 Study of mitochondrial recycling process in human fibroblasts after the overexpression of *Tau* and *APP*

Although APP is ubiquitously expressed, Tau is abundant in neurons. Therefore, one may think that this protein plays an important role in the preferential sensitivity of this cell type in AD pathology. With this idea, we next evaluated the effect of the addition of Tau over the autophagy-mitophagy alterations observed after APP overexpression.

1.2.1 Synergistic effect of Tau and APP causes an increased autophagy flux

To achieve the effect of Tau and APP in the process of autophagy we overexpressed both proteins at the same time in a human line of skin fibroblasts by lentiviral infection. As a control we

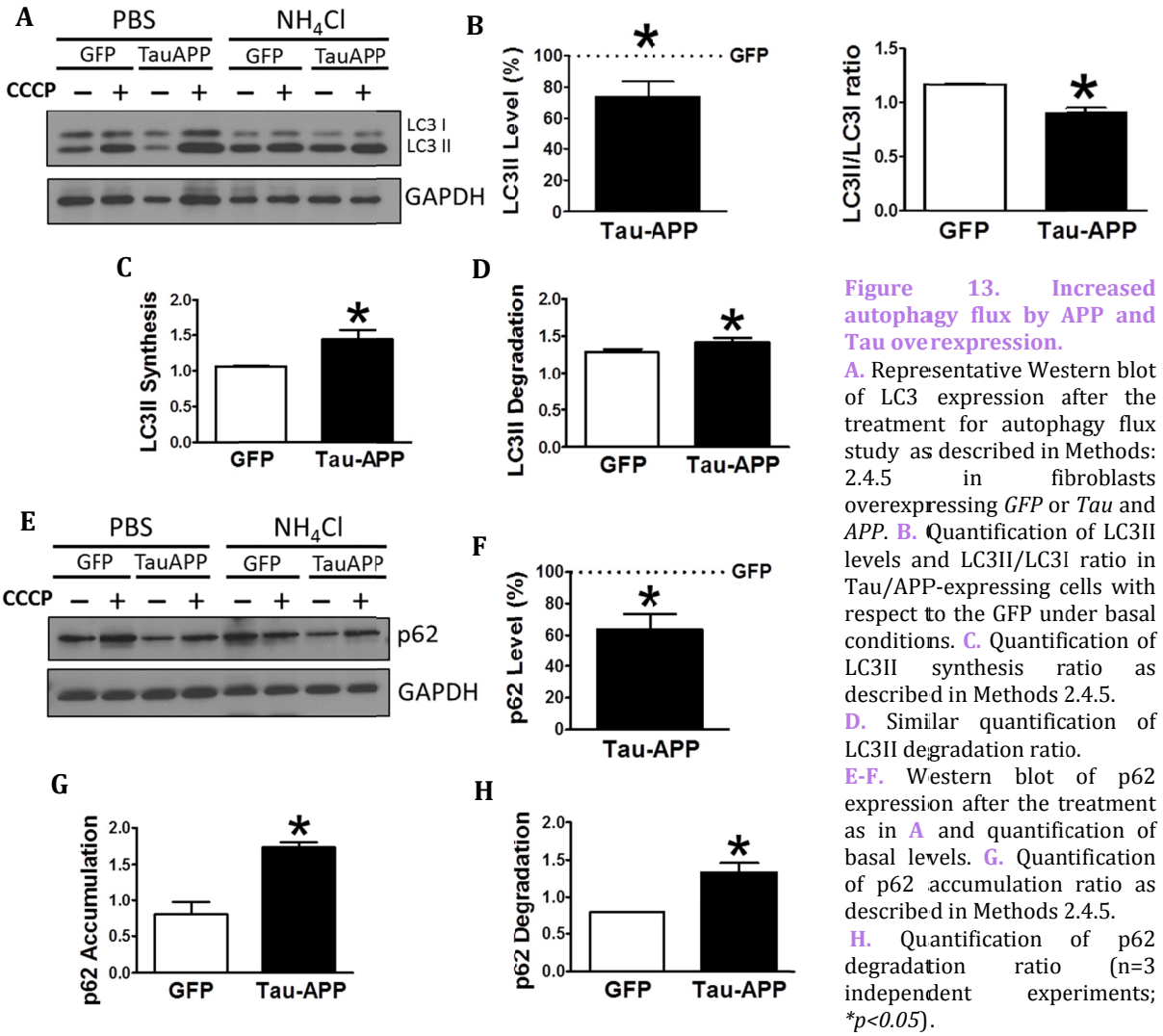

Figure 13. Increased autophagy flux by APP and Tau overexpression.
A. Representative Western blot of LC3 expression after the treatment for autophagy flux study as described in Methods: 2.4.5 in fibroblasts overexpressing *GFP* or *Tau* and *APP*. **B.** Quantification of LC3II levels and LC3II/LC3I ratio in Tau/APP-expressing cells with respect to the GFP under basal conditions. **C.** Quantification of LC3II synthesis ratio as described in Methods 2.4.5. **D.** Similar quantification of LC3II degradation ratio. **E-F.** Western blot of p62 expression after the treatment as in **A** and quantification of basal levels. **G.** Quantification of p62 accumulation ratio as described in Methods 2.4.5. **H.** Quantification of p62 degradation ratio (n=3 independent experiments; **p<0.05*).

used a GFP lentivirus like in previous experiments. Then, cells were treated for 24h with CCCP followed by an additional treatment of NH_4Cl for 6h in the presence of CCCP. First, we showed that Tau-APP overexpression causes a reduction of AVs content exhibited by lower levels of LC3II protein as well as LC3II/LC3I ratio under basal conditions which may correlate with the activation of autophagy (Fig. 13A-B). This activation was reflected by the markedly elevated synthesis of AVs besides the significant increase of LC3II degradation when *Tau* and *APP* are overexpressed (Fig. 13C-D). Under the same conditions, we next examined levels of p62, an adaptor protein that recognizes substrates to be recycled by autophagy being itself degraded in this process (Katsuragi et al, 2015). Western blot revealed diminished p62 levels in cells that overexpressed *Tau* and *APP* under basal conditions (Fig. 13E-F). Similar to previous situation, the accumulation and degradation rates of p62 were increased promoting the turnover of this protein and preventing their accumulation corroborating an increased autophagy flux (Fig. 13G-H). Lysosomal system plays a pivotal role during autophagy degradation phase. We could observe an increased lysosomal content after the overexpression of APP and Tau suggested by the augmented levels of LAMP1 and active Cathepsin B (Fig 14A-C). To ascertain if these lysosomes are functional we studied their pH by LysoTracker assay finding that Tau/APP-expressing cells exhibited a higher capacity to retain LysoTracker probe suggesting an increased amount of lysosomes (Fig. 14D). All these data together indicated that the overexpression of Tau and APP caused a marked increase in the number of lysosomes which seem to be active due their acidic pH and the enhanced degradation phase of autophagy observed.

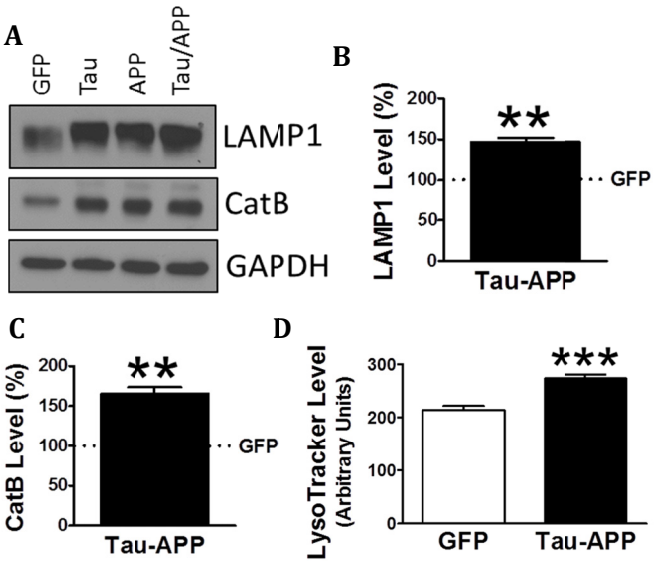

Figure 14. Increased lysosomal activity in Tau/APP-expressing cells. A. Representative Western blot of LAMP1 and Cathepsin B protein levels in fibroblasts overexpressing *GFP*, *Tau*, *APP* or *Tau/APP*. **B.** Quantification of LAMP1 protein levels of *Tau/APP*-expressing cells with respect to *GFP*-. **C.** Similar quantification of Cathepsin B protein levels. **D.** Quantification of the amount of lysosomes per cell in GFP- or *Tau/APP*-expressing cells. (n=3 independent experiments; ***p<0.01, ***p<0.001*).

1.2.1 *Tau* and *APP* overexpression induces mitophagy impairment

Taking into account that Tau and APP contribute to mitochondrial pathogenesis in AD (Garcia-Escudero et al, 2013), we wanted to evaluate whether their overexpression could be promote a defect in the mitochondrial recycling process. On one hand, basal PARK2 levels were strongly

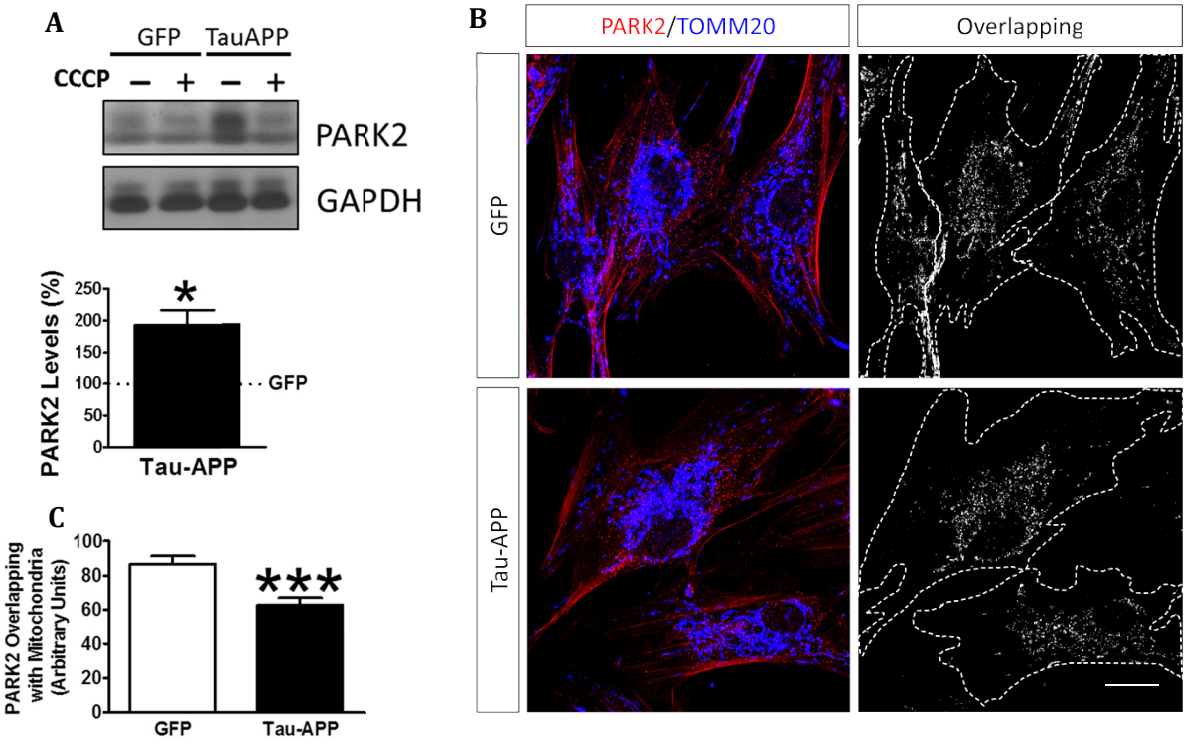

Figure 15. Imbalance pattern of PARK2 in Tau/APP-expressing cells. A. Representative Western blot of PARK2 in fibroblasts overexpressing *GFP* or *Tau* and *APP* in the absence or presence of CCCP (20 μM) and quantification of the levels under basal conditions. **B.** Representative confocal microscopy immunofluorescence images showing PARK2 in red and TOMM20 as a mitochondria constitutive marker in blue of GFP- or Tau/APP-expressing fibroblasts treated with CCCP (20 μM) for 1h. On the right, binary image representing the colocalization of both labels and dotted line delimits cytoplasm of each cell according to phalloidin label (not shown). **C.** Quantification of the colocalization between PARK2 and TOMM20 expressed as area occupied by the overlapping elements per cell. Scale bar: 40 μm. (n=3 independent experiments; **p<0.05, ***p<0.001*).

increased in Tau/APP-expressing cells respect to controls (Fig. 15A). This situation may reflect an activation of detoxification system (Witte et al, 2009). However, the recruitment of PARK2 to the mitochondria after CCCP treatment for 1h was decreased in Tau/APP-expressing cells suggesting a defective labeling of damaged mitochondria (Fig. 15B-C). Similarly, Western blot analysis displayed that both FL-PINK1 and Δ1-PINK1 were significantly increased in Tau/APP-expressing cells as compared to controls after a mitochondrial insult for 24h (Fig. 16A). Strikingly, immunofluorescence analysis of the subcellular localization of PINK1 after CCCP challenge for 1h showed a strongly increased stabilization of PINK1 in the mitochondria in these cells which may reflect an accumulation of depolarized mitochondria

	APP	Tau/APP
LC3	–	–
Autophagy Flux		
Synthesis	–	+
Degradation	+	+
Lysosomes	+	+
CatB	+	+
PARK2		
Accumulation	+	++
Mito. targeting	–	–
PINK1		
Accumulation	++	+
Mito. targeting	–	++
Mito. accumulation	+	++
ΔΨm	=	<

Table 5. Summary of results in APP and Tau/APP-expressing cells.

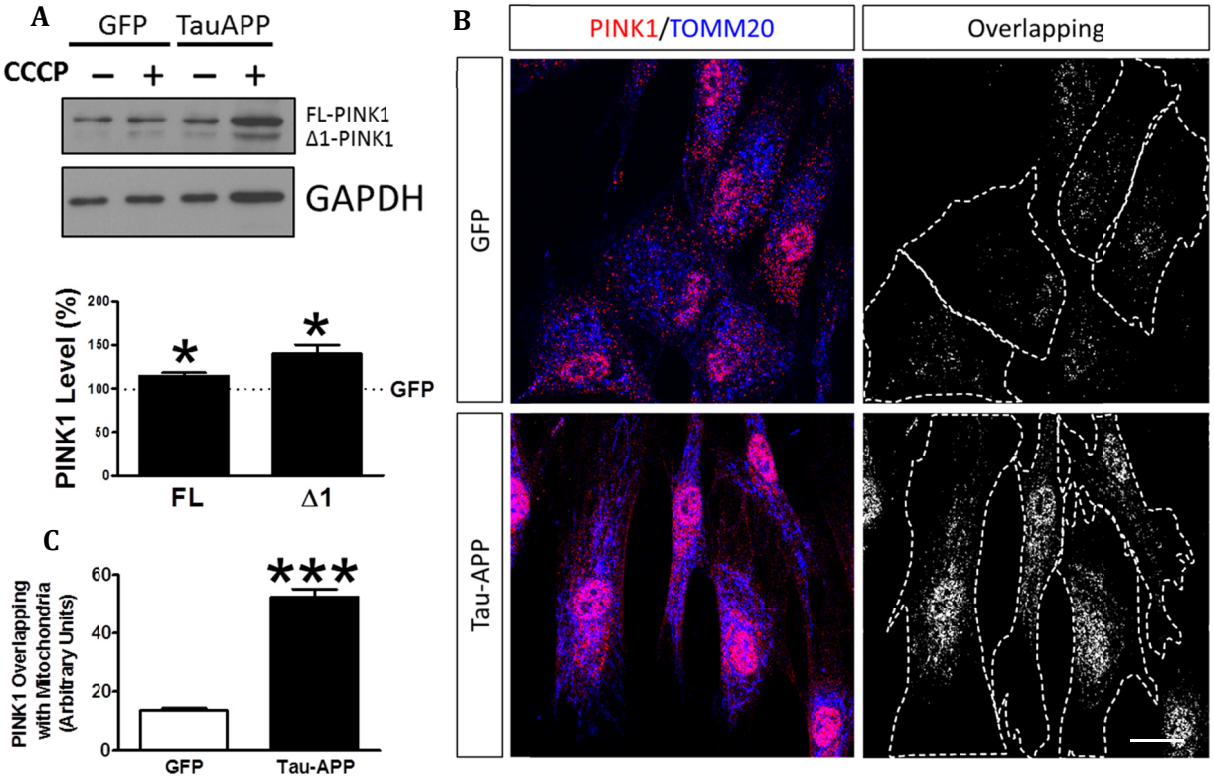

Figure 16. Imbalance pattern of PINK1 by *APP* and *Tau* overexpression. A. Representative Western blot of the expression of PINK1 in fibroblasts overexpersing *GFP* or *Tau/APP* treated with CCCP (20 μM) for 24h. Quantification of the levels of FL-PINK1 and Δ1-PINK1 isoforms in Tau/APP-expressing cells with respect to GFP in the presence of CCCP. **B-C.** Representative confocal microscopy immunofluorescence images and quantification showing PINK1 in red and TOMM20 in blue of GFP- and Tau/APP-expressing fibroblasts treated with CCCP (20 μM) for 1h. On the right, binary image representing the colocalization of both labels and dotted line delimits cytoplasm of each cell according to phalloidin label (not shown). Scale bar: 40 μm. (n=3 independent experiments; **p<0.05, ***p<0.001*).

(**Fig. 16B-C**). These data indicated that although there was a correct stabilization of PINK1 in depolarized mitochondria, PARK2 was not properly targeted to this organelle suggesting a deficient crosstalk between these two proteins. The increased levels of Δ1-PINK1 may sequester PARK2 in the cytosol impairing its targeting to mitochondria. These data substantially correlates with the elevated levels of TOMM20 shown in Tau/APP-expressing cells demonstrating evident mitophagy impairment resulting in the accumulation of mitochondria (**Fig. 17A**). This was corroborated by the significantly diminished ΔΨm recovery observed in Tau/APP-expressing cells after a CCCP reversible challenge (**Fig. 17B**). Once again, these results suggest that Tau and APP overexpression hinders the mitochondrial recycling process (**Table 5**).

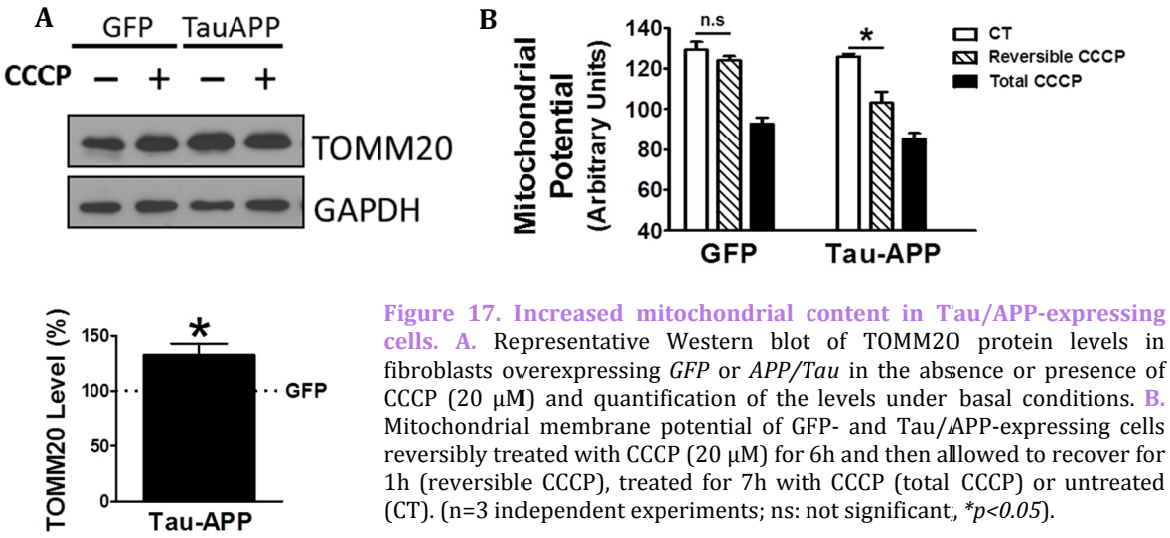

Figure 17. Increased mitochondrial content in Tau/APP-expressing cells. A. Representative Western blot of TOMM20 protein levels in fibroblasts overexpressing *GFP* or *APP/Tau* in the absence or presence of CCCP (20 μM) and quantification of the levels under basal conditions. **B.** Mitochondrial membrane potential of GFP- and Tau/APP-expressing cells reversibly treated with CCCP (20 μM) for 6h and then allowed to recover for 1h (reversible CCCP), treated for 7h with CCCP (total CCCP) or untreated (CT). (n=3 independent experiments; ns: not significant, **p<0.05*).

2. Mitophagy analysis in a familial model of Alzheimer disease.

In order to deepen in the differential susceptibility of neurons in AD, our next goal was to study the mitophagy alterations observed in *APP/Tau*-overexpression model in fibroblasts and neurons derived from AD patients. To achieve this we have taken advantage of the new techniques of cell reprogramming that allowed us to get induced pluripotent stem cells (iPSC) from fibroblasts that can be subsequently differentiated into neurons. To model the disease we have chosen a familiar form of AD associated to PSEN1 mutation which has been previously demonstrated to cause an autophagy failure (Lee et al, 2010).

Early-onset Alzheimer disease is the term used for cases of Alzheimer disease diagnosed before the age of 65 (Campion et al, 1999). It is an uncommon form of Alzheimer, accounting for only 5% of all Alzheimer's cases. Approximately 13% of the cases of early-onset AD are FAD, where a genetic predisposition leads to the disease (Campion et al, 1999). Although this condition only represents a small proportion of Alzheimer patients, we wanted to evaluate whether the failure in mitochondrial recycling process observed after the overexpression of APP and Tau may be also present in an unmodified human cell model harboring a well characterized AD related mutation.

Presenilin 1 (PSEN1) gene mutations are the most prevalent in FAD (Bekris et al, 2010; Piaceri et al, 2013). Presenilin 1 protein is a proteolytic subunit of γ-secretase which carries out the main function of the complex which is the proteolysis of other proteins (De Strooper et al, 2012). The γ-secretase complex is located in the plasma membrane and it is well known for its role in generation

of Aβ from amyloid precursor protein (APP), which is produced in the brain and other tissues (Haass, 1993 (Haass & Selkoe, 1993), (Thinakaran & Koo, 2008).

Over 180 mutations in PSEN1 have been reported as the cause of early onset Alzheimer disease (Cruts et al, 2012). Defective Presenilin 1 interferes with the function of the γ-secretase complex, which alters the processing of APP and leads to the overproduction of a longer, toxic version of Aβ peptide (Aβ42) (Borchelt et al, 1996). Generation of toxic Aβ peptide and the formation of amyloid plaques likely lead to the death of neurons and the progressive signs and symptoms of this disorder. To develop this work we have focused in the PSEN1 Ala246Glu mutation known as FAD1. This mutation was originally reported in 1995 in conjunction with the cloning of the PSEN1 gene (Sherrington et al, 1995). It was detected in a Canadian family of Anglo Saxon-Celtic origin. The pattern of transmission is consistent with autosomal-dominant inheritance, and genetic analysis confirmed that the mutation segregated with disease.

Besides the generation of Aβ, little is known about PSEN1 implication in mitochondrial dysfunction and oxidative damage. Previous study defined an essential role for PSEN1 in the maturation and trafficking of the v-ATPase responsible for lysosome acidification which is essential for the normal turnover of proteins and organelles by autophagy (Lee et al, 2010). Taking into account these data, the next goal of this work is the evaluation of mitochondrial recycling process by autophagy in two different human cell models of AD -associated *PSEN1* mutations, unmodified skin fibroblasts and iPSC-derived neurons.

2.1 Study of mitochondrial recycling process in fibroblasts from patients harboring AD-associated *PSEN1* mutation.

To achieve the first part of this project, we used human primary cell lines of skin fibroblasts from FAD patients obtained from Coriell Institute (**Table 2**) carrying the mutation FAD1: *PSEN1* Ala246Glu compared to their correspondent age- and sex-matched samples from non-demented individuals.

2.1.1 Autophagy degradation impairment in PSEN1-FAD fibroblasts.

To identify whether autophagy may be altered in our PSEN1-FAD (FAD1) fibroblasts, as it was previously published (Lee et al, 2010), we treated the cells with CCCP for 24h followed by an additional treatment of NH_4Cl for 6h in the presence of CCCP to block the degradation phase of autophagy. As expected, Western blot analysis revealed an increase of LC3II and LC3II/LC3I ratio levels in FAD1 fibroblasts compared to healthy samples, being more significance the second one (**Fig. 18A-B**). This may reflect an accumulation of autophagic vesicles in FAD1 cells. According to this, we could observe a diminished autophagy flux where the autophagosome (LC3II) synthesis was slightly decreased but the degradation was drastically reduced in FAD1 samples (**Fig. 18C-D**). These data

correlates with the significant increase of LC3II levels indicating that the degradation phase of autophagy is blocked by PSEN1 deficiency. To confirm this hypothesis we examined the turnover of p62, an adaptor protein degraded by autophagy, under the same conditions. We observed that basal levels of p62 were notably elevated in FAD1 cells compared with healthy samples (Fig. 18E-F) as had been previously reported (Lee et al, 2010). Moreover, these cells exhibited decreased p62 accumulation besides a remarkably lower degradation of p62 (Fig. 18G-H). Accumulation of LC3II and p62 together with a reduction of degradation phase strongly suggests that lysosomal function may be inhibited in FAD1 fibroblasts. Consistently, lysosomal protein levels measured by LAMP1 were markedly lower in FAD1 cells which could contribute to an impaired degradation process (Fig. 19A-B). Additionally we could observe that the acidification of lysosomes was diminished in FAD1 cell with respect to controls (Fig. 19C). All these data correlate with previously published results that indicate that PSEN1 function is necessary for the targeting of the v-ATPase V0a1 subunit to lysosomes, their acidification and function; therefore, PSEN1 mutations impair degradative phase of autophagy (Lee et al, 2010).

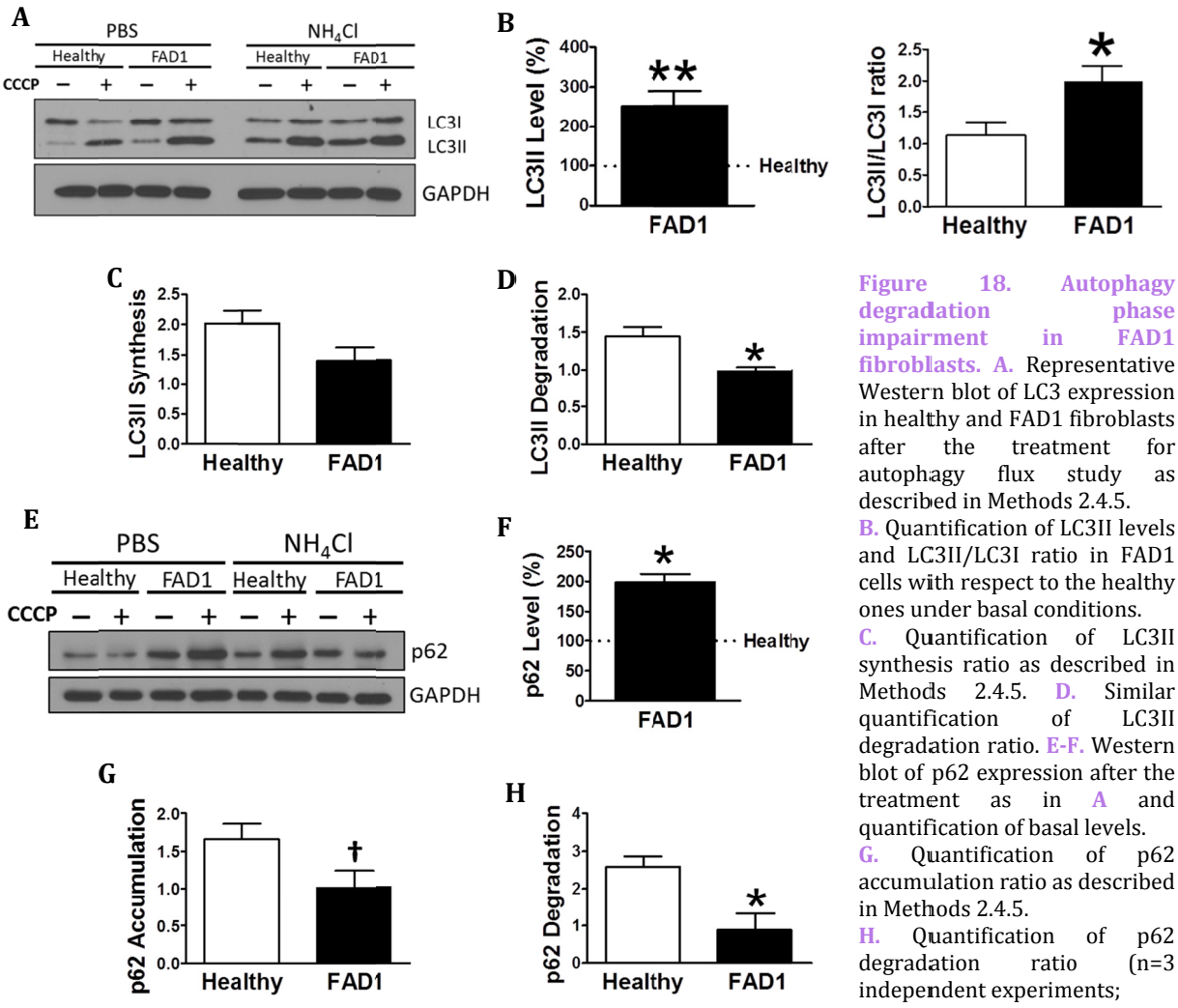

Figure 18. Autophagy degradation phase impairment in FAD1 fibroblasts. **A.** Representative Western blot of LC3 expression in healthy and FAD1 fibroblasts after the treatment for autophagy flux study as described in Methods 2.4.5. **B.** Quantification of LC3II levels and LC3II/LC3I ratio in FAD1 cells with respect to the healthy ones under basal conditions. **C.** Quantification of LC3II synthesis ratio as described in Methods 2.4.5. **D.** Similar quantification of LC3II degradation ratio. **E-F.** Western blot of p62 expression after the treatment as in **A** and quantification of basal levels. **G.** Quantification of p62 accumulation ratio as described in Methods 2.4.5. **H.** Quantification of p62 degradation ratio (n=3 independent experiments; *†p< 0.08; *p<0.05; **p<0.01*).

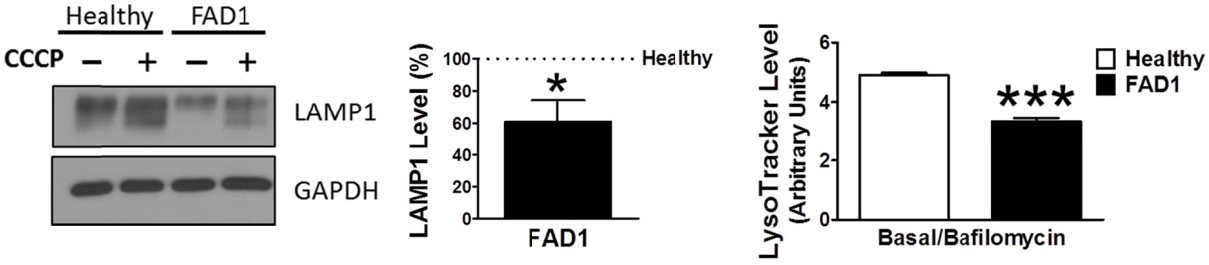

Figure 19. Imbalance of lysosomal properties of FAD1 cells. A. Representative Western blot of LAMP1 protein in healthy and FAD1 fibroblasts in the absence or presence of CCCP (20 μM). **B.** Quantification of LAMP1 protein levels under basal conditions. **C.** Quantification of the lysosomal acidity represented by the ratio between untreated and bafilomycin (100 nM) treated cells. (n=3 independent experiments; **p<0.05, ***p<0.001*).

2.1.2 FAD1 fibroblasts exhibit misbalance of mitophagy involved proteins.

Once a defect in autophagy had been corroborated in our FAD1-fibroblasts, we wondered if the proteins implicated in mitochondrial recycling process could be deregulated under PSEN1 mutation. FAD1-fibroblasts showed an abnormal increased PARK2 levels compared with healthy samples (**Fig. 20A-B**). On the other hand, Western blot analysis displayed that both FL and Δ1 isoforms of PINK1 were slightly decreased in PSEN1-FAD cells compared to controls after the treatment with CCCP for 24h (**Fig. 20C-D**). Additionally, we studied the recruitment of PARK2 to the mitochondria by immunofluorescence after CCCP insult for 1h (**Fig. 21**). We observed that mitochondrial localization of PARK2 was increased in FAD1-fibroblasts suggesting an accumulation of damaged mitochondria which are not able to be recycled by mitophagy due to the degradation phase deficiency described before. Accordingly, we could observe an accumulation of mitochondria in autophagic vesicles after CCCP treatment measured by the increased colocalization of TOMM20 and LC3II (**Fig. 22**). Moreover, diminished membrane potential recovery after a reversible treatment with CCCP was observed in FAD1-fibroblasts indicating a defect in mitochondrial recycling by mitophagy (**Fig. 23A**).

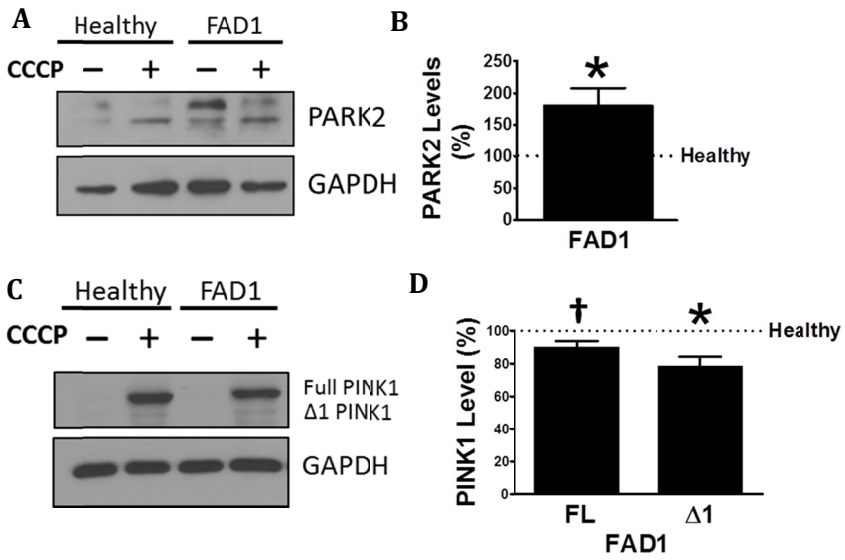

Figure 20. Deregulated pattern of PARK2 and PINK1 proteins in FAD1 fibroblasts. **A.** Representative Western blot of PARK2 in healthy and FAD1 fibroblasts in the absence or presence of CCCP (20 μM). **B.** Quantification of PARK2 levels under basal conditions. **C.** Representative Western blot of the expression of PINK1 in these fibroblasts treated with CCCP (20 μM) for 24h. **D.** Quantification of the levels of FL-PINK1 and Δ1-PINK1 isoform FAD1 fibroblasts with respect to healthy ones in the presence of CCCP. (n=3 independent experiments; *†p< 0.08, *p<0.05*).

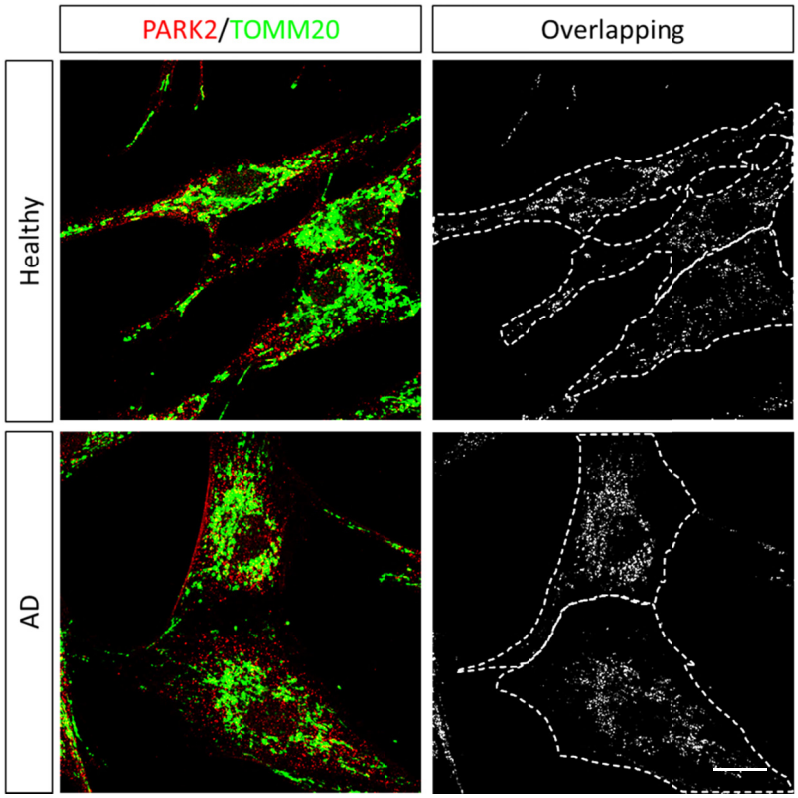

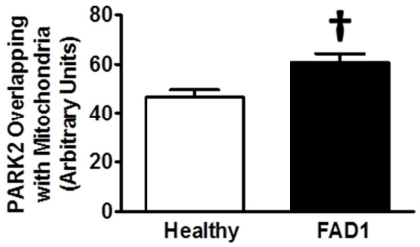

Figure 21. FAD1 fibroblasts showed increased PARK2 mitochondrial localization. Representative confocal microscopy immunofluorescence images showing PARK2 in red and TOMM20 as a mitochondria constitutive marker in green of healthy and FAD1 fibroblasts cells treated with CCCP (20 µM) for 1h. On the right, binary image representing the colocalization of both labels and dotted line delimits cytoplasm of each cell according to phalloidin staining (not shown). Quantification of the colocalization between PARK2 and TOMM20 expressed as area occupied by the overlapping elements per cell. Scale bar: 40 µm. *†p< 0.08*.

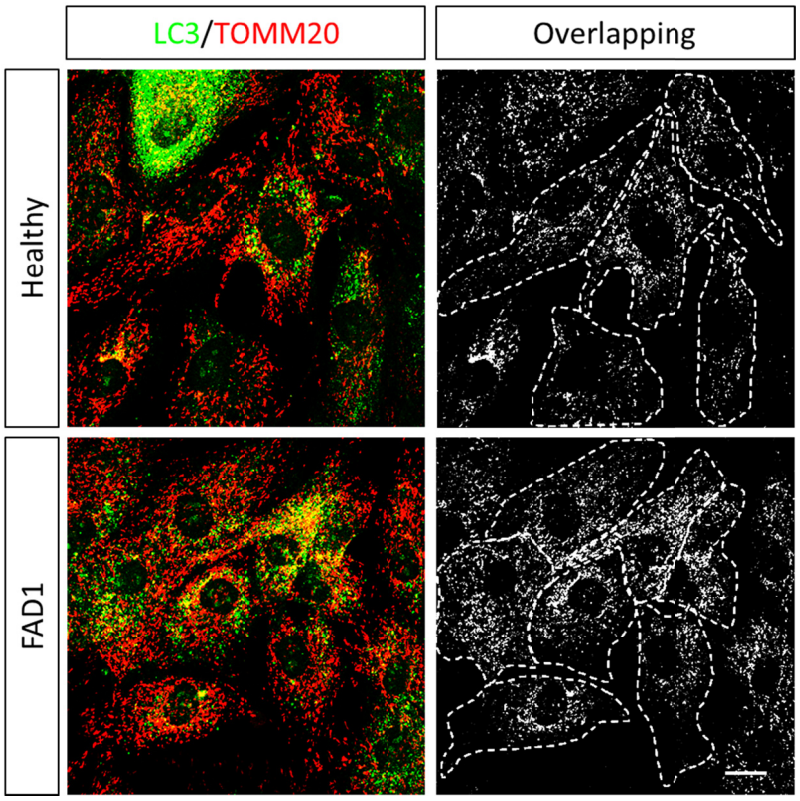

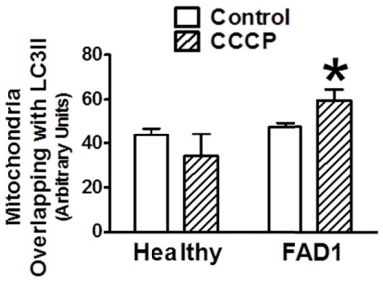

Figure 22. Accumulation of mitochondria in autophagic vesicles in FAD1 fibroblasts. Representative confocal microscopy immunofluorescence images showing LC3 in green and TOMM20 in red of healthy and FAD1 fibroblasts treated with CCCP (20 µM) for 24h. On the right, binary image representing the colocalization of both labels and dotted line delimits cytoplasm of each cell delimited according to phalloidin staining (note shown). Quantification of the colocalization between LC3 and TOMM20 expressed as area occupied by the overlapping elements per cell. Scale bar: 40 µm. **p<0.05*.

Consistently, mitochondrial surface analysis revealed increased levels of TOMM20 protein (**Fig. 23B-C**) in FAD1 cells respect to healthy controls. Therefore, these results indicate an impairment of the clearance of mitochondria by mitophagy.

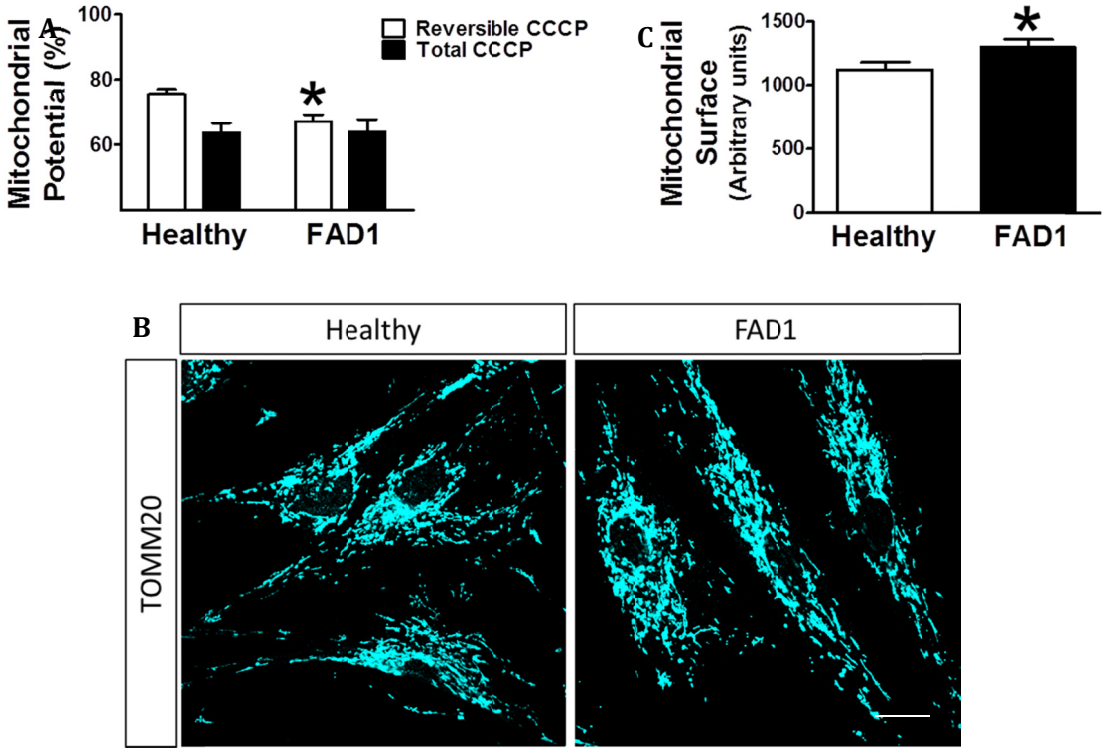

Figure 23. Dysfunctional mitochondria clearance impairment in FAD1 cells. A. Mitochondrial membrane potential of healthy and FAD1 fibroblasts reversibly treated with CCCP (20 µM) for 6h and then allowed to recover for 1h (reversible CCCP) or treated for 7h with CCCP (total CCCP) with respect to untreated condition. **B.** Representative confocal images of these fibroblasts showing TOMM20 in cyan in basal conditions. **C.** Quantification of the mitochondrial surface per cell in the confocal images. (n=3 independent experiments; *$p<0.05$). Scale bar: 40 µm.

2.2 Study of mitochondrial recycling process in human iPSC-derived neurons from PSEN1 Alzheimer patients.

To understand the onset and progression of a human disease, an effective model that combines known genetic elements with a predictive phenotypic readout is required. Recent advances in iPSC technology grant access to unique human samples and enable the generation of disease- and patient-specific cell lines. Terminally differentiated cell types, such as neurons, derived from iPSC lines are extremely useful for understanding the patho-physiological mechanisms of neurodegenerative disorders. For that reason we focused our efforts in the study of mitochondrial recycling in a human model of PSEN1-FAD iPSC-derived neurons from patients carrying the mutation FAD1: Ala246Glu.

2.2.1 Generation and characterization of healthy and Alzheimer iPSC lines.

To carry out this project, we worked in collaboration with Andrew Sproul and Scott Noggle from New York Stem Cell Foundation (NYSCF) as well as Ottavio Arancio from Columbia University. We worked with iPSC lines previously prepared by them within the collection of iPSC lines from Alzheimer patients' skin samples developed by the NYSCF Global Stem Cell Array. The iPSC lines were generated from established fibroblast lines from a healthy control and PSEN1 mutant patients carrying the mutation FAD1 (Ala246Glu) obtained from the cell bank repository of Coriell Institute (Camden, NJ) (**Table 2**).

Fibroblast lines were reprogrammed using four high-titer retroviral constructs prepared by the Harvard Gene Therapy Core Facility encoding human Oct4, KLF4, SOX2 and c-Myc, respectively (Dimos et al, 2008). iPSC colonies from both healthy and FAD1 patients (**Fig. 24**) were initially selected by morphology, passaged several times to remove untransformed cells, and expanded before characterization. Although iPSC lines were previously characterized using a variety of quality control assays (Sproul et al, 2014) we performed some of them to ascertain the pluripotency of the cells used for our experiments. First of all, we conducted a study of stem properties with two different approaches. Double immunofluorescence staining showed high expression of pluripotency markers NANOG, SSEA-4, OCT4, Tra-1-60, SOX2 and Tra1-81 in both healthy and FAD1 colonies (**Fig. 25**). Secondly, we confirmed a dramatic increase of pluripotency marker genes in iPSC lines compa-

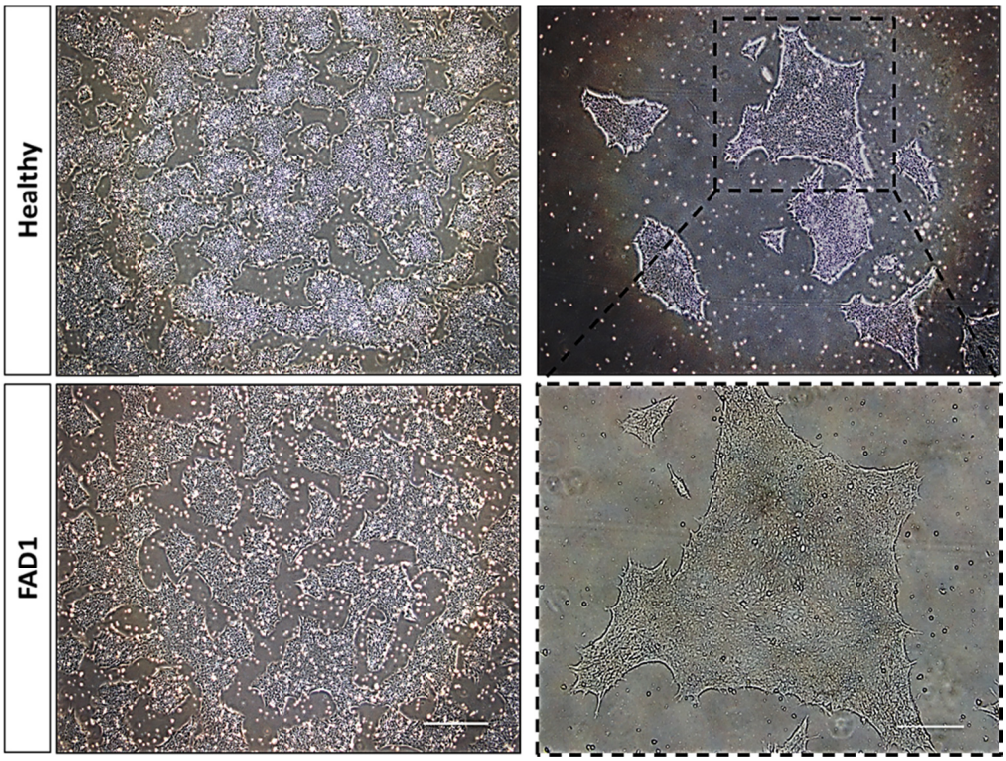

Figure 24. Healthy and FAD1 iPSC colonies. Representative images showing both healthy and FAD1 colonies *in vitro* in a feeder-free culture system. Scale bar: 50 µm.

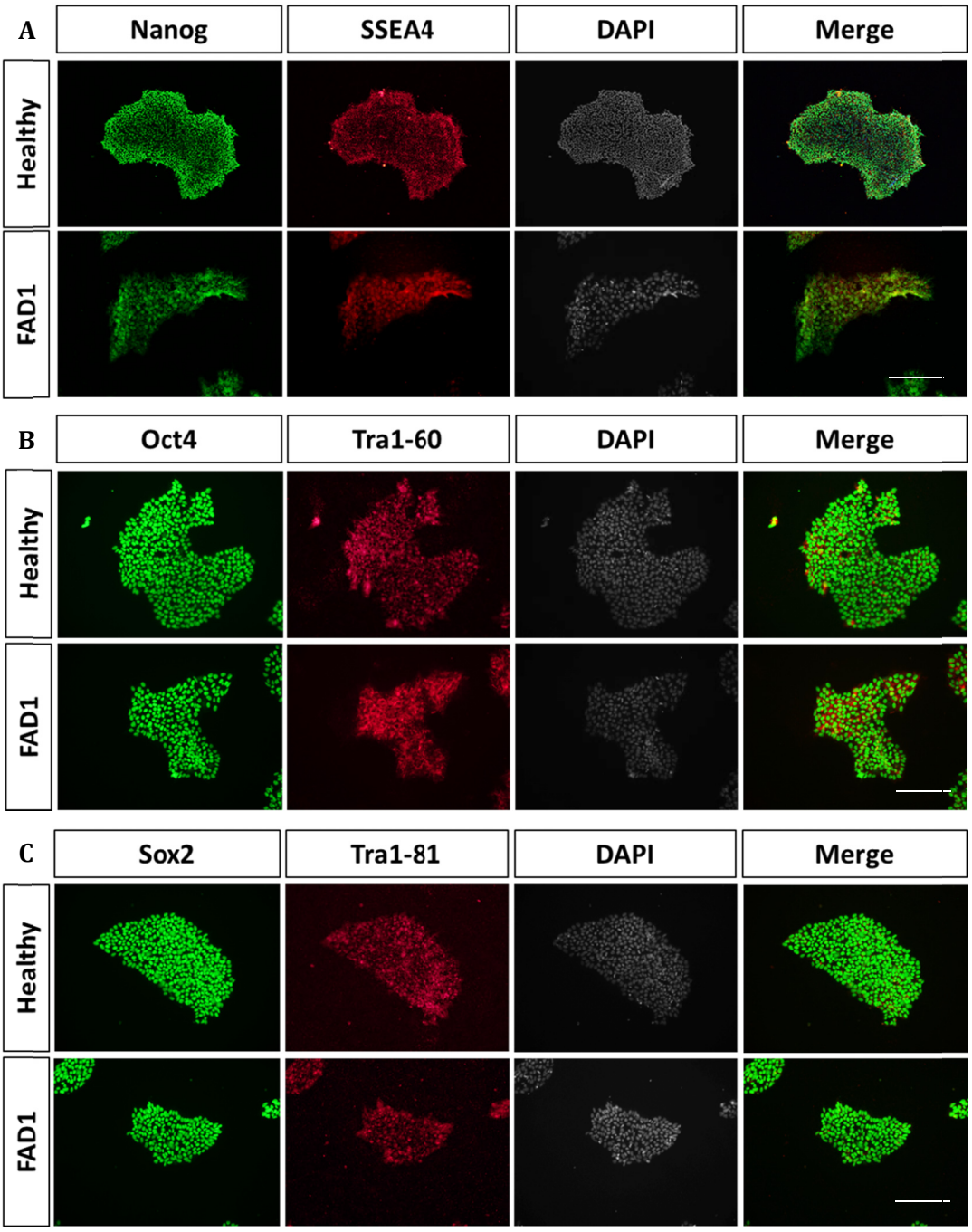

Figure 25. Expression of pluripotency markers in healthy and FAD1 iPSC colonies. Representative images of double immunofluorescence staining of pluripotency markers, DAPI staining for nuclei and merged channels in both healthy and FAD1 iPSC colonies. **A.** NANOG/SSEA-4 expression. **B.** OCT4/Tra-1-60 expression. **C.** SOX2/Tra1-81 expression. Scale bar: 50 μm.

red with the parental fibroblast line through NanoString Technology, a system that analyzes expression of hundreds of genes, miRNAs, or copy number variations simultaneously with high sensitivity and precision (**Fig. 26A**). We next examined the differentiation capacity of the iPSC cells *in vitro* through the formation of embryoid bodies (EBs). The lysates of spontaneously differentiated EBs were analyzed by NanoString Technology. As the graph shows, the expression of canonical germ

layer targets were notably elevated relative to undifferentiated iPSC control not shown (Fig. 26B). These data together with the previously published ones indicate successful reprogramming of healthy and FAD1 fibroblasts to a pluripotent state.

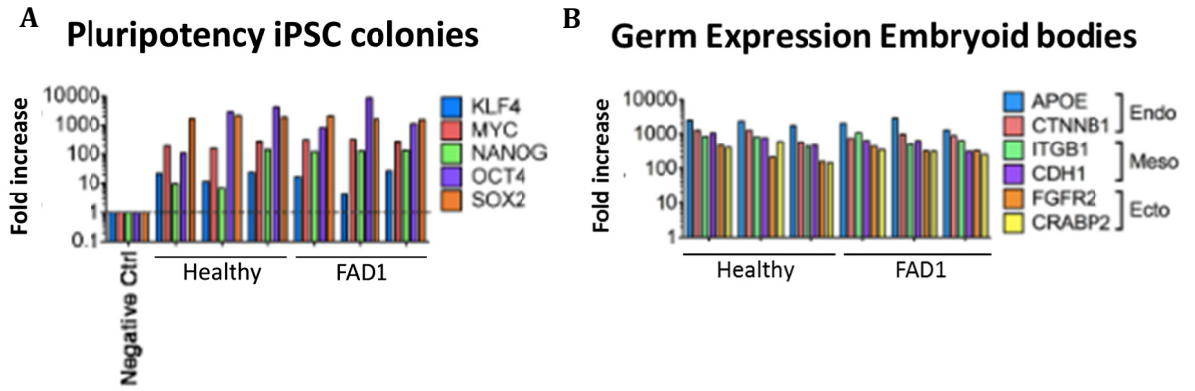

Figure 26. Characterization of pluripotency markers of iPSC colonies by RNA expression. A. Relative change in RNA expression of detailed canonical pluripotency genes in healthy and FAD1 iPSC lines. The negative control is a fibroblast line. **B.** RNA expression of specified canonical germ layer markers in spontaneously differentiated embryoid bodies relative to healthy iPSCs (not shown). Graphs show the median t-score of the expression levels of n=3.

2.2.2 Neural differentiation, characterization and AD pattern.

Both healthy control and FAD1 iPSC cell lines were subsequently differentiated into cortical neurons using a protocol that achieves rapid neuronal conversion (within 25–30 days) on adherent cell culture (Chambers et al, 2009) (Fig. 27A). Traditional EB formation (that takes 30–50 days) was found to be inefficient for neural differentiation from iPSC cell cultures, and stromal feeders could contribute undefined factors to the cell culture (Chambers et al, 2009). In the first step, undifferentiated iPSC colonies were dissociated into single cells and re-plated onto Cultrex-coated dishes in mTesR1 medium, supplemented with a ROCK inhibitor (Y-27632). When the culture reached a cell density of 80%, differentiation was started by changing the medium to custom mTesR1 media containing SMAD inhibitors (Fig. 27B): SB431542, a potent and specific inhibitor of transforming growth factor beta (TGFβ) superfamily type I which activates receptor-like kinase (ALK) receptors ALK4, ALK5 and ALK7 and Noggin analog LDN-193189, an inhibitor of bone morphogenetic protein type I receptors ALK2 and ALK3 (Chambers et al, 2009). The blockade of SMAD signaling has been shown to help destabilize pluripotency while promoting neuralization of primitive ectoderm (Lee et al, 2007; Xu et al, 2008). By day 11 of culture, a dense layer of cells was mechanically isolated and replated on Poly-L-ornithine/Matrigel-coated dishes. To push the differentiation of precursor cells, the medium was replaced by neuronal differentiation media.

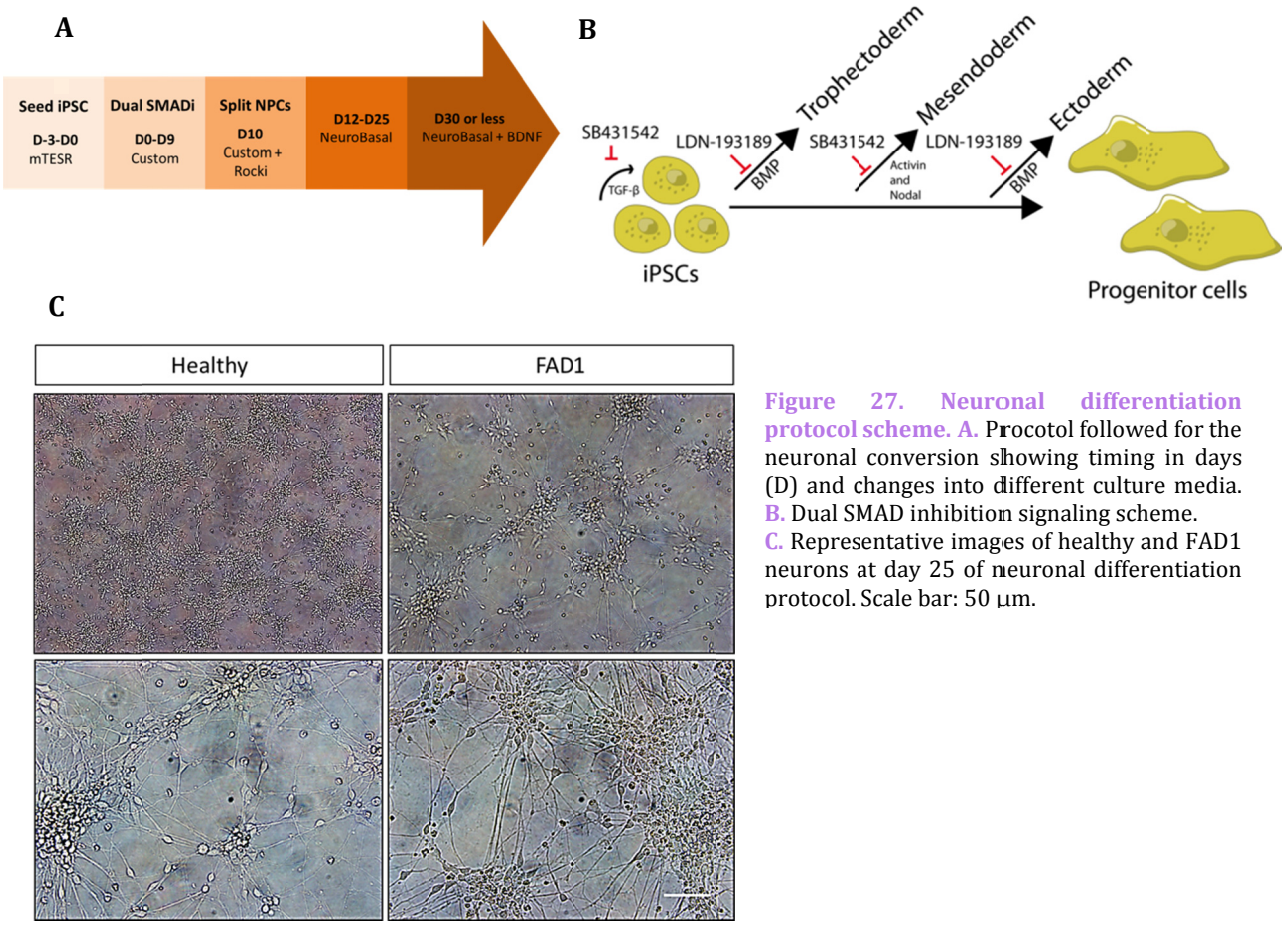

Figure 27. Neuronal differentiation protocol scheme. A. Procotol followed for the neuronal conversion showing timing in days (D) and changes into different culture media. **B.** Dual SMAD inhibition signaling scheme. **C.** Representative images of healthy and FAD1 neurons at day 25 of neuronal differentiation protocol. Scale bar: 50 µm.

We assayed our cell lines at day 25 of neuronal differentiation (Fig. 27C) through the analysis of several neuronal markers. Immunofluorescence staining displayed an elevated amount of cells derived from healthy and FAD1 cells expressing MAP2, a specific cytoskeletal protein that are enriched in dentrites, implicated in determining and stabilizing dentritic shape during neuron development, as well as 514 antibody staining which recognizes high molecular weight MAP2 isoforms independently of their phosphorylation state (Fig. 28A). Moreover, cells were positive for Tau, a protein expressed in neurons that modulates the stability of axonal microtubules as one of its main functions (Fig. 28B). On the other hand, most of healthy- and FAD1-derived neurons exhibited vGlut1 staining suggesting that a large population of neuronal differentiated cells obtained with this protocol have glutamatergic properties as the majority of excitatory neurons in the central nervous system (Fig. 28B). Then, we analyzed cells at day 30 of neuronal differentiation. At this point, cells were stained with post-mitotic markers such as NeuN/Fox3, a specific mature neuronal nuclear protein, as well as Calbindin, a mature granule cell marker. A huge proportion of healthy and FAD1 cells were positive for both markers at the same time (Fig. 29A-B). After 40 days of differentiation protocol both healthy and FAD1 neurons displayed all the morphological features of *in vitro* cultured neurons (Fig. 30).

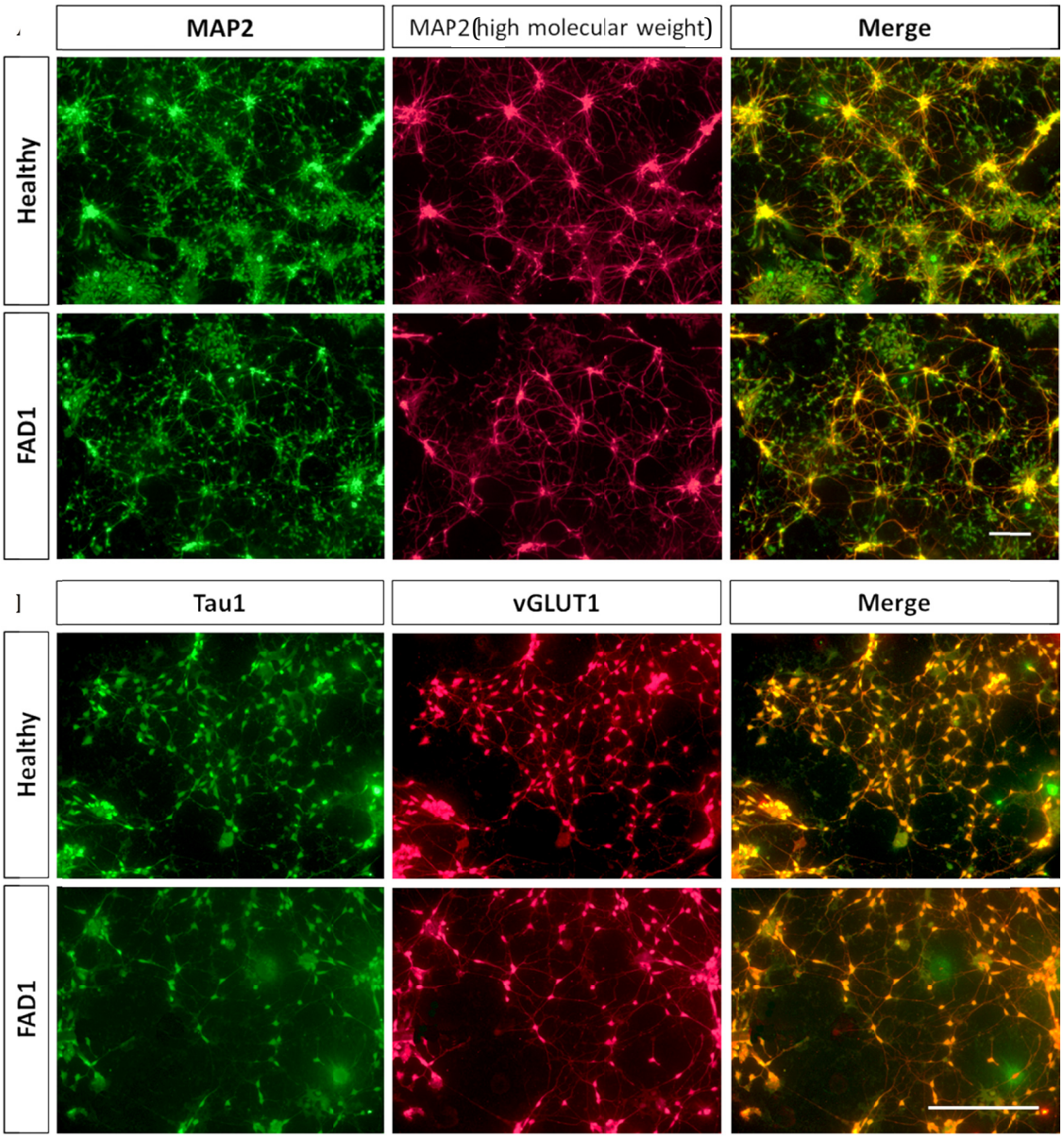

Figure 28. Characterization of iPSC-derived neurons at day 25 of neuronal differentiation. Representative images of immunofluorescence staining of the specified neuronal markers in both healthy and FAD1-derived neurons. **A.** MAP2 and high molecular weight MAP2 isoforms markers. **B.** Tau and vGlut1 markers. Scale bar: 500 µm.

Once iPCS cells were differentiated into mature neurons (40 days of differentiation), we wondered whether FAD1 neurons could recapitulate the hallmarks of AD pathology. Thus, we next investigated proteins associated with the disease and we observed that levels of APP were increased in FAD1 neurons respect to healthy ones and the levels of this protein were still high when autophagy process is activated by the treatment with CCCP (Fig. 31A-B). On the other hand, we showed no differences in basal levels of Tau in both cell types but the levels remained increased after the treatment with CCCP only in FAD1 neurons (Fig. 31A-C). However, FAD1 cells exhibited elevated levels of PHF1, Tau phosphorylated at Ser396/Ser404 sites, that stayed increased after autophagy

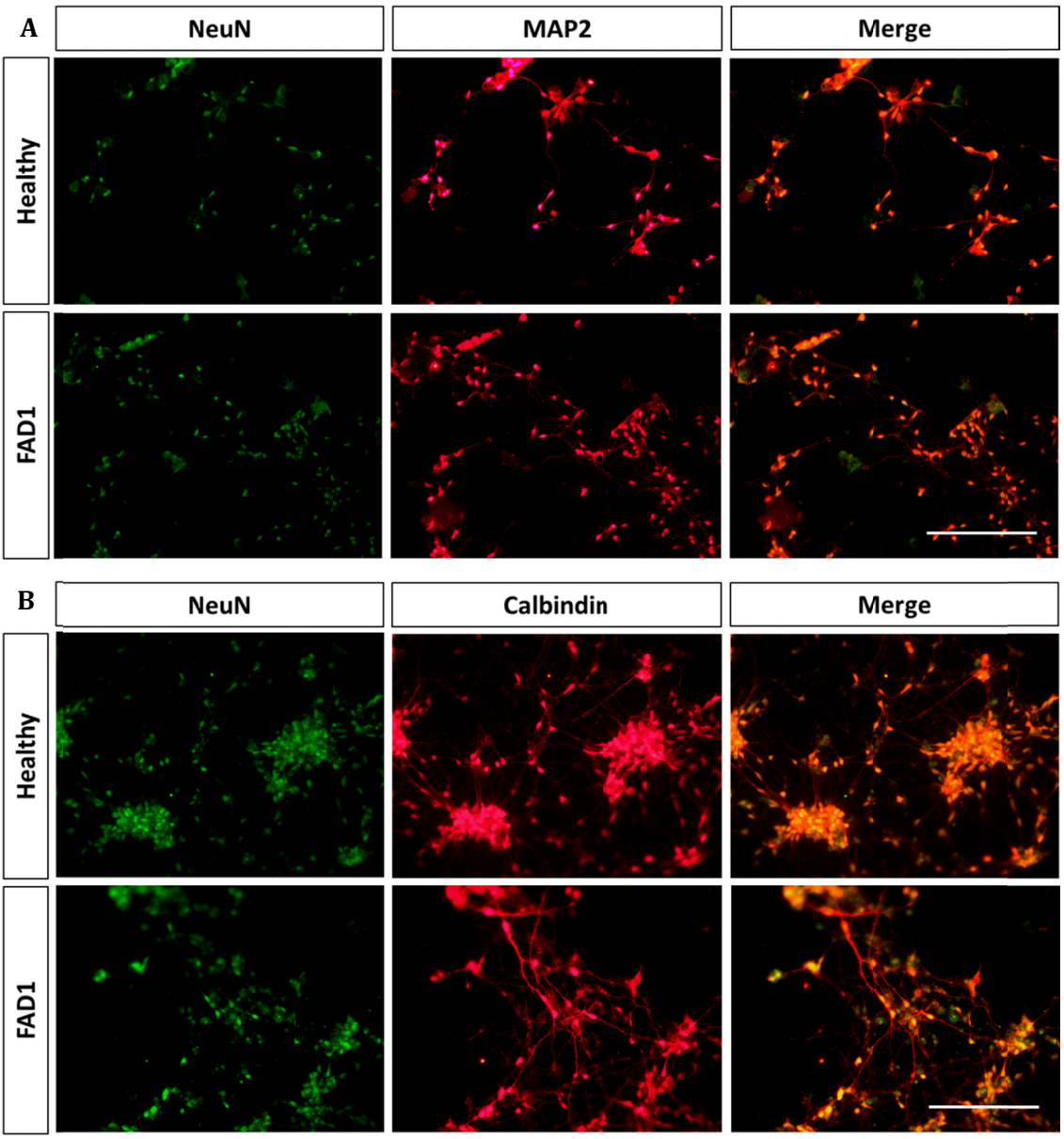

Figure 29. Characterization iPSC-derived neurons at day 30 of neuronal differentiation. Representative images of immunofluorescence staining of post-mitotic neuronal markers in both healthy and FAD1-derived neurons. **A.** NeuN and MAP2 markers. **B.** NeuN and Calbindin markers. Scale bar: 500 µm.

induction as in the previous cases (**Fig. 31A-D**). These results together indicate that AD-related hallmarks such as APP and phospho-Tau accumulation can also be found in FAD1 iPSC-derived neurons. Moreover, the indirect activation of autophagy by a mitophagy inducer was able to reduce these features in healthy neurons but not in FAD1 ones, suggesting a deficiency in the autophagy process in these neurons.

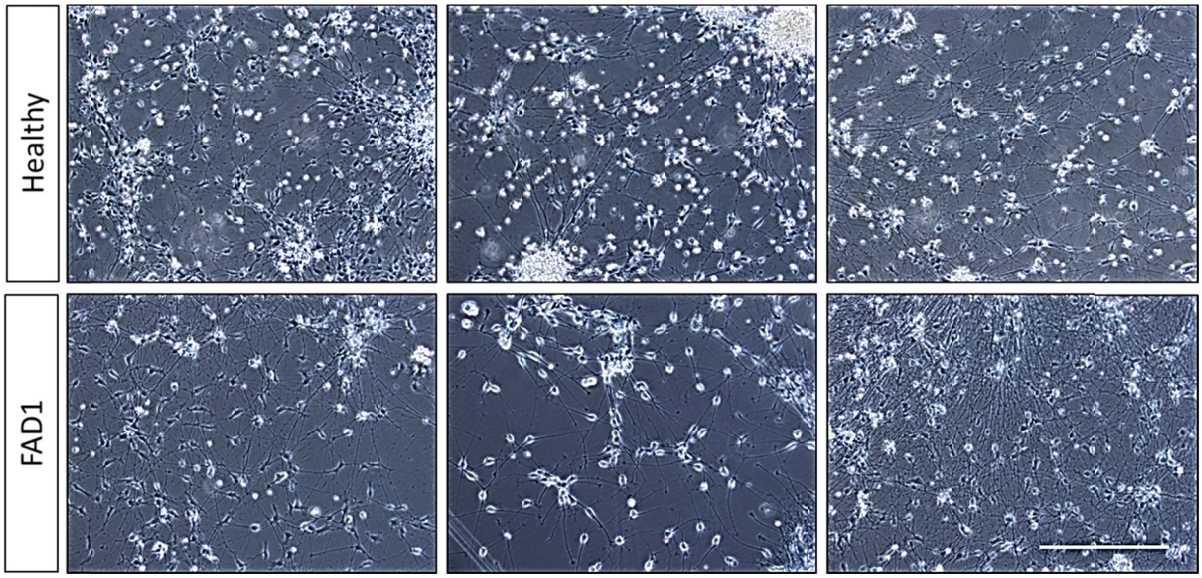

Figure 30. Healthy and FAD1-derived neurons after day 40 of neuronal differentiation. Representative phase contrast images of both healthy and FAD1-derived neurons after 40 days of differentiation protocol. Scale bar: 500 µm.

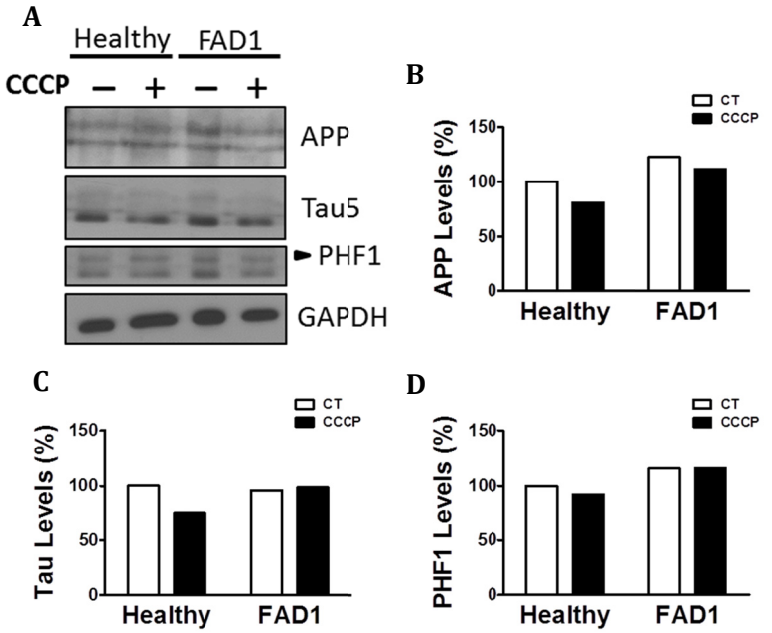

Figure 31. AD-related protein expression pattern in iPSC-derived neurons. A. Representative Western blot of the proteins involved in AD pathology in healthy- and FAD1-derived neurons in the absence or presence of CCCP (20 µM). Quantification of APP (**B**), total Tau (**C**) and phospho-Tau (PHF-1) levels (**D**) with respect to untreated healthy neurons.

2.2.3 Study of recycling process in iPSC-derived neurons.

2.2.3.1 Autophagy failure in PSEN1-FAD iPSC-derived neurons.

Taking into account our previous results in FAD1 fibroblasts, we asked whether mitophagy was impaired in human cortical neurons that contain an endogenous PSEN1 mutation. To address this question, neurons derived from healthy iPSC and FAD1 iPSC lines at day 40 of differentiation protocol, were treated with CCCP for 24h followed by an additional treatment of NH_4Cl for 6h in the

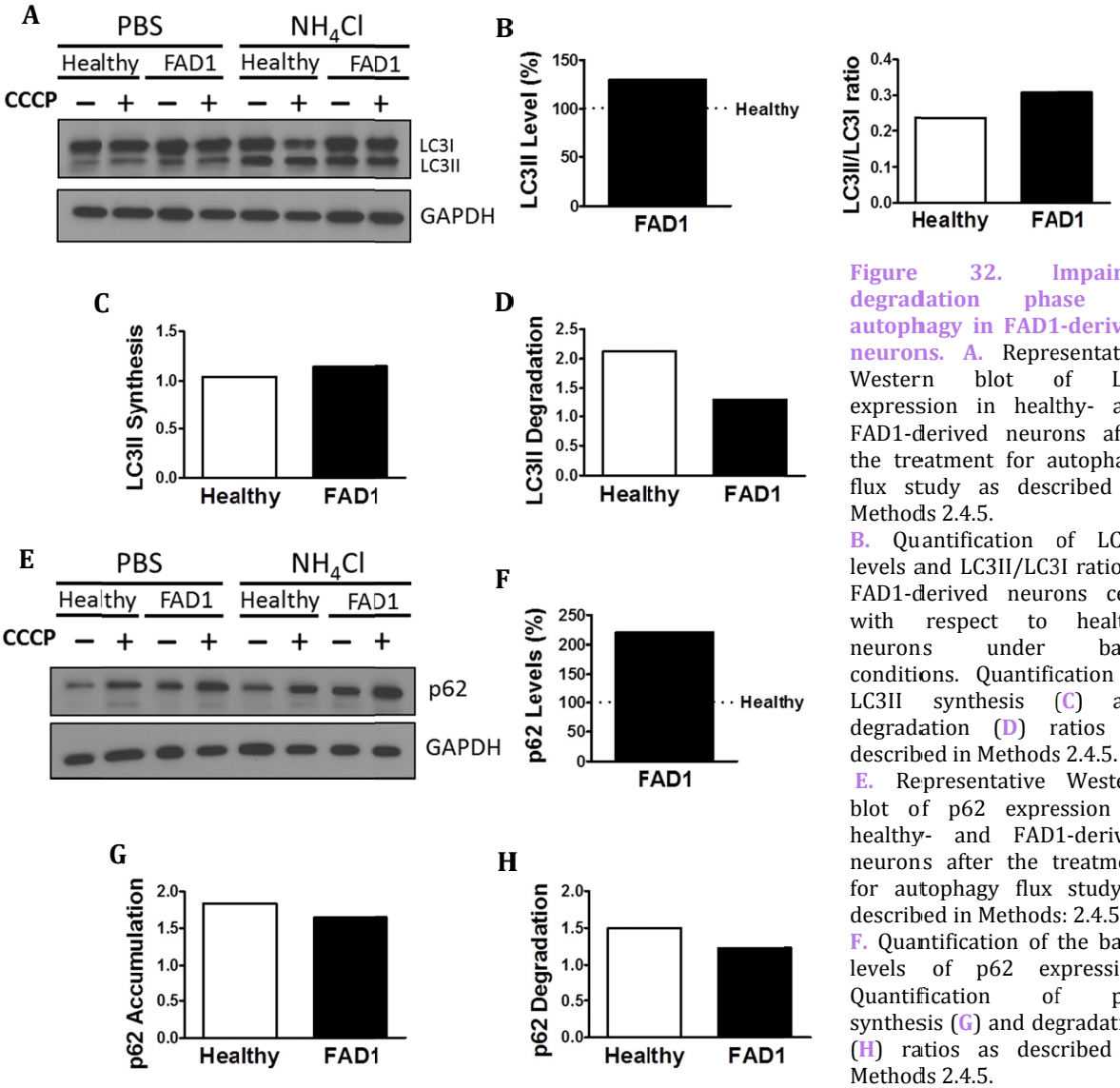

Figure 32. Impaired degradation phase of autophagy in FAD1-derived neurons. A. Representative Western blot of LC3 expression in healthy- and FAD1-derived neurons after the treatment for autophagy flux study as described in Methods 2.4.5. **B.** Quantification of LC3II levels and LC3II/LC3I ratio in FAD1-derived neurons cells with respect to healthy neurons under basal conditions. Quantification of LC3II synthesis (**C**) and degradation (**D**) ratios as described in Methods 2.4.5. **E.** Representative Western blot of p62 expression in healthy- and FAD1-derived neurons after the treatment for autophagy flux study a described in Methods: 2.4.5. **F.** Quantification of the basal levels of p62 expression. Quantification of p62 synthesis (**G**) and degradation (**H**) ratios as described in Methods 2.4.5.

presence of CCCP. Similar to what we showed for fibroblasts, FAD1 neurons exhibited an increased amount of autophagic vacuoles due to the high levels of LC3II and LC3II/LC3I ratio under basal conditions (**Fig. 32A-B**). These results correlate with the increased synthesis and markedly decreased degradation of AV observed in FAD1 neurons (**Fig. 32C-D**). Parallel to this inhibition of degradation phase of autophagy, we found a drastic increment of p62 levels in FAD1 neurons with respect to healthy ones under basal conditions (**Fig. 32E-F**) together with reduced p62 degradation ratio (**Fig. 32H**). Moreover, there was a misregulation of lysosomal levels showed in the increase of LAMP1 in FAD1 neurons compared with healthy samples (**Fig. 33A-B**).

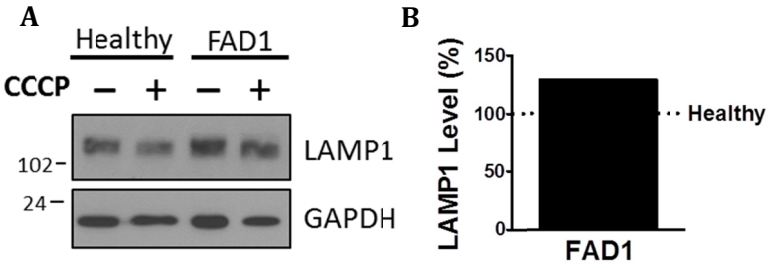

Figure 33. Increased lysosomal content in FAD1-derived neurons. A. Representative Western blot of LAMP1 protein in healthy- and FAD1-derived neurons in the absence or presence of CCCP (20 μM). **B.** Quantification of the LAMP1 levels under basal conditions.

2.2.4.2 Misregulation of the proteins involved in mitophagy in FAD1 iPSC-derived neurons.

Once FAD1 neurons demonstrated similar autophagy alterations to what was observed in fibroblasts, we turned our attention to the proteins involved in mitophagy. Under basal conditions, FAD1 neurons revealed increased levels of PARK2 compared to healthy neurons (Fig. 34A-B).

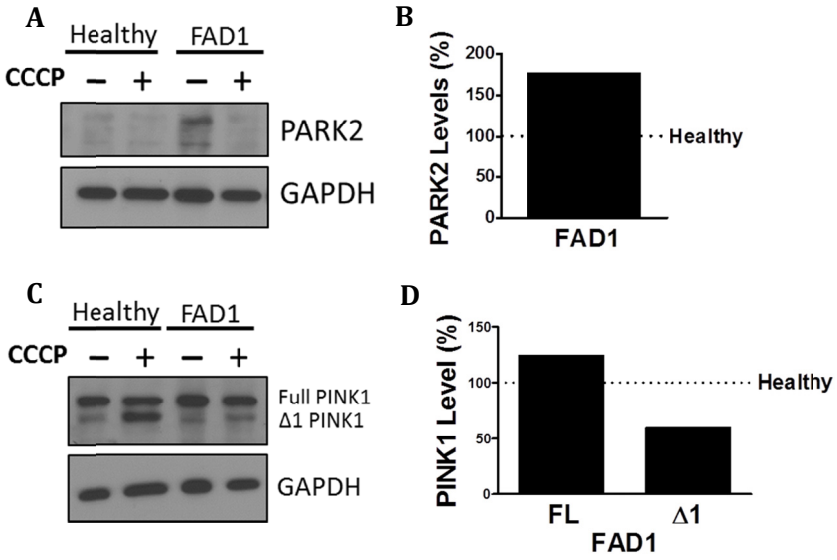

Figure 34. Deregulation of PARK2 and PINK1 proteins pattern in FAD1-derived neurons. A. Representative Western blot of PARK2 in healthy- and FAD1-derived neurons in the absence or presence of CCCP (20 μM) for 24h. **B.** Quantification of PARK2 levels under basal conditions. **C.** Representative Western blot of the expression of PINK1 in these neurons similarly treated. **D.** Quantification of the levels of FL-PINK1 and Δ1-PINK1 isoform in FAD1-derived neurons with respect to healthy ones in the presence of CCCP.

Surprisingly, FAD1 neurons exhibited elevated levels of FL-PINK1 in contrast to Δ1-PINK1 isoform which were diminished after the treatment with CCCP for 24h (Fig. 34C-D). In consonance, immunostaining displayed an elevated PARK2 localization on mitochondria in FAD1 neurons after 1h treatment with CCCP, similar to the situation founded in FAD1 fibroblasts (Fig. 35). This result was accompanied by markedly increased mitochondrial surface in FAD1 neurons respect to healthy controls (Fig. 36). All these result together suggest that, after CCCP treatment, FL-PINK1 was stabilized in dysfunctional mitochondria to where PARK2 was correctly recruited but, due to the previously

FAD1	Fibrob.	Neurons
LC3	+	+
Autophagy Flux		
Synthesis	–	+
Degradation	–	–
Lysosomes	-	+
CatB	ND	ND
pH	>	ND
PARK2		
Accumulation	+	++
Mito. targeting	+	+
PINK1		
Accumulation	–	+
Mito. targeting	ND	ND
Mito. accumulation	+	++
ΔΨm	<	ND

Table 6. Summary of results in FAD1 fibroblasts and FAD1 neurons. ND: not determined.

demonstrated defect in the degradation phase of autophagy, they were not able to be recycled causing the observed accumulation (**Table 6**).

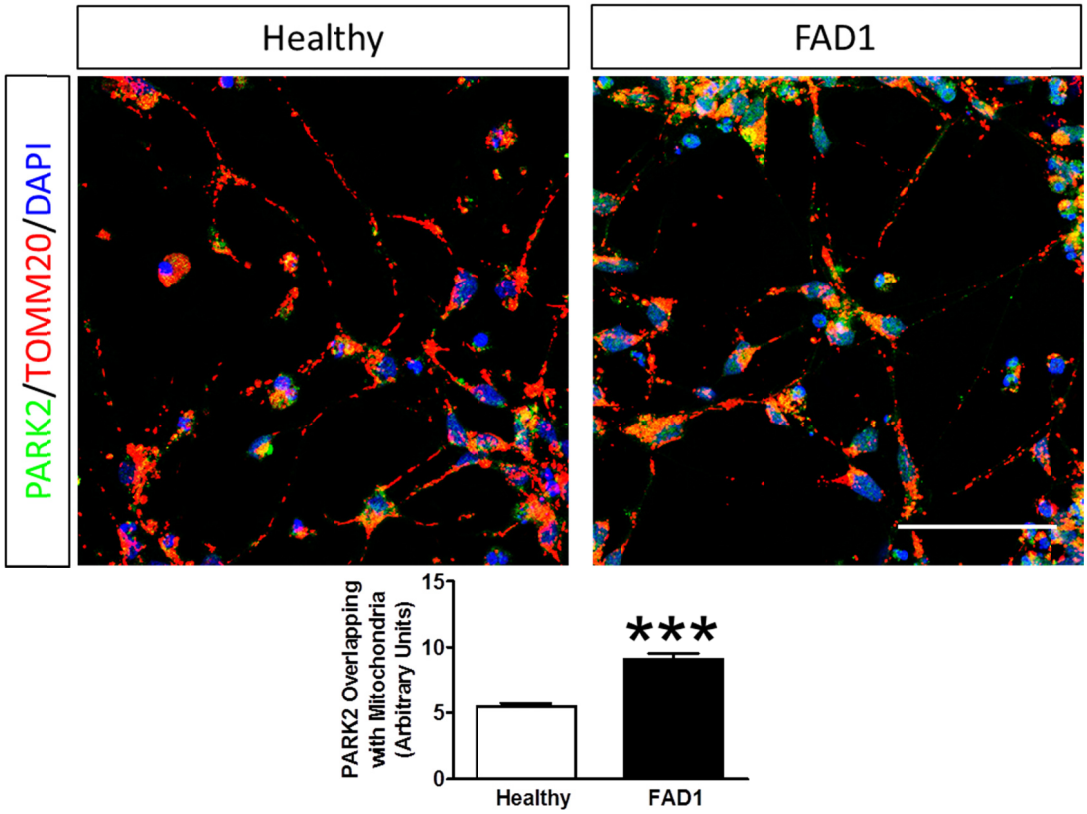

Figure 35. FAD1-derived neurons exhibited elevated PARK2 localization on mitochondria. Representative confocal microscopy immunofluorescence images showing PARK2 in green, TOMM20 in red and DAPI in blue of healthy- and FAD1-derived neurons treated with CCCP (20 µM) for 1h. Quantification of the colocalization between PARK2 and TOMM20 expressed as area occupied by the overlapping elements per cell. Scale bar: 100 µm. ****p<0.001*.

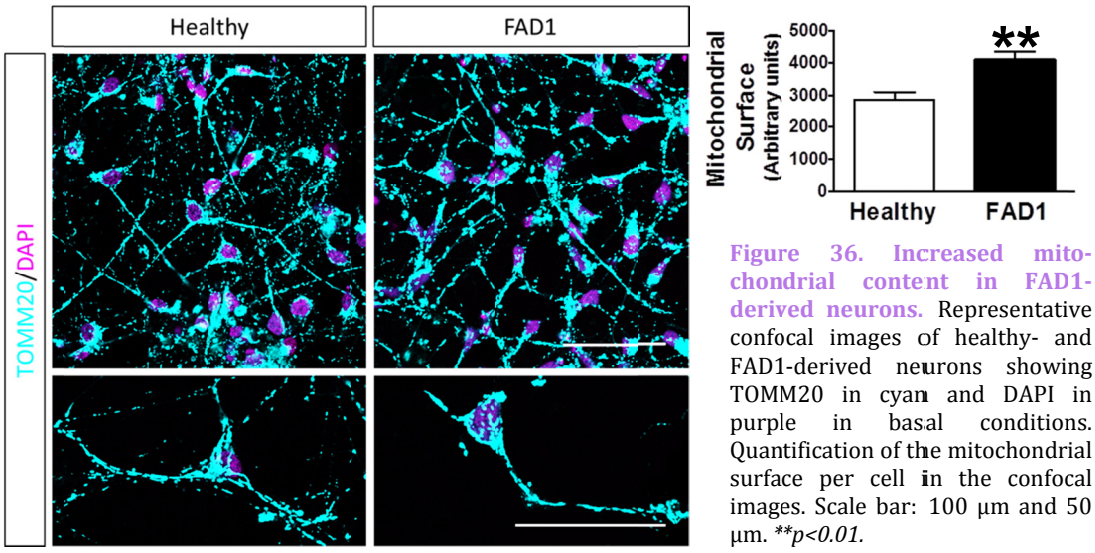

Figure 36. Increased mitochondrial content in FAD1-derived neurons. Representative confocal images of healthy- and FAD1-derived neurons showing TOMM20 in cyan and DAPI in purple in basal conditions. Quantification of the mitochondrial surface per cell in the confocal images. Scale bar: 100 µm and 50 µm. ***p<0.01.*

3. Mitophagy study in a model of sporadic Alzheimer disease.

The majority of AD cases have a sporadic etiology, in which the disease could arise through interactions among various genetic and environmental risk factors that potentially contribute to the pathology development (Stozicka et al, 2007). The leading AD molecular paradigm, the "amyloid cascade hypothesis", is based on studies of rare autosomal dominant variants and does not represent what initiates the most common late-onset sporadic form. It has been proposed for SAD a "mitochondrial cascade hypothesis" that posits mitochondrial dysfunction as primary pathology and comprehensively reconciles seemingly histopathologic and pathophysiologic features (Swerdlow & Khan, 2004).

Sporadic disease models are indispensable tools for understanding the molecular mechanisms that drive pathogenesis and enable the development of novel therapies. Although our ability to model diseases in mice is improving rapidly, owing to the advent of sophisticated molecular tools, sporadic diseases usually have a much more complex pathogenesis that can be difficult to model accurately. Therefore, search and study of SAD in a human model is the key to decipher the mechanisms underlying the pathology.

Taking into account these premises, the next step of this thesis consisted in the study of a possible impairment in the mitochondrial recycling in a human unmodified cell model of SAD that could support the important role of mitochondria in late-onset AD.

3.1 Study of mitochondrial recycling process in fibroblasts from sporadic AD patients.

Human fibroblast cell culture systems have been used to model both molecular events associated with the aging process and the biochemical anomalies found in AD. Our first goal was to evaluate the autophagy-mitophagy system function in human primary cell line of skin fibroblasts from SAD patients obtained from Coriell Institute as well as their correspondent age-matched healthy samples (Table 2).

3.1.1 Mitochondrial anomalies in SAD fibroblasts

Consistent with previous findings demonstrating increased ROS levels in familial AD fibroblasts (Naderi et al, 2006), we analyzed oxidation of proteins in fibroblasts from SAD patients compared with its correspondent age-matched healthy samples. Through OxyBlot analysis we observed that SAD cells showed an increased amount of oxidized proteins under basal conditions (Fig. 37). Abnormal mitochondrial distribution and morphology has been described in SAD fibro-

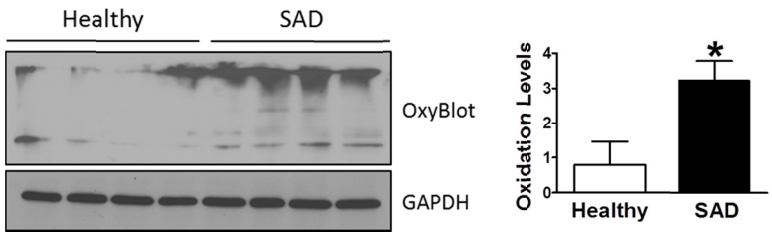

Figure 37. Increased oxidized proteins in SAD fibroblasts. Representative OxyBlot showing oxidized proteins of healthy and SAD fibroblasts in basal conditions and quantification of the whole set of data. n=4 healthy/AD sex- and age-matched couple samples; *p<0.05.

blasts (Wang et al, 2008a), therefore we studied a possible functional defect in mitochondrial dynamics by inducing a reversible process of mitochondrial fragmentation. Healthy and SAD cells, which had similar growth rates, were plated and infected with a lentivector encoding mito-DsRed2 for better mitochondria visualization. Fibroblasts were treated with CCCP for 6h, after which they were allowed to recover for 1h. These conditions induce a reversible depolarization of mitochondria without causing any toxic effect (Fig. 38A). Also, after 24h of CCCP treatment the viability of fibroblasts was not compromised (Fig. 38B).

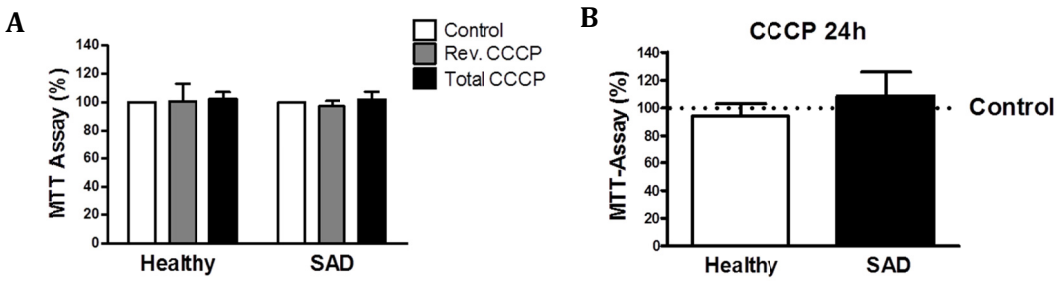

Figure 38. Viability of fibroblasts was not compromised during experimental conditions. A. MTT assay of healthy and SAD fibroblasts in a reversible treatment with CCCP (20 μM) for 6 h and then allowed to recover for 1 h (Rev.CCCP) or treated for 7h with CCCP (Total CCCP). **B.** MTT assay after the treatment with CCCP for 24h. n=4 healthy/AD sex- and age-matched couple samples.

The patterns of mitochondria were classified into three categories: filamentous, fragmented and intermediate (Fig. 39A). Analysis was carried out by the quantification of mitochondria shape in all the different experimental conditions (Fig. 39B-C-D-E). SAD and control cells exhibited similar mitochondrial patter under resting conditions (Fig. 39B-C) or after 7h treatment with CCCP (Fig. 39B-D). However, after the reversible challenge with CCCP, SAD fibroblasts exhibited significantly increased percentage of cells with fragmented mitochondria with respect to their correspondent healthy fibroblasts which showed a significantly higher proportion of cells that had recovered filamentous morphology (Fig. 39B-E). This result suggests a delayed recovery of mitochondrial filamentous morphology in SAD fibroblasts after a reversible insult. This observation was accompanied by a deregulation of proteins that control mitochondrial dynamics such as a decrease in fission DLP1 protein level, in SAD cells as it was previously described by Zhu and coworkers (Wang et al, 2008a) (Fig. 40A-B). DLP1 function depends on its subcellular localization (Smirnova et al, 2001) therefore we studied its distribution by immunofluorescence analysis of mitochondria labeled with TOMM20 (Fig. 40C). Quantitative analysis revealed a decrease of DLP1 on mitochondria in SAD

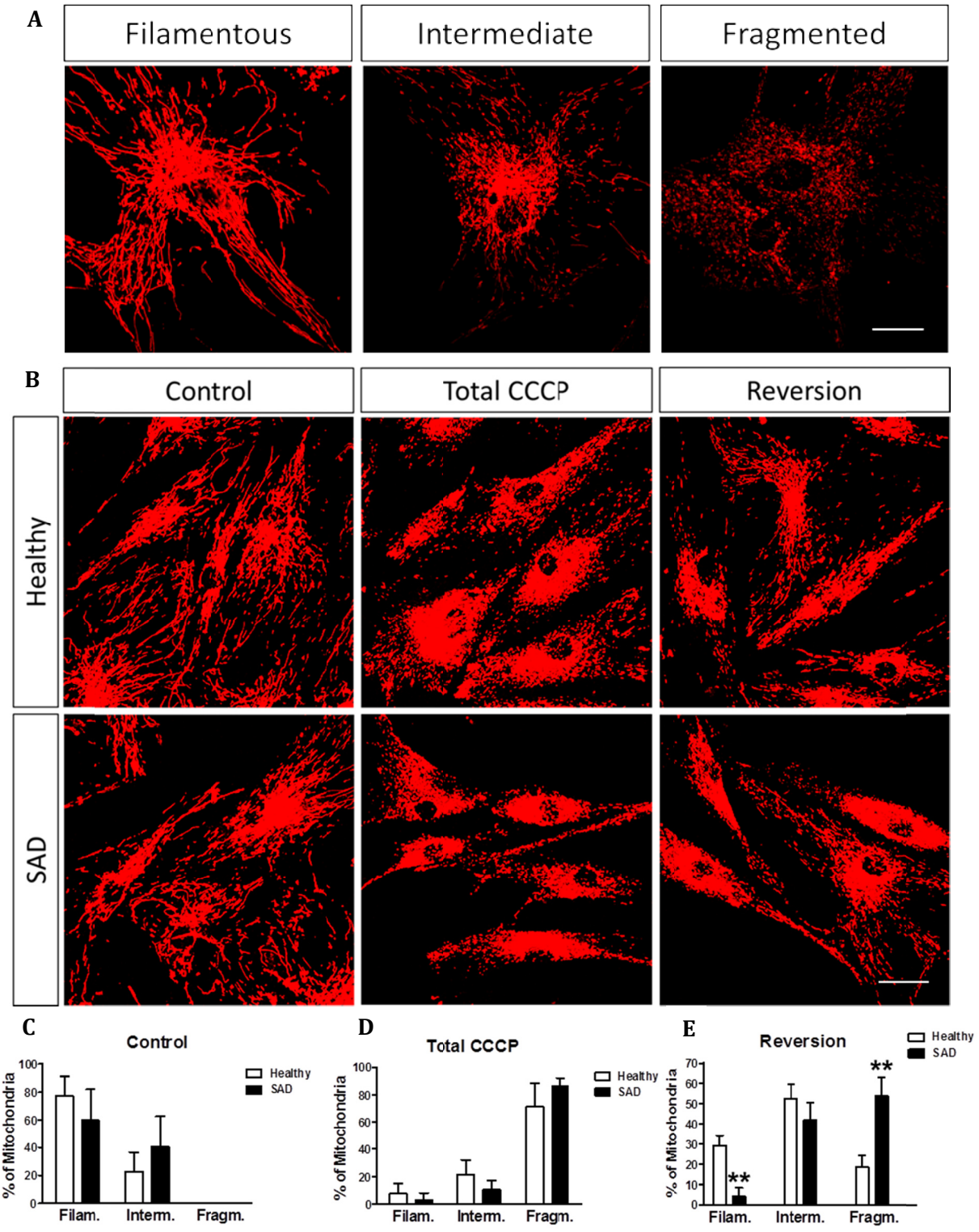

Figure 39 Mitochondrial dynamics alteration in SAD fibroblasts. A. Representative confocal microscopy images showing the three different mitochondrial morphologies in which they will be classified. **B.** Representative images showing the mitochondrial morphology of healthy and SAD fibroblasts untreated (Control) or after 7h with 20 µM CCCP (Total CCCP) or after 6 h treatment with CCCP followed by 1 h without it (Reversion). **C-E.** Quantification of mitochondrial morphology of healthy-SAD couples when the cells remain untreated (**C**) treated with CCCP for 7h (**D**) or reversibly treated with CCCP (**E**). n=3 different healthy/AD sex- and age-matched couple samples. Scale bar: 20 and 40 µm respectively. ***p<0.01*.

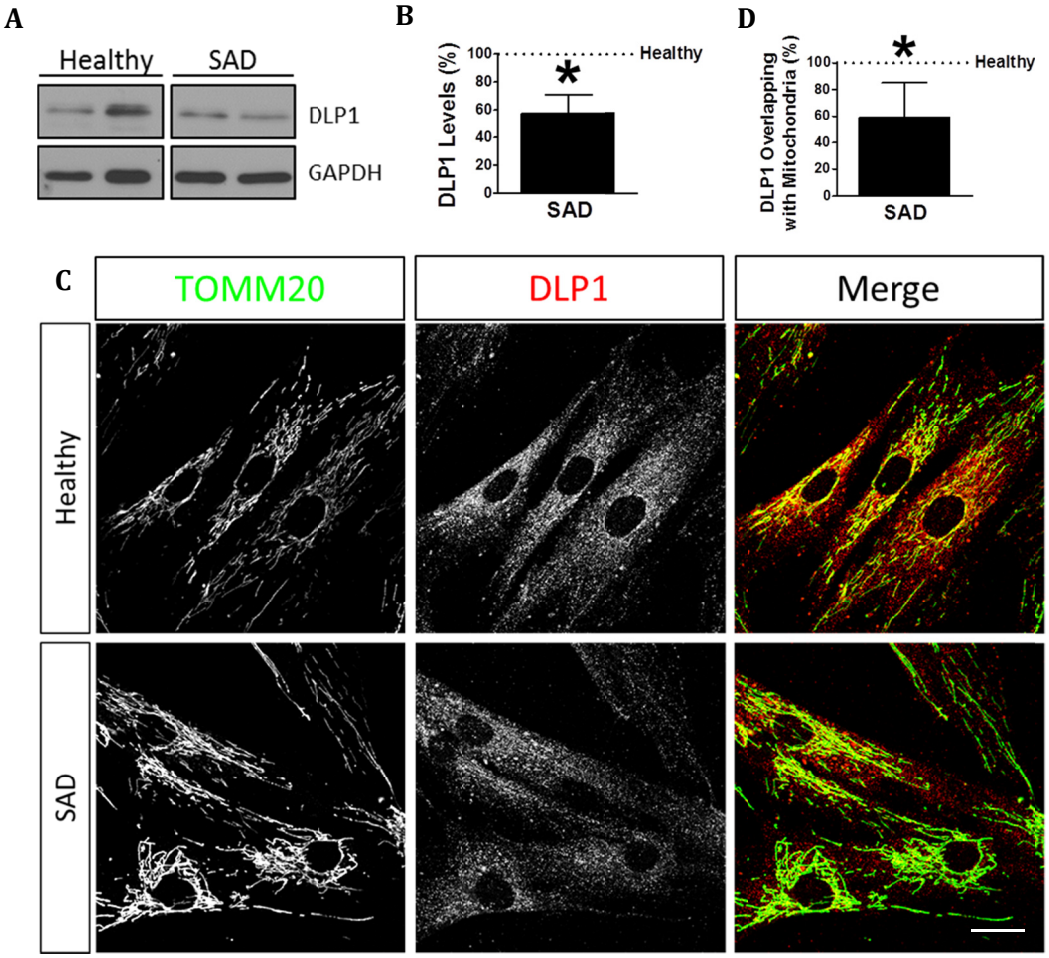

Figure 40. Decreased fission DLP1 protein level in SAD cells. A-B. Representative Western blot analysis and quantification of DLP1 protein in healthy and SAD fibroblasts under basal conditions. **C.** Representative confocal microscopy images showing TOMM20 in green and DLP1 in red in basal conditions. **D.** Quantification of the amount of DLP1 in mitochondria per cell in the images represented in (**B**). Graphs represent means and standard deviations of the healthy/AD age- and sex-matched couple samples (n=5). Scale bar: 40 μm. **p<0.05*.

fibroblasts compared to healthy ones (**Fig. 40D**). To determine whether altered mitochondrial dynamics showed in SAD fibroblasts may have functional consequences that might increase oxidative stress levels, we studied the ΔΨm recovery after the treatment with CCCP. Membrane potential recovery was higher in healthy cells compared to SAD ones, in which there was negligible recovery during the studied period (**Fig. 41A**). In parallel, we measured ATP content of the cells as functional readout of mitochondrial status (**Fig. 41B-C**). There were no differences in ATP levels between healthy and SAD samples (Fig. 5B). Accordingly, after CCCP challenge for 7h, similar ATP levels were observed (**Fig. 41C, Tot. CCCP**), indicating that after a long term CCCP exposure the cells activate other catalytic mechanisms to recover ATP homeostasis when the mitochondrial function is compromised. Additionally, the recovery of ΔΨm after the reversible treatment is an ATP demanding process as it can be inferred from the lower ATP levels in this condition in SAD cells (**Fig. 41C, Rev.**

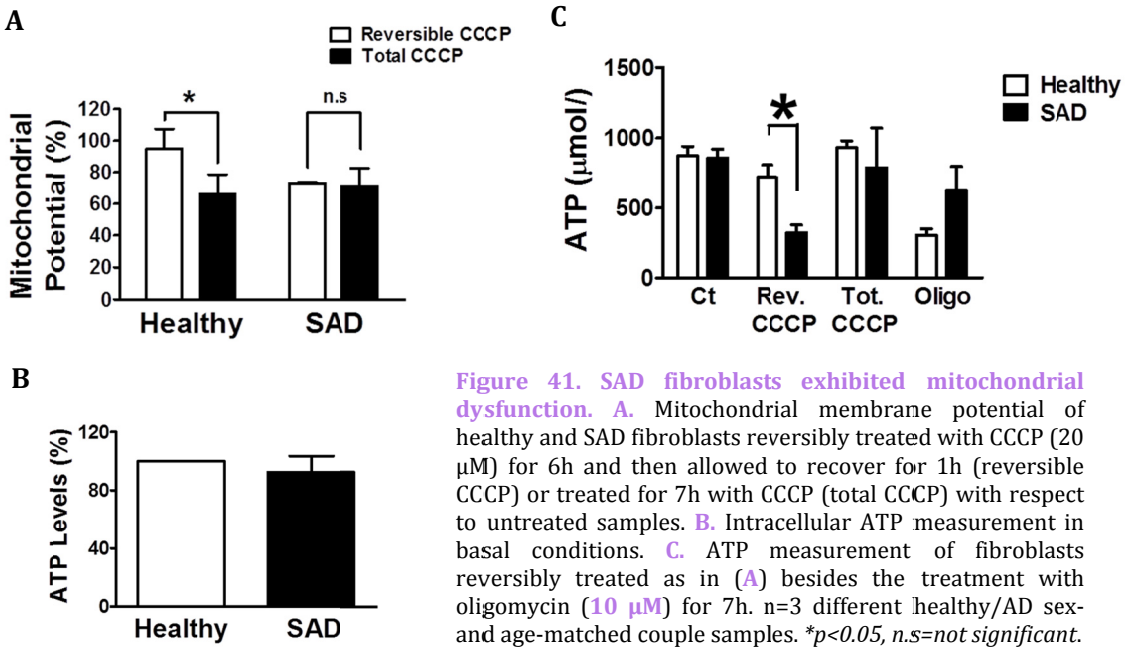

Figure 41. SAD fibroblasts exhibited mitochondrial dysfunction. A. Mitochondrial membrane potential of healthy and SAD fibroblasts reversibly treated with CCCP (20 µM) for 6h and then allowed to recover for 1h (reversible CCCP) or treated for 7h with CCCP (total CCCP) with respect to untreated samples. **B.** Intracellular ATP measurement in basal conditions. **C.** ATP measurement of fibroblasts reversibly treated as in (**A**) besides the treatment with oligomycin (**10 µM**) for 7h. n=3 different healthy/AD sex- and age-matched couple samples. **p<0.05, n.s=not significant.*

CCCP). On the contrary, healthy cells exhibited ATP levels close to the untreated condition indicating that mitochondrial function was recovered. As a control we used oligomycin that inhibits mitochondrial H^+-ATP-synthase causing the drop of ATP levels which was more evident in healthy fibroblasts indicating higher dependence on mitochondrial function in these cells to maintain ATP homeostasis (**Fig. 41C, Oligo**). Nonetheless, these cells exhibited higher levels of TOMM20 by immunofluorescence (**Fig. 42A-B**) and Western blot (**Fig. 42C**). As stated before, the increase of mitochondria content has been previously related with the impairment of mitochondrial recycling by autophagy (Kuo et al, 2012; Martinez-Vicente et al, 2010; Ozawa et al, 2013). Therefore, the observed accumulation of mitochondria joined to the alterations in mitochondrial dynamics and functional recovery strongly suggest a possible defect in mitophagy.

3.1.2 Autophagy alterations in SAD fibroblasts

Several studies have revealed autophagic vacuole (AV) accumulation affecting both neuronal and peripheral cells in AD (Cuervo, 2004; Lee et al, 2010; Nixon, 2005). We sought a possible defect in the process of autophagy in our SAD cells. To determine autophagy flux, both healthy and SAD fibroblasts were treated with CCCP for 24h followed by an additional treatment of NH_4Cl for 6h in the presence of CCCP. Surprisingly, Western blot analysis revealed a significantly diminished amount of AVs in SAD fibroblasts exhibiting a decrease in LC3II protein levels as well as lower levels of LC3II/LC3I ratio under basal conditions (**Fig. 43A-B**). Although all samples showed induction of AVs after CCCP treatment, we observed a reduction of autophagosome synthesis in SAD cells due to the significantly smaller LC3II accumulation compared to healthy samples after CCCP treatment when vacuole degradation is blocked by NH_4Cl (**Fig. 43C**). In contrast, we do not observe

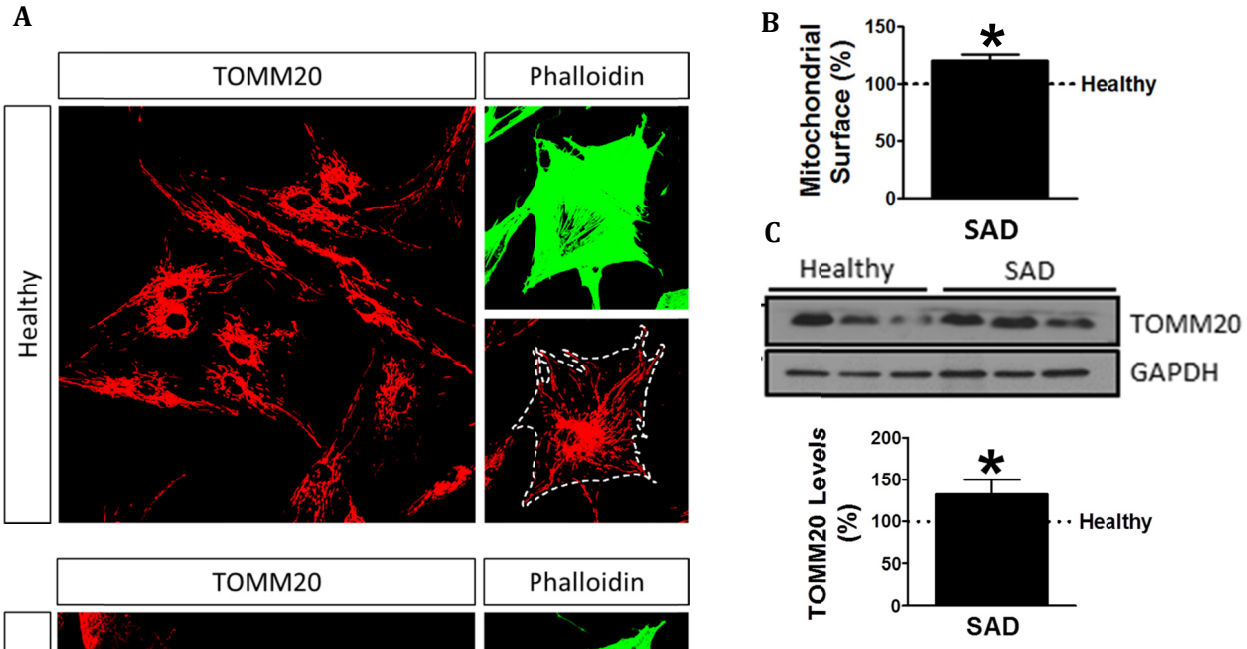

Figure 42. Increased mitochondrial content in SAD cells. A. Representative confocal images of healthy and SAD fibroblasts showing TOMM20 in red in basal conditions. Phalloidin staining was used to delineate the boundary of the cell represented by discontinuous line. **B.** Quantification of mitochondrial surface per cell in the confocal images shown in (**A**). **C.** Representative Western blot and quantification of TOMM20 expression under basal conditions. n=3 different healthy/AD sex- and age-matched couple samples. Scale bar: 20 and 40 μm respectively. **p<0.05*.

significant differences in LC3II degradation between SAD and healthy fibroblasts (Fig. 43D). This data suggests a decreased autophagy flux mainly due to a deficient in autophagic vacuole formation. To further study autophagic protein degradation we have studied p62 levels. Additionally, similar levels of p62 protein were observed in both SAD and healthy fibroblasts under basal conditions (Fig. 43E-F). Accordingly, accumulation of p62 was diminished in SAD samples although differences were not significant (Fig. 43G). Finally, the degradation of p62 was comparable in both samples confirming no differences in the degradation phase (Fig. 43H). Conversely, the levels of Beclin1 were not altered in SAD fibroblasts compared to healthy ones under basal conditions (Fig. 43I-J), as well as its induction and degradation (Fig. 43K-L) occurring during autophagy. Consistent with these autophagy alterations, we also detected a significant accumulation of ubiquitinated proteins in SAD cells (Fig. 44).

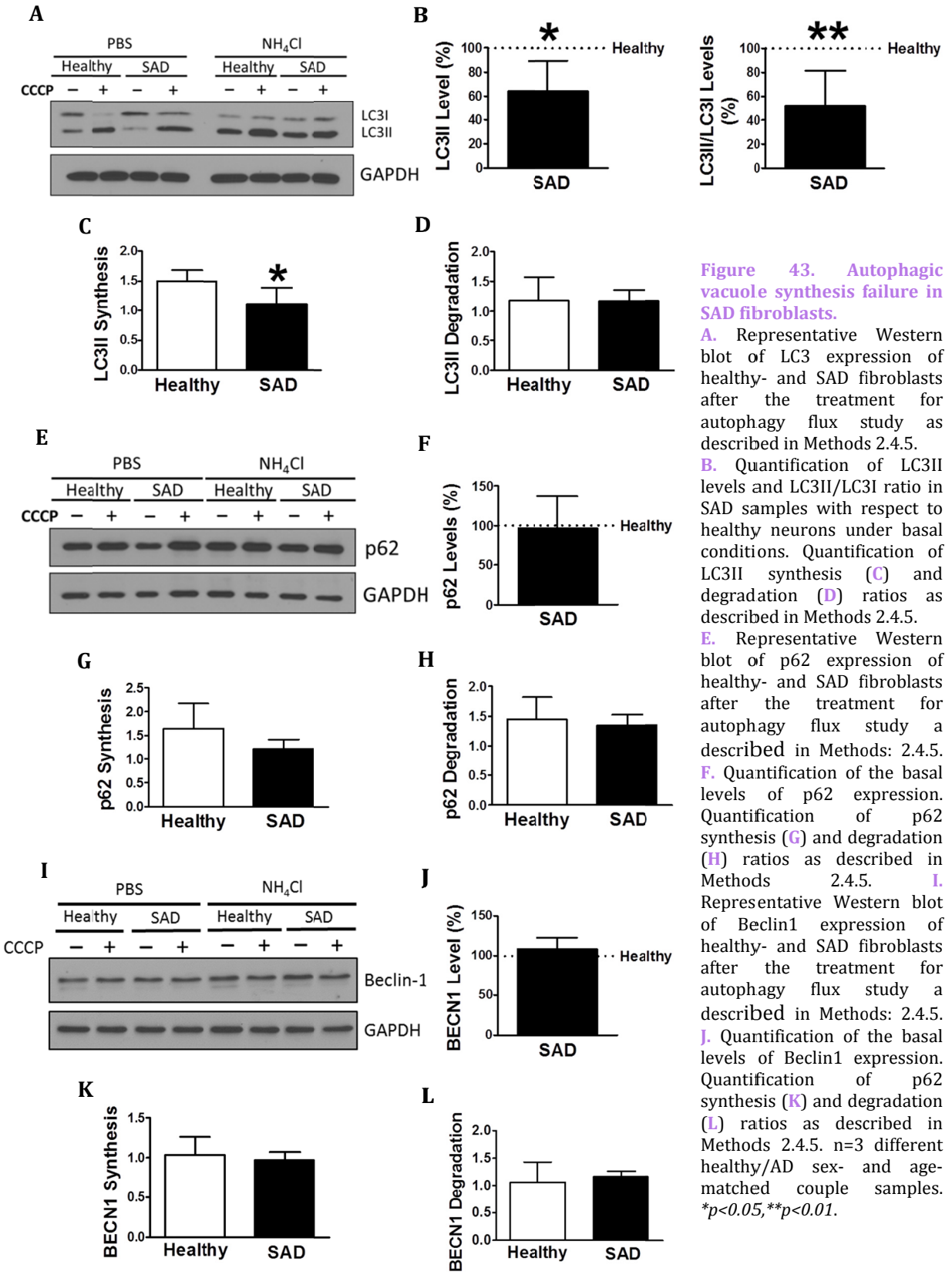

Figure 43. Autophagic vacuole synthesis failure in SAD fibroblasts.
A. Representative Western blot of LC3 expression of healthy- and SAD fibroblasts after the treatment for autophagy flux study as described in Methods 2.4.5.
B. Quantification of LC3II levels and LC3II/LC3I ratio in SAD samples with respect to healthy neurons under basal conditions. Quantification of LC3II synthesis (**C**) and degradation (**D**) ratios as described in Methods 2.4.5.
E. Representative Western blot of p62 expression of healthy- and SAD fibroblasts after the treatment for autophagy flux study a described in Methods: 2.4.5.
F. Quantification of the basal levels of p62 expression. Quantification of p62 synthesis (**G**) and degradation (**H**) ratios as described in Methods 2.4.5.
I. Representative Western blot of Beclin1 expression of healthy- and SAD fibroblasts after the treatment for autophagy flux study a described in Methods: 2.4.5.
J. Quantification of the basal levels of Beclin1 expression. Quantification of p62 synthesis (**K**) and degradation (**L**) ratios as described in Methods 2.4.5. n=3 different healthy/AD sex- and age-matched couple samples. **p<0.05,**p<0.01*.

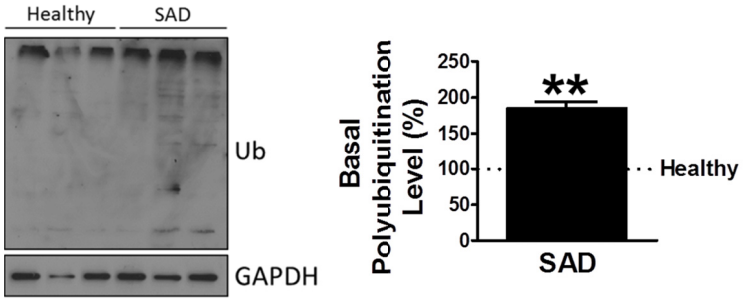

Figure 44. Increased ubiquitinated proteins in SAD fibroblasts. Representative Western blot and quantification of the basal levels of ubiquitinated proteins in healthy and SAD fibroblasts. n=3 different healthy/AD sex- and age-matched couple samples. ***p<0.01*.

3.1.3 Lysosomal alterations in SAD fibroblasts

As stated previously in this work, lysosomal function is fundamental for the degradative phase of autophagy, therefore we wanted to evaluate lysosomal properties in SAD cases. The pH of lysosomes was analyzed by using LysoTracker assay with and without the treatment with bafilomycin. Under basal conditions, SAD fibroblasts exhibited a lower capacity to retain LysoTracker probe suggesting an increase in pH (Fig. 45A). However, when we compared the LysoTracker label

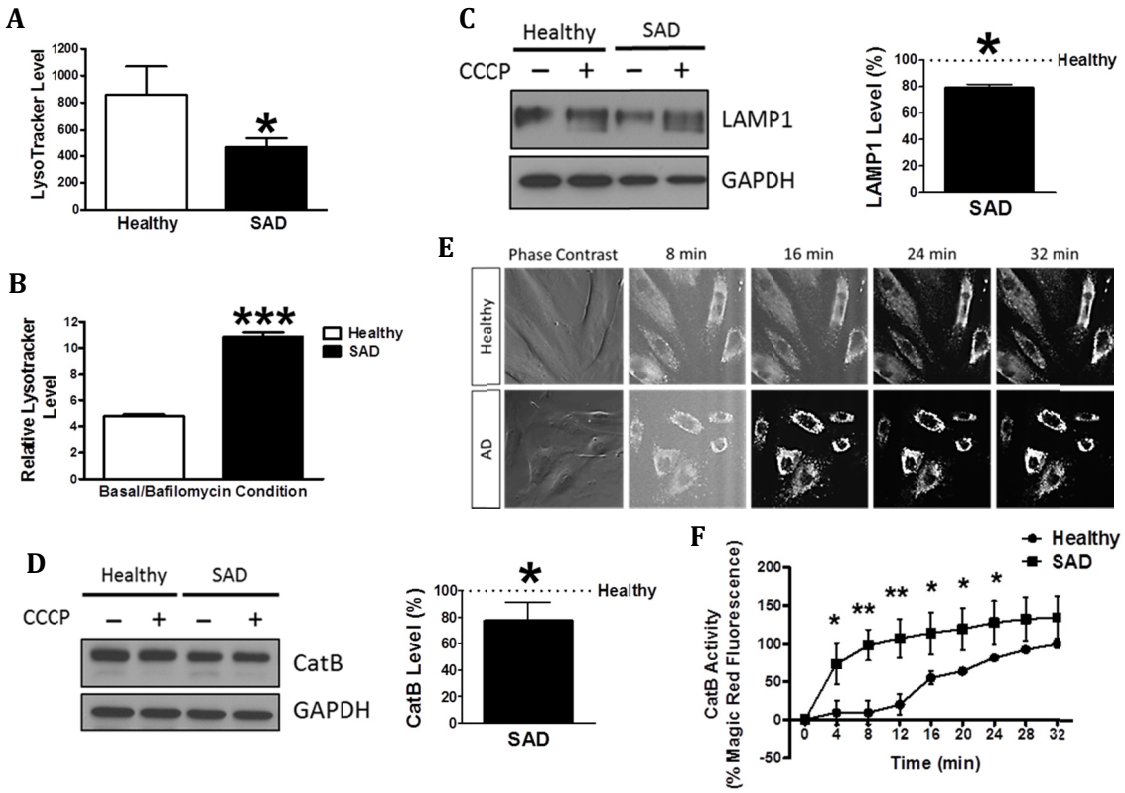

Figure 45. Lysosomal alterations in SAD fibroblasts. A. Quantification of the lysosomal content per cell in healthy and SAD fibroblasts. **B.** Quantification of the lysosomal acidity represented by the ratio between untreated and bafilomycin (100 nM) treated cells. **C.** Representative Western blot of LAMP1 protein in the absence or presence of CCCP (20 µM) for 24h and quantification of the levels under basal conditions. **D.** Representative Western blot analysis of Cathepsin B and quantification of the protein levels under basal conditions. **E.** Representative field of fibroblasts showing phase contrast and fluorescence images exhibiting the time course of intracellular Cathepsin B activity as red fluorescence. **F.** Cathepsin B activity along time. The activity was normalized by the maximum fluorescence detected in the last time point of the healthy sample. n=3 (except for C, n=4) different healthy/AD sex- and age-matched couple samples. Scale bar: 40 µm. **p<0.05,**p<0.01, ***p<0.001*.

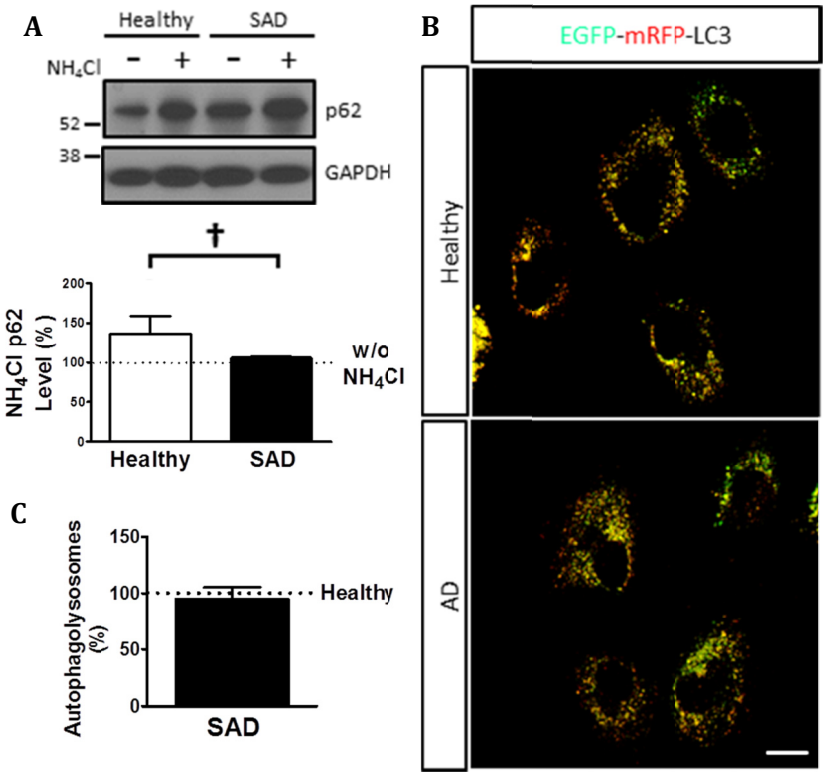

Figure 46. Lysosomal function was not affected in SAD fibroblasts.
A. Representative Western blot analysis of p62 and quantification of the levels in the presence of NH_4Cl with respect to the absence of NH_4Cl in healthy and SAD fibroblasts. **B.** Representative confocal microscopy images of these fibroblasts expressing mRFP-EGFP-LC3. **C.** Quantification of autophagolysosomes per cell corresponding to the percentage of only red structures. n=3 different healthy/AD age-matched couple samples. Scale bar: 40 µm. *$p<0.05$.

in basal conditions with respect to bafilomycin, SAD fibroblasts showed a higher ratio (Fig. 45B). These apparently contradictory results suggest that SAD fibroblasts had a small number of lysosomes but the pH of each lysosome is more acidic, giving higher ratio between basal and bafilomycin condition. We confirmed this hypothesis by studying levels of LAMP1, which was markedly lower in SAD cells, consistent with a diminished amount of lysosomes (Fig. 45C). On the other hand, the cysteine protease Cathepsin B levels were decreased in SAD cells (Fig. 45D). Conversely, activity was significantly increased in SAD fibroblasts compared to controls especially at short time points (Fig. 45E-F). A lower amount of Cathepsin B protein but increased activity confirmed our hypothesis of a lower amount of lysosomes but having each one lower pH. Despite these alterations, lysosomal function does not appear to be affected because, as previously stated, there were no differences in degradation phase of autophagy (Fig. 43D). Moreover, when lysosomal function was blocked we could observe the accumulation of p62 which is normally degraded by autophagy (Katsuragi et al, 2015) in both healthy and SAD samples leading to conclude that lysosomal was active in both cases (Fig. 46A). p62 accumulation was higher in healthy cells (Fig. 46A) probably due to a major autophagy induction in these samples (Fig. 43C). Accordingly, autophagolysosomes formation that depends on lysosomal function was similar in healthy and SAD cells (Fig. 46B-C).

3.1.4 Imbalance of PARK2 and PINK1 pattern in SAD fibroblasts

In agreement with our previous results that demonstrated alterations in mitochondrial dynamics and function as well as in autophagy and lysosomes, we hypothesize that a possible defect in mitochondrial recycling may take place in our SAD samples. Thus, we examined PARK2 protein

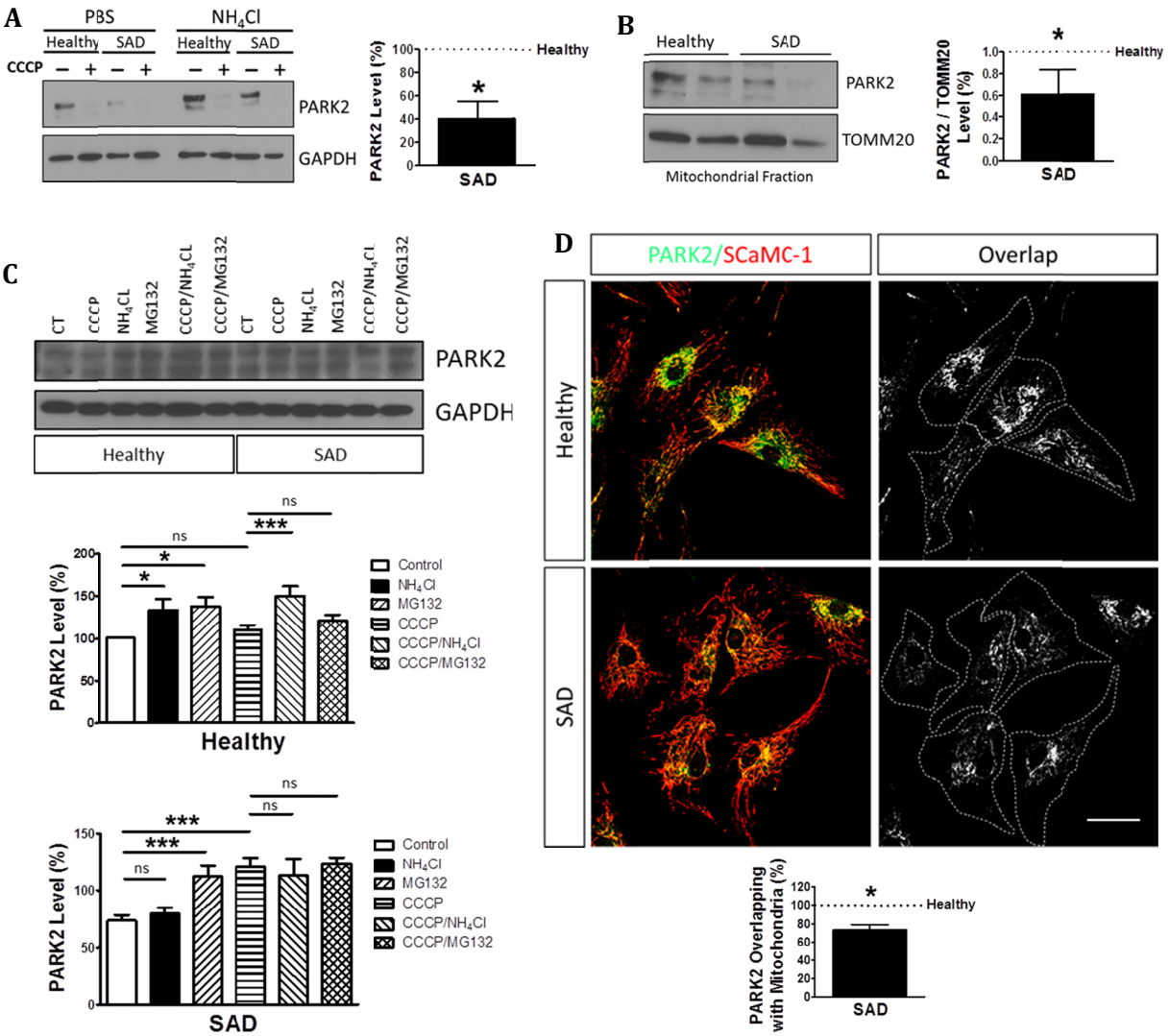

Figure 47. SAD fibroblasts showed imbalance PARK2 pattern and impairment of its degradation by autophagy. A. Representative Western blot of PARK2 expression in healthy and SAD fibroblasts treated with CCCP (20 µM) for 24 h followed by an additional treatment of PBS or NH_4Cl (15 mM) for 6 h and quantification of PARK2 expression under basal conditions. **B.** Representative Western blot and quantification of the mitochondrial fraction of cells treated with CCCP as indicated in (**A**) normalized by TOMM20 expression as a mitochondrial housekeeping marker. **C.** Representative Western blot and the correspondent quantification of PARK2 levels in cells treated for 3h with CCCP (20 µM) followed by 6h with NH_4Cl (15 mM) or 6 h MG132 (10 µM). **D.** Representative confocal microscopy immunofluorescence images showing PARK2 in green and SCaMC-1 as a mitochondria constitutive marker in red of fibroblasts treated with CCCP (20 µM) for 1h. On the right, binary image representing the colocalization of both labels and dotted line delimits cytoplasm of each cell according to phalloidin staining (not shown). Quantification of the colocalization between PARK2 and SCaMC-1 expressed as area occupied by the overlapping elements per cell. n=3 different healthy/AD sex- and age-matched couple samples. Scale bar: 40 µm. ns: not significant, **p<0.05, ***p<0.001*.

and we observed that PARK2 levels were substantially diminished in SAD cells (Fig. 47A). In addition, these cells showed a reduction in PARK2 levels in a mitochondria-enriched fraction compared with healthy samples (Fig. 47B). Degradation of PARK2 in resting conditions was mediated by autophagy and proteasome in healthy cells but, after mitophagy induction by CCCP, degradation was mainly by autophagy as it would be expected (Fig. 47C). In SAD samples, there was a significant accumulation of PARK2 after 3h of CCCP challenge that correlates with the previously

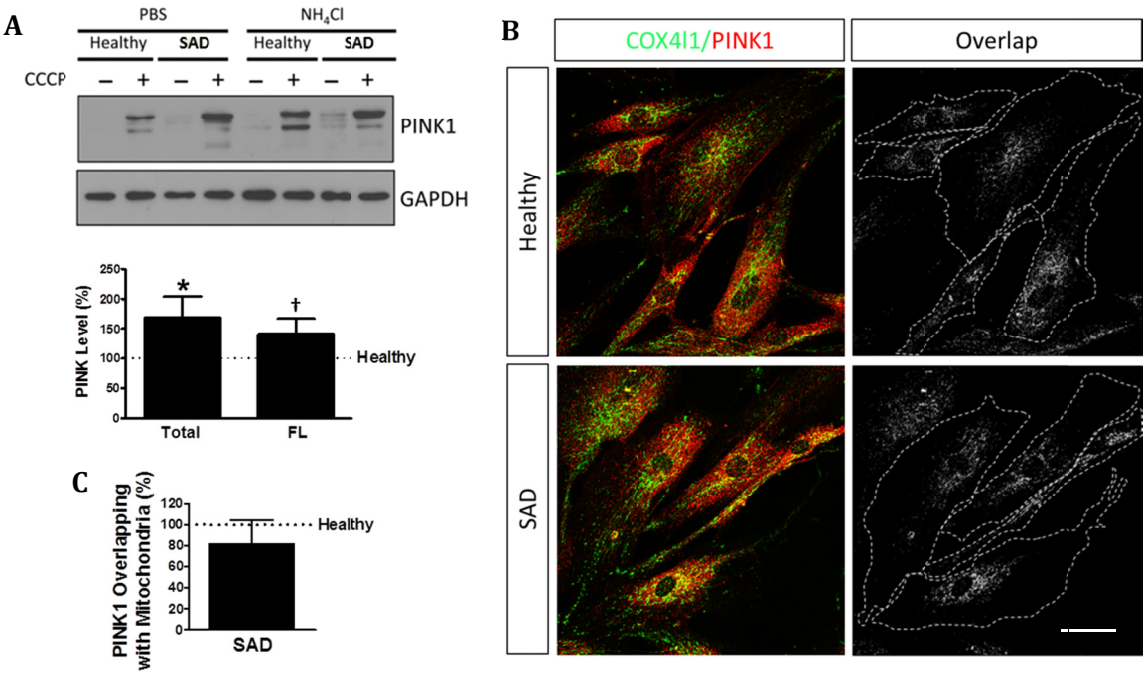

Figure 48. Imbalance of PINK1 pattern in SAD fibroblasts. **A.** Representative Western blot of the expression of PINK1 in healthy and SAD fibroblasts treated with CCCP (20 μM) for 24 h followed by an additional treatment of PBS or NH_4Cl (15 mM) for 6 h. Quantification of the levels of all isoforms of PINK1 (total) or only full length isoform (FL) in SAD fibroblasts in the presence of CCCP. **B-C.** Representative confocal microscopy immunofluorescence images and quantification showing PINK1 in red and COX4I1 as a mitochondria constitutive marker in green of fibroblasts treated with CCCP (20 μM) for 1h. On the right, binary image representing the colocalization of both labels and dotted line delimits cytoplasm of each cell according to phalloidin staining (not shown). n=4 (**A**) or n=3 (**B**) different healthy/AD sex- and age-matched couple samples. Scale bar: 40 μm. *†p< 0.08, *p<0.05*.

described failure in autophagy. Accordingly, in these cells there was no significant degradation of PARK2 mediated by lysosome. The recruitment of PARK2 to the mitochondria after CCCP treatment was significantly decreased in SAD fibroblasts suggesting a defective labeling of damaged mitochondria to be recycled by mitophagy (**Fig. 47D**). Additionally, both FL and all isoforms of PINK1 were significantly increased in SAD cells after a mitochondrial insult (**Fig. 48A**). However, immunofluorescence analysis of the stabilization of PINK1 in the mitochondria after CCCP challenge showed that there were no significant differences between SAD and healthy fibroblasts (**Fig. 48B-C**). Moreover, there was similar colocalization of PARK2 and PINK1 (**Fig. 49**), suggesting that PINK1 was able to recruit PARK2 in these conditions.

3.1.5 Cross-talk disruption between PINK1 and PARK2 by phosphorylation impairment in SAD fibroblasts

To determine whether phospho-PARK2 and phospho-PINK1 are deregulated in SAD fibroblasts we have performed a Phos-tag assay in which phosphorylated Ser, Thr, and Tyr are retained by a phosphate-binding tag shifting the electrophoretic mobility which is detected as slower migrating

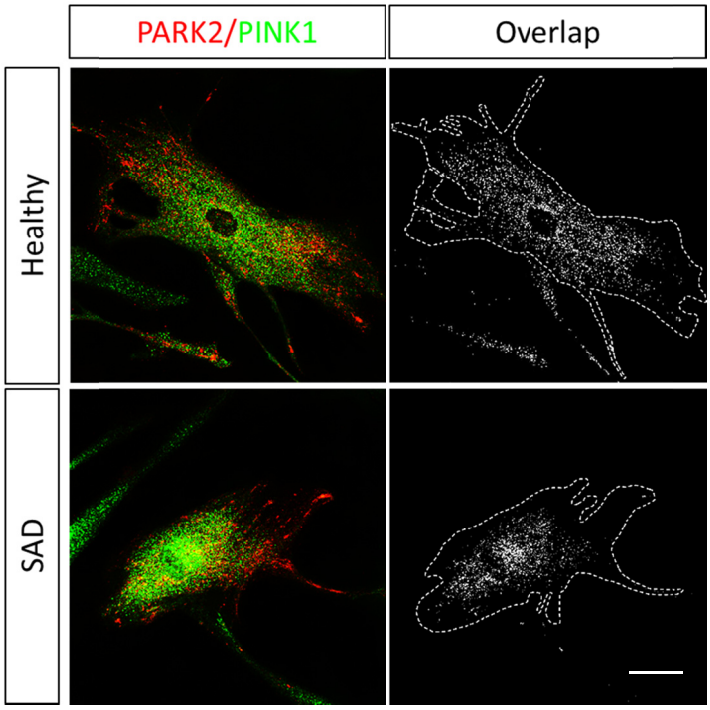

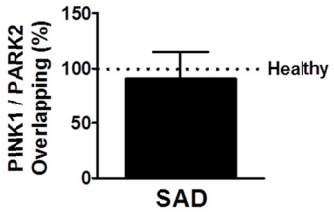

Figure 49. PINK1 was able to recruit PARK2 in SAD fibroblasts. Representative confocal microscopy immunofluorescence images showing PARK2 in red and PINK1 in green in healthy and SAD fibroblasts treated with CCCP (20 µM) for 1h. On the right, binary images representing the colocalization of both labels and dotted line delimits cytoplasm of each cell according to phalloidin label (not shown). Quantification of the colocalization between PARK2 and PINK1 expressed as area occupied by the overlapping elements per cell. n=3 different healthy/AD sex- and age-matched couple samples. Scale bar: 40 µm.

bands compared with the corresponding non-phosphorylated proteins ones (Fig. 50) (Kinoshita et al, 2006). Accordingly with our previous results, we observed that basal levels of non-phosphorylated PARK2 were significantly decreased in SAD cells (Fig. 50A-B). Phos-tag analysis revealed that, although there were no differences in PARK2 phosphorylation in basal conditions (data not shown), after 1h of CCCP treatment SAD fibroblasts exhibited a decreased PARK2 phosphorylation as well as a diminished phosphorylation ratio (Fig. 50C-D). In contrast, after CCCP challenge, non-phosphorylated FL-PINK1 isoform appeared to be significantly increased in SAD fibroblasts as we observed by conventional Western blot (Fig. 50E-F). Moreover, in these conditions, we detected an increased PINK1 phosphorylation and phosphorylation ratio in SAD cells with respect to healthy ones (Fig. 50G-H). After dissipation of ΔΨm, PINK1 auto-phosphorylation is fundamental for PARK2 recruitment and phosphorylation (Okatsu et al, 2012). Taking these results together, strongly suggests that there is a disruption of the crosstalk between PINK1 and PARK2. Although there is a stabilization and auto-phosphorylation of PINK1, the recruitment and activation of PARK2 was severely compromised and, consequently, a failure in the later processes of mitophagy promotes PINK1 accumulation in SAD fibroblasts. Remarkably, SAD cells exhibited significantly higher Δ1-PINK1 levels respect to the controls (Fig. 50I), which is known to inhibit PAKR2 translocation to the mitochondria (Fedorowicz et al, 2014). This data together with the deficit in the recruitment and activation of PINK1, strongly suggests an additional inhibition of PARK2 by cytosolic Δ1-PINK1 isoform that impairs its translocation to the mitochondria and subsequent activation

which in turn causes a deficit in mitophagy showed in the accumulation of damaged mitochondria and the increase of PINK1 in SAD fibroblasts (Fig. 51).

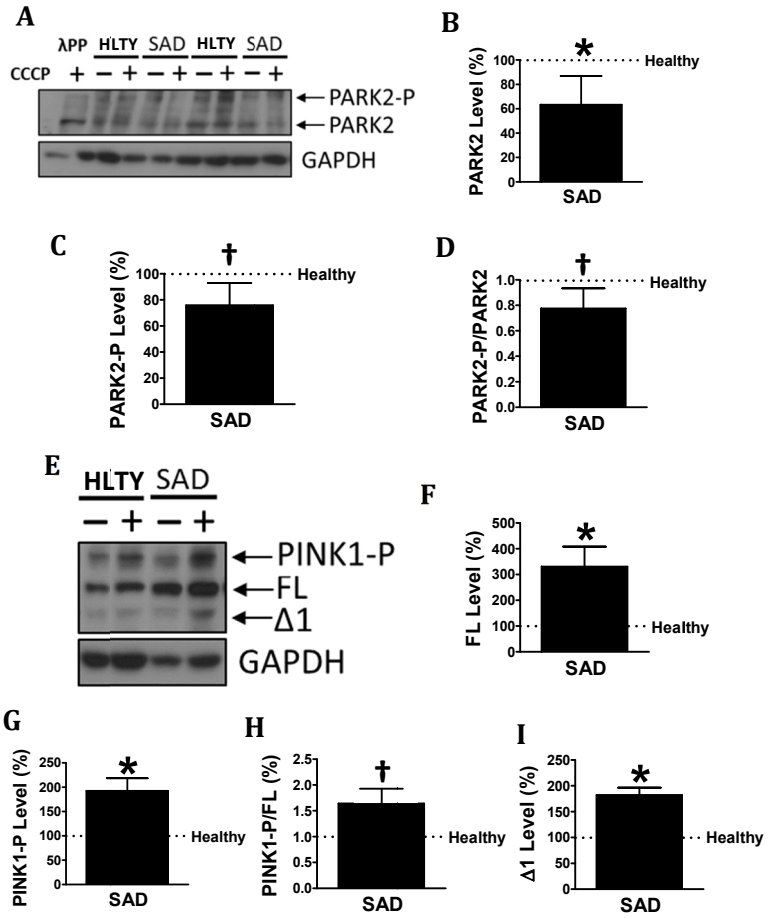

Figure 50. Mitophagy-related phosphorylation patter dysregulation in SAD fibroblasts. A. Representative Phos-tag Western blot showing PARK2 and GAPDH pattern of healthy (HLTY) and SAD fibroblasts treated or not with CCCP (20 μM) for 1h. Phosphorylated bands of PARK2 were confirmed by their disappearance after lambda protein phosphatase (λPP) treatment. **B.** Quantification of non-phosphorylated PARK2 levels in SAD samples with respect to the healthy ones under basal conditions. **C.** Quantification of PARK2 phosphorylation in cells treated with CCCP for 1h. **D.** Quantification of PARK2 phosphorylation ratio in the presence of CCCP represented as the relation of phospho-PARK2 with respect to non-phosphorylated PARK2 protein levels. **E.** Representative Phos-tag Western blot of PINK1 of fibroblasts treated as described in (**A**). **F.** Quantification of non-phosphorylated full-length PINK1 levels in fibroblasts treated with CCCP. **G.** Similar quantification of PINK1 phosphorylation levels in cells treated with CCCP. **H.** Quantification of PINK1 phosphorylation ratio of cells treated with CCCP similar to what was described for (**D**). **I.** Quantification of Δ1-PINK1 fragment under basal conditions. All graphs represent values corrected by GAPDH signal and normalized by each sex- and age-matched healthy sample (n=3). *†p< 0.08, *p<0.05.*

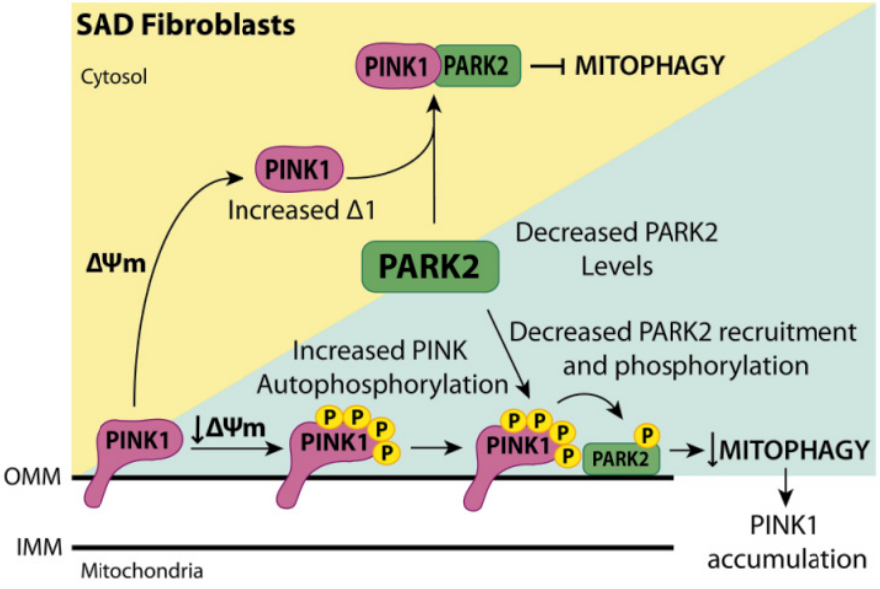

Figure 51. Schematic model representing the mitophagy failure in SAD cells. PARK2 can follow two different pathways in a mitochondrial membrane potential-dependent manner.

3.2 Study of mitochondrial recycling process in brains from sporadic AD patients.

Once we showed that fibroblasts are a good model to study mitophagy failure in SAD and our results were clear and robust, we wanted to know whether these alterations found in peripheral tissue could be representative of what it is taking place in the patient's brain. The translation of new findings from basic laboratory studies to human brain diseases relies heavily on the use of postmortem tissue.

Braak and Braak demonstrated that the progression of neurofibrillary pathology follow a characteristic pattern which, in turn, correlates with the stage of dementia in AD (Braak & Braak, 1991). This progression is used to classified AD in different stages. Neurofibrillary tangle accumulation starts at transentorhinal cortex (early-stage I and II), progresses to the entorhinal cortex, hippocampus, amygdala and temporal cortex adjacent (middle-stage III and IV) to finish with extensive spread throughout the cortex (late-stage V and VI). This should not be confused with the stage of senile plaque involvement, which progresses differently.

To carry out this work we used postmortem brain tissue from SAD patients classified according to their Braak stage as well as healthy control samples obtained from the brain bank of *Fundación CIEN* (Madrid) (Table 3).

3.2.1 Mitophagy alterations in SAD brain

It is well known that one of the brain structures mainly affected in SAD patients is the hippocampus (Braak & Braak, 1991), so we focused our study in this region. In contrast to what we observed in SAD fibroblasts (Fig. 47A), by Western blot we could not detect significant differences in PARK2 levels in hippocampus at early stages (Braak II-III) but at later stages (Braak V and VI) of the disease there was an increase of PARK2 being significant at Braak VI. (Fig. 52). On the contrary, the study of PINK1 showed an accumulation of this protein at the first stages on the disease (Braak II-III) (Fig. 53A-B-C). Accordingly to what we have

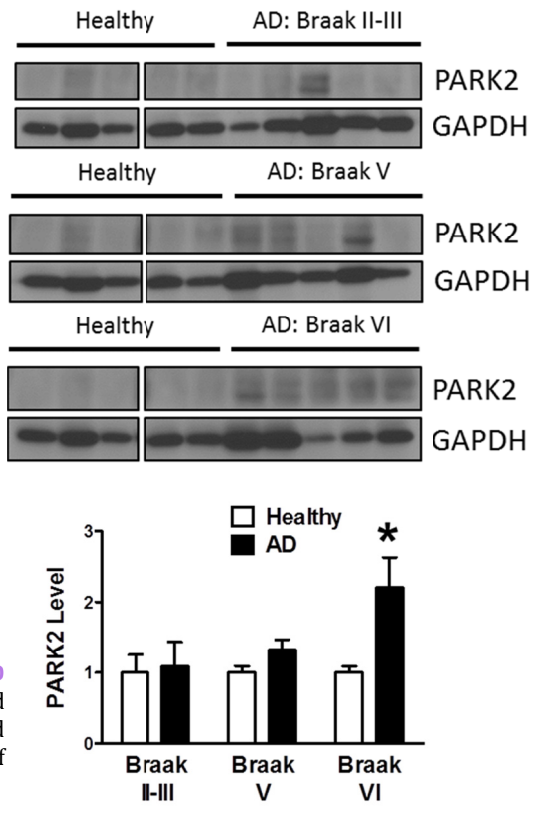

Figure 52. Increased PARK2 protein levels at late stage of AD in patient brains. Representative Western blot and quantification of PARK2 of human hippocampal samples divided accordingly to Braak stage compared to the same group of healthy donors. Healthy n=6; AD n=5). **p<0.05*.

described for SAD fibroblasts (Fig. 50E-I), we could also find an increase of Δ1 PINK1 fragment at early stages of the disease (Braak II-III) (Fig. 53D). This data strongly indicates that a similar inhibitory mechanism over PARK2 translocation may be taking place in the brain. Moreover, the study of TOMM20 showed an increase of mitochondrial content (Fig. 54), according to what we demonstrated for fibroblasts under basal conditions (Fig. 42C).

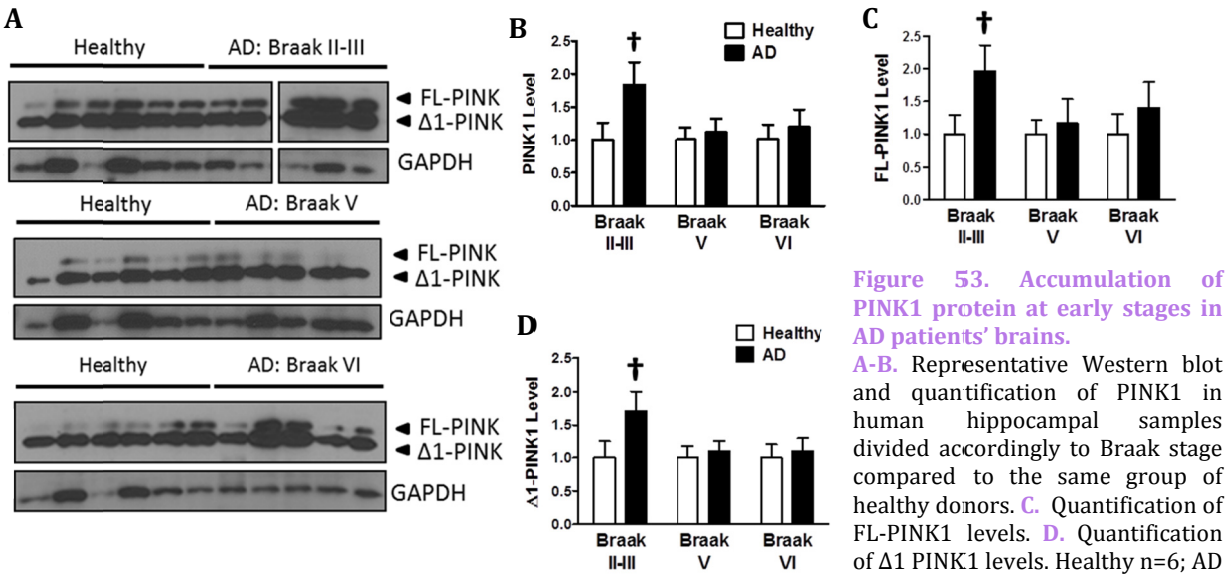

Figure 53. Accumulation of PINK1 protein at early stages in AD patients' brains.
A-B. Representative Western blot and quantification of PINK1 in human hippocampal samples divided accordingly to Braak stage compared to the same group of healthy donors. **C.** Quantification of FL-PINK1 levels. **D.** Quantification of Δ1 PINK1 levels. Healthy n=6; AD n=5). *†p< 0.08.*

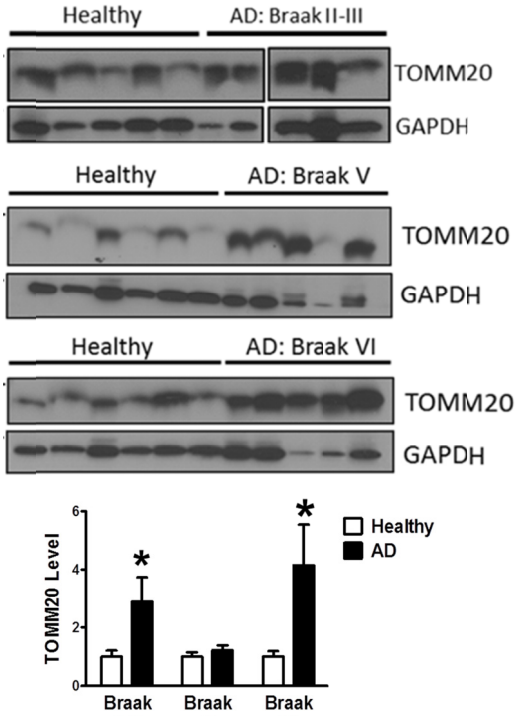

SAD	Fibrob.	Brain Early AD	Brain Late AD
LC3	–	ND	ND
Autophagy Flux			
Synthesis	–	ND	ND
Degradation	=	ND	ND
Lysosomes	–	ND	ND
CatB	+	ND	ND
pH	>	ND	ND
PARK2			
Accumulation	–	=	+
Mito. targeting	–	ND	ND
PINK1			
Accumulation	+	++	=
Mito. targeting	=	ND	ND
Mito. accumulation	+	++	++
ΔΨm	<	ND	ND

Table 7. Summary of results in SAD fibroblasts and AD brains. **ND:** not determined.

Figure 54. Mitochondrial accumulation at early and late stage of AD in patient brains. Representative Western blot and quantification of the levels of TOMM20 protein in human hippocampus samples divided accordingly to Braak stage compared to the same group of healthy donors. Healthy n=6; AD n=5. **p<0.05.*

3.2.2 Diminished gene expression of mitophagy-related proteins in AD patient brains

The analysis of *PARK2* expression levels by RT-qPCR showed similar RNA levels in AD and healthy brain (Fig. 55A). However, when a larger set of brain samples was used such in Hisayama study (Hokama et al, 2014), a reduction in *PARK2* RNA levels could be observed (Fig. 55E) correlating with decreased PARK2 protein levels exhibited by our fibroblasts. The absence of differences in *PINK1* RNA levels observed in our samples (Fig. 55B) or the reduction observed in Hisayama study (Fig. 55F) indicate that the protein accumulation of PINK1 was due to an impaired degradation rather than an excess of synthesis. Finally, although *TOMM20* RNA levels were significantly diminished in our brain samples (Fig. 55C) and in Hisayama study (Fig. 55G), the levels of 16S/MTNRN2 RNA (Fig. 55D), a mitochondrial DNA encoded constitutive protein which should be proportional to the amount mitochondria, were markedly increased. This clearly indicates higher mitochondrial content due to an accumulation rather than an increased synthesis. All these evidences together suggest that in brain samples there is a strong mitophagy alteration at early stages of the disease that may cause the accumulation of dysfunctional mitochondria similar to what we have described for fibroblasts (Table 7).

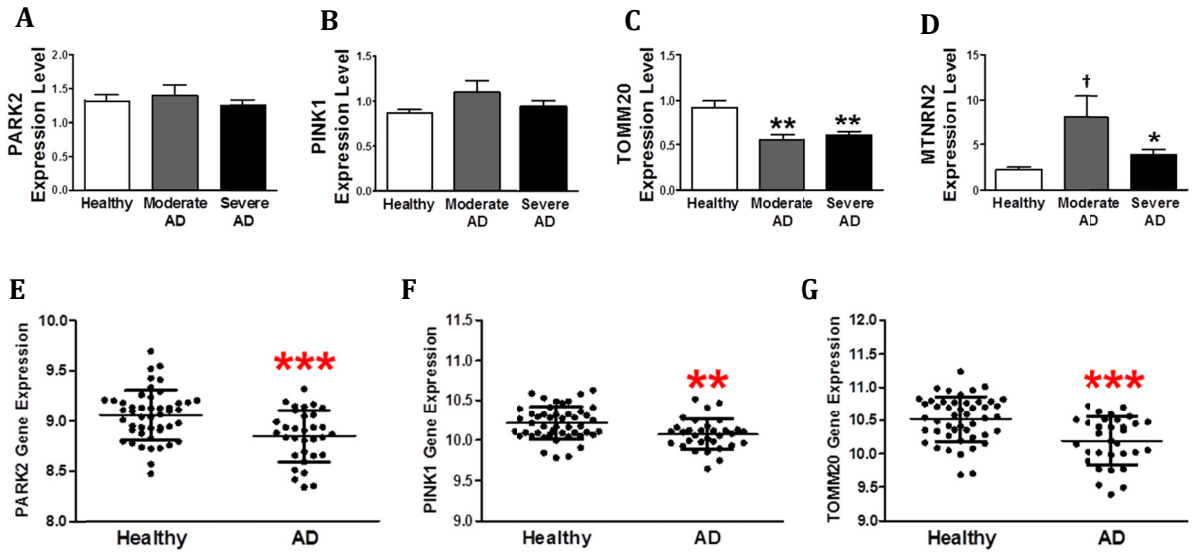

Figure 55. Altered gene expression of mitophagy-related proteins in AD patient brains. A-D Expression levels of PARK2 (A), PINK1 (B), TOMM20 (C) and MTNRN2 (D) measured by RT-qPCR in brain samples (Healthy n=6; AD n=5). **E-G.** Graphs show expression profiling by array (Affymetrix Human Gene 1.0 ST Array) of PARK2 (E), PINK1 (F), and TOMM20 (G) of human brain samples classified into healthy (n= 47) vs AD (n=32) retrieved from the Hisayama study. *†p< 0.08, *p<0.05, **p<0.01, ***p<0.001*.

3.3 *PARK2* overexpression as a potential therapeutic target in sporadic AD

Most adult-onset neurodegenerative diseases are characterized by the formation of protein inclusions or aggregates inside neurons that are autophagy substrates (Berger et al, 2006; Webb et al, 2003). Autophagy defects can occur at different stages of the pathway in different diseases, and this may influence treatment strategies. Autophagy may be impaired at both levels of autophago-

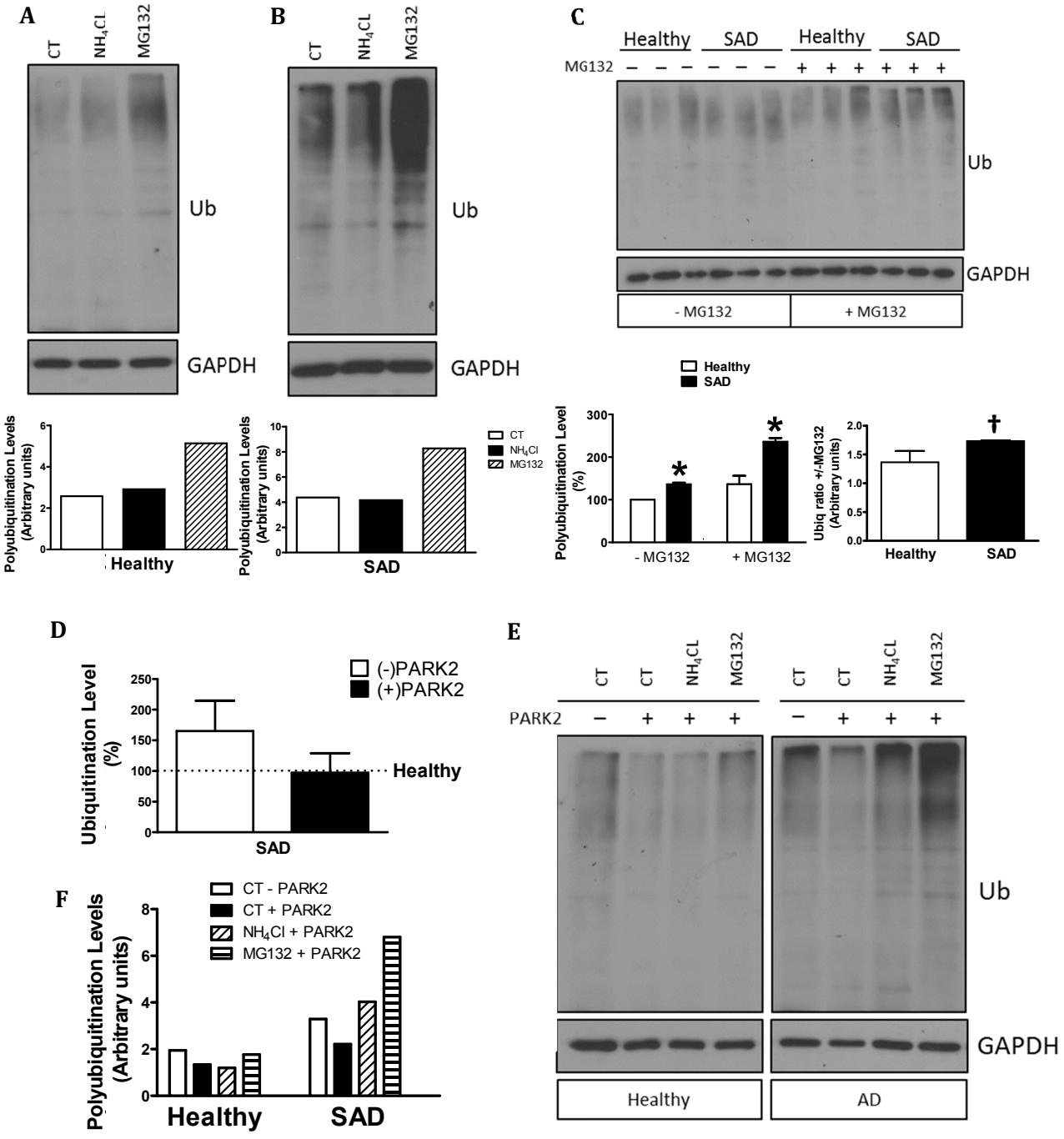

Figure 56. Study of polyubiquitinated protein degradation in healthy and SAD cells. **A.** Representative Western blot and quantification of ubiquitination levels after the treatment with NH_4Cl (15 mM) and MG132 (10 μM) for 6h in healthy fibroblasts. **B.** Similar analysis as in (**A**) in SAD fibroblasts. **C.** Representative Western blot and quantification of healthy and AD ubiquitination levels after the treatment with MG132 (10 μM) for 6h. **D.** Protein ubiquitination levels of SAD samples when they are infected or not with a lentivector encoding *WT PARK2*. **E-F.** Representative Western blot and quantification of ubiquitination levels when the cells were infected or not with a lentivector encoding *WT PARK2* and treated with NH_4Cl (15 mM) and MG132 (10 μM) for 6h. Results are normalized with respect to the levels found in the correspondent sex- and age-matched healthy fibroblasts (n=3). *†p< 0.08, *p<0.05.*

some degradation (Lee et al, 2010) and autophagosome formation (Pickford et al, 2008) in AD, even though these effects may vary according to the relevant genotype of the patients or the stage of the disease. There are different studies that revealed the possibility of upregulating autophagy to enable the clearance of intracytoplasmic aggregation proteins. Although it has been identified drugs that induce or inhibit autophagy it may be able to influence the clearance of autophagy substrates by acting not only on the autophagy pathway itself but also on processes influencing substrate recruitment (Orvedahl et al, 2011). Substrate recruitment may be influenced by altered activities of autophagy adaptor molecules that help to recruit substrates to autophagosomes (Dupont et al, 2010). By altering the levels of such adaptors, it is possible that modifications of these adaptors may be a more effective means of influencing substrate recognition. In order to investigate whether increa-

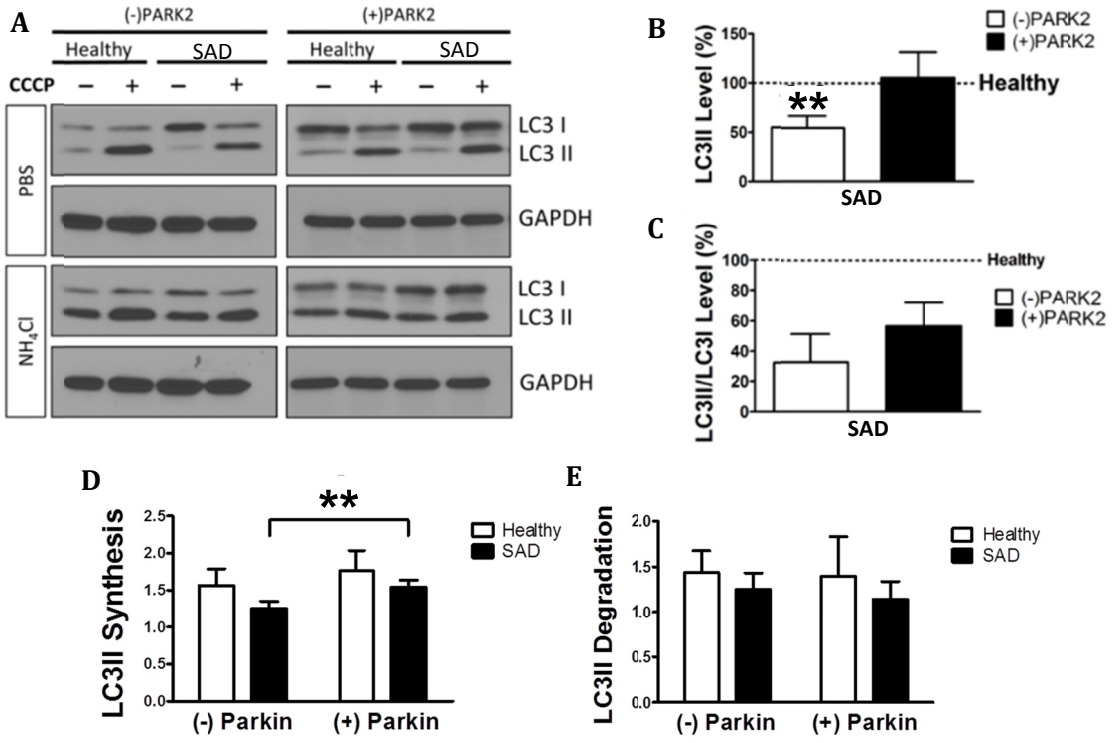

Figure 57. Improvement of autophagy process after PARK2 overexpression in SAD fibroblasts. **A.** Representative Western blot of LC3 expression in healthy and SAD fibroblasts infected with a lentivector encoding *WT PARK2*. Then, cells were treated to study the autophagy flux as described in Methods 2.4.5. **B-C.** Quantification of the levels of LC3II (**B**) or LC3II/LC3I ratio (**C**) of SAD fibroblasts infected or not with a lentivector encoding *PARK2* under basal conditions. **D-E.** Quantification of LC3II synthesis (**D**) and degradation (**E**) ratio as described in Methods 2.4.5. n=3 different healthy/AD sex- and age-matched couple samples. **p<0.05, **p<0.01*.

sing the levels of PARK2 would be able to modulate the observed autophagy defect in sporadic SAD cells, we induced the overexpression of *PARK2* by a lentivector encoding wild type *PARK2* in healthy and SAD fibroblasts. Being PARK2 an ubiquitin ligase, we first focus our attention in polyubiquitinated proteins turnover which may be recycled via proteasome as well as via autophagy. In our fibroblasts, degradation of polyubiquitinated proteins was mainly mediated by proteasome and, only in healthy cells, there was a slight contribution of autophagy (**Fig. 56A-B**). Proteasome-mediated degradation flux is higher in SAD samples probably due to compensatory mechanism to counteract autophagy impairment in these samples (**Fig. 56C**). Surprisingly, although PARK2 is an ubiquitin ligase, its overexpression in SAD fibroblasts, far from increasing ubiquitination levels, decreased them to the levels found in healthy samples (**Fig. 56D**). This can be explained because *PARK2* overexpression favored ubiquitinated proteins degradation by autophagy and proteasome especially in SAD samples (**Fig. 56E-F**).

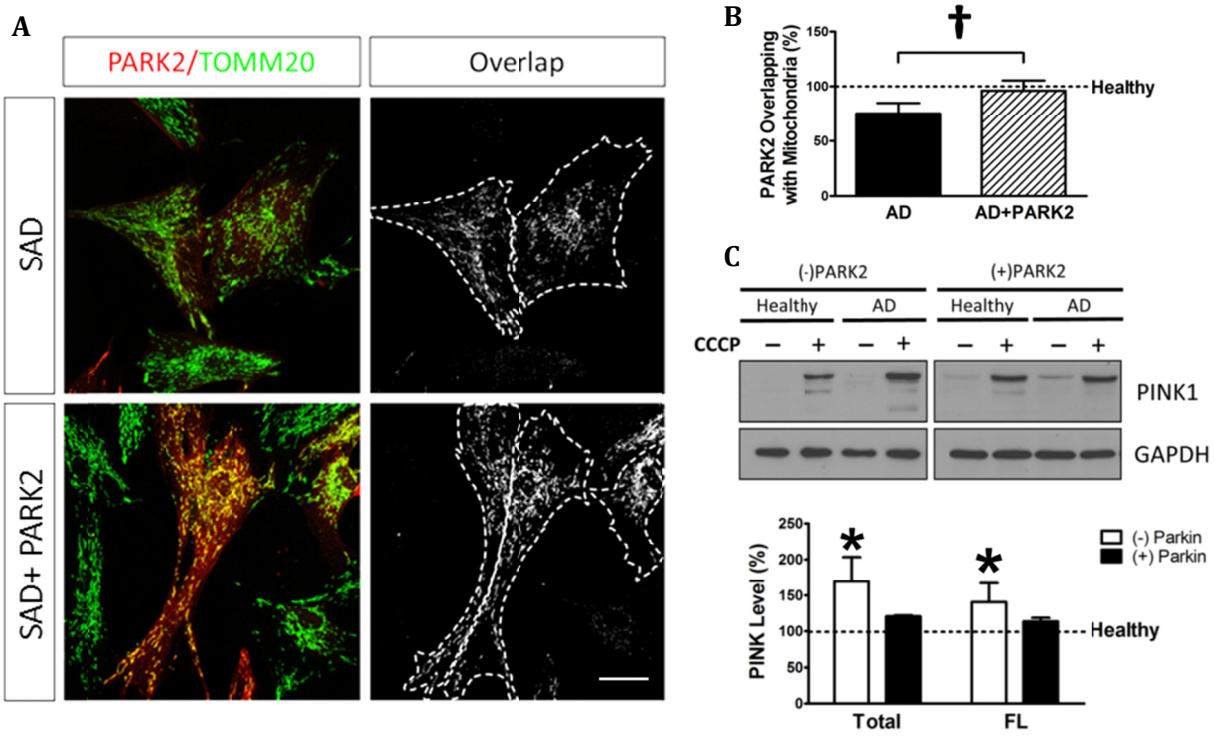

Figure 58. *PARK2* overexpression compensates mitophagy deficiency proteins in SAD cells. A. Representative confocal microscopy immunofluorescence images showing PARK2 in red and TOMM20 as a mitochondria constitutive marker in green of healthy and SAD fibroblasts infected with a lentivector encoding *PARK2* treated with CCCP (20 µM) for 1 h. On the right, binary images representing the colocalization of both labels and dotted line delimits cytoplasm of each cell according to phalloidin label (not shown). **B.** Quantification of the colocalization between PARK2 and TOMM20 expressed as area occupied by the overlapping elements per cell. **C.** Representative Western blot of PINK1 expression in fibroblasts treated with CCCP for 24h, when indicated, infected or not with a lentivirus encoding PARK2. Quantification of the levels of total and full length (FL) PINK1 in the cells treated with CCCP with respect to the correspondent healthy sample treated with CCCP. n=3 (**A-B**) or n=4 (**C**) different healthy/AD sex-and age-matched couple samples (n=3). *†p< 0.08, *p<0.05*.

We next analyzed a putative improvement of autophagy process after *PARK2* overexpression. In fact we could observe a restauration of the basal levels of AVs in SAD samples what was shown in the increase of LC3II protein levels up to the ones observed in healthy samples (**Fig. 57A-B**). However, the induction of AVs represented by the LC3II/LC3I ratio, were not significantly increased (**Fig. 57C**). Noteworthy, we also could observe a significant improvement of AV synthesis (**Fig. 57D**). This also correlates with the increased degradation of polyubiquitinated proteins via autophagy observed (**Fig. 56E**). On the other hand, the autophagosome degradation after *PARK2* overexpression maintains similar levels to the ones found in the absence of *PARK2* in both SAD and healthy fibroblasts (**Fig. 57E**), highlighting that the improvement of autophagy flux is due to an increase in AV generation.

Then, we assessed the possible effects of *PARK2* overexpression in mitophagy process. *PARK2* transduction improved the targeting of PARK2 to the mitochondria after CCCP treatment in SAD fibroblasts (**Fig. 58A**). Additionally, the accumulation of either total or full length isoforms of PINK1 in SAD samples was reduced after *PARK2* overexpression to levels closer to the ones observed in healthy cells (**Fig. 58B**). Remarkably, PARK2 enhancement allowed a significant mitochondrial function improvement indicated by the ΔΨm recovery in SAD cells after a reversible CCCP challenge (**Fig. 59A**) which was negligible when they were uninfected (**Fig. 41A**). Finally, we could observe that the accumulation of TOMM20 label in SAD fibroblasts in basal conditions was restored by *PARK2* overexpression up to healthy levels (**Fig. 59B-C**). Moreover, in normal conditions or after CCCP treatment there was a clear recycling of mitochondria by lysosomal degradation in healthy samples that was not observed AD samples where there was an accumulation of mitochondria (**Fig. 59D**). But *PARK2* overexpression dramatically improved mitochondrial recycling bypassing the impairment due to NH_4Cl treatment (**Fig. 59E**). Overall, these data indicate that *PARK2* overexpression compensates autophagy deficiency and restores mitophagy in SAD fibroblasts.

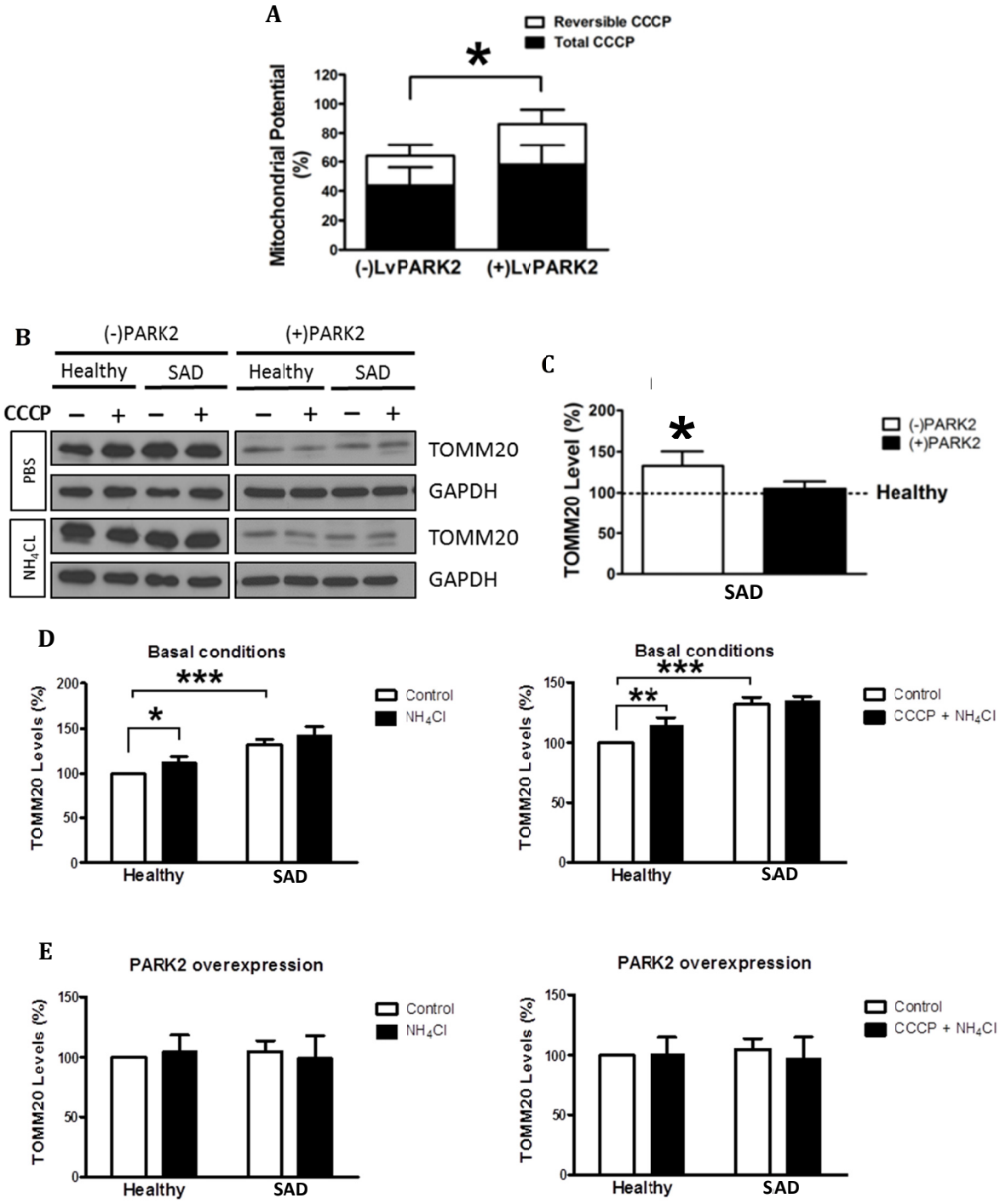

Figure 59. PARK2 overexpression restored accumulation of dysfunctional mitochondria in SAD fibroblasts. **A.** Mitochondrial membrane potential of SAD fibroblasts treated with CCCP (20 μM) for 6h and allowed then to recover for 1h (reversible) or treated for 7h with CCCP (total) when the cells were infected or not with a lentivector encoding *WT PARK2*. **B.** Representative Western blot of TOMM20 expression in healthy and SAD fibroblasts infected with a lentivector encoding *WT PARK2*, when cells were treated as described in Methods 2.4.5. **C.** Quantification of the levels of TOMM20 of SAD fibroblasts infected or not with a lentivector encoding *PARK2* with respect to the healthy fibroblasts under basal conditions. **D.** Quantification of Western blot showing the levels of TOMM20 under basal condition, after treatment with NH_4Cl or CCCP plus NH_4Cl. **E.** Quantification of Western blot showing the levels of TOMM20 when PARK2 is overexpressed after treatment with NH_4Cl or CCCP plus NH4Cl. n=3 different healthy/AD sex- and age-matched couple samples. **p<0.05, **p<0.01, ***p<0.001*.

Discussion

1. Peripheral vs neuronal models for the study of Alzheimer disease: Is there a peripheral failure in AD?

Fibroblasts offer us an accessible cell source that can be obtained by a small skin biopsy from living patients. Furthermore, skin fibroblasts represent a model of primary human cells, involving the chronological and biological aging of patients according to their genetic and environmental predisposition factors. However, it is imperative to demonstrate that fibroblasts retain certain hallmarks of the disease, and, being the skin a tissue that is not affected in AD pathology, this is not a trivial issue. Several works have previously demonstrated that fibroblasts exhibit oxidized proteins accumulation and mitochondrial anomalies that can also be found in AD brain (Wang et al, 2014b). Moreover, accumulation of Aβ has been also demonstrated in these cells (Citron et al, 1994). It is well known that the loss of mitochondrial membrane potential with the uncoupler ionophore CCCP induces autophagic clearance of mammalian mitochondria (Narendra et al, 2008). In this thesis, we have demonstrated a deregulation in the proteins involved in the degradation of mitochondria under basal conditions, even though the activation of this process by the treatment with CCCP helped us to elucidate the mechanisms underlying the pathogenesis exacerbating the possible differences between AD and healthy cells. For biochemical studies, the ability to depolarize the mitochondria in a cell culture with CCCP has clear advantages (Narendra et al, 2008; Wang et al, 2011). It has been well demonstrated that endogenous PARK2 is able to be recruited to the mitochondria after 1h of CCCP treatment besides the induction of autophagy system (Narendra et al, 2008). The concentration and time of the treatment should be optimized depending of the cell type as well as the items to be addressed in each specific experiment. Thus, by immunostaining and biochemical methods is possible to analyze the subcellular location and interaction of the variety of proteins involve in mitophagy/autophagy process.

Fibroblasts are a good tool for the study of the disease but it should be kept in mind that there are several important differences between peripheral cells and neurons. The differences in metabolic energy cost exhibited by these cells are substantial (Savage et al, 2007). Epithelial cells require a high metabolic rate for the frequent replacement to maintain function, turning over rapidly with many cell divisions to replace cells during the lifespan of the organism, but neurons are among the most metabolically active cells in the body and require constant maintenance due to the complexity of the molecular signaling that have. Fibroblasts reflect cumulative cell damage at the age of the patient, but the continuous replacement of these cells ameliorates the possible failure generated by the pathology. Although AD patients does not exhibit severe dermal changes, recently it has been published a work where patients with Rosacea, a chronic and potentially life-disruptive disorder primarily of the facial skin, have increased risk of dementia (Egeberg et al, 2016). On the other hand, neurons are cells which cannot be replaced and particularly sensitive to oxidative damage and protein aggregation. Thus, neurons require all the machinery involve in detoxification to

maintain cell homeostasis. Therefore, the susceptibility of these cells to proteopathy and oxidative stress, as the main features of AD, are determinedly higher than fibroblasts. Additionally, it is fundamental to considerate that gene expression profile and their signaling could vary due to the differences in the expression of APP and Tau, the proteins involve in AD, in these cell models. Although APP is expressed in many tissues and fibroblasts revealed expression of this protein, APP is mainly concentrated in AD neurons (Israel et al, 2012). On the other hand, Tau is mostly expressed in neuronal and glial cells but it is also present in non-neural cells such as fibroblasts and lymphocytes (Ingelson et al, 1996; Rossi et al, 2008; Thurston et al, 1996). Contrary to these works, we could not report protein expression of Tau in our cell lines, therefore the difference between our fibroblast and neural models is the presence of Tau. We could observe that Tau plays an important role in the reclycling of mitochondria and its overexpression in fibroblasts reflects a similar failure obtained in FAD and SAD models. Moreover, we need to highlight that when Tau was present in each model, either by overexpression or in neurons derived from FAD1-iPSCs or in AD brain, the defect in mitophagy was increased reflected in a major accumulation of dysfunctional mitochondria. Therefore, we may conclude that Tau is a pivotal protein in mitophagy failure walking together with the deregulation pattern of several proteins involved in the process.

Although fibroblasts and neurons exhibit basic differences in their biology we could recapitulate the mitophagy impairment in these two cells types in both FAD and SAD pathology.

2. Opportunities and limitations of modelling Alzheimer disease with induced pluripotent stem cells

The ability to generate patient-specific iPSCs through reprogramming of somatic cells and their subsequent differentiation into neuronal cell types, have boosted the investigation regarding the etiology of human neurodegenerative diseases, such as AD. While human iPSCs certainly provide great opportunities to repeatedly interrogate specific human brain cell types of individuals with familial and sporadic forms of the disease, the complex etiology and timescale over which AD develops in humans poses particular challenges to iPSC-based AD models.

Literature indicates that most of the iPSC-AD studies are limited and larger cohorts of iPSCs from AD patients are being generated worldwide through various consortia, industry or iPSC banks. *New York Stem Cell Foundation (NYSCF)* research is focused on the modeling of different diseases and the development of cell therapies. This research center houses the platform "*The NYSCF Global Stem Cell Array*", a new technology platform that, for the first time, creates and manipulates stem cell lines in a massively parallel process using automation. The NYSCF Alzheimer's disease team is developing a massive collection of iPSC lines on this platform from hundreds of Alzheimer patients' skin samples. The Array fully automates the generation of standardized iPSC that can be used to study Alzheimer pathology. Moreover, it should be noted that work with this type of cells are expensive because the

general range for the iPSC line generation is $5,000 - $40,000 based on reprogramming method and specifications.

We need to take into account the advantages and limitations that iPSC model system demonstrates. There is evidence that iPSCs, even from the same individual, can vary in terms of DNA mutation load (Gore et al, 2011), gene expression (Schondorf et al, 2014) and epigenetic signatures (Bock et al, 2011; Kim et al, 2010), often resulting in differences that may affect their propensity to differentiate into particular cell types (Nazor et al, 2012). Some of the variability appears to be driven by the method chosen to reprogram the somatic cells (non-integrating methods showing the least variability (Hartjes et al, 2014; Ma et al, 2014)), allelic variation (Lo et al, 2003), the age and type of cells used for reprogramming (Polo et al, 2010) and the culture time and method used to expand iPSC following establishment (Wutz, 2012). Moreover, the choice of the appropriate control for comparative studies of human samples is not a trivial one. Unaffected relative or parental control samples are preferable but these are not always available or come from family members of different age or gender and different genetic backgrounds. On the other hand, iPSCs are amenable to manipulation and genome editing while maintaining genome stability (Zhang et al, 2014). A variety of gene-editing techniques, such as zinc-finger nucleases (Carroll, 2011), transcription activator-like effector nucleases (Woodruff et al, 2013), and the clustered regularly interspaced short palindromic repeat/Cas9 RNA-guided nuclease system (Paquet et al, 2016; Shalem et al, 2014) have been developed to facilitate investigation of specific genes and their functions. The advantage of isogenic lines is that only the disease-associated difference is studied, as the genetic background of the lines should be identical. Therefore, it seems advisable to both correct the mutation of interest in a patient-derived cell line, while in parallel introducing it in a control line. Therefore, genome editing will be an important strategy to minimize the effect of background variations in human iPS cell-derived lines. Neural cells differentiated from iPSC lines with SAD backgrounds can display a number of AD-like phenotypes that can be characterized *in vitro* and represent an improvement of the knowledge of this AD phenotype. However, due to SAD may result from a combinatorial effect of genetic and non-genetic risk factors, the lack of a defined mutation makes difficult the generation of isogenic iPSC lines from SAD and control patients. The large scale analysis developed by human genome wide association studies (GWAS) have allowed the identification of AD markers that can predict disease risk and age onset. There is a recent study focused in iPSC derived from patients with SAD-associated variants in the SORL1 gene, which encodes a protein involved in endocytic trafficking, whose loss of expression has been reported in AD brains (Young et al, 2015). Therefore, the increased feasibility of genome editing in iPSCs will be relevant to elucidate the roles of SAD risk genetic variants in iPSC-derived neural models. Additionally, although it is difficult to be able to artificially recreate such a complex three-dimensional tissue as the human brain, iPSC technology is well suited to study paracrine interactions in the dish through the co-cultured of neurons from control or AD patients with astrocytes (Marchetto et al, 2008).

Glutamatergic and basal forebrain cholinergic neurons in the cerebral cortex and the hippocampus are thought to be cells that are affected at early stages and lost during AD pathogenesis (Braak & Braak, 1994). Thank to iPSC technology we have generated glutamatergic cortical forebrain neurons as most iPSC-AD modelling studies, that employed either embryoid body/neurosphere or small molecule-based neuronal differentiation protocols (Israel et al, 2012; Sproul et al, 2014). These iPSC-derived neurons from patient with the familiar etiology have reproduced the mitochondrial recycling failure observed in FAD1 fibroblasts. However, the development of protocols that allow the generation of specific and relevant cell types, such as basal forebrain cholinergic neurons are necessary. Additionally, protocols that mimic or accelerate the maturation and "ageing" processes are also fundamental to decipher the gene-regulatory networks involved in the disease.

Finally, several studies reported the direct conversion or transdifferentiation of fibroblasts to neurons avoiding the pluripotent stage. It has been described that three neurodevelopmental factors, Brn2, Ascl1 and Myth1l, directly converted fibroblasts into neuronal cells, called induced neurons (iNs) (Vierbuchen et al, 2010). From this publication, it has appeared a collection of papers where the protocol has improved facilitating the conversion of fibroblasts into neuronal cells by using small molecules and also was reported for AD patients' fibroblasts (Hu et al, 2015). Although the results have not been presented in this manuscript, we first tried to carry out the transdifferentiation in our cell lines due to this technology may seem easier. We tried the original protocol (Vierbuchen et al, 2010) using the human analogs of the mentioned genes but, in our hands we could not reproduce successfully the results previously reported. Additionaly we tried the protocol described by Ladewig et al (2012) in which a combination of small molecules (SB-431542, Noggin and CHIR-99021) and two neuronal gene factors (Ascl1 and Ngn2) were used. In this case, we could obtain neuron-like cells that showed expression for mature neuron markers such as Tau, calbindin and NSE, but we could not achieve electric function in these cells. In our experience, transdifferentiation compared to iPSCs derived neurons is less efficient, poorly reproducible and the phenotype obtained is not always mature neurons with electric activity.

3. Implication of *PSEN1* Ala246Glu mutation in the mitochondrial recycling failure

Presenilins are ubiquitously detected in many human tissues, including brain, heart, kidney and muscle (Lee et al, 1996). Moreover, it has described high levels of *PSEN1* mRNA in both skin fibroblasts and brains from AD patients (Ikeda et al, 2000). Presenilin mutations are the main cause of autosomal-dominant FAD. Moreover, mutations in the *PSEN1* gene, located on chromosome 14, occur most frequently in FAD (Cruts et al, 1998; Sherrington et al, 1995). Familial models bring the opportunity to characterize the pathology working with a specific mutation. We have focused our research in *PSEN1* Ala246Glu mutation since it is a well-characterized FAD mutation that shows

typical phenotypes of AD with complete penetrance. *PSEN1* A246E is reported to induce elevation of Aβ42 in human plasma, patient-derived fibroblasts, forced-expressed cells and showing strong toxicity in mice (Borchelt et al, 1996).

We have analyzed the mitochondrial recycling process in fibroblasts from FAD patients carrying the mutation FAD1: *PSEN1* Ala246Glu. The aim was to compare the results obtained in peripheral cells with a human neural model generated from iPSC harboring the same FAD1 mutation. We have demonstrated a deregulation of autophagy as a result of a reduction of degradation phase in both FAD1 fibroblasts and iPSC-derived neurons. This may be caused by an impaired fusion of the autophagic vesicles with lysosome or inhibition of lysosomal function. Consistently, we could observe that the acidification of lysosomes in FAD1 fibroblasts was diminished correlating with the lysosome acidification deficiency reported by Lee et al. (2010). In mentioned work, PSEN1 was demonstrated to act as chaperone protein that facilitates the N-glycosylation of V-ATPase subunit V0a1, which help V-ATPase traffic to lysosome and complete lysosome acidification. Furthermore, the accumulation of autophagic vesicles has been observed in dystrophic neurites around the amyloid plaques for decades. Likewise, the accumulation of p62 has been observed in neuronal and glial ubiquitin-containing inclusions (Kuusisto et al, 2001) as well as in neurofibrillary tangles (Kuusisto et al, 2002) in AD brain. Therefore, all these results together demonstrate that PSEN1 mutations impair degradative phase of autophagy.

The study of mitophagy after a mitochondrial insult indicates that this process is severely affected due to the mitochondrial accumulation exhibited in both fibroblasts and iPSC-derived neurons from FAD1 patients (See final model **Fig. 60**). These two cell types showed a correct FL-PINK1 stabilization and PARK2 recruitment to mitochondria but, due to the degradation phase deficiency described before, there is an accumulation of damaged mitochondria which are not able to be recycled by mitophagy. This results correlate with the increased mitochondria in AVs, previously reported in pyramidal neurons from AD patients suggesting a mitophagy alteration (Moreira et al, 2007b; Moreira et al, 2007c), as well as the PARK2/PINK1 accumulation observed. It is well known the accumulation of PINK1 and PARK2 in depolarized mitochondria to be degraded by autophagy (Narendra et al, 2010b; Tanaka, 2010). Moreover, PARK2 accumulation could be due to a proteasome degradation system saturation as a result of the autophagy impairment (Yamano et al, 2016). Additionally, we observed that FAD1 fibroblasts revealed lower levels of PINK1. It has been previously described that deficiency of PINK1 is a fundamental mechanism leading to accumulation of depolarized mitochondria (Bueno et al, 2015), therefore lower PINK1 expression in fibroblasts can contribute to a diminish targeting of dysfunctional mitochondria to be recycled by mitophagy. Conversely, in FAD1-iPSCs derived neurons the accumulation of mitochondria and PARK2 is substantially higher hence is logical to expect an additional accumulation of PINK1 stabilized in those mitochondria although its signaling was originally diminished.

On the other hand, it is relevant to remark a different role of presenilins in autophagy system. Presenilins mutations, including *PSEN1* Ala246Glu, have been reported to cause abnormal intracellular calcium signaling promoting the release of Ca^{2+} from overloaded endoplasmic reticulum stores through inositol triphosphate receptor (IP3R) (Ito et al, 1994). It has described that *PSEN1* Ala246Glu enhances gating of the IP3R Ca^{2+} release channel by a gain of function effect, and is independent of the secretase function of PSEN1 (Cheung et al, 2010). Mutant PSEN1 enhances single channel activity of the IP3R by affecting modal gating kinetics, the major mechanism by which IP3 and Ca^{2+} regulate the channel (Ionescu et al, 2007). This is important because autophagy appears to be directly dependent on the levels of endoplasmic reticulum's Ca^{2+} and on the activity of IP3R. According to this, lysosomal fusion depends on both luminal acidification and local lysosomal Ca^{2+} release (Luzio et al, 2007; Saftig & Klumperman, 2009). It has described that PSEN1 deficient cells exhibited decreased Ca^{2+} storage in degradative organelles besides a significantly decreased lysosomal Ca^{2+} release demonstrating a cell type-independent function for PSEN1 in lysosomal Ca^{2+} homeostasis. The accumulation of AVs observed in FAD could be interpreted by PSEN1-related calcium abnormality promoting the consequent defect in lysosomal fusion and protein clearance (Coen et al, 2012). Moreover, neurons are more sensitive than fibroblasts to deregulation of Ca^{2+} levels, being an additional explanation for the preferential toxicity in this cell type.

With respect to our FAD study, although we only could work with a couple of healthy/FAD1 age- and sex-matched samples of fibroblast and iPS-derived neurons and further studies with more patients are needed, we have demonstrated for the first time a problem in mitochondrial recycling by mitophagy that correlates with previously described alterations in lysosomal function (Coen et al, 2012; Lee et al, 2010; Neely et al, 2011). Moreover, we have recapitulated the mitochondrial recycling impairment showed in FAD1 fibroblasts in iPSC-derived neurons. In conclusion, our findings demonstrate that FAD1 iPSC-derived neurons are a valid model for the study of mitophagy impairment in AD.

4. APP and Tau contribution in mitophagy.

Extensive literature exists supporting a role of mitochondrial dysfunction and oxidative damage in the early AD pathogenesis (Moreira et al, 2006; Nunomura et al, 2001). There are strong indications that oxidative stress occurs prior to the onset of symptoms in AD and oxidative damage is found not only in the vulnerable regions of the brain affected in the disease (Casadesus et al, 2007; Nunomura et al, 2001) but also in peripheral cells (Moreira et al, 2007a). Mitochondrial function is regulated by autophagy and, for this porpose, segregation of damaged mitochondria depends on fission and fusion events that are altered in AD. It has been described an abnormal interaction of Aβ monomers and oligomers as well as hyperphosphorylated Tau with the mitochondrial fission protein DLP1 suggesting a possible cause of mitochondrial dynamics alteration and synaptic damage

(Manczak et al, 2011). In addition, the microtubule-directed traffic is a main player in the regulation of autophagy. Altered microtubule assembly impairs microtubule-dependent mitochondrial and autophagosomal transport toward lysosomes (Arduino et al, 2013). It is known that Aβ induces a reduction in motile mitochondria (Rui et al, 2006) and hyperphosphorylated Tau may block the transport of mitochondria and may disrupt the microtubule network trafficking leading to energy deprivation and oxidative stress (Stamer et al, 2002). Autophagy plays a fundamental role in neuronal function and is intensively involved in AD-related protein aggregation (Nixon et al, 2005) but little is known about the implication of APP and Tau in mitophagy dysfunction.

We have analyzed the mitochondrial recycling process by the overexpression of *APP* and *Tau* in a human line of fibroblasts (See final model **Fig. 60**). We have demonstrated that overexpression of both APP and Tau proteins generates an activation of autophagy flux revealed by the enhanced activity of the autophagy degradation phase correlating with higher lysosomal activity. It might be reasonable to speculate that the boosting of autophagy flux may be a consequence of the proteotoxic stress generated by the overexpression of APP and Tau which are prone to aggregate (Bandyopadhyay et al, 2007; Spires et al, 2005). Further studies are needed regarding the increased autophagy degradation to discard a possible artefact of protein overexpression (Lamark & Johansen, 2012).

The study of mitochondrial recycling process revealed an increased mitochondrial content suggesting a compromised mitophagy in both APP and APP/Tau-expressing cells. Although we have demonstrated the same defect in both cases there are some differences. In the case of APP-expressing cells, we hypothesize that increased levels of PARK2 and PINK1 could be explain as an attempt to increase the mitochondrial recycling system. However, the diminished targeting of PARK2 and PINK1 to mitochondria may reflect either an improvement of the recycling of mitochondria by the increased degradation phase of autophagy observed or an insufficient labelling of depolarized mitochondria to be degraded. In this regard, enhanced levels of Δ1-PINK1 may play an inhibitory effect over PARK2 mitochondrial translocation contributing to defective label of damage mitochondria (Fedorowicz et al, 2014). Nevertheless, the study of mitochondrial ΔΨm recovery after CCCP insult indicates that a main part of mitochondria are able to be recycled properly although not as efficiently as control cells what may explain the slight accumulation of mitochondria, FL-PINK and PARK2. On the other hand, APP/Tau-expressing cells exhibited a dramatic accumulation of PINK1 in mitochondria after an insult but the recruitment of PARK2 to the mitochondria was decreased resulting in a defective labeling of damaged mitochondria demonstrating a deficient crosstalk between these two proteins. This resulted in a deficient mitochondrial ΔΨm recovery after CCCP challenge correlating with an major accumulation of mitochondria. According to our results, it has been recently described that Tau accumulation may induce mitophagy deficits by reducing level of PARK2 in the mitochondrial fraction (Hu et al, 2016). Moreover, increased levels of Δ1-PINK1 may also contribute to this deficit in mitochondrial targeting of PARK2 (Fedorowicz et al, 2014). This data together demonstrate a

worsening of mitophagy failure due to the presence of Tau. This can be related with two factors. First, the deterioration of mitochondrial function caused by the deregulation of mitochondrial respiratory chain complexes V and I (David et al, 2005; Schulz et al, 2012) as well as by the block of mitochondrial pores through VDAC1 interaction (Manczak & Reddy, 2012). And secondly, the mitochondrial dynamics alteration by Tau interaction with the fission protein DLP1 (Manczak et al, 2011) accompanied with the interference of mitochondrial axonal transport by competition with their binding site to microtubules (Hagiwara et al, 1994).

In summary, we have demonstrate that the presence of Tau aggravates the defect showed by *APP* overexpression leading to a clear mitophagy failure showed by unachievable recovery of mitochondrial membrane potential after an insult that results in the accumulation of dysfunctional mitochondria labeled by PINK1.

We have been able to demonstrate mitophagy impairment by overexpression of the two proteins mainly involved in AD. Although this is a good proof of concept and may help to understand the mechanisms involved in this pathology, this is only the simplest model and putative artifacts generated by supraphysiological expression levels need to be ruled out. Therefore it is crucial to validate these findings in more physiological models of the disease as well as in patients' brain. With this aim, unmodified human skin fibroblasts and brain samples of sporadic AD patients have been used. Sporadic AD is not only the most prevalent form of this dementia but also is closely related to the accumulation of Aβ plaques derived from APP and neurofibrillary tangles generated by Tau.

5. Mitophagy failure in sporadic AD.

The majority of AD cases occur sporadically. SAD is a multifactorial neurodegenerative disorder arising from a number of different, but related biological alterations that contribute to the pathogenesis of the disease. In addition to the molecular, structural, and functional changes exhibited in AD patients, the individual differences in genetic background, environmental stimuli, lifestyle, and other risk factors potentially contribute to the pathology development (Stozicka et al, 2007). Several genes involved in various metabolic pathways were presented as the genetic risk factors in SAD. The majority of these genes may influence the vulnerability of the central nerve system without direct impact on the primary causes of AD (Stozicka et al, 2007).

Findings from recent AD genetic studies suggest that mitochondrial defects may play an important role in SAD progression, and that mitochondrial abnormalities and oxidative damage may play a significant role to initiate the disease (Reddy & Beal, 2005). The "mitochondrial cascade hypothesis" could explain many of the biochemical, genetic, and pathological features of sporadic AD (Swerdlow & Khan, 2004). Somatic mutations in mtDNA could cause energy failure, increased oxidative stress, and accumulation of Aβ, which in a vicious cycle reinforce the mtDNA damage and the oxidative stress (Mancuso et al, 2009). In addition, this hypothesis reconciles AD research with

brain aging research, provides insight into late-onset AD epidemiology and phenotype studies, and explains biochemical and physiologic changes that occur outside the AD brain.

Taking into account the mitochondrial relevance in SAD, we have analyzed the mitochondrial recycling process in fibroblasts from SAD patients and have validated the mitophagy impairment in brains from AD patients (See final model **Fig. 60**). We have demonstrated that mitochondrial function was compromised due to the lack of membrane potential and ATP homeostasis recovery after the reversible treatment with CCCP suggesting an inefficient recycling of damaged mitochondria by autophagy in SAD fibroblasts. Accordingly, SAD cells showed a deficiency in autophagy induction and the accumulation of oxidized and ubiquitinated proteins. The absence of significant differences in BECN1 levels in SAD samples may be explained because autophagy can also occur independently of BECN1 (Chu et al, 2007; Zhu et al, 2007). Lysosomal anomalies have been also found in our SAD samples. We assume a reduction in the amount of lysosomes reflected by the diminished levels of LAMP1 and Cathepsin B proteins. However, we hypothesize that these lysosomes have a more acidic pH which correlates with enhanced Cathepsin B activity. In fact, it was previously described that lysosomal Cathepsin B exopeptidase activity is increased as the pH decreases (Polgar & Csoma, 1987). Despite these anomalies, the lack of significant differences in the degradative phase of autophagy together with the active degradation of proteins mediated by autophagy such as p62 as well as similar rates of autophagosomes/lysosomes fusion, indicate that these lysosomes may be functional and suggest that the altered properties may be a consequence of autophagy failure. SAD fibroblasts demonstrated a failure in the induction of autophagy, meanwhile FAD1 fibroblasts showed a defective degradative phase of autophagy. These divergent phenotypes observed in SAD and FAD1 fibroblasts suggest different mechanisms for a common final failure in autophagy process.

The study of mitophagy after a mitochondrial insult indicates that this process is severely affected in SAD fibroblasts. Upon mitochondrial depolarization, although there is a correct stabilization and auto-phosphorylation of PINK1, there is not a proper PARK2 activation. This may be due to the lower levels of PARK2 and its inhibition mediated the sequestration of cytosolic PARK2 by Δ1-PINK1. Accordingly, it has been described that defects in PARK2 recruitment correlates with declining ATP levels after the treatment with CCCP, such as we have observed for SAD samples, suggesting that CCCP-induced PARK2 mitochondrial translocation is ATP-sensitive (Lee et al, 2015). The deficient PARK2 recruitment to mitochondria in our SAD samples caused the accumulation of damaged mitochondria, reflected in the increase of FL- and phosphorylated-PINK1 and diminished phosphorylated-PARK2, emphasizing the deficiency in the crosstalk between PINK1 and PARK2. Furthermore, the defect in mitochondrial recycling may explain the accumulation of oxidized proteins observed. The situation observed in SAD fibroblasts was similar to what can be found in hippocampus from AD patients at early stages of the disease where we observed accumulation of both FL- and Δ1-PINK1 accompanied by abnormally increased mitochondrial content due to an impaired degradation rather than an increase in synthesis. This strongly suggests that mitophagy

failure may play an important role in the onset of the disease. At latest stages of the disease the increase of PARK2 may correlate with recently published results in which accumulation of insoluble PARK2 with intraneuronal Aβ and phospho-Tau was detected in autophagosomes in AD brains reflecting an autophagy failure (Lonskaya et al, 2013). Moreover, the upregulation of PARK2 in these patients' brain has been suggested as a defense mechanism to counteract stress-induced damage in AD pathogenesis (Witte et al, 2009). Our findings demonstrate that SAD fibroblasts are a suitable model for the study of this dementia because they recapitulate similar alterations in mitophagy process to what it can be observed in patients' brain.

Finally, it is important to highlight that the autophagy and mitophagy failure uncovered in SAD samples must be substantially relevant since we have been able to characterize these deficiencies in a small collection of fibroblasts from different patients in which we have found similar features despite the multifactorial origin of SAD pathology.

6. Relevance of Autophagy-Mitophagy system in AD

Protein degradation is critical in cell quality control (Ciechanover, 2005). Disturbances in intracellular proteostasis trigger the accumulation of altered proteins and toxic aggregates as Aβ and hyperphosphorylated Tau widely recognized hallmarks of AD (Serrano-Pozo et al, 2011) . The major consequence of the accumulation of such pathogenic aggregates is the downregulation of proteolytic pathways triggering a feed-forward loop that at the end alter essential proteolytic networks. In addition, neurons are post-mitotic cells unable to dilute or remove abnormal protein aggregates via cell division and therefore are more sensitive to these toxic proteinaceous species compared to mitotic cells (Sitte et al, 2000a; Sitte et al, 2000b).

Mounting evidence has implicated defective autophagy in the pathogenesis of AD. Autophagy is considerably involved in amyloid degradation (Yang et al, 2011). Autophagy and the Beclin1–PIK3C3 complex regulate APP processing in AD (Jaeger et al, 2010). In addition, autophagic vesicles have been demonstrated to be an active compartment for Aβ generation and their abnormal accumulation in affected neurons of the AD brain contributes to Aβ deposition (Yu et al, 2004). Inhibition of Aβ peptide aggregation rescues the autophagic deficits in a model of AD (Lai & McLaurin, 2012). On the other hand, the autophagy system plays a role in the clearance of Tau and the use of autophagy inhibitors delays Tau degradation favouring the formation of high molecular weight species of Tau including oligomers and insoluble aggregates (Hamano et al, 2008). Moreover, autophagy stimulation successfully reduces the number of Tau inclusions and improves nerve cell survival in a mouse model of human tauopathy (Schaeffer et al, 2012). Additionally, the lysosomal hydrolase cathepsin D was shown to degrade Tau proteins in cultured hippocampal slices (Bednarski & Lynch, 1996) demonstrating that Tau is susceptible of being degraded by autophagy.

Neurons represent a particularly interesting cell type for mitophagy because they combine high demand for mitochondria and high mitochondrial stress with extremely complex cellular architecture. Neurons face a unique challenge for mitochondrial turnover because a large fraction of the mitochondrial mass resides in distal axonal and dendritic processes, far away from the soma where most of the biogenesis is likely to occur and most of the lysosomes are thought to be located (Holtzman & Novikoff, 1965). Neuronal autophagy plays a critical role in the maintenance of homeostasis in distal axons and rapid elimination of dysfunctional mitochondria is probably critical for protection of neurons due to its impairment promotes the accumulation of oxidative damage and degeneration (Son et al, 2012).

Taking into account the "mitochondrial cascade hypothesis" as a primary event in AD, a defective elimination of mitochondria could be taken place in the early pathology as we could observe (**Fig. 53-54**). Moreover, accumulation of damage mitochondria release high levels of Ca^{2+} and cytochrome c to the cytosol triggering apoptosis (Parsons & Green, 2010). Several articles have described mitophagy impairment in AD. It has been found an increase of autophagic vesicles containing mitochondria in pyramidal neurons from AD patients suggesting a mitophagy alteration (Moreira et al, 2007b; Moreira et al, 2007c). According to this, PARK2 has been shown to be reduced in the cortex of AD brains (Rosen et al, 2010) as we have described for SAD fibroblasts. Moreover, it has been shown that Tau accumulation impairs mitophagy reducing mitochondrial PARK2 (Hu et al, 2016) as well as NH2-truncated human Tau induces deregulated mitophagy in neurons by aberrant recruitment of PARK2 (Corsetti et al, 2015). The present work adds new insights to previously suggested mitochondrial recycling deregulation in AD by deciphering the mechanisms involved in this failure in familial and sporadic forms of the disease as well as the contribution of APP and Tau to this pathology. Our results also support "mitochondrial cascade hypothesis" by proposing mitochondrial dysfunction as the onset of SAD.

Along with the autophagy system, the proteasome mediates the degradation of short-lived, oxidatively damaged, modified and misfolded proteins both in the cytoplasm and the nucleus (Jung et al, 2009). Proteasome plays a crucial role in the processing of proteins involved in the onset of AD and its activity is heavily downregulated by protein aggregates in AD neurons (Cecarini et al, 2007; Keck et al, 2003). According to this, we also have demonstrated an increased in the ubiquitinated proteins suggesting dysfunctional proteasome degradation. Nevertheless, recent advances strongly suggest that autophagy/proteasome pathways are carefully orchestrated and some crosstalk mechanisms have been suggested (Kraft et al, 2010). In neurodegenerative conditions, when one proteolytic system is damaged and shows a reduced functionality, the enhanced activity of the other pathway may become a compensatory mechanism necessary to protect neuronal cells against the accumulation of toxic species (Ding et al, 2007; Pandey et al, 2007). Therefore, the fine collaboration between these two pathways is essential to protein quality control. In our hands, healthy fibroblasts exhibited a dual contribution of autophagy and proteasome systems for PARK2 degradation. Howev-

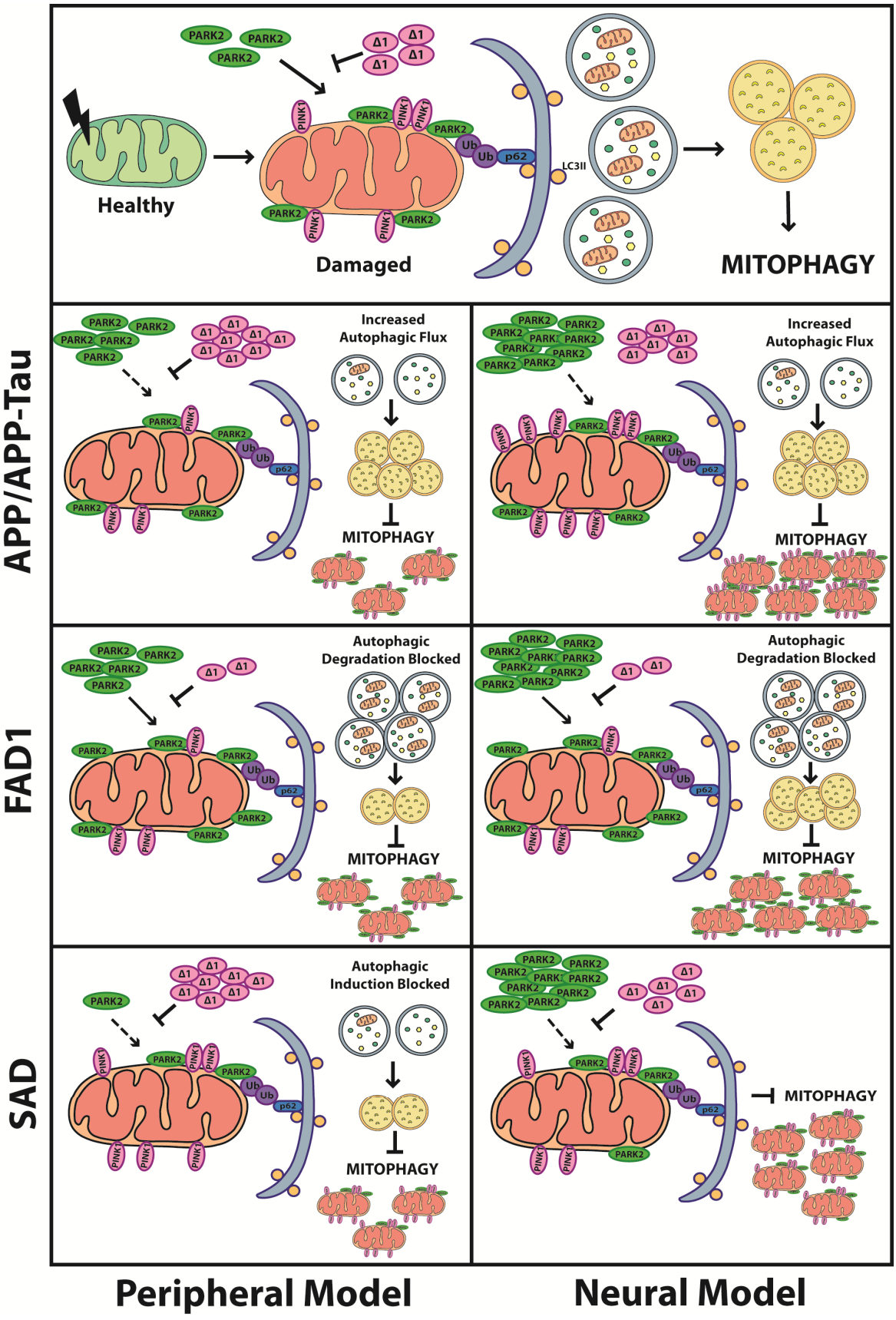

Figure 60. Summary of the mitophagy impairment studied in Alzheimer disease.

er, the contribution of autophagy for the degradation of polyubiquitinated proteins in healthy cells was only moderated and the majority was degraded by proteasome. Conversely, proteasome-mediated degradation flux was enhanced in SAD samples while autophagy was completely blocked with respect to PARK2 degradation. This fact closely correlates with the behavior of polyubiquitinated protein levels in SAD fibroblasts where there was a null contribution of autophagy in degradation while proteasome role was enhanced, probably due to a compensatory mechanism to counteract autophagy impairment in SAD cells.

Finally, although we studied the two distinct types of AD exhibiting different deregulation pattern of the mitochondrial recycling process, both SAD and FAD models converge on the same mitochondrial problem as is the mitophagy failure.

7. PARK2: a potential therapeutic target in SAD

Promoting the clearance of aggregated proteins via pharmacological induction of autophagy has proved to be a useful strategy for protecting against the toxic effects of these proteins in a range of cell and animal models (Berger et al, 2006; Ravikumar et al, 2002; Rose et al, 2010). In addition, mitochondrial biology represents a potentially useful, but relatively unexploited, area of therapeutic innovation. Emerging concepts of mitochondrial turnover and dynamics provides the opportunity to develop and evaluate mitochondrial based therapies.

Taking into consideration our results in SAD fibroblasts where PARK2 levels were dimished we wanted to evaluate if PARK2 enhancement would be able to reverse the observed mitophagy deficiency in fibroblast. The overexpression of wild type PARK2 was able to improve autophagy shown in the recovery of autophagic vesicles under basal conditions up to the levels found in healthy samples. This improvement was reflected in the clearance of ubiquitinated proteins and the decrease of abnormal accumulated mitochondria. Additionally, PARK2 enhancement would exceed the inhibitory effect of Δ1 PINK1 and, upon CCCP treatment, PARK2 would be recruited by FL-PINK1 to damaged mitochondria leading them to be degraded by mitophagy. Consequently, the levels of PINK1 were diminished and the ΔΨm was recovered by increasing of autophagy vesicle synthesis. We may thus assume that PARK2 overexpression restored autophagy and was able to compensate mitochondrial anomalies found in SAD fibroblasts. Previous work has demonstrated that the overexpression of PARK2 mediated the clearance of Aβ and phospho-Tau by enhancing autophagy and it was able to increase tricarboxylic acid cycle activity suggesting an improvement of mitochondrial function as well as a restored synaptic function in a triple transgenic AD mice model (Khandelwal et al, 2011; Lonskaya et al, 2013). Additionally, Parkin-induced autophagy facilitated clearance of vesicles containing debris and defective mitochondria counteracting oxidative stress and preventing mitochondrial dysfunction (Khandelwal et al, 2011). Taking all these evidences together, we may conclude that promoting autophagy by PARK2 overexpression restores mitochondrial

recycling and function, induces Aβ and phospho-Tau clearance and improves synaptic function. In this way, elimination of unsalvageable mitochondria prevents excessive intracellular oxidative stress and the pathologic accumulation of oxidized macromolecules that may propagate damage and interfere with redox signaling mechanisms. The most important point is that the therapeutic capacity of PARK2 enhancement that we have demonstrated in sporadic cases highlights not only the similarities with FAD but also with other neuropathies such as Parkinson's disease, where the role of PARK2 has been widely demonstrated (Kitada et al, 1998).

Other strategies for the induction of autophagy as a therapeutic target in AD have been tested in animal models for the disease. One of the best characterized autophagy inducer is rapamycin, which is already in clinical use for other indications (Cloughesy et al, 2008). In mammalian cells, rapamycin inhibits the kinase activity of mTOR by forming a complex with the immunophilin FK506-binding protein of 12 kDa that binds to and inactivates mTOR, leading to the upregulation of autophagy (Caccamo et al, 2010; Spilman et al, 2010). On the other hand, Trehalose a natural disaccharide that can be found in animals, plants, and microorganisms induces autophagy via an mTOR independent pathway promoting the removal of aggregated proteins in a mouse model of human tauopathy (Schaeffer et al, 2012). In addition, Cystatin B deletion, an endogenous inhibitor of lysosomal cysteine proteases, can rescue autophagic-lysosomal pathology, reducing abnormal accumulations of Aβ peptide, ubiquitinated proteins and other autophagic substrates (Yang et al, 2011). Latrepirdine, is an antihistamine drug that stimulates mTOR- and ATG5-dependent autophagy, leading to the reduction of intracellular levels of APP metabolites, including Aβ (Steele & Gandy, 2013). Moreover, scyllo-Inositol is an endogenous inositol stereoisomer known to inhibit aggregation and fibril formation of Aβ. It has described that inhibition of Aβ peptide aggregation rescues the autophagic deficits by the decrease in the size and number of accumulated autophagic vesicles in a mouse model of Alzheimer disease (Lai & McLaurin, 2012).

To conclude, given the results obtained in this thesis, it must to be taken in consideration that autophagy defects in AD can occur at different points of the pathway. We have revealed an impairment of autophagosome induction as well as degradation in SAD and FAD, respectively. For that reason, every disease case should be carefully studied to determine the origin of autophagy failure to adjust the therapeutic approach to each patient problem. Therefore, Alzheimer disease is another complex disease whose efficient treatment will depend on future personalized medicine.

Conclusions

1. Sporadic and familial AD fibroblasts as well as familial AD iPSC-derived neurons are suitable models for the study of mitophagy impairment in Alzheimer disease.

2. *APP* overexpression promotes a mitochondrial recycling defect by impairing of PINK1 stabilization on mitochondria and the subsequent PARK2 recruitment leading to mitochondrial accumulation.

3. The addition of *Tau* to the *APP* overexpression cellular model exacerbates the mitophagy failure promoting an increased accumulation of dysfunctional mitochondria labeled with PINK1.

4. Patients-derived skin fibroblasts harboring *PSEN1* Ala246Glu mutation demonstrate a defect in degradation phase of autophagy correlating with lysosomal anomalies, leading to dysfunctional mitochondria accumulation consistent with mitophagy impairment.

5. Neurons derived from Alzheimer disease patients' iPSC harboring *PSEN1* Ala246Glu mutation demonstrate an exacerbation of mitophagy failure leading to increased mitochondrial accumulation together with augmented PINK1 and PARK2 levels.

6. Fibroblasts derived from sporadic Alzheimer patients exhibit alterations in mitochondrial dynamics and function. This is accompanied by a deficiency in autophagy induction together with a defective labeling of mitochondria to be degraded by mitophagy due to decreased levels of PARK2, leading to the accumulation of dysfunctional mitochondria as well as oxidized and ubiquitinated proteins.

7. Brains from Alzheimer disease patients show similar but aggravated mitophagy impairment exhibited by sporadic Alzheimer disease fibroblasts reflected in major accumulation of PINK1 and mitochondrial content especially at early stages of the disease.

8. Neuronal models display an enhanced mitophagy failure compared to peripheral cells pattern in both sporadic and familial Alzheimer forms of the disease.

9. *PARK2* overexpression recover mitochondrial dynamics and functional defect besides autophagy and mitochondrial recycling failure revealed by sporadic Alzheimer disease fibroblasts, demonstrating that autophagy induction could be a relevant therapeutic strategy for Alzheimer disease.

10. Mitochondrial recycling impairment is a common defect over all sporadic and familial Alzheimer disease models studied.

1. Los fibroblastos de pacientes tanto con la forma esporádica como familiar de la enfermedad de Alzheimer así como las neuronas derivadas de iPSC procedentes de pacientes de Alzheimer familiar son modelos adecuados para el estudio del defecto en mitofagia en dicha patología.

2. La sobreexpresión de *APP* promueve un fallo en el reciclaje mitocondrial debido a un impedimento de la estabilización de PINK1 en la mitocondria y la consiguiente translocación de PARK2 que provoca la acumulación de mitocondrias.

3. La adición de *Tau* al modelo celular de sobreexpresión de *APP* agrava el fallo en mitofagia promoviendo un aumento de la acumulación de mitocondrias no funcionales marcadas con PINK1.

4. Los fibroblastos de la piel derivados de pacientes portadores de la mutación *PSEN1* Ala246Glu presentan un defecto en la fase degradativa de la autofagia en correlación con anomalías lisosomales que conducen a la acumulación de mitocondrias no funcionales consecuente con el fallo en mitofagia.

5. Las neuronas derivadas de iPSC de pacientes de Alzheimer portadores de la mutación *PSEN1* Ala246Glu muestran una exacerbación de la deficiencia en mitofagia lo que causa una mayor acumulación mitocondrial, junto con el aumento de los niveles de PINK1 y PARK2.

6. Los fibroblastos derivados de pacientes con la forma esporádica de la enfermedad de Alzheimer manifiestan alteraciones en la dinámica y la función mitocondrial. Esto va acompañado de una inducción de autofagia deficiente junto con un marcaje defectuoso de las mitocondrias que van a ser degradadas por mitofagia como consecuencia de la disminución de los niveles de PARK2, lo que favorece la acumulación de mitocondrias no funcionales, así como de proteínas oxidadas y ubiquitinadas.

7. Los cerebros de pacientes de la enfermedad de Alzheimer muestran un deterioro en mitofagia similar, pero agravado, del presentado por los fibroblastos de la enfermedad de Alzheimer esporádica, lo que se refleja en una mayor acumulación de PINK1 y del contenido mitocondrial, especialmente en las etapas tempranas de la enfermedad.

8. Los modelos neuronales muestran un fallo en autofagia exacerbado en comparación con el patrón mostrado por las células periféricas en ambas formas, esporádica y familiar, de la enfermedad de Alzheimer.

9. La sobreexpresión de *PARK2* recupera la dinámica mitocondrial y el defecto funcional además del fallo en autofagia y reciclaje mitocondrial mostrado por los fibroblastos con la forma esporádica de Alzheimer, lo que demuestra que la inducción de la autofagia podría ser una estrategia terapéutica relevante para la enfermedad de Alzheimer.

10. El fallo en el reciclaje mitocondrial es un defecto común en todos los modelos, tanto esporádicos como familiares, de la enfermedad de Alzheimer estudiados.

References

Aasen T, Raya A, Barrero MJ, Garreta E, Consiglio A, Gonzalez F, Vassena R, Bilic J, Pekarik V, Tiscornia G, Edel M, Boue S, Izpisua Belmonte JC (2008) Efficient and rapid generation of induced pluripotent stem cells from human keratinocytes. *Nat Biotechnol* **26:** 1276-1284

Aizenstein HJ, Nebes RD, Saxton JA, Price JC, Mathis CA, Tsopelas ND, Ziolko SK, James JA, Snitz BE, Houck PR, Bi W, Cohen AD, Lopresti BJ, DeKosky ST, Halligan EM, Klunk WE (2008) Frequent amyloid deposition without significant cognitive impairment among the elderly. *Arch Neurol* **65:** 1509-1517

Alikhani N, Ankarcrona M, Glaser E (2009) Mitochondria and Alzheimer's disease: amyloid-beta peptide uptake and degradation by the presequence protease, hPreP. *J Bioenerg Biomembr* **41:** 447-451

Alzheimer A, Stelzmann RA, Schnitzlein HN, Murtagh FR (1995) An English translation of Alzheimer's 1907 paper, "Uber eine eigenartige Erkankung der Hirnrinde". *Clin Anat* **8:** 429-431

Ankarcrona M, Hultenby K (2002) Presenilin-1 is located in rat mitochondria. *Biochem Biophys Res Commun* **295:** 766-770

Arduino DM, Esteves AR, Cardoso SM (2013) Mitochondria drive autophagy pathology via microtubule disassembly: a new hypothesis for Parkinson disease. *Autophagy* **9:** 112-114

Area-Gomez E, Del Carmen Lara Castillo M, Tambini MD, Guardia-Laguarta C, de Groof AJ, Madra M, Ikenouchi J, Umeda M, Bird TD, Sturley SL, Schon EA (2012) Upregulated function of mitochondria-associated ER membranes in Alzheimer disease. *EMBO J* **31:** 4106-4123

Auburger G, Klinkenberg M, Drost J, Marcus K, Morales-Gordo B, Kunz WS, Brandt U, Broccoli V, Reichmann H, Gispert S, Jendrach M (2012) Primary skin fibroblasts as a model of Parkinson's disease. *Mol Neurobiol* **46:** 20-27

Avila J, Lucas JJ, Perez M, Hernandez F (2004) Role of tau protein in both physiological and pathological conditions. *Physiol Rev* **84:** 361-384

Bandyopadhyay B, Li G, Yin H, Kuret J (2007) Tau aggregation and toxicity in a cell culture model of tauopathy. *J Biol Chem* **282:** 16454-16464

Bednarski E, Lynch G (1996) Cytosolic proteolysis of tau by cathepsin D in hippocampus following suppression of cathepsins B and L. *J Neurochem* **67:** 1846-1855

Behbahani H, Shabalina IG, Wiehager B, Concha H, Hultenby K, Petrovic N, Nedergaard J, Winblad B, Cowburn RF, Ankarcrona M (2006) Differential role of Presenilin-1 and -2 on mitochondrial membrane potential and oxygen consumption in mouse embryonic fibroblasts. *J Neurosci Res* **84:** 891-902

Bekris LM, Yu CE, Bird TD, Tsuang DW (2010) Genetics of Alzheimer disease. *J Geriatr Psychiatry Neurol* **23:** 213-227

Belkacemi A, Ramassamy C (2012) Time sequence of oxidative stress in the brain from transgenic mouse models of Alzheimer's disease related to the amyloid-beta cascade. *Free Radic Biol Med* **52:** 593-600

Berger Z, Ravikumar B, Menzies FM, Oroz LG, Underwood BR, Pangalos MN, Schmitt I, Wullner U, Evert BO, O'Kane CJ, Rubinsztein DC (2006) Rapamycin alleviates toxicity of different aggregate-prone proteins. *Hum Mol Genet* **15:** 433-442

Birgisdottir A, Lamark T, Johansen T (2013) The LIR motif - crucial for selective autophagy. *J Cell Sci* **126:** 3237-47

Bissonnette CJ, Lyass L, Bhattacharyya BJ, Belmadani A, Miller RJ, Kessler JA (2011) The controlled generation of functional basal forebrain cholinergic neurons from human embryonic stem cells. *Stem Cells* **29:** 802-811

Bock C, Kiskinis E, Verstappen G, Gu H, Boulting G, Smith ZD, Ziller M, Croft GF, Amoroso MW, Oakley DH, Gnirke A, Eggan K, Meissner A (2011) Reference Maps of human ES and iPS cell variation enable high-throughput characterization of pluripotent cell lines. *Cell* **144:** 439-452

Bonda DJ, Wang X, Perry G, Nunomura A, Tabaton M, Zhu X, Smith MA (2010a) Oxidative stress in Alzheimer disease: a possibility for prevention. *Neuropharmacology* **59:** 290-294

Bonda DJ, Wang X, Perry G, Smith MA, Zhu X (2010b) Mitochondrial dynamics in Alzheimer's disease: opportunities for future treatment strategies. *Drugs Aging* **27:** 181-192

Borchelt DR, Thinakaran G, Eckman CB, Lee MK, Davenport F, Ratovitsky T, Prada CM, Kim G, Seekins S, Yager D, Slunt HH, Wang R, Seeger M, Levey AI, Gandy SE, Copeland NG, Jenkins NA, Price DL, Younkin SG, Sisodia SS (1996) Familial Alzheimer's disease-linked presenilin 1 variants elevate Abeta1-42/1-40 ratio in vitro and in vivo. *Neuron* **17:** 1005-1013

Bossy B, Petrilli A, Klinglmayr E, Chen J, Lutz-Meindl U, Knott AB, Masliah E, Schwarzenbacher R, Bossy-Wetzel E (2010) S-Nitrosylation of DRP1 does not affect enzymatic activity and is not specific to Alzheimer's disease. *J Alzheimers Dis* **20 Suppl 2:** S513-526

Braak H, Braak E (1991) Neuropathological stageing of Alzheimer-related changes. *Acta Neuropathol* **82:** 239-259

Braak H, Braak E (1994) Morphological criteria for the recognition of Alzheimer's disease and the distribution pattern of cortical changes related to this disorder. *Neurobiol Aging* **15:** 355-356; discussion 379-380

Bueno M, Lai YC, Romero Y, Brands J, St Croix CM, Kamga C, Corey C, Herazo-Maya JD, Sembrat J, Lee JS, Duncan SR, Rojas M, Shiva S, Chu CT, Mora AL (2015) PINK1 deficiency impairs mitochondrial homeostasis and promotes lung fibrosis. *J Clin Invest* **125:** 521-538

Butterfield DA (2002) Amyloid beta-peptide (1-42)-induced oxidative stress and neurotoxicity: implications for neurodegeneration in Alzheimer's disease brain. A review. *Free Radic Res* **36:** 1307-1313

Caccamo A, Majumder S, Richardson A, Strong R, Oddo S (2010) Molecular interplay between mammalian target of rapamycin (mTOR), amyloid-beta, and Tau: effects on cognitive impairments. *J Biol Chem* **285:** 13107-13120

Calkins MJ, Manczak M, Mao P, Shirendeb U, Reddy PH (2011) Impaired mitochondrial biogenesis, defective axonal transport of mitochondria, abnormal mitochondrial dynamics and synaptic degeneration in a mouse model of Alzheimer's disease. *Hum Mol Genet* **20:** 4515-4529

Campion D, Dumanchin C, Hannequin D, Dubois B, Belliard S, Puel M, Thomas-Anterion C, Michon A, Martin C, Charbonnier F, Raux G, Camuzat A, Penet C, Mesnage V, Martinez M, Clerget-Darpoux F, Brice A, Frebourg T (1999) Early-onset autosomal dominant Alzheimer disease: prevalence, genetic heterogeneity, and mutation spectrum. *Am J Hum Genet* **65:** 664-670

Carlsson CM (2010) Type 2 diabetes mellitus, dyslipidemia, and Alzheimer's disease. *J Alzheimers Dis* **20:** 711-722

Carroll D (2011) Genome engineering with zinc-finger nucleases. *Genetics* **188:** 773-782

Casadesus G, Smith MA, Basu S, Hua J, Capobianco DE, Siedlak SL, Zhu X, Perry G (2007) Increased isoprostane and prostaglandin are prominent in neurons in Alzheimer disease. *Mol Neurodegener* **2:**

Cataldo AM, Barnett JL, Pieroni C, Nixon RA (1997) Increased neuronal endocytosis and protease delivery to early endosomes in sporadic Alzheimer's disease: neuropathologic evidence for a mechanism of increased beta-amyloidogenesis. *J Neurosci* **17:** 6142-6151

Cataldo AM, Nixon RA (1990) Enzymatically active lysosomal proteases are associated with amyloid deposits in Alzheimer brain. *Proc Natl Acad Sci U S A* **87:** 3861-3865

Cecarini V, Ding Q, Keller JN (2007) Oxidative inactivation of the proteasome in Alzheimer's disease. *Free Radic Res* **41:** 673-680

Cecchi C, Fiorillo C, Sorbi S, Latorraca S, Nacmias B, Bagnoli S, Nassi P, Liguri G (2002) Oxidative stress and reduced antioxidant defenses in peripheral cells from familial Alzheimer's patients. *Free Radic Biol Med* **33:** 1372-1379

Ciechanover A (2005) Intracellular protein degradation: from a vague idea, through the lysosome and the ubiquitin-proteasome system, and onto human diseases and drug targeting (Nobel lecture). *Angew Chem Int Ed Engl* **44:** 5944-5967

Cipolat S, Rudka T, Hartmann D, Costa V, Serneels L, Craessaerts K, Metzger K, Frezza C, Annaert W, D'Adamio L, Derks C, Dejaegere T, Pellegrini L, D'Hooge R, Scorrano L, De Strooper B (2006) Mitochondrial rhomboid PARL regulates cytochrome c release during apoptosis via OPA1-dependent cristae remodeling. *Cell* **126:** 163-175

Citron M, Diehl TS, Gordon G, Biere AL, Seubert P, Selkoe DJ (1996) Evidence that the 42- and 40-amino acid forms of amyloid beta protein are generated from the beta-amyloid precursor protein by different protease activities. *Proc Natl Acad Sci U S A* **93:** 13170-13175

Citron M, Vigo-Pelfrey C, Teplow DB, Miller C, Schenk D, Johnston J, Winblad B, Venizelos N, Lannfelt L, Selkoe DJ (1994) Excessive production of amyloid beta-protein by peripheral cells of symptomatic and presymptomatic patients carrying the Swedish familial Alzheimer disease mutation. *Proc Natl Acad Sci U S A* **91:** 11993-11997

Clayton KB, Podlesniy P, Figueiro-Silva J, Lopez-Domenech G, Benitez L, Enguita M, Abad MA, Soriano E, Trullas R (2012) NP1 regulates neuronal activity-dependent accumulation of BAX in mitochondria and mitochondrial dynamics. *J Neurosci* **32:** 1453-1466

Cloughesy TF, Yoshimoto K, Nghiemphu P, Brown K, Dang J, Zhu S, Hsueh T, Chen Y, Wang W, Youngkin D, Liau L, Martin N, Becker D, Bergsneider M, Lai A, Green R, Oglesby T, Koleto M, Trent J, Horvath S, Mischel PS, Mellinghoff IK, Sawyers CL (2008) Antitumor activity of rapamycin in a Phase I trial for patients with recurrent PTEN-deficient glioblastoma. *PLoS Med* **5:** e8

Coen K, Flannagan RS, Baron S, Carraro-Lacroix LR, Wang D, Vermeire W, Michiels C, Munck S, Baert V, Sugita S, Wuytack F, Hiesinger PR, Grinstein S, Annaert W (2012) Lysosomal calcium homeostasis defects, not proton pump defects, cause endo-lysosomal dysfunction in PSEN-deficient cells. *J Cell Biol* **198:** 23-35

Coon KD, Myers AJ, Craig DW, Webster JA, Pearson JV, Lince DH, Zismann VL, Beach TG, Leung D, Bryden L, Halperin RF, Marlowe L, Kaleem M, Walker DG, Ravid R, Heward CB, Rogers J, Papassotiropoulos A, Reiman EM, Hardy J, Stephan DA (2007) A high-density whole-genome association study reveals that APOE is the major susceptibility gene for sporadic late-onset Alzheimer's disease. *J Clin Psychiatry* **68:** 613-618

Corder EH, Saunders AM, Strittmatter WJ, Schmechel DE, Gaskell PC, Small GW, Roses AD, Haines JL, Pericak-Vance MA (1993) Gene dose of apolipoprotein E type 4 allele and the risk of Alzheimer's disease in late onset families. *Science* **261:** 921-923

Corsetti V, Florenzano F, Atlante A, Bobba A, Ciotti MT, Natale F, Della Valle F, Borreca A, Manca A, Meli G, Ferraina C, Feligioni M, D'Aguanno S, Bussani R, Ammassari-Teule M, Nicolin V, Calissano P, Amadoro G (2015) NH2-truncated human tau induces deregulated mitophagy in neurons by

aberrant recruitment of Parkin and UCHL-1: implications in Alzheimer's disease. *Hum Mol Genet* **24:** 3058-3081

Coulson EJ, Paliga K, Beyreuther K, Masters CL (2000) What the evolution of the amyloid protein precursor supergene family tells us about its function. *Neurochem Int* **36:** 175-184

Cruts M, Theuns J, Van Broeckhoven C (2012) Locus-specific mutation databases for neurodegenerative brain diseases. *Hum Mutat* **33:** 1340-1344

Cruts M, van Duijn CM, Backhovens H, Van den Broeck M, Wehnert A, Serneels S, Sherrington R, Hutton M, Hardy J, St George-Hyslop PH, Hofman A, Van Broeckhoven C (1998) Estimation of the genetic contribution of presenilin-1 and -2 mutations in a population-based study of presenile Alzheimer disease. *Hum Mol Genet* **7:** 43-51

Cuervo AM (2004) Autophagy: in sickness and in health. *Trends Cell Biol* **14:** 70-77

Cuervo AM (2010) Chaperone-mediated autophagy: selectivity pays off. *Trends Endocrinol Metab* **21:** 142-150

Cummings JL (2004) Alzheimer's disease. *N Engl J Med* **351:** 56-67

Cunningham M, Cho JH, Leung A, Savvidis G, Ahn S, Moon M, Lee PK, Han JJ, Azimi N, Kim KS, Bolshakov VY, Chung S (2014) hPSC-derived maturing GABAergic interneurons ameliorate seizures and abnormal behavior in epileptic mice. *Cell Stem Cell* **15:** 559-573

Chambers SM, Fasano CA, Papapetrou EP, Tomishima M, Sadelain M, Studer L (2009) Highly efficient neural conversion of human ES and iPS cells by dual inhibition of SMAD signaling. *Nat Biotechnol* **27:** 275-280

Chandrasekaran K, Hatanpaa K, Brady DR, Rapoport SI (1996) Evidence for physiological down-regulation of brain oxidative phosphorylation in Alzheimer's disease. *Exp Neurol* **142:** 80-88

Chandrasekaran K, Hatanpaa K, Rapoport SI, Brady DR (1997) Decreased expression of nuclear and mitochondrial DNA-encoded genes of oxidative phosphorylation in association neocortex in Alzheimer disease. *Brain Res Mol Brain Res* **44:** 99-104

Cheung KH, Mei L, Mak DO, Hayashi I, Iwatsubo T, Kang DE, Foskett JK (2010) Gain-of-function enhancement of IP3 receptor modal gating by familial Alzheimer's disease-linked presenilin mutants in human cells and mouse neurons. *Sci Signal* **3:** ra22

Chiong M, Cartes-Saavedra B, Norambuena-Soto I, Mondaca-Ruff D, Morales PE, Garcia-Miguel M, Mellado R (2014) Mitochondrial metabolism and the control of vascular smooth muscle cell proliferation. *Front Cell Dev Biol* **2:** 72

Chu CT, Zhu J, Dagda R (2007) Beclin 1-independent pathway of damage-induced mitophagy and autophagic stress: implications for neurodegeneration and cell death. *Autophagy* **3:** 663-666

da Costa CA, Sunyach C, Giaime E, West A, Corti O, Brice A, Safe S, Abou-Sleiman PM, Wood NW, Takahashi H, Goldberg MS, Shen J, Checler F (2009) Transcriptional repression of p53 by parkin and impairment by mutations associated with autosomal recessive juvenile Parkinson's disease. *Nat Cell Biol* **11:** 1370-1375

Dagda RK, Cherra SJ, 3rd, Kulich SM, Tandon A, Park D, Chu CT (2009) Loss of PINK1 function promotes mitophagy through effects on oxidative stress and mitochondrial fission. *J Biol Chem* **284:** 13843-13855

David DC, Hauptmann S, Scherping I, Schuessel K, Keil U, Rizzu P, Ravid R, Drose S, Brandt U, Muller WE, Eckert A, Gotz J (2005) Proteomic and functional analyses reveal a mitochondrial dysfunction in P301L tau transgenic mice. *J Biol Chem* **280:** 23802-23814

De Strooper B, Iwatsubo T, Wolfe MS (2012) Presenilins and gamma-secretase: structure, function, and role in Alzheimer Disease. *Cold Spring Harb Perspect Med* **2:** a006304

de Toledo Ferraz Alves TC, Ferreira LK, Wajngarten M, Busatto GF (2010) Cardiac disorders as risk factors for Alzheimer's disease. *J Alzheimers Dis* **20:** 749-763

Detmer SA, Chan DC (2007) Functions and dysfunctions of mitochondrial dynamics. *Nat Rev Mol Cell Biol* **8:** 870-879

Devi L, Prabhu BM, Galati DF, Avadhani NG, Anandatheerthavarada HK (2006) Accumulation of amyloid precursor protein in the mitochondrial import channels of human Alzheimer's disease brain is associated with mitochondrial dysfunction. *J Neurosci* **26:** 9057-9068

Dickson DW, Crystal HA, Mattiace LA, Masur DM, Blau AD, Davies P, Yen SH, Aronson MK (1992) Identification of normal and pathological aging in prospectively studied nondemented elderly humans. *Neurobiol Aging* **13:** 179-189

Dimos JT, Rodolfa KT, Niakan KK, Weisenthal LM, Mitsumoto H, Chung W, Croft GF, Saphier G, Leibel R, Goland R, Wichterle H, Henderson CE, Eggan K (2008) Induced pluripotent stem cells generated from patients with ALS can be differentiated into motor neurons. *Science* **321:** 1218-1221

Ding WX, Ni HM, Gao W, Yoshimori T, Stolz DB, Ron D, Yin XM (2007) Linking of autophagy to ubiquitin-proteasome system is important for the regulation of endoplasmic reticulum stress and cell viability. *Am J Pathol* **171:** 513-524

Ding WX, Yin XM (2012) Mitophagy: mechanisms, pathophysiological roles, and analysis. *Biol Chem* **393:** 547-564

Drechsel DN, Hyman AA, Cobb MH, Kirschner MW (1992) Modulation of the dynamic instability of tubulin assembly by the microtubule-associated protein tau. *Mol Biol Cell* **3:** 1141-1154

Du H, Guo L, Fang F, Chen D, Sosunov AA, McKhann GM, Yan Y, Wang C, Zhang H, Molkentin JD, Gunn-Moore FJ, Vonsattel JP, Arancio O, Chen JX, Yan SD (2008) Cyclophilin D deficiency attenuates mitochondrial and neuronal perturbation and ameliorates learning and memory in Alzheimer's disease. *Nat Med* **14:** 1097-1105

Duan L, Bhattacharyya BJ, Belmadani A, Pan L, Miller RJ, Kessler JA (2014) Stem cell derived basal forebrain cholinergic neurons from Alzheimer's disease patients are more susceptible to cell death. *Mol Neurodegener* **9:** 3

DuBoff B, Gotz J, Feany MB (2012) Tau promotes neurodegeneration via DRP1 mislocalization in vivo. *Neuron* **75:** 618-632

Duce JA, Tsatsanis A, Cater MA, James SA, Robb E, Wikhe K, Leong SL, Perez K, Johanssen T, Greenough MA, Cho HH, Galatis D, Moir RD, Masters CL, McLean C, Tanzi RE, Cappai R, Barnham KJ, Ciccotosto GD, Rogers JT, Bush AI (2010) Iron-export ferroxidase activity of beta-amyloid precursor protein is inhibited by zinc in Alzheimer's disease. *Cell* **142:** 857-867

Dupont N, Temime-Smaali N, Lafont F (2010) How ubiquitination and autophagy participate in the regulation of the cell response to bacterial infection. *Biol Cell* **102:** 621-634

Ebneth A, Godemann R, Stamer K, Illenberger S, Trinczek B, Mandelkow E (1998) Overexpression of tau protein inhibits kinesin-dependent trafficking of vesicles, mitochondria, and endoplasmic reticulum: implications for Alzheimer's disease. *J Cell Biol* **143:** 777-794

Egeberg A, Hansen PR, Gislason GH, Thyssen JP (2016) Patients with rosacea have increased risk of dementia. *Ann Neurol*

Eiraku M, Watanabe K, Matsuo-Takasaki M, Kawada M, Yonemura S, Matsumura M, Wataya T, Nishiyama A, Muguruma K, Sasai Y (2008) Self-organized formation of polarized cortical tissues from ESCs and its active manipulation by extrinsic signals. *Cell Stem Cell* **3:** 519-532

Esclatine A, Chaumorcel M, Codogno P (2009) Macroautophagy signaling and regulation. *Curr Top Microbiol Immunol* **335:** 33-70

Escobar-Khondiker M, Hollerhage M, Muriel MP, Champy P, Bach A, Depienne C, Respondek G, Yamada ES, Lannuzel A, Yagi T, Hirsch EC, Oertel WH, Jacob R, Michel PP, Ruberg M, Hoglinger GU (2007) Annonacin, a natural mitochondrial complex I inhibitor, causes tau pathology in cultured neurons. *J Neurosci* **27:** 7827-7837

Fedorowicz MA, de Vries-Schneider RL, Rub C, Becker D, Huang Y, Zhou C, Alessi Wolken DM, Voos W, Liu Y, Przedborski S (2014) Cytosolic cleaved PINK1 represses Parkin translocation to mitochondria and mitophagy. *EMBO Rep* **15:** 86-93

Fodero-Tavoletti MT, Okamura N, Furumoto S, Mulligan RS, Connor AR, McLean CA, Cao D, Rigopoulos A, Cartwright GA, O'Keefe G, Gong S, Adlard PA, Barnham KJ, Rowe CC, Masters CL, Kudo Y, Cappai R, Yanai K, Villemagne VL (2011) 18F-THK523: a novel in vivo tau imaging ligand for Alzheimer's disease. *Brain* **134:** 1089-1100

Fotuhi M, Hachinski V, Whitehouse PJ (2009) Changing perspectives regarding late-life dementia. *Nat Rev Neurol* **5:** 649-658

Fraldi A, Annunziata F, Lombardi A, Kaiser HJ, Medina DL, Spampanato C, Fedele AO, Polishchuk R, Sorrentino NC, Simons K, Ballabio A (2010) Lysosomal fusion and SNARE function are impaired by cholesterol accumulation in lysosomal storage disorders. *EMBO J* **29:** 3607-3620

Frank S, Gaume B, Bergmann-Leitner ES, Leitner WW, Robert EG, Catez F, Smith CL, Youle RJ (2001) The role of dynamin-related protein 1, a mediator of mitochondrial fission, in apoptosis. *Dev Cell* **1:** 515-525

Frazier AE, Kiu C, Stojanovski D, Hoogenraad NJ, Ryan MT (2006) Mitochondrial morphology and distribution in mammalian cells. *Biol Chem* **387:** 1551-1558

Fridman AL, Tainsky MA (2008) Critical pathways in cellular senescence and immortalization revealed by gene expression profiling. *Oncogene* **27:** 5975-5987

Funderburk SF, Marcellino BK, Yue Z (2010) Cell "self-eating" (autophagy) mechanism in Alzheimer's disease. *Mt Sinai J Med* **77:** 59-68

Gallego MJ, Porayette P, Kaltcheva MM, Bowen RL, Vadakkadath Meethal S, Atwood CS (2010) The pregnancy hormones human chorionic gonadotropin and progesterone induce human embryonic stem cell proliferation and differentiation into neuroectodermal rosettes. *Stem Cell Res Ther* **1:** 28

Galluzzi L, Kepp O, Trojel-Hansen C, Kroemer G (2012) Mitochondrial control of cellular life, stress, and death. *Circ Res* **111:** 1198-1207

Ganley IG, Wong PM, Gammoh N, Jiang X (2011) Distinct autophagosomal-lysosomal fusion mechanism revealed by thapsigargin-induced autophagy arrest. *Mol Cell* **42:** 731-743

Garcia-Escudero V, Garcia-Gomez A, Gargini R, Martin-Bermejo MJ, Langa E, de Yebenes JG, Delicado A, Avila J, Moreno-Flores MT, Lim F (2010) Prevention of senescence progression in reversibly immortalized human ensheathing glia permits their survival after deimmortalization. *Mol Ther* **18:** 394-403

Garcia-Escudero V, Martin-Maestro P, Perry G, Avila J (2013) Deconstructing mitochondrial dysfunction in Alzheimer disease. *Oxid Med Cell Longev* **2013:** 162152

Geisler S, Holmstrom KM, Skujat D, Fiesel FC, Rothfuss OC, Kahle PJ, Springer W (2010) PINK1/Parkin-mediated mitophagy is dependent on VDAC1 and p62/SQSTM1. *Nat Cell Biol* **12:** 119-131

Gibson GE, Sheu KF, Blass JP, Baker A, Carlson KC, Harding B, Perrino P (1988) Reduced activities of thiamine-dependent enzymes in the brains and peripheral tissues of patients with Alzheimer's disease. *Arch Neurol* **45:** 836-840

Goedert M, Wischik CM, Crowther RA, Walker JE, Klug A (1988) Cloning and sequencing of the cDNA encoding a core protein of the paired helical filament of Alzheimer disease: identification as the microtubule-associated protein tau. *Proc Natl Acad Sci U S A* **85:** 4051-4055

Gore A, Li Z, Fung HL, Young JE, Agarwal S, Antosiewicz-Bourget J, Canto I, Giorgetti A, Israel MA, Kiskinis E, Lee JH, Loh YH, Manos PD, Montserrat N, Panopoulos AD, Ruiz S, Wilbert ML, Yu J, Kirkness EF, Izpisua Belmonte JC, Rossi DJ, Thomson JA, Eggan K, Daley GQ, Goldstein LS, Zhang K (2011) Somatic coding mutations in human induced pluripotent stem cells. *Nature* **471:** 63-67

Greene AW, Grenier K, Aguileta MA, Muise S, Farazifard R, Haque ME, McBride HM, Park DS, Fon EA (2012) Mitochondrial processing peptidase regulates PINK1 processing, import and Parkin recruitment. *EMBO Rep* **13:** 378-385

Grundke-Iqbal I, Iqbal K, Quinlan M, Tung YC, Zaidi MS, Wisniewski HM (1986a) Microtubule-associated protein tau. A component of Alzheimer paired helical filaments. *J Biol Chem* **261:** 6084-6089

Grundke-Iqbal I, Iqbal K, Tung YC, Quinlan M, Wisniewski HM, Binder LI (1986b) Abnormal phosphorylation of the microtubule-associated protein tau (tau) in Alzheimer cytoskeletal pathology. *Proc Natl Acad Sci U S A* **83:** 4913-4917

Haass C, Hung AY, Schlossmacher MG, Teplow DB, Selkoe DJ (1993) beta-Amyloid peptide and a 3-kDa fragment are derived by distinct cellular mechanisms. *J Biol Chem* **268:** 3021-3024

Haass C, Schlossmacher MG, Hung AY, Vigo-Pelfrey C, Mellon A, Ostaszewski BL, Lieberburg I, Koo EH, Schenk D, Teplow DB, et al. (1992) Amyloid beta-peptide is produced by cultured cells during normal metabolism. *Nature* **359:** 322-325

Haass C, Selkoe DJ (1993) Cellular processing of beta-amyloid precursor protein and the genesis of amyloid beta-peptide. *Cell* **75:** 1039-1042

Hagiwara H, Yorifuji H, Sato-Yoshitake R, Hirokawa N (1994) Competition between motor molecules (kinesin and cytoplasmic dynein) and fibrous microtubule-associated proteins in binding to microtubules. *J Biol Chem* **269:** 3581-3589

Hamano T, Gendron TF, Causevic E, Yen SH, Lin WL, Isidoro C, Deture M, Ko LW (2008) Autophagic-lysosomal perturbation enhances tau aggregation in transfectants with induced wild-type tau expression. *Eur J Neurosci* **27:** 1119-1130

Hanna J, Markoulaki S, Schorderet P, Carey BW, Beard C, Wernig M, Creyghton MP, Steine EJ, Cassady JP, Foreman R, Lengner CJ, Dausman JA, Jaenisch R (2008) Direct reprogramming of terminally differentiated mature B lymphocytes to pluripotency. *Cell* **133:** 250-264

Hanna JH, Saha K, Jaenisch R (2010) Pluripotency and cellular reprogramming: facts, hypotheses, unresolved issues. *Cell* **143:** 508-525

Hansson CA, Frykman S, Farmery MR, Tjernberg LO, Nilsberth C, Pursglove SE, Ito A, Winblad B, Cowburn RF, Thyberg J, Ankarcrona M (2004) Nicastrin, presenilin, APH-1, and PEN-2 form active gamma-secretase complexes in mitochondria. *J Biol Chem* **279:** 51654-51660

Hartjes KA, Li X, Martinez-Fernandez A, Roemmich AJ, Larsen BT, Terzic A, Nelson TJ (2014) Selection via pluripotency-related transcriptional screen minimizes the influence of somatic origin on iPSC differentiation propensity. *Stem Cells* **32:** 2350-2359

Hauptmann S, Scherping I, Drose S, Brandt U, Schulz KL, Jendrach M, Leuner K, Eckert A, Muller WE (2009) Mitochondrial dysfunction: an early event in Alzheimer pathology accumulates with age in AD transgenic mice. *Neurobiol Aging* **30:** 1574-1586

He C, Klionsky DJ (2009) Regulation mechanisms and signaling pathways of autophagy. *Annu Rev Genet* **43:** 67-93

Hirano A, Dembitzer HM, Kurland LT, Zimmerman HM (1968) The fine structure of some intraganglionic alterations. Neurofibrillary tangles, granulovacuolar bodies and "rod-like" structures as seen in Guam amyotrophic lateral sclerosis and parkinsonism-dementia complex. *J Neuropathol Exp Neurol* **27:** 167-182

Hokama M, Oka S, Leon J, Ninomiya T, Honda H, Sasaki K, Iwaki T, Ohara T, Sasaki T, LaFerla FM, Kiyohara Y, Nakabeppu Y (2014) Altered expression of diabetes-related genes in Alzheimer's disease brains: the Hisayama study. *Cereb Cortex* **24:** 2476-2488

Holtzman E, Novikoff AB (1965) Lysomes in the rat sciatic nerve following crush. *J Cell Biol* **27:** 651-669

Hu W, Qiu B, Guan W, Wang Q, Wang M, Li W, Gao L, Shen L, Huang Y, Xie G, Zhao H, Jin Y, Tang B, Yu Y, Zhao J, Pei G (2015) Direct Conversion of Normal and Alzheimer's Disease Human Fibroblasts into Neuronal Cells by Small Molecules. *Cell Stem Cell* **17:** 204-212

Hu Y, Li XC, Wang ZH, Luo Y, Zhang X, Liu XP, Feng Q, Wang Q, Yue Z, Chen Z, Ye K, Wang JZ, Liu GP (2016) Tau accumulation impairs mitophagy via increasing mitochondrial membrane potential and reducing mitochondrial parkin. *Oncotarget*

Huang C, Andres AM, Ratliff EP, Hernandez G, Lee P, Gottlieb RA (2011) Preconditioning involves selective mitophagy mediated by Parkin and p62/SQSTM1. *PLoS One* **6:** e20975

Iijima-Ando K, Sekiya M, Maruko-Otake A, Ohtake Y, Suzuki E, Lu B, Iijima KM (2012) Loss of axonal mitochondria promotes tau-mediated neurodegeneration and Alzheimer's disease-related tau phosphorylation via PAR-1. *PLoS Genet* **8:** e1002918

Ikeda K, Urakami K, Arai H, Wada K, Wakutani Y, Ji Y, Adachi Y, Okada A, Kowa H, Sasaki H, Ohno K, Ohtsuka Y, Ishikawa Y, Nakashima K (2000) The expression of presenilin 1 mRNA in skin fibroblasts and brains from sporadic Alzheimer's disease. *Dement Geriatr Cogn Disord* **11:** 245-250

Imai Y (2012) Mitochondrial Regulation by PINK1-Parkin Signaling. *ISRN Cell Biology* **2012:** 15

Ingelson M, Vanmechelen E, Lannfelt L (1996) Microtubule-associated protein tau in human fibroblasts with the Swedish Alzheimer mutation. *Neurosci Lett* **220:** 9-12

Ionescu L, White C, Cheung KH, Shuai J, Parker I, Pearson JE, Foskett JK, Mak DO (2007) Mode switching is the major mechanism of ligand regulation of InsP3 receptor calcium release channels. *J Gen Physiol* **130:** 631-645

Ishihara N, Fujita Y, Oka T, Mihara K (2006) Regulation of mitochondrial morphology through proteolytic cleavage of OPA1. *EMBO J* **25:** 2966-2977

Israel MA, Yuan SH, Bardy C, Reyna SM, Mu Y, Herrera C, Hefferan MP, Van Gorp S, Nazor KL, Boscolo FS, Carson CT, Laurent LC, Marsala M, Gage FH, Remes AM, Koo EH, Goldstein LS (2012) Probing sporadic and familial Alzheimer's disease using induced pluripotent stem cells. *Nature* **482:** 216-220

Itakura E, Kishi-Itakura C, Mizushima N (2012) The hairpin-type tail-anchored SNARE syntaxin 17 targets to autophagosomes for fusion with endosomes/lysosomes. *Cell* **151:** 1256-1269

Ito E, Oka K, Etcheberrigaray R, Nelson TJ, McPhie DL, Tofel-Grehl B, Gibson GE, Alkon DL (1994) Internal Ca2+ mobilization is altered in fibroblasts from patients with Alzheimer disease. *Proc Natl Acad Sci U S A* **91:** 534-538

Jaeger PA, Pickford F, Sun CH, Lucin KM, Masliah E, Wyss-Coray T (2010) Regulation of amyloid precursor protein processing by the Beclin 1 complex. *PLoS One* **5:** e11102

Jahreiss L, Menzies FM, Rubinsztein DC (2008) The itinerary of autophagosomes: from peripheral formation to kiss-and-run fusion with lysosomes. *Traffic* **9:** 574-587

Jicha GA, Rockwood JM, Berenfeld B, Hutton M, Davies P (1999) Altered conformation of recombinant frontotemporal dementia-17 mutant tau proteins. *Neurosci Lett* **260:** 153-156

Jin SM, Lazarou M, Wang C, Kane LA, Narendra DP, Youle RJ (2010) Mitochondrial membrane potential regulates PINK1 import and proteolytic destabilization by PARL. *J Cell Biol* **191:** 933-942

Jung SS, Nalbantoglu J, Cashman NR (1996) Alzheimer's beta-amyloid precursor protein is expressed on the surface of immediately ex vivo brain cells: a flow cytometric study. *J Neurosci Res* **46:** 336-348

Jung T, Catalgol B, Grune T (2009) The proteasomal system. *Mol Aspects Med* **30:** 191-296

Kadowaki H, Nishitoh H, Urano F, Sadamitsu C, Matsuzawa A, Takeda K, Masutani H, Yodoi J, Urano Y, Nagano T, Ichijo H (2005) Amyloid beta induces neuronal cell death through ROS-mediated ASK1 activation. *Cell Death Differ* **12:** 19-24

Kagan BL, Azimov R, Azimova R (2004) Amyloid peptide channels. *J Membr Biol* **202:** 1-10

Kahler DJ, Ahmad FS, Ritz A, Hua H, Moroziewicz DN, Sproul AA, Dusenberry CR, Shang L, Paull D, Zimmer M, Weiss KA, Egli D, Noggle SA (2013) Improved methods for reprogramming human dermal fibroblasts using fluorescence activated cell sorting. *PLoS One* **8:** e59867

Kane LA, Lazarou M, Fogel AI, Li Y, Yamano K, Sarraf SA, Banerjee S, Youle RJ (2014) PINK1 phosphorylates ubiquitin to activate Parkin E3 ubiquitin ligase activity. *J Cell Biol* **205:** 143-153

Kang DE, Roh SE, Woo JA, Liu T, Bu JH, Jung AR, Lim Y (2011) The Interface between Cytoskeletal Aberrations and Mitochondrial Dysfunction in Alzheimer's Disease and Related Disorders. *Exp Neurobiol* **20:** 67-80

Katsuragi Y, Ichimura Y, Komatsu M (2015) p62/SQSTM1 functions as a signaling hub and an autophagy adaptor. *FEBS J***:** 10.1111/febs.13540

Katzman R, Terry R, DeTeresa R, Brown T, Davies P, Fuld P, Renbing X, Peck A (1988) Clinical, pathological, and neurochemical changes in dementia: a subgroup with preserved mental status and numerous neocortical plaques. *Ann Neurol* **23:** 138-144

Kawas CH, Corrada MM (2006) Alzheimer's and dementia in the oldest-old: a century of challenges. *Curr Alzheimer Res* **3:** 411-419

Keck S, Nitsch R, Grune T, Ullrich O (2003) Proteasome inhibition by paired helical filament-tau in brains of patients with Alzheimer's disease. *J Neurochem* **85:** 115-122

Khandelwal PJ, Herman AM, Hoe HS, Rebeck GW, Moussa CE (2011) Parkin mediates beclin-dependent autophagic clearance of defective mitochondria and ubiquitinated Abeta in AD models. *Hum Mol Genet* **20:** 2091-2102

Kim K, Doi A, Wen B, Ng K, Zhao R, Cahan P, Kim J, Aryee MJ, Ji H, Ehrlich LI, Yabuuchi A, Takeuchi A, Cunniff KC, Hongguang H, McKinney-Freeman S, Naveiras O, Yoon TJ, Irizarry RA, Jung N, Seita J, Hanna J, Murakami P, Jaenisch R, Weissleder R, Orkin SH, Weissman IL, Feinberg AP, Daley GQ (2010) Epigenetic memory in induced pluripotent stem cells. *Nature* **467:** 285-290

Kim TS, Misumi S, Jung CG, Masuda T, Isobe Y, Furuyama F, Nishino H, Hida H (2008a) Increase in dopaminergic neurons from mouse embryonic stem cell-derived neural progenitor/stem cells is mediated by hypoxia inducible factor-1alpha. *J Neurosci Res* **86:** 2353-2362

Kim Y, Park J, Kim S, Song S, Kwon SK, Lee SH, Kitada T, Kim JM, Chung J (2008b) PINK1 controls mitochondrial localization of Parkin through direct phosphorylation. *Biochem Biophys Res Commun* **377:** 975-980

Kimura S, Noda T, Yoshimori T (2007) Dissection of the autophagosome maturation process by a novel reporter protein, tandem fluorescent-tagged LC3. *Autophagy* **3:** 452-460

Kinoshita E, Kinoshita-Kikuta E, Takiyama K, Koike T (2006) Phosphate-binding tag, a new tool to visualize phosphorylated proteins. *Mol Cell Proteomics* **5:** 749-757

Kirkin V, McEwan DG, Novak I, Dikic I (2009) A role for ubiquitin in selective autophagy. *Mol Cell* **34:** 259-269

Kitada T, Asakawa S, Hattori N, Matsumine H, Yamamura Y, Minoshima S, Yokochi M, Mizuno Y, Shimizu N (1998) Mutations in the parkin gene cause autosomal recessive juvenile parkinsonism. *Nature* **392:** 605-608

Klionsky DJ (2005) The molecular machinery of autophagy: unanswered questions. *J Cell Sci* **118:** 7-18

Klionsky DJ (2007) Autophagy: from phenomenology to molecular understanding in less than a decade. *Nat Rev Mol Cell Biol* **8:** 931-937

Klionsky DJ, et al (2016) Guidelines for the use and interpretation of assays for monitoring autophagy (3rd edition). *Autophagy* **12:** 1-222

Klunk WE, Engler H, Nordberg A, Wang Y, Blomqvist G, Holt DP, Bergstrom M, Savitcheva I, Huang GF, Estrada S, Ausen B, Debnath ML, Barletta J, Price JC, Sandell J, Lopresti BJ, Wall A, Koivisto P, Antoni G, Mathis CA, Langstrom B (2004) Imaging brain amyloid in Alzheimer's disease with Pittsburgh Compound-B. *Ann Neurol* **55:** 306-319

Ko LW, Sheu KF, Thaler HT, Markesbery WR, Blass JP (2001) Selective loss of KGDHC-enriched neurons in Alzheimer temporal cortex: does mitochondrial variation contribute to selective vulnerability? *J Mol Neurosci* **17:** 361-369

Koch P, Tamboli IY, Mertens J, Wunderlich P, Ladewig J, Stuber K, Esselmann H, Wiltfang J, Brustle O, Walter J (2012) Presenilin-1 L166P mutant human pluripotent stem cell-derived neurons exhibit partial loss of gamma-secretase activity in endogenous amyloid-beta generation. *Am J Pathol* **180:** 2404-2416

Komatsu M, Waguri S, Koike M, Sou YS, Ueno T, Hara T, Mizushima N, Iwata J, Ezaki J, Murata S, Hamazaki J, Nishito Y, Iemura S, Natsume T, Yanagawa T, Uwayama J, Warabi E, Yoshida H, Ishii T, Kobayashi A, Yamamoto M, Yue Z, Uchiyama Y, Kominami E, Tanaka K (2007) Homeostatic levels of p62 control cytoplasmic inclusion body formation in autophagy-deficient mice. *Cell* **131:** 1149-1163

Kondo T, Asai M, Tsukita K, Kutoku Y, Ohsawa Y, Sunada Y, Imamura K, Egawa N, Yahata N, Okita K, Takahashi K, Asaka I, Aoi T, Watanabe A, Watanabe K, Kadoya C, Nakano R, Watanabe D, Maruyama K, Hori O, Hibino S, Choshi T, Nakahata T, Hioki H, Kaneko T, Naitoh M, Yoshikawa K, Yamawaki S, Suzuki S, Hata R, Ueno S, Seki T, Kobayashi K, Toda T, Murakami K, Irie K, Klein WL, Mori H, Asada

T, Takahashi R, Iwata N, Yamanaka S, Inoue H (2013) Modeling Alzheimer's disease with iPSCs reveals stress phenotypes associated with intracellular Abeta and differential drug responsiveness. *Cell Stem Cell* **12:** 487-496

Korolchuk VI, Mansilla A, Menzies FM, Rubinsztein DC (2009) Autophagy inhibition compromises degradation of ubiquitin-proteasome pathway substrates. *Mol Cell* **33:** 517-527

Kosik KS, Joachim CL, Selkoe DJ (1986) Microtubule-associated protein tau (tau) is a major antigenic component of paired helical filaments in Alzheimer disease. *Proc Natl Acad Sci U S A* **83:** 4044-4048

Koyano F, Okatsu K, Kosako H, Tamura Y, Go E, Kimura M, Kimura Y, Tsuchiya H, Yoshihara H, Hirokawa T, Endo T, Fon EA, Trempe JF, Saeki Y, Tanaka K, Matsuda N (2014) Ubiquitin is phosphorylated by PINK1 to activate parkin. *Nature* **510:** 162-166

Kraft C, Peter M, Hofmann K (2010) Selective autophagy: ubiquitin-mediated recognition and beyond. *Nat Cell Biol* **12:** 836-841

Kukull WA, Higdon R, Bowen JD, McCormick WC, Teri L, Schellenberg GD, van Belle G, Jolley L, Larson EB (2002) Dementia and Alzheimer disease incidence: a prospective cohort study. *Arch Neurol* **59:** 1737-1746

Kuo SH, Tang G, Ma K, Babij R, Cortes E, Vonsattel JP, Faust PL, Sulzer D, Louis ED (2012) Macroautophagy abnormality in essential tremor. *PLoS One* **7:** e53040

Kuusisto E, Salminen A, Alafuzoff I (2001) Ubiquitin-binding protein p62 is present in neuronal and glial inclusions in human tauopathies and synucleinopathies. *Neuroreport* **12:** 2085-2090

Kuusisto E, Salminen A, Alafuzoff I (2002) Early accumulation of p62 in neurofibrillary tangles in Alzheimer's disease: possible role in tangle formation. *Neuropathol Appl Neurobiol* **28:** 228-237

Ladewig J, Mertens J, Kesavan J, Doerr J, Poppe D, Glaue F, Herms S, Wernet P, Kogler G, Muller FJ, Koch P, Brustle O (2012) Small molecules enable highly efficient neuronal conversion of human fibroblasts. *Nat Methods* **9:** 575-578

Lai AY, McLaurin J (2012) Inhibition of amyloid-beta peptide aggregation rescues the autophagic deficits in the TgCRND8 mouse model of Alzheimer disease. *Biochim Biophys Acta* **1822:** 1629-1637

Lamark T, Johansen T (2012) Aggrephagy: selective disposal of protein aggregates by macroautophagy. *Int J Cell Biol* **2012:** 736905

Lancaster MA, Renner M, Martin CA, Wenzel D, Bicknell LS, Hurles ME, Homfray T, Penninger JM, Jackson AP, Knoblich JA (2013) Cerebral organoids model human brain development and microcephaly. *Nature* **501:** 373-379

Lazarou M, Jin SM, Kane LA, Youle RJ (2012) Role of PINK1 binding to the TOM complex and alternate intracellular membranes in recruitment and activation of the E3 ligase Parkin. *Dev Cell* **22:** 320-333

Lee H, Shamy GA, Elkabetz Y, Schofield CM, Harrsion NL, Panagiotakos G, Socci ND, Tabar V, Studer L (2007) Directed differentiation and transplantation of human embryonic stem cell-derived motoneurons. *Stem Cells* **25:** 1931-1939

Lee JH, Yu WH, Kumar A, Lee S, Mohan PS, Peterhoff CM, Wolfe DM, Martinez-Vicente M, Massey AC, Sovak G, Uchiyama Y, Westaway D, Cuervo AM, Nixon RA (2010) Lysosomal proteolysis and autophagy require presenilin 1 and are disrupted by Alzheimer-related PS1 mutations. *Cell* **141:** 1146-1158

Lee MK, Slunt HH, Martin LJ, Thinakaran G, Kim G, Gandy SE, Seeger M, Koo E, Price DL, Sisodia SS (1996) Expression of presenilin 1 and 2 (PS1 and PS2) in human and murine tissues. *J Neurosci* **16:** 7513-7525

Lee S, Zhang C, Liu X (2015) Role of glucose metabolism and ATP in maintaining PINK1 levels during Parkin-mediated mitochondrial damage responses. *J Biol Chem* **290:** 904-917

Lee VM, Balin BJ, Otvos L, Jr., Trojanowski JQ (1991) A68: a major subunit of paired helical filaments and derivatized forms of normal Tau. *Science* **251:** 675-678

Lemasters JJ (2005) Selective mitochondrial autophagy, or mitophagy, as a targeted defense against oxidative stress, mitochondrial dysfunction, and aging. *Rejuvenation Res* **8:** 3-5

Li WW, Li J, Bao JK (2012) Microautophagy: lesser-known self-eating. *Cell Mol Life Sci* **69:** 1125-1136

Lin T, Ambasudhan R, Yuan X, Li W, Hilcove S, Abujarour R, Lin X, Hahm HS, Hao E, Hayek A, Ding S (2009) A chemical platform for improved induction of human iPSCs. *Nat Methods* **6:** 805-808

Lister R, Pelizzola M, Kida YS, Hawkins RD, Nery JR, Hon G, Antosiewicz-Bourget J, O'Malley R, Castanon R, Klugman S, Downes M, Yu R, Stewart R, Ren B, Thomson JA, Evans RM, Ecker JR (2011) Hotspots of aberrant epigenomic reprogramming in human induced pluripotent stem cells. *Nature* **471:** 68-73

Liu Q, Spusta SC, Mi R, Lassiter RN, Stark MR, Hoke A, Rao MS, Zeng X (2012) Human neural crest stem cells derived from human ESCs and induced pluripotent stem cells: induction, maintenance, and differentiation into functional schwann cells. *Stem Cells Transl Med* **1:** 266-278

Lo HS, Wang Z, Hu Y, Yang HH, Gere S, Buetow KH, Lee MP (2003) Allelic variation in gene expression is common in the human genome. *Genome Res* **13:** 1855-1862

Loh YH, Agarwal S, Park IH, Urbach A, Huo H, Heffner GC, Kim K, Miller JD, Ng K, Daley GQ (2009) Generation of induced pluripotent stem cells from human blood. *Blood* **113:** 5476-5479

Lonskaya I, Shekoyan AR, Hebron ML, Desforges N, Algarzae NK, Moussa CE (2013) Diminished parkin solubility and co-localization with intraneuronal amyloid-beta are associated with autophagic defects in Alzheimer's disease. *J Alzheimers Dis* **33:** 231-247

LoPresti P, Szuchet S, Papasozomenos SC, Zinkowski RP, Binder LI (1995) Functional implications for the microtubule-associated protein tau: localization in oligodendrocytes. *Proc Natl Acad Sci U S A* **92:** 10369-10373

Loson OC, Song Z, Chen H, Chan DC (2013) Fis1, Mff, MiD49, and MiD51 mediate Drp1 recruitment in mitochondrial fission. *Mol Biol Cell* **24:** 659-667

Lustbader JW, Cirilli M, Lin C, Xu HW, Takuma K, Wang N, Caspersen C, Chen X, Pollak S, Chaney M, Trinchese F, Liu S, Gunn-Moore F, Lue LF, Walker DG, Kuppusamy P, Zewier ZL, Arancio O, Stern D, Yan SS, Wu H (2004) ABAD directly links Abeta to mitochondrial toxicity in Alzheimer's disease. *Science* **304:** 448-452

Luzio JP, Bright NA, Pryor PR (2007) The role of calcium and other ions in sorting and delivery in the late endocytic pathway. *Biochem Soc Trans* **35:** 1088-1091

Llorens-Martin M, Lopez-Domenech G, Soriano E, Avila J (2011) GSK3beta is involved in the relief of mitochondria pausing in a Tau-dependent manner. *PLoS One* **6:** e27686

Ma H, Morey R, O'Neil RC, He Y, Daughtry B, Schultz MD, Hariharan M, Nery JR, Castanon R, Sabatini K, Thiagarajan RD, Tachibana M, Kang E, Tippner-Hedges R, Ahmed R, Gutierrez NM, Van Dyken C, Polat A, Sugawara A, Sparman M, Gokhale S, Amato P, Wolf DP, Ecker JR, Laurent LC, Mitalipov S

(2014) Abnormalities in human pluripotent cells due to reprogramming mechanisms. *Nature* **511:** 177-183

Mahairaki V, Ryu J, Peters A, Chang Q, Li T, Park TS, Burridge PW, Talbot CC, Jr., Asnaghi L, Martin LJ, Zambidis ET, Koliatsos VE (2014) Induced pluripotent stem cells from familial Alzheimer's disease patients differentiate into mature neurons with amyloidogenic properties. *Stem Cells Dev* **23:** 2996-3010

Mancuso M, Calsolaro V, Orsucci D, Carlesi C, Choub A, Piazza S, Siciliano G (2009) Mitochondria, cognitive impairment, and Alzheimer's disease. *Int J Alzheimers Dis* **2009**

Manczak M, Calkins MJ, Reddy PH (2011) Impaired mitochondrial dynamics and abnormal interaction of amyloid beta with mitochondrial protein Drp1 in neurons from patients with Alzheimer's disease: implications for neuronal damage. *Hum Mol Genet* **20:** 2495-2509

Manczak M, Reddy PH (2012) Abnormal interaction of VDAC1 with amyloid beta and phosphorylated tau causes mitochondrial dysfunction in Alzheimer's disease. *Hum Mol Genet* **21:** 5131-5146

Manley S, Williams JA, Ding WX (2013) Role of p62/SQSTM1 in liver physiology and pathogenesis. *Exp Biol Med (Maywood)* **238:** 525-538

Marchetto MC, Muotri AR, Mu Y, Smith AM, Cezar GG, Gage FH (2008) Non-cell-autonomous effect of human SOD1 G37R astrocytes on motor neurons derived from human embryonic stem cells. *Cell Stem Cell* **3:** 649-657

Martinez-Vicente M, Talloczy Z, Wong E, Tang G, Koga H, Kaushik S, de Vries R, Arias E, Harris S, Sulzer D, Cuervo AM (2010) Cargo recognition failure is responsible for inefficient autophagy in Huntington's disease. *Nat Neurosci* **13:** 567-576

Massey A, Kiffin R, Cuervo AM (2004) Pathophysiology of chaperone-mediated autophagy. *Int J Biochem Cell Biol* **36:** 2420-2434

Masters CL, Multhaup G, Simms G, Pottgiesser J, Martins RN, Beyreuther K (1985) Neuronal origin of a cerebral amyloid: neurofibrillary tangles of Alzheimer's disease contain the same protein as the amyloid of plaque cores and blood vessels. *EMBO J* **4:** 2757-2763

Matteoni R, Kreis TE (1987) Translocation and clustering of endosomes and lysosomes depends on microtubules. *J Cell Biol* **105:** 1253-1265

Meissner C, Lorenz H, Weihofen A, Selkoe DJ, Lemberg MK (2011) The mitochondrial intramembrane protease PARL cleaves human Pink1 to regulate Pink1 trafficking. *J Neurochem* **117:** 856-867

Melov S, Adlard PA, Morten K, Johnson F, Golden TR, Hinerfeld D, Schilling B, Mavros C, Masters CL, Volitakis I, Li QX, Laughton K, Hubbard A, Cherny RA, Gibson B, Bush AI (2007) Mitochondrial oxidative stress causes hyperphosphorylation of tau. *PLoS One* **2:** e536

Mertens J, Stuber K, Wunderlich P, Ladewig J, Kesavan JC, Vandenberghe R, Vandenbulcke M, van Damme P, Walter J, Brustle O, Koch P (2013) APP processing in human pluripotent stem cell-derived neurons is resistant to NSAID-based gamma-secretase modulation. *Stem Cell Reports* **1:** 491-498

Mishra P, Chan DC (2014) Mitochondrial dynamics and inheritance during cell division, development and disease. *Nat Rev Mol Cell Biol* **15:** 634-646

Misko A, Jiang S, Wegorzewska I, Milbrandt J, Baloh RH (2010) Mitofusin 2 is necessary for transport of axonal mitochondria and interacts with the Miro/Milton complex. *J Neurosci* **30:** 4232-4240

Moore S, Evans LD, Andersson T, Portelius E, Smith J, Dias TB, Saurat N, McGlade A, Kirwan P, Blennow K, Hardy J, Zetterberg H, Livesey FJ (2015) APP metabolism regulates tau proteostasis in human cerebral cortex neurons. *Cell Rep* **11:** 689-696

Moreira PI, Cardoso SM, Santos MS, Oliveira CR (2006) The key role of mitochondria in Alzheimer's disease. *J Alzheimers Dis* **9:** 101-110

Moreira PI, Carvalho C, Zhu X, Smith MA, Perry G (2010) Mitochondrial dysfunction is a trigger of Alzheimer's disease pathophysiology. *Biochim Biophys Acta* **1802:** 2-10

Moreira PI, Harris PL, Zhu X, Santos MS, Oliveira CR, Smith MA, Perry G (2007a) Lipoic acid and N-acetyl cysteine decrease mitochondrial-related oxidative stress in Alzheimer disease patient fibroblasts. *J Alzheimers Dis* **12:** 195-206

Moreira PI, Siedlak SL, Wang X, Santos MS, Oliveira CR, Tabaton M, Nunomura A, Szweda LI, Aliev G, Smith MA, Zhu X, Perry G (2007b) Autophagocytosis of mitochondria is prominent in Alzheimer disease. *J Neuropathol Exp Neurol* **66:** 525-532

Moreira PI, Siedlak SL, Wang X, Santos MS, Oliveira CR, Tabaton M, Nunomura A, Szweda LI, Aliev G, Smith MA, Zhu X, Perry G (2007c) Increased autophagic degradation of mitochondria in Alzheimer disease. *Autophagy* **3:** 614-615

Morris JC, Storandt M, McKeel DW, Jr., Rubin EH, Price JL, Grant EA, Berg L (1996) Cerebral amyloid deposition and diffuse plaques in "normal" aging: Evidence for presymptomatic and very mild Alzheimer's disease. *Neurology* **46:** 707-719

Mosmann T (1983) Rapid colorimetric assay for cellular growth and survival: application to proliferation and cytotoxicity assays. *J Immunol Methods* **65:** 55-63

Muratore CR, Rice HC, Srikanth P, Callahan DG, Shin T, Benjamin LN, Walsh DM, Selkoe DJ, Young-Pearse TL (2014) The familial Alzheimer's disease APPV717I mutation alters APP processing and Tau expression in iPSC-derived neurons. *Hum Mol Genet* **23:** 3523-3536

Naderi J, Lopez C, Pandey S (2006) Chronically increased oxidative stress in fibroblasts from Alzheimer's disease patients causes early senescence and renders resistance to apoptosis by oxidative stress. *Mech Ageing Dev* **127:** 25-35

Narendra D, Kane LA, Hauser DN, Fearnley IM, Youle RJ (2010a) p62/SQSTM1 is required for Parkin-induced mitochondrial clustering but not mitophagy; VDAC1 is dispensable for both. *Autophagy* **6:** 1090-1106

Narendra D, Tanaka A, Suen DF, Youle RJ (2008) Parkin is recruited selectively to impaired mitochondria and promotes their autophagy. *J Cell Biol* **183:** 795-803

Narendra DP, Jin SM, Tanaka A, Suen DF, Gautier CA, Shen J, Cookson MR, Youle RJ (2010b) PINK1 is selectively stabilized on impaired mitochondria to activate Parkin. *PLoS Biol* **8:** e1000298

Nazor KL, Altun G, Lynch C, Tran H, Harness JV, Slavin I, Garitaonandia I, Muller FJ, Wang YC, Boscolo FS, Fakunle E, Dumevska B, Lee S, Park HS, Olee T, D'Lima DD, Semechkin R, Parast MM, Galat V, Laslett AL, Schmidt U, Keirstead HS, Loring JF, Laurent LC (2012) Recurrent variations in DNA methylation in human pluripotent stem cells and their differentiated derivatives. *Cell Stem Cell* **10:** 620-634

Neely KM, Green KN, LaFerla FM (2011) Presenilin is necessary for efficient proteolysis through the autophagy-lysosome system in a gamma-secretase-independent manner. *J Neurosci* **31:** 2781-2791

Neve RL, McPhie DL, Chen Y (2000) Alzheimer's disease: a dysfunction of the amyloid precursor protein(1). *Brain Res* **886:** 54-66

Ni HM, Williams JA, Ding WX (2015) Mitochondrial dynamics and mitochondrial quality control. *Redox Biol* **4:** 6-13

Nicholas CR, Chen J, Tang Y, Southwell DG, Chalmers N, Vogt D, Arnold CM, Chen YJ, Stanley EG, Elefanty AG, Sasai Y, Alvarez-Buylla A, Rubenstein JL, Kriegstein AR (2013) Functional maturation of hPSC-derived forebrain interneurons requires an extended timeline and mimics human neural development. *Cell Stem Cell* **12:** 573-586

Nikfarjam L, Farzaneh P (2012) Prevention and detection of Mycoplasma contamination in cell culture. *Cell J* **13:** 203-212

Nixon RA (2005) Endosome function and dysfunction in Alzheimer's disease and other neurodegenerative diseases. *Neurobiol Aging* **26:** 373-382

Nixon RA, Wegiel J, Kumar A, Yu WH, Peterhoff C, Cataldo A, Cuervo AM (2005) Extensive involvement of autophagy in Alzheimer disease: an immuno-electron microscopy study. *J Neuropathol Exp Neurol* **64:** 113-122

Nunomura A, Perry G, Aliev G, Hirai K, Takeda A, Balraj EK, Jones PK, Ghanbari H, Wataya T, Shimohama S, Chiba S, Atwood CS, Petersen RB, Smith MA (2001) Oxidative damage is the earliest event in Alzheimer disease. *J Neuropathol Exp Neurol* **60:** 759-767

Okatsu K, Oka T, Iguchi M, Imamura K, Kosako H, Tani N, Kimura M, Go E, Koyano F, Funayama M, Shiba-Fukushima K, Sato S, Shimizu H, Fukunaga Y, Taniguchi H, Komatsu M, Hattori N, Mihara K, Tanaka K, Matsuda N (2012) PINK1 autophosphorylation upon membrane potential dissipation is essential for Parkin recruitment to damaged mitochondria. *Nat Commun* **3:** 1016

Okatsu K, Saisho K, Shimanuki M, Nakada K, Shitara H, Sou YS, Kimura M, Sato S, Hattori N, Komatsu M, Tanaka K, Matsuda N (2010) p62/SQSTM1 cooperates with Parkin for perinuclear clustering of depolarized mitochondria. *Genes Cells* **15:** 887-900

Orvedahl A, Sumpter R, Jr., Xiao G, Ng A, Zou Z, Tang Y, Narimatsu M, Gilpin C, Sun Q, Roth M, Forst CV, Wrana JL, Zhang YE, Luby-Phelps K, Xavier RJ, Xie Y, Levine B (2011) Image-based genome-wide siRNA screen identifies selective autophagy factors. *Nature* **480:** 113-117

Ozawa K, Komatsubara AT, Nishimura Y, Sawada T, Kawafune H, Tsumoto H, Tsuji Y, Zhao J, Kyotani Y, Tanaka T, Takahashi R, Yoshizumi M (2013) S-nitrosylation regulates mitochondrial quality control via activation of parkin. *Sci Rep* **3:** 2202

Pagani L, Eckert A (2011) Amyloid-Beta interaction with mitochondria. *Int J Alzheimers Dis* **2011:** 925050

Palmer CS, Osellame LD, Laine D, Koutsopoulos OS, Frazier AE, Ryan MT (2011) MiD49 and MiD51, new components of the mitochondrial fission machinery. *EMBO Rep* **12:** 565-573

Pandey UB, Nie Z, Batlevi Y, McCray BA, Ritson GP, Nedelsky NB, Schwartz SL, DiProspero NA, Knight MA, Schuldiner O, Padmanabhan R, Hild M, Berry DL, Garza D, Hubbert CC, Yao TP, Baehrecke EH, Taylor JP (2007) HDAC6 rescues neurodegeneration and provides an essential link between autophagy and the UPS. *Nature* **447:** 859-863

Pankiv S, Clausen TH, Lamark T, Brech A, Bruun JA, Outzen H, Overvatn A, Bjorkoy G, Johansen T (2007) p62/SQSTM1 binds directly to Atg8/LC3 to facilitate degradation of ubiquitinated protein aggregates by autophagy. *J Biol Chem* **282:** 24131-24145

Paquet D, Kwart D, Chen A, Sproul A, Jacob S, Teo S, Olsen KM, Gregg A, Noggle S, Tessier-Lavigne M (2016) Efficient introduction of specific homozygous and heterozygous mutations using CRISPR/Cas9. *Nature* **533:** 125-129

Parsons MJ, Green DR (2010) Mitochondria in cell death. *Essays Biochem* **47:** 99-114

Perry EK, Perry RH, Tomlinson BE, Blessed G, Gibson PH (1980) Coenzyme A-acetylating enzymes in Alzheimer's disease: possible cholinergic 'compartment' of pyruvate dehydrogenase. *Neurosci Lett* **18:** 105-110

Piaceri I, Nacmias B, Sorbi S (2013) Genetics of familial and sporadic Alzheimer's disease. *Front Biosci (Elite Ed)* **5:** 167-177

Pickford F, Masliah E, Britschgi M, Lucin K, Narasimhan R, Jaeger PA, Small S, Spencer B, Rockenstein E, Levine B, Wyss-Coray T (2008) The autophagy-related protein beclin 1 shows reduced expression in early Alzheimer disease and regulates amyloid beta accumulation in mice. *J Clin Invest* **118:** 2190-2199

Polgar L, Csoma C (1987) Dissociation of ionizing groups in the binding cleft inversely controls the endo- and exopeptidase activities of cathepsin B. *J Biol Chem* **262:** 14448-14453

Polo JM, Liu S, Figueroa ME, Kulalert W, Eminli S, Tan KY, Apostolou E, Stadtfeld M, Li Y, Shioda T, Natesan S, Wagers AJ, Melnick A, Evans T, Hochedlinger K (2010) Cell type of origin influences the molecular and functional properties of mouse induced pluripotent stem cells. *Nat Biotechnol* **28:** 848-855

Porayette P, Gallego MJ, Kaltcheva MM, Bowen RL, Vadakkadath Meethal S, Atwood CS (2009) Differential processing of amyloid-beta precursor protein directs human embryonic stem cell proliferation and differentiation into neuronal precursor cells. *J Biol Chem* **284:** 23806-23817

Priller C, Bauer T, Mitteregger G, Krebs B, Kretzschmar HA, Herms J (2006) Synapse formation and function is modulated by the amyloid precursor protein. *J Neurosci* **26:** 7212-7221

Raber J, Huang Y, Ashford JW (2004) ApoE genotype accounts for the vast majority of AD risk and AD pathology. *Neurobiol Aging* **25:** 641-650

Rademakers R, Cruts M, Van Broeckhoven C (2003) Genetics of early-onset Alzheimer dementia. *ScientificWorldJournal* **3:** 497-519

Ravikumar B, Duden R, Rubinsztein DC (2002) Aggregate-prone proteins with polyglutamine and polyalanine expansions are degraded by autophagy. *Hum Mol Genet* **11:** 1107-1117

Reddy PH, Beal MF (2005) Are mitochondria critical in the pathogenesis of Alzheimer's disease? *Brain Res Brain Res Rev* **49:** 618-632

Rose C, Menzies FM, Renna M, Acevedo-Arozena A, Corrochano S, Sadiq O, Brown SD, Rubinsztein DC (2010) Rilmenidine attenuates toxicity of polyglutamine expansions in a mouse model of Huntington's disease. *Hum Mol Genet* **19:** 2144-2153

Rosen KM, Moussa CE, Lee HK, Kumar P, Kitada T, Qin G, Fu Q, Querfurth HW (2010) Parkin reverses intracellular beta-amyloid accumulation and its negative effects on proteasome function. *J Neurosci Res* **88:** 167-178

Rossi G, Dalpra L, Crosti F, Lissoni S, Sciacca FL, Catania M, Di Fede G, Mangieri M, Giaccone G, Croci D, Tagliavini F (2008) A new function of microtubule-associated protein tau: involvement in chromosome stability. *Cell Cycle* **7:** 1788-1794

Rowe CC, Ng S, Ackermann U, Gong SJ, Pike K, Savage G, Cowie TF, Dickinson KL, Maruff P, Darby D, Smith C, Woodward M, Merory J, Tochon-Danguy H, O'Keefe G, Klunk WE, Mathis CA, Price JC, Masters CL, Villemagne VL (2007) Imaging beta-amyloid burden in aging and dementia. *Neurology* **68:** 1718-1725

Rui Y, Tiwari P, Xie Z, Zheng JQ (2006) Acute impairment of mitochondrial trafficking by beta-amyloid peptides in hippocampal neurons. *J Neurosci* **26:** 10480-10487

Saftig P, Klumperman J (2009) Lysosome biogenesis and lysosomal membrane proteins: trafficking meets function. *Nat Rev Mol Cell Biol* **10:** 623-635

Sandoe J, Eggan K (2013) Opportunities and challenges of pluripotent stem cell neurodegenerative disease models. *Nat Neurosci* **16:** 780-789

Santa-Maria I, Hernandez F, Martin CP, Avila J, Moreno FJ (2004) Quinones facilitate the self-assembly of the phosphorylated tubulin binding region of tau into fibrillar polymers. *Biochemistry* **43:** 2888-2897

Santos RX, Correia SC, Wang X, Perry G, Smith MA, Moreira PI, Zhu X (2010) A synergistic dysfunction of mitochondrial fission/fusion dynamics and mitophagy in Alzheimer's disease. *J Alzheimers Dis* **20 Suppl 2:** S401-412

Savage VM, Allen AP, Brown JH, Gillooly JF, Herman AB, Woodruff WH, West GB (2007) Scaling of number, size, and metabolic rate of cells with body size in mammals. *Proc Natl Acad Sci U S A* **104:** 4718-4723

Saxton WM, Hollenbeck PJ (2012) The axonal transport of mitochondria. *J Cell Sci* **125:** 2095-2104

Schaeffer V, Lavenir I, Ozcelik S, Tolnay M, Winkler DT, Goedert M (2012) Stimulation of autophagy reduces neurodegeneration in a mouse model of human tauopathy. *Brain* **135:** 2169-2177

Scheper W, Nijholt DA, Hoozemans JJ (2011) The unfolded protein response and proteostasis in Alzheimer disease: preferential activation of autophagy by endoplasmic reticulum stress. *Autophagy* **7:** 910-911

Schmidt ML, Zhukareva V, Newell KL, Lee VM, Trojanowski JQ (2001) Tau isoform profile and phosphorylation state in dementia pugilistica recapitulate Alzheimer's disease. *Acta Neuropathol* **101:** 518-524

Schmitt K, Grimm A, Kazmierczak A, Strosznajder JB, Gotz J, Eckert A (2012) Insights into mitochondrial dysfunction: aging, amyloid-beta, and tau-A deleterious trio. *Antioxid Redox Signal* **16:** 1456-1466

Schon EA, Area-Gomez E (2010) Is Alzheimer's disease a disorder of mitochondria-associated membranes? *J Alzheimers Dis* **20 Suppl 2:** S281-292

Schondorf DC, Aureli M, McAllister FE, Hindley CJ, Mayer F, Schmid B, Sardi SP, Valsecchi M, Hoffmann S, Schwarz LK, Hedrich U, Berg D, Shihabuddin LS, Hu J, Pruszak J, Gygi SP, Sonnino S, Gasser T, Deleidi M (2014) iPSC-derived neurons from GBA1-associated Parkinson's disease patients show autophagic defects and impaired calcium homeostasis. *Nat Commun* **5:** 4028

Schuessel K, Frey C, Jourdan C, Keil U, Weber CC, Muller-Spahn F, Muller WE, Eckert A (2006) Aging sensitizes toward ROS formation and lipid peroxidation in PS1M146L transgenic mice. *Free Radic Biol Med* **40:** 850-862

Schulz KL, Eckert A, Rhein V, Mai S, Haase W, Reichert AS, Jendrach M, Muller WE, Leuner K (2012) A new link to mitochondrial impairment in tauopathies. *Mol Neurobiol* **46:** 205-216

Selkoe DJ (2001) Alzheimer's disease: genes, proteins, and therapy. *Physiol Rev* **81:** 741-766

Selkoe DJ (2002) Alzheimer's disease is a synaptic failure. *Science* **298:** 789-791

Serrano-Pozo A, Frosch MP, Masliah E, Hyman BT (2011) Neuropathological alterations in Alzheimer disease. *Cold Spring Harb Perspect Med* **1:** a006189

Sha D, Chin LS, Li L (2010) Phosphorylation of parkin by Parkinson disease-linked kinase PINK1 activates parkin E3 ligase function and NF-kappaB signaling. *Hum Mol Genet* **19:** 352-363

Shalem O, Sanjana NE, Hartenian E, Shi X, Scott DA, Mikkelsen TS, Heckl D, Ebert BL, Root DE, Doench JG, Zhang F (2014) Genome-scale CRISPR-Cas9 knockout screening in human cells. *Science* **343:** 84-87

Sherrington R, Rogaev EI, Liang Y, Rogaeva EA, Levesque G, Ikeda M, Chi H, Lin C, Li G, Holman K, Tsuda T, Mar L, Foncin JF, Bruni AC, Montesi MP, Sorbi S, Rainero I, Pinessi L, Nee L, Chumakov I, Pollen D, Brookes A, Sanseau P, Polinsky RJ, Wasco W, Da Silva HA, Haines JL, Perkicak-Vance MA, Tanzi RE, Roses AD, Fraser PE, Rommens JM, St George-Hyslop PH (1995) Cloning of a gene bearing missense mutations in early-onset familial Alzheimer's disease. *Nature* **375:** 754-760

Sheu KF, Cooper AJ, Koike K, Koike M, Lindsay JG, Blass JP (1994) Abnormality of the alpha-ketoglutarate dehydrogenase complex in fibroblasts from familial Alzheimer's disease. *Ann Neurol* **35:** 312-318

Shin RW, Iwaki T, Kitamoto T, Tateishi J (1991) Hydrated autoclave pretreatment enhances tau immunoreactivity in formalin-fixed normal and Alzheimer's disease brain tissues. *Lab Invest* **64:** 693-702

Sitte N, Merker K, Von Zglinicki T, Davies KJ, Grune T (2000a) Protein oxidation and degradation during cellular senescence of human BJ fibroblasts: part II--aging of nondividing cells. *FASEB J* **14:** 2503-2510

Sitte N, Merker K, Von Zglinicki T, Grune T, Davies KJ (2000b) Protein oxidation and degradation during cellular senescence of human BJ fibroblasts: part I--effects of proliferative senescence. *FASEB J* **14:** 2495-2502

Smirnova E, Griparic L, Shurland DL, van der Bliek AM (2001) Dynamin-related protein Drp1 is required for mitochondrial division in mammalian cells. *Mol Biol Cell* **12:** 2245-2256

Soba P, Eggert S, Wagner K, Zentgraf H, Siehl K, Kreger S, Lower A, Langer A, Merdes G, Paro R, Masters CL, Muller U, Kins S, Beyreuther K (2005) Homo- and heterodimerization of APP family members promotes intercellular adhesion. *EMBO J* **24:** 3624-3634

Son JH, Shim JH, Kim KH, Ha JY, Han JY (2012) Neuronal autophagy and neurodegenerative diseases. *Exp Mol Med* **44:** 89-98

Spilman P, Podlutskaya N, Hart MJ, Debnath J, Gorostiza O, Bredesen D, Richardson A, Strong R, Galvan V (2010) Inhibition of mTOR by rapamycin abolishes cognitive deficits and reduces amyloid-beta levels in a mouse model of Alzheimer's disease. *PLoS One* **5:** e9979

Spires TL, Meyer-Luehmann M, Stern EA, McLean PJ, Skoch J, Nguyen PT, Bacskai BJ, Hyman BT (2005) Dendritic spine abnormalities in amyloid precursor protein transgenic mice demonstrated by gene transfer and intravital multiphoton microscopy. *J Neurosci* **25:** 7278-7287

Sprenger A, Kuttner V, Biniossek ML, Gretzmeier C, Boerries M, Mack C, Has C, Bruckner-Tuderman L, Dengjel J (2010) Comparative quantitation of proteome alterations induced by aging or immortalization in primary human fibroblasts and keratinocytes for clinical applications. *Mol Biosyst* **6:** 1579-1582

Sproul AA, Jacob S, Pre D, Kim SH, Nestor MW, Navarro-Sobrino M, Santa-Maria I, Zimmer M, Aubry S, Steele JW, Kahler DJ, Dranovsky A, Arancio O, Crary JF, Gandy S, Noggle SA (2014) Characterization and molecular profiling of PSEN1 familial Alzheimer's disease iPSC-derived neural progenitors. *PLoS One* **9:** e84547

Stadtfeld M, Brennand K, Hochedlinger K (2008) Reprogramming of pancreatic beta cells into induced pluripotent stem cells. *Curr Biol* **18:** 890-894

Stadtfeld M, Hochedlinger K (2010) Induced pluripotency: history, mechanisms, and applications. *Genes Dev* **24:** 2239-2263

Stamer K, Vogel R, Thies E, Mandelkow E, Mandelkow EM (2002) Tau blocks traffic of organelles, neurofilaments, and APP vesicles in neurons and enhances oxidative stress. *J Cell Biol* **156:** 1051-1063

Steele JW, Gandy S (2013) Latrepirdine (Dimebon(R)), a potential Alzheimer therapeutic, regulates autophagy and neuropathology in an Alzheimer mouse model. *Autophagy* **9:** 617-618

Stozicka Z, Zilka N, Novak M (2007) Risk and protective factors for sporadic Alzheimer's disease. *Acta Virol* **51:** 205-222

Strazielle C, Jazi R, Verdier Y, Qian S, Lalonde R (2009) Regional brain metabolism with cytochrome c oxidase histochemistry in a PS1/A246E mouse model of autosomal dominant Alzheimer's disease: correlations with behavior and oxidative stress. *Neurochem Int* **55:** 806-814

Strittmatter WJ, Saunders AM, Schmechel D, Pericak-Vance M, Enghild J, Salvesen GS, Roses AD (1993) Apolipoprotein E: high-avidity binding to beta-amyloid and increased frequency of type 4 allele in late-onset familial Alzheimer disease. *Proc Natl Acad Sci U S A* **90:** 1977-1981

Swerdlow RH, Khan SM (2004) A "mitochondrial cascade hypothesis" for sporadic Alzheimer's disease. *Med Hypotheses* **63:** 8-20

Takahashi K, Yamanaka S (2006) Induction of pluripotent stem cells from mouse embryonic and adult fibroblast cultures by defined factors. *Cell* **126:** 663-676

Tan JM, Wong ES, Kirkpatrick DS, Pletnikova O, Ko HS, Tay SP, Ho MW, Troncoso J, Gygi SP, Lee MK, Dawson VL, Dawson TM, Lim KL (2008) Lysine 63-linked ubiquitination promotes the formation and autophagic clearance of protein inclusions associated with neurodegenerative diseases. *Hum Mol Genet* **17:** 431-439

Tanaka A (2010) Parkin-mediated selective mitochondrial autophagy, mitophagy: Parkin purges damaged organelles from the vital mitochondrial network. *FEBS Lett* **584:** 1386-1392

Tanzi RE, Kovacs DM, Kim TW, Moir RD, Guenette SY, Wasco W (1996) The gene defects responsible for familial Alzheimer's disease. *Neurobiol Dis* **3:** 159-168

Thinakaran G, Koo EH (2008) Amyloid precursor protein trafficking, processing, and function. *J Biol Chem* **283:** 29615-29619

Thurston TL, Ryzhakov G, Bloor S, von Muhlinen N, Randow F (2009) The TBK1 adaptor and autophagy receptor NDP52 restricts the proliferation of ubiquitin-coated bacteria. *Nat Immunol* **10:** 1215-1221

Thurston VC, Zinkowski RP, Binder LI (1996) Tau as a nucleolar protein in human nonneural cells in vitro and in vivo. *Chromosoma* **105:** 20-30

Trinczek B, Ebneth A, Mandelkow EM, Mandelkow E (1999) Tau regulates the attachment/detachment but not the speed of motors in microtubule-dependent transport of single vesicles and organelles. *J Cell Sci* **112 (Pt 14):** 2355-2367

Turner PR, O'Connor K, Tate WP, Abraham WC (2003) Roles of amyloid precursor protein and its fragments in regulating neural activity, plasticity and memory. *Prog Neurobiol* **70:** 1-32

Twig G, Elorza A, Molina AJ, Mohamed H, Wikstrom JD, Walzer G, Stiles L, Haigh SE, Katz S, Las G, Alroy J, Wu M, Py BF, Yuan J, Deeney JT, Corkey BE, Shirihai OS (2008) Fission and selective fusion govern mitochondrial segregation and elimination by autophagy. *EMBO J* **27:** 433-446

van der Bliek AM, Shen Q, Kawajiri S (2013) Mechanisms of mitochondrial fission and fusion. *Cold Spring Harb Perspect Biol* **5**

Van Humbeeck C, Cornelissen T, Hofkens H, Mandemakers W, Gevaert K, De Strooper B, Vandenberghe W (2011) Parkin interacts with Ambra1 to induce mitophagy. *J Neurosci* **31:** 10249-10261

Vazin T, Ball KA, Lu H, Park H, Ataeijannati Y, Head-Gordon T, Poo MM, Schaffer DV (2014) Efficient derivation of cortical glutamatergic neurons from human pluripotent stem cells: a model system to study neurotoxicity in Alzheimer's disease. *Neurobiol Dis* **62:** 62-72

Verwer RW, Dubelaar EJ, Hermens WT, Swaab DF (2002) Tissue cultures from adult human postmortem subcortical brain areas. *J Cell Mol Med* **6:** 429-432

Vierbuchen T, Ostermeier A, Pang ZP, Kokubu Y, Sudhof TC, Wernig M (2010) Direct conversion of fibroblasts to functional neurons by defined factors. *Nature* **463:** 1035-1041

Vives-Bauza C, Zhou C, Huang Y, Cui M, de Vries RL, Kim J, May J, Tocilescu MA, Liu W, Ko HS, Magrane J, Moore DJ, Dawson VL, Grailhe R, Dawson TM, Li C, Tieu K, Przedborski S (2010) PINK1-dependent recruitment of Parkin to mitochondria in mitophagy. *Proc Natl Acad Sci U S A* **107:** 378-383

Wang D, Epstein D, Khalaf O, Srinivasan S, Williamson WR, Fayyazuddin A, Quiocho FA, Hiesinger PR (2014a) Ca2+-Calmodulin regulates SNARE assembly and spontaneous neurotransmitter release via v-ATPase subunit V0a1. *J Cell Biol* **205:** 21-31

Wang X, Perry G, Smith MA, Zhu X (2010) Amyloid-beta-derived diffusible ligands cause impaired axonal transport of mitochondria in neurons. *Neurodegener Dis* **7:** 56-59

Wang X, Su B, Fujioka H, Zhu X (2008a) Dynamin-like protein 1 reduction underlies mitochondrial morphology and distribution abnormalities in fibroblasts from sporadic Alzheimer's disease patients. *Am J Pathol* **173:** 470-482

Wang X, Su B, Lee HG, Li X, Perry G, Smith MA, Zhu X (2009) Impaired balance of mitochondrial fission and fusion in Alzheimer's disease. *J Neurosci* **29:** 9090-9103

Wang X, Su B, Siedlak SL, Moreira PI, Fujioka H, Wang Y, Casadesus G, Zhu X (2008b) Amyloid-beta overproduction causes abnormal mitochondrial dynamics via differential modulation of mitochondrial fission/fusion proteins. *Proc Natl Acad Sci U S A* **105:** 19318-19323

Wang X, Wang W, Li L, Perry G, Lee HG, Zhu X (2014b) Oxidative stress and mitochondrial dysfunction in Alzheimer's disease. *Biochim Biophys Acta* **1842:** 1240-1247

Wang X, Winter D, Ashrafi G, Schlehe J, Wong YL, Selkoe D, Rice S, Steen J, LaVoie MJ, Schwarz TL (2011) PINK1 and Parkin target Miro for phosphorylation and degradation to arrest mitochondrial motility. *Cell* **147:** 893-906

Webb JL, Ravikumar B, Atkins J, Skepper JN, Rubinsztein DC (2003) Alpha-Synuclein is degraded by both autophagy and the proteasome. *J Biol Chem* **278:** 25009-25013

Wild P, McEwan DG, Dikic I (2014) The LC3 interactome at a glance. *J Cell Sci* **127:** 3-9

Wischik CM, Novak M, Edwards PC, Klug A, Tichelaar W, Crowther RA (1988) Structural characterization of the core of the paired helical filament of Alzheimer disease. *Proc Natl Acad Sci U S A* **85:** 4884-4888

Witte ME, Bol JG, Gerritsen WH, van der Valk P, Drukarch B, van Horssen J, Wilhelmus MM (2009) Parkinson's disease-associated parkin colocalizes with Alzheimer's disease and multiple sclerosis brain lesions. *Neurobiol Dis* **36:** 445-452

Wolf DS, Gearing M, Snowdon DA, Mori H, Markesbery WR, Mirra SS (1999) Progression of regional neuropathology in Alzheimer disease and normal elderly: findings from the Nun study. *Alzheimer Dis Assoc Disord* **13:** 226-231

Wolozin BL, Pruchnicki A, Dickson DW, Davies P (1986) A neuronal antigen in the brains of Alzheimer patients. *Science* **232:** 648-650

Wong E, Cuervo AM (2010) Autophagy gone awry in neurodegenerative diseases. *Nat Neurosci* **13:** 805-811

Wong YC, Holzbaur EL (2014) Optineurin is an autophagy receptor for damaged mitochondria in parkin-mediated mitophagy that is disrupted by an ALS-linked mutation. *Proc Natl Acad Sci U S A* **111:** E4439-4448

Wood JG, Mirra SS, Pollock NJ, Binder LI (1986) Neurofibrillary tangles of Alzheimer disease share antigenic determinants with the axonal microtubule-associated protein tau (tau). *Proc Natl Acad Sci U S A* **83:** 4040-4043

Woodruff G, Young JE, Martinez FJ, Buen F, Gore A, Kinaga J, Li Z, Yuan SH, Zhang K, Goldstein LS (2013) The presenilin-1 DeltaE9 mutation results in reduced gamma-secretase activity, but not total loss of PS1 function, in isogenic human stem cells. *Cell Rep* **5:** 974-985

Wutz A (2012) Epigenetic alterations in human pluripotent stem cells: a tale of two cultures. *Cell Stem Cell* **11:** 9-15

Xie Z, Nair U, Klionsky DJ (2008) Atg8 controls phagophore expansion during autophagosome formation. *Mol Biol Cell* **19:** 3290-3298

Xu RH, Sampsell-Barron TL, Gu F, Root S, Peck RM, Pan G, Yu J, Antosiewicz-Bourget J, Tian S, Stewart R, Thomson JA (2008) NANOG is a direct target of TGFbeta/activin-mediated SMAD signaling in human ESCs. *Cell Stem Cell* **3:** 196-206

Yagi T, Ito D, Okada Y, Akamatsu W, Nihei Y, Yoshizaki T, Yamanaka S, Okano H, Suzuki N (2011) Modeling familial Alzheimer's disease with induced pluripotent stem cells. *Hum Mol Genet* **20:** 4530-4539

Yamano K, Matsuda N, Tanaka K (2016) The ubiquitin signal and autophagy: an orchestrated dance leading to mitochondrial degradation. *EMBO Rep* **17:** 300-316

Yang DS, Stavrides P, Mohan PS, Kaushik S, Kumar A, Ohno M, Schmidt SD, Wesson D, Bandyopadhyay U, Jiang Y, Pawlik M, Peterhoff CM, Yang AJ, Wilson DA, St George-Hyslop P, Westaway D, Mathews PM, Levy E, Cuervo AM, Nixon RA (2011) Reversal of autophagy dysfunction in the TgCRND8 mouse model of Alzheimer's disease ameliorates amyloid pathologies and memory deficits. *Brain* **134:** 258-277

Youle RJ, Narendra DP (2011) Mechanisms of mitophagy. *Nat Rev Mol Cell Biol* **12:** 9-14
Young JE, Boulanger-Weill J, Williams DA, Woodruff G, Buen F, Revilla AC, Herrera C, Israel MA, Yuan SH, Edland SD, Goldstein LS (2015) Elucidating molecular phenotypes caused by the SORL1 Alzheimer's disease genetic risk factor using human induced pluripotent stem cells. *Cell Stem Cell* **16:** 373-385

Yu WH, Kumar A, Peterhoff C, Shapiro Kulnane L, Uchiyama Y, Lamb BT, Cuervo AM, Nixon RA (2004) Autophagic vacuoles are enriched in amyloid precursor protein-secretase activities:

implications for beta-amyloid peptide over-production and localization in Alzheimer's disease. *Int J Biochem Cell Biol* **36:** 2531-2540

Yue Z (2007) Regulation of neuronal autophagy in axon: implication of autophagy in axonal function and dysfunction/degeneration. *Autophagy* **3:** 139-141

Zeng H, Guo M, Martins-Taylor K, Wang X, Zhang Z, Park JW, Zhan S, Kronenberg MS, Lichtler A, Liu HX, Chen FP, Yue L, Li XJ, Xu RH (2010) Specification of region-specific neurons including forebrain glutamatergic neurons from human induced pluripotent stem cells. *PLoS One* **5:** e11853

Zhang F, Wen Y, Guo X (2014) CRISPR/Cas9 for genome editing: progress, implications and challenges. *Hum Mol Genet* **23:** R40-46

Zhu JH, Horbinski C, Guo F, Watkins S, Uchiyama Y, Chu CT (2007) Regulation of autophagy by extracellular signal-regulated protein kinases during 1-methyl-4-phenylpyridinium-induced cell death. *Am J Pathol* **170:** 75-86

Zhu X, Perry G, Smith MA, Wang X (2013) Abnormal mitochondrial dynamics in the pathogenesis of Alzheimer's disease. *J Alzheimers Dis* **33 Suppl 1:** S253-262

Appendix